University of Dundee

DOCTOR OF PHILOSOPHY

The regulation of TGF/BMP signalling by deubiquitylating enzymes

Herhaus, Lina

Award date:
2014

Awarding institution:
University of Dundee

Link to publication

DOCTOR OF PHILOSOPHY

The regulation of TGF/BMP signalling by deubiquitylating enzymes

Lina Herhaus

2014

University of Dundee

The regulation of TGFβ/BMP signalling by deubiquitylating enzymes

Lina Herhaus

TABLE OF CONTENTS

3   OTUB1 ENHANCES TGFB SIGNALLING BY INHIBITING THE UBIQUITYLATION AND DEGRADATION OF ACTIVE SMAD2/3 .... - 93 -

LIST OF FIGURES

LIST OF TABLES

DECLARATIONS

I declare that the following thesis is based on the results of investigations conducted by myself, and that this thesis is of my own composition. Work other than my own is clearly indicated in the text by reference to the relevant researchers or to their publications. This dissertation has not in whole, or in part, been previously submitted for a higher degree.

Lina Herhaus

I certify that Lina Herhaus has spent the equivalent of at least nine terms in research work at the School of Life Sciences, University of Dundee, and that she has fulfilled the conditions of the Ordinance General No. 14 of the University of Dundee and is qualified to submit the accompanying thesis in application for the degree of Doctor of Philosophy.

Dr Gopal P. Sapkota

ACKNOWLEDGEMENTS

I would like to thank my supervisor Gopal Sapkota for giving me the opportunity to perform my PhD studies under his supervision. I am grateful for all his guidance and encouragement, as his mentorship enabled the start of my scientific career.

I also want to thank past and present members of the MRC unit and Sapkota group, in particular Ana, Janis, David, Alejandro and Tim who have made the lab an enjoyable place to work.

I would like to acknowledge and thank all the technical and administrative MRC support staff, especially Simone and Tom for cloning my constructs and Bob, Dave and Joby for help with mass spectrometry.

Finally, I would like to thank my family, especially my parents and grandparents for all their support throughout my studies and most of all: my husband Marco, without whom this would not have been possible.

THESIS SUMMARY

The transforming growth factor-β (TGFβ) pathway, including the bone morphogenetic protein (BMP), plays critical roles during embryogenesis and in adult tissue homeostasis. Hence, malfunctions in TGFβ/BMP signalling result in several diseases. Signalling is initiated by ligand binding to cell surface receptor kinases, which phosphorylate and activate the R-SMAD transcription factors. R-SMADs translocate to the nucleus and regulate the transcription of hundreds of genes. The cellular responses to TGFβ/BMP signals are tightly controlled and highly regulated. TGFβ/BMP receptors and R-SMADs, as the intracellular mediators of TGFβ/BMP ligands, are key targets for regulation to control duration and potency of signalling. Reversible ubiquitylation of R-SMADs and TGFβ/BMP receptors is a key mechanism to control TGFβ/BMP signalling. Several E3 ubiquitin ligases have been reported to regulate the turnover and activity of TGFβ/BMP receptors and R-SMADs, however little is known about their cognate deubiquitylating enzymes (DUBs). A proteomic screen identified the DUBs OTUB1 and USP15 as potential novel regulators of the TGFβ and BMP pathways respectively.

Endogenous OTUB1 was recruited to the active phospho-SMAD2/3 complex only upon TGFβ induction and OTUB1 had a crucial role in TGFβ-mediated gene transcription and cellular migration. OTUB1 inhibited the ubiquitylation of phospho-SMAD2/3 by binding to and inhibiting the E2 ubiquitin-conjugating enzymes independently of its catalytic activity. Consequently, the depletion of OTUB1 in cells caused a rapid loss in levels of TGFβ-induced phospho-SMAD2/3, which was rescued by the proteasomal inhibitor Bortezomib. These findings demonstrated a novel signal-induced

phosphorylation-dependent recruitment of OTUB1 to its target. Hence, OTUB1 could be exploited as a target to intervene against diseases that are provoked by an imbalance in TGFβ signalling.

DUBs are highly regulated enzymes and recent reports have shed light into the molecular regulation OTUB1. The N-terminal region of OTUB1 harbours an ubiquitin binding domain, which is critical for its function to inhibit ubiquitylation. While investigating the role of OTUB1 in TGFβ signalling, it became apparent that OTUB1 itself could be post-translationally modified by phosphorylation. Two phosphorylation sites at the OTUB1 N-terminal region have been identified by mass spectrometry. S18 of OTUB1 was phosphorylated *in vitro* by the type I TGFβ receptor (ALK5), whereas S16 was phosphorylated by the constitutively active kinase CK2 *in vitro* and *in vivo*. Phosphorylation of the OTUB1 N-terminal region could affect its physiological function and requires further investigation.

Although much is known about DUBs that target the type I TGFβ receptor, no DUBs that target the type I BMP receptors had been identified. USP15 was identified in a proteomic screen as an interactor of SMAD6, which is a negative regulator of the BMP pathway. USP15 also binds to and deubiquitylates the type I BMP receptor (ALK3), thereby enhancing BMP signalling. Consequently, USP15 impacts BMP-induced SMAD1 phosphorylation, mouse osteoblastic differentiation and *Xenopus* embryogenesis.

A proteomic approach identified O-GlcNAc transferase (OGT) as an interactor of SMAD2. SMADs have not been associated with O-GlcNAc modifications and the regulation of TGFβ/BMP signalling by O-GlcNAcylation

has not been investigated. Endogenous SMADs1-3 bound OGT and pulled down potential O-GlcNAc modified proteins. Furthermore, SMAD4 was possibly O-GlcNAcylated, which implies that O-GlcNAc modification could regulate TGFβ/BMP signalling. Further investigation is needed to decipher the precise molecular mechanisms of this potential regulation.

ABBREVIATIONS

A	adenosine
aa	amino acids
ACN	Acetonitrile
AGC	protein kinase A, G, and C family
AKT	protein kinase B
ALK	Activin receptor like kinase
AMH	anti-Müllerian hormone
AMSH(-LP)	Associated Molecule with the SH3 domain of STAM (-like protein)
AP	alkaline phosphatase
AP1	Activator Protein 1 C-Jun proto-oncogene
APC	anaphase-promoting complex
APS	ammonium persulphate
ARKADIA	E3 ubiquitin ligase RING Finger Protein 111
ATG8/12	autophagy-8/12
ATP	adenosine 5'-triphosphate sodium salt
BAMBI	BMP and Activin receptor membrane bound inhibitor
BIRC6	Baculoviral IAP Repeat Containing 6
BMDM	bone marrow derived macrophage
BMP	bone morphogenic protein
bp	base pairs
BRAP	BRCA1 Associated Protein
BRE	BMP responsive element
BSA	bovine serum albumin
BTB	Broad-complex, tamtrack and bab
C	cytosine
C/EBPβ	CCAAT/enhancer-binding protein β
CAMK	calcium/calmodulin-dependent protein kinases
Cbl	Casitas B-lineage Lymphoma E3 ubiquitin ligase
CBP	CREB-binding protein
CD109	CD109 molecule
CDC37	Cell Division Cycle 37 homolog
CDK	cyclin dependent protein kinase

X

cDNA	complementary DNA
cf.	*confer*
CHIP	carboxy terminus of Hsc70-interacting protein
c-IAP1	cellular inhibitor of apoptosis 1
CK1/2	Casein kinase 1/2
CLK1/2	CDC-like kinase 1/2
CMGC	CDKs, MAP kinases, GSK and CDK-like kinases
c-Myc	V-Myc Avian Myelocytomatosis Viral Oncogene homolog
cpm	counts per minute
CREB	cAMP response element-binding protein
c-SKI	V-Ski Avian Sarcoma Viral Oncogene homolog
C-terminal	carboxy-terminal
CTGF	connective tissue growth factor
CYLD	Cylindromatosis
Da	Dalton
DAPI	4',6-diamidino-2-phenylindole
DMEM	Dulbecco's modified Eagle medium
DMSO	dimethylsulphoxide
DNA	deoxyribonucleic acid
DSP	dithiobis (succinimidyl propionate)
DSTT	Division of Signal Transduction Therapy
DTT	dithiothreitol
DUB	deubiquitylating enzyme
DUSP	domain present in USPs
DYRK1A	Dual specificity tyrosine-phosphorylation-regulated kinase 1A
E. coli	*Escherichia coli*
E1	E1 ubiquitin activating enzyme
E2	E2 ubiquitin conjugating enzyme
E2F	E2F Transcription Factor
E3	E3 ubiquitin ligase
ECL	enhanced chemiluminescence
ECM	extracellular matrix
EDTA	ethylenediaminetetraacetic acid

eEF1A1	elongation factor 1 A1
EGFR	epidermal growth factor receptor
EGTA	ethyleneglycol bis (2-aminoethylether)-N'N'tetraacetic acid
EMEM	Eagle's Minimum essential medium
EMT	epithelial to mesenchymal transition
EndoMT	endothelial to mesenchymal transition
ERBB2IP	Erbb2 interacting protein
ERK1/2	Mitogen-Activated Protein Kinase 3/1
ERα	Estrogen receptor α
FAT10	human leukocyte antigen F associated
FBS	foetal bovine serum
FDS	Ferguson-Smith disease
FKBP12	FK506 Binding Protein 1A, 12 kDa
FOX	Forkhead box
FT	flow-through extracts
FUB1	Fau ubiquitin-like protein
g	gram or gravity
G	guanosine
G418	geneticin
GADD34	growth arrest and DNA damage-inducible protein 34
GDF	growth and differentiation factor
GFAT	glutamine:fructose-6-phosphate amidotransferase
GFP	green fluorescent protein
GRK2	G protein-coupled receptor kinase 2
GSK3	glycogen synthase kinase 3
GST	glutathione-S-transferase
h	hours
HA	haemagglutinin
HAT	histone acetyltransferase
HBP	hexosamine biosynthetic pathway
HDAC	histone deacetylase
HECT	Homologous to E6-AP C-Terminus
HEK293	human embryonic kidney 293 cells

HEPES	N-[2-hydroxyethyl]piperazine-N'-[2-ethanesulphonic acid]
HHT	Hereditary Haemorrhagic Telangiectasia
HIF-1α	Hypoxia-inducible factor 1-α
HOX	homeotic genes
HPLC	high-pressure liquid chromatography
HPV16	Human papillomavirus 16
HRP	horseradish peroxidase
HSCARG	NmrA-like family domain containing 1
IBR	in-between RING
ID-1	inhibitor of differentiation 1
IgG	immunoglobulin G
IL1β	Interleukin-1 β
IP	immunoprecipitation
IPTG	isopropyl β-D-thiogalactoside
ISG15	interferon-α-stimulated gene-15
I-SMAD	inhibitory SMAD
ITCH	Itchy E3 ubiquitin ligase
JAMM/MPN+	zinc metalloproteases JAB1/MPN/MOV34
JNK	c-Jun N-terminal kinase
k	kilo
Keap1	Kelch-like ECH-associated protein 1
KLH	keyhole limpet haemocyanin
l	litre
LAP	latent association peptide
LB	Luria-Bertani medium
LC-MS/MS	liquid chromatography coupled to high-resolution tandem mass spectrometry
LDS	Loeys-Dietz syndrome
LPS	Lipopolysaccharide
LTBPs	latent TGFβ binding proteins
m	milli or meter
M	molar
MAD	mothers against decapentaplegic

MAPK	mitogen-activated protein kinase
M-CSF	macrophage colony-stimulating factor
MDM2	mouse double minute 2 homolog
MEF	mouse embryonic fibroblast
MEK	mitogen-activated protein kinase kinase
MES	2-(*N*-morpholino) ethane sulfonic acid
MET	mesenchymal to epithelial transition
MH	MAD homology
MH1	N-terminal MAD homology 1 domain
MH2	C-terminal MAD homology 2 domain
min	minute
miRNA	microRNA
MKK4	mitogen-activated protein kinase kinase 4
MMP2	matrix metalloprotease 2
mOGT	mitochondrial OGT
mol	mole
MOPS	3-(*N*-morpholino) propanesulfonic acid
MRC PPU	Medical Research Council Protein Phosphorylation and Ubiquitylation Unit
mRNA	messenger RNA
MTMR4	myotubularin related protein 4
mTORC1	mammalian target of rapamycin complex 1
n	nano
NADPH	nicotinamide adenine dinucleotide phosphate-oxidase
ncOGT	nucleo-cytoplasmic OGT
NEDD	neural precursor cell expressed, developmentally down-regulated
NFκB	nuclear factor kappa-light-chain-enhancer of activated B cells
NLS	nuclear localisation signal
N-terminal	amino-terminal
O1	OTUB1
OD	optical density
OGA	O-GlcNAcase
O-GlcNAc	O-linked β-N-acetylglucosamine

OGT	O-GlcNAc transferase
OTU	ovarian tumour domain
p	pico
p300	E1A Binding Protein P300
p38 MAPK	mitogen-activated protein kinase 14
p53	Tumour Protein p53
PAGE	polyacrylamide gel electrophoresis
PAI-1	Plasminogen activator inhibitor-1
PAR6	Partitioning defective 6 homolog
PAWS1	Protein Associated With SMAD1
PBS	phosphate-buffered saline
PCR	polymerase chain reaction
PDP	mitochondrial enzyme Pyruvate dehydrogenase
PDZ	post synaptic density protein, Drosophila disc large tumor suppressor and zonula occludens-1 protein
PEI	polyethylenimine
PHD	Plant Homeo Domain
PI3K	Phosphatidylinositol-4,5-bisphosphate 3-kinase
PIAS	protein inhibitor of activated STAT E3 SUMO ligase
PIM1	proto-oncogene Serine/Threonine-protein kinase 1
PIN1	peptidyl-prolyl *cis-trans* isomerase
PKA	protein kinase A
PKC	protein kinase C
PKG	protein kinase G
PMDS	Persistent Müllerian Duct syndrome
PMSF	phenylmethanesulphonylfluoride
PP1	protein phosphatase 1
PP2A	protein phosphatase 2
PPM1A	protein phosphatase Mg^{2+}/Mn^{2+} dependent 1A
pS16	phospho-Serine 16
PTMs	post-translational modifications
PVDF	polyvinylidene difluoride
qRT-PCR	quantitative reverse transcriptase PCR

RAS	rat sarcoma protein family
RBR	RING, in-between RING and RING2
REST	RE1-Silencing Transcription factor
RhoA	RAS homolog gene family member A
RIG1	retinoic acid-inducible gene 1
RING	really interesting new gene
RNA	ribonucleic acid
RNAi	RNA interference
RNF12	RING Finger Protein 12
ROC1	RING box protein 1
rpm	revolutions per minute
R-SMADs	receptor-regulated SMAD
RT	room temperature
RUNX(2)	Runt-related transcription factor 2
s	seconds
S1	site 1
SARA	SMAD anchor for receptor activation
SART3	Squamous cell carcinoma antigen recognized by T-cells 3
SBE	SMAD binding element
SCF	Skp, Cullin, F-box containing complex
SCP(1-3)	small C-terminal domain phosphatase (1-3)
SDS	sodium dodecyl sulphate
SH	Src Homology
ShcA	Src Homology 2 Domain Containing Transforming Protein 1
siRNA	small interfering RNA
SIRT1	Sirtuin 1
SLIM1	skeletal muscle LIM protein 1
SMAD-LP	linker-phosphorylated SMAD
SMAD-TP	tail-phosphorylated SMAD
SMURF1/2	SMAD ubiquitylation regulatory factor 1/2
SnoN	Ski-related novel protein N
SOCS	BC box-Suppressor of Cytokine Signalling
sOGT	short cytoplasmic form of OGT

SOS	Son of Sevenless
SRE	SMAD-Response Element
STAT	Signal Transducer and Activator of Transcription
STE	Homologs of the yeast STE7, STE11 and STE20
SUMO	small ubiquitin-like modifier
T	thymidine
T/B miRNAs	TGFβ/BMP-regulated miRNAs
TAB1	TGFβ Activated Kinase 1/MAP3K7 Binding Protein 1
TACE	TNFα-converting enzyme
TAE	Tris-acetate-EDTA
TAK1	TGFβ Activated Kinase 1/MAP3K7
TBS	Tris-buffered saline
TBS-T	Tris-buffered saline-Tween
TCEP	Tris(2-carboxyethyl)phosphine
TEAB	triethylammonium bicarbonate
TEMED	tetramethylethylenediamine
TFA	trifluoroacetic acid
TGFβ	transforming growth factor-β
TGIF	TG-interacting factor
Th17	T helper 17 cells
TIF1γ	transcriptional intermediary factor 1 γ
TK	Tyrosine kinases
TKL	Tyrosine kinase-like
TMEPAI	transmembrane prostate androgen-induced protein
TNFα	tumour necrosis factor α
TPR	terminal tetratricopeptide repeat
TRAF6	tumour necrosis factor receptor associated protein 6
TRIM25/33	Tripartite motif-containing 25/33
Tris	Tris(hydroxymethyl)methylamine
Triton X-100	t-octylphenoxypolyethoxyethanol-X-100
TSC22(D3)	TGFβ-stimulated clone 22 (domain 3)
Tween-20	polyethylene glycol sorbitan monolaurate
U	uracil

UBA	ubiquitin-associated domains
UBD	ubiquitin-binding domain
UBL fold	ubiquitin-like fold
UBL5	ubiquitin-like protein-5
UBLs	ubiquitin-like modifiers
UCH	ubiquitin C-terminal hydrolase
UDP-GlcNAc	uridine diphosphate N-acetylglucosamine
UFM1	ubiquitin fold-modifier-1
UIM	ubiquitin-interacting motif
ULP	ubiquitin-like protease
URM1	ubiquitin-related modifier-1
USP	ubiquitin specific protease
V	volts
v/v	volume to volume
VHL box	Von Hippel–Lindau box
w/v	weight to volume
WT	wild type
WWP1/2	WW domain-containing E3 ubiquitin protein ligase 1/2
XTT	2,3-Bis-(2-Methoxy-4-Nitro-5-Sulfophenyl)-2H-Tetrazolium-5-Carboxanilide
YAP	Yes-associated protein
YpkA	Yersinia protein kinase A
YY1	Ying Yang 1
ZnF-UBP	zinc finger ubiquitin-specific protease domains
α	alpha
β	beta
β-ME	β-mercaptoethanol
βTRCP1	F-box/WD repeat-containing protein 1A
γ	gamma
λ	lambda phosphatase
μ	micro
°C	degree Celsius

AMINO ACID CODE

amino acid	thee letter code	one letter symbol
Alanine	Ala	A
Arginine	Arg	R
Asparagine	Asn	N
Aspartic acid	Asp	D
Cysteine	Cys	C
Glutamic acid	Glu	E
Glutamine	Gln	Q
Glycine	Gly	G
Histidine	His	H
Isoleucine	Ile	I
Leucine	Leu	L
Lysine	Lys	K
Methionine	Met	M
Phenylalanine	Phe	F
Proline	Pro	P
Serine	Ser	S
Threonine	Thr	T
Tryptophan	Trp	W
Tyrosine	Tyr	Y
Valine	Val	V
any amino acid	Xaa	X

LIST OF PUBLICATIONS

1. **Herhaus, L.,** and Sapkota, G. P. (2014) The emerging roles of deubiquitylating enzymes (DUBs) in the TGFβ and BMP pathways. *Cellular Signalling* 26, 2186-2192.

2. **Herhaus, L.***, Al-Salihi, M.A.*, Dingwell, K. S., Cummins, T. D., Wasmus, L., Vogt, J., Ewan, R., Bruce, D., Macartney, T., Weidlich, S., Smith, J. C., Sapkota, G. P. (2014) USP15 targets ALK3/BMPR1A for deubiquitylation to enhance BMP signalling. *Open Biology* 4, 140065, *equal contribution.

3. Vogt, J., Dingwell, K. S., **Herhaus, L.,** Gourlay, R., Macartney, T., Campbell, D., Smith, J. C., Sapkota, G. P. (2014) Protein Associated With SMAD1 (PAWS1/FAM83G) is a substrate for type I BMP receptors and modulates BMP signalling. *Open Biology* 4, 130210.

4. **Herhaus, L.**, Al-Salihi, M.A., Macartney, T., Weidlich, S., Sapkota, G. P. (2013) OTUB1 enhances TGFβ signalling by inhibiting the ubiquitylation and degradation of active SMAD2/3. *Nature Communications* 4, 2519.

5. Al-Salihi, M. A., **Herhaus, L.**, Macartney, T., Sapkota, G. P. (2012) USP11 augments TGFβ signalling by deubiquitylating ALK5. *Open Biology* 2, 120063.

6. Al-Salihi, M. A., **Herhaus, L.**, Sapkota, G. P. (2012) Regulation of the transforming growth factor beta pathway by reversible ubiquitylation. *Open Biology* 2, 120082.

1 Introduction

1.1 Post-translational modifications

Most proteins undergo post-translational modifications (PTMs), which affect their cellular roles through modulation of their subcellular localisation, protein-protein interactions, transcriptional ability, stability and activity. PTMs include phosphorylation, ubiquitylation, acetylation, glycosylation, methylation, glycation, nitration, carbonylation, hydroxylation, palmitoylation, crotonylation, succinylation, hypusination and biotinylation (Markiv *et al.*, 2012, Tan *et al.*, 2011, Weinert *et al.*, 2013, Park *et al.*, 1993, Hwang *et al.*, 2014). Enzymatic generation of reversible PTMs, which are subject to feedback control, provide a dynamic basis for eukaryotic cells to respond to external stimuli and modulate signal transduction. The PTMs can be permanent or transient due to their reversibility, which allows for competition and reciprocal occupancy of different PTMs at the same residues. Certain PTMs on target proteins can trigger the formation of other PTMs at proximal residues, highlighting the interplay between them. The most studied PTMs are phosphorylation and ubiquitylation.

1.1.1 Reversible Phosphorylation

Protein phosphorylation is one of the most abundant PTMs and controls a wide range of cellular processes including transcription, trafficking and metabolism. Protein phosphorylation is catalysed by protein kinases, which represent one of the largest groups of enzymes with at least 550 reported so far. Protein kinases are responsible for the catalysis of the γ-phosphate from ATP to the hydroxyl group of a residue in the substrate protein. Primarily, protein kinases phosphorylate Serine, Threonine, or Tyrosine residues on target proteins. The human protein kinases can further be classified into distinct

groups according to their evolutionary divergences: AGC (containing the PKA, PKG and PKC families), CAMK (calcium/calmodulin-dependent protein kinases), CK1 (Casein kinase 1), CMGC (containing the CDK, MAPK, GSK3, CLK families), STE (containing the homologues of yeast Sterile kinases), TK (Tyrosine kinases), TKL (Tyrosine kinase–like) and the atypical kinases (Manning *et al.*, 2002, Cohen, 2002).

The majority of eukaryotic proteins are phosphorylated at multiple residues and each phosphate introduces a change in the local charge of the substrate. This can cause conformational changes in the modified protein, thereby directly altering its affinity or activity towards ligand or substrate (Figure 1-1). The phosphorylated substrate can also be recognised by other proteins, which might then lead to a change in protein function, stability or localisation (Manning *et al.*, 2002).

The human kinome is now increasingly targeted for structure-based drug design to generate specific ATP competitive inhibitors or allosteric modulators, as kinase malfunctioning is found to drive various diseases (Cohen and Alessi, 2013, Fang *et al.*, 2013).

Protein phosphorylation can be reversed by the action of protein phosphatases (Figure 1-1). Protein phosphatases hydrolyse the phosphoric acid monoesters into a phosphate ion and a molecule with a free hydroxyl group. They can be classified into three distinct groups based on sequence similarity, structure and catalytic activity: protein Tyrosine phosphatases, Serine-Threonine phosphatases and dual (S/T-Y) phosphatases (Cohen, 2009). Due to the limited number of phosphatases encoded in the human genome, phosphatases are likely to be more promiscuous with regards to their substrate specificity than protein kinases (Bruce and Sapkota, 2012).
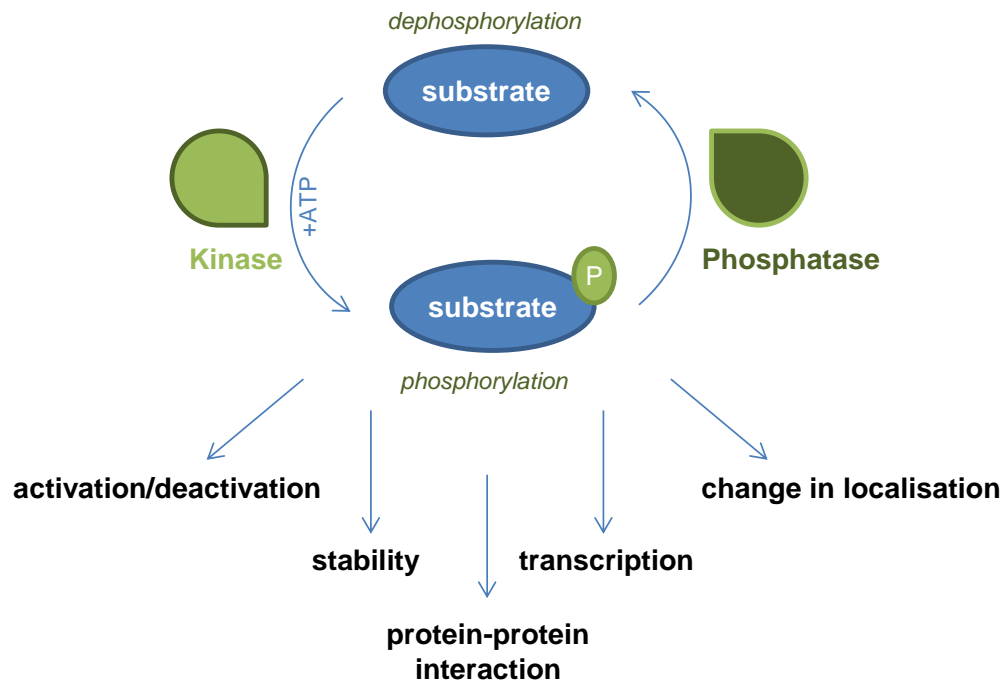
Figure 1-1 Protein phosphorylation

Protein kinases can phosphorylate their substrates in the presence of ATP. This mechanism can be reversed by the action of phosphatases. Protein phosphorylation can lead to conformational changes in the substrate leading to changes in activity (in case of enzymes), stability, localisation and interaction partners.

1.1.2 Reversible Ubiquitylation

1.1.2.1 Ubiquitylation

Ubiquitylation is a reversible post-translational modification that is essential in many cellular regulatory mechanisms (Fraile *et al.*, 2011, Frappier and Verrijzer, 2011). Discovered in 1975, ubiquitin is a 76 amino acid protein that is evolutionarily conserved from yeast to human (Hershko *et al.*, 1979, Varshavsky, 2006, Schlesinger and Goldstein, 1975). Ubiquitin is part of a highly conserved family of small proteins that share homology in a common-fold structure. This family also includes ubiquitin-like modifiers (UBLs): small ubiquitin-like modifier (SUMO), neural precursor cell expressed developmentally down-regulated protein 8 (NEDD8), ubiquitin-like protein-5 (UBL5), ubiquitin-related modifier-1 (URM1), interferon-α-stimulated gene-15 (ISG15), autophagy-

8 (ATG8) and -12 (ATG12), human leukocyte antigen F associated (FAT10), ubiquitin fold-modifier-1 (UFM1) and Fau ubiquitin-like protein (FUB1) (Hochstrasser, 2009).

During the ubiquitylation cascade, ubiquitin is attached to target proteins through the action of an E1 ubiquitin activating enzyme, an E2 ubiquitin conjugating enzyme and an E3 ubiquitin ligase. This cascade is initiated upon the ATP-dependent activation of ubiquitin by the E1. One of the two E1 enzymes encoded in the human genome links the C-terminal Glycine residue of ubiquitin via a thioester bond to a Cysteine residue within its active site. The activated ubiquitin intermediate is then transferred to the catalytic Cysteine residue of one of the ~45 E2 enzymes (E2~ub). The E3 ubiquitin ligase then conjugates the C-terminal Glycine of ubiquitin via an isopeptide bond to the ε-amino group of the target Lysine of the substrate (Figure 1-2). There are over 600 E3 ubiquitin ligases, which are divided into two families based on their catalytic domain structure and mode of catalysis (Hershko *et al.*, 1983, Pickart, 2001, Ye and Rape, 2009, Hochstrasser, 2009, Schulman, 2011).

The HECT E3 ligases (Homologous to E6-AP C-Terminus) bind E2~ub through a thioester bond formed with its catalytic Cysteine residue. The ubiquitin loaded HECT E3 can then directly ubiquitylate the target protein (Kamadurai *et al.*, 2013, Kamadurai *et al.*, 2009). The conserved HECT domain, which includes the catalytic Cysteine residue and E2 binding site, is located at the C-terminus, whereas the N-terminus is diverse and mediates substrate binding (Berndsen and Wolberger, 2014, Scheffner and Kumar, 2014, Metzger *et al.*, 2012). HECT E3 ligases are further classified into three subfamilies, with the mammalian NEDD4 family comprising NEDD4, NEDD4L, ITCH, WWP1/2, SMURF1/2 and NEDL1/2. The N-terminal regions of the NEDD4 family contain

a C2 domain that regulates autoinhibition and sub-cellular localisation and two to four WW domains which are characterised by two highly conserved Tryptophans that associate with Proline-rich motifs and assist in substrate binding (Scheffner and Kumar, 2014, Rotin and Kumar, 2009, Wiesner *et al.*, 2007).

The other class of E3 ubiquitin ligases with a RING (really interesting new gene) domain, or the closely related U-Box and PHD domain, catalyse ubiquitylation without accepting the activated ubiquitin. RING E3 ligases catalyse the direct transfer of ubiquitin from the E2 enzyme to the substrate, simultaneously binding both the E2~ub thioester and the substrate, thereby facilitating the positioning of the E2 enzyme in an orientation that assists the transfer of ubiquitin to the substrate protein (Plechanovova *et al.*, 2012, Metzger *et al.*, 2014). RING domain E3 ligases are usually found in large complexes (e.g. cullin RING ligases including SCF) or dimers; however some can also be single protein E3 ubiquitin ligases. The canonical RING finger is a two Zn^{2+} ion-coordinating domain that binds a hydrophobic patch on the donor ubiquitin, E2 enzymes and in some cases directly recognises substrates. Usually, interchangeable components of large RING E3 ligase complexes that contain F-box, SOCS box, VHL box or BTB domain proteins assist in substrate recognition, in addition to alternative substrate recognition motifs (such as UBD, SH and PDZ). Some RING E3 ligases also have other domains that interact with the "backside" of E2s (Metzger *et al.*, 2014, Deshaies and Joazeiro, 2009, Berndsen and Wolberger, 2014).

The RBR family of E3 ubiquitin ligases comprise a canonical RING domain, an in-between RING (IBR) domain and a RING2 domain. Some ligases

belonging to this family act as RING–HECT E3 ligase hybrids (Deshaies and Joazeiro, 2009, Wenzel *et al.*, 2011, Spratt *et al.*, 2014).

Target proteins can be monoubiquitylated, multi-monoubiquitylated or by repeated action of the E1, E2 and E3, ubiquitin can be added onto one of several Lysine residues or the α-amino group of the first ubiquitin to form unique polyubiquitin chains. Monoubiquitylation can alter protein sub-cellular localisation and function in signalling pathways. Polyubiquitin chains can have a distinct structure depending on which Lysine (K) residue within ubiquitin is utilised to anchor the subsequent ubiquitin molecule. These linkages can occur on K6, K11, K27, K29, K33, K48 or K63 as well as the N-terminus of ubiquitin (linear chains, M1). Branched chains and mixed linkage types are also possible. These different linkage types function as signals that can be identified by other ubiquitin-binding proteins (ubiquitin receptors) and ultimately determine the fate of the target protein. Ubiquitin-mediated protein degradation can occur through the proteasomal, lysosomal or autophagosomal pathway (Komander and Rape, 2012, Pickart and Eddins, 2004, Kulathu and Komander, 2012, Husnjak and Dikic, 2012, Emmerich *et al.*, 2013).

The 26S proteasome is a multisubunit enzyme complex that has one or two 19S regulatory caps, which bind polyubiquitin chains. The ubiquitylated proteins are then degraded in the 20S proteolytic core, which is composed of two inner β and two outer α rings. The β rings contain proteolytic sites, which can be inhibited by various proteasome inhibitors (Figure 1-2). Bortezomib is a selective and potent proteasomal inhibitor that reversibly binds the Threonine residue in the β ring, which is essential for chymotryptic activity (Adams, 2003). Bortezomib confers antitumor activity

and is now approved in the treatment of multiple myeloma or relapsed mantel cell lymphoma (Grosicki *et al.*, 2014).

Two of the most commonly studied ubiquitin chain linkages are the K48-linked chains, which generally mark proteins for proteasomal degradation, and the K63-linked chains, which confer degradation via the lysosome or non-degradative fates of target proteins (Nathan *et al.*, 2013). K63, K11 and linear chains are usually implicated in signal transduction. K63-linked polyubiquitin chains convey a signalling function, especially in the innate immune system, in response to DNA damage and in endocytosis (Deng *et al.*, 2000, Duncan *et al.*, 2006, Hofmann and Pickart, 1999). K11-linked polyubiquitin chains are implicated in the regulation of cell cycle progression in eukaryotes and can mediate endocytosis, TNFα and Wnt signalling (Bremm and Komander, 2011, Wickliffe *et al.*, 2011). Linear chains are implicated in the activation of NFκB by TNFα (Tokunaga *et al.*, 2009). The functions of the remaining chain linkages are not well established.
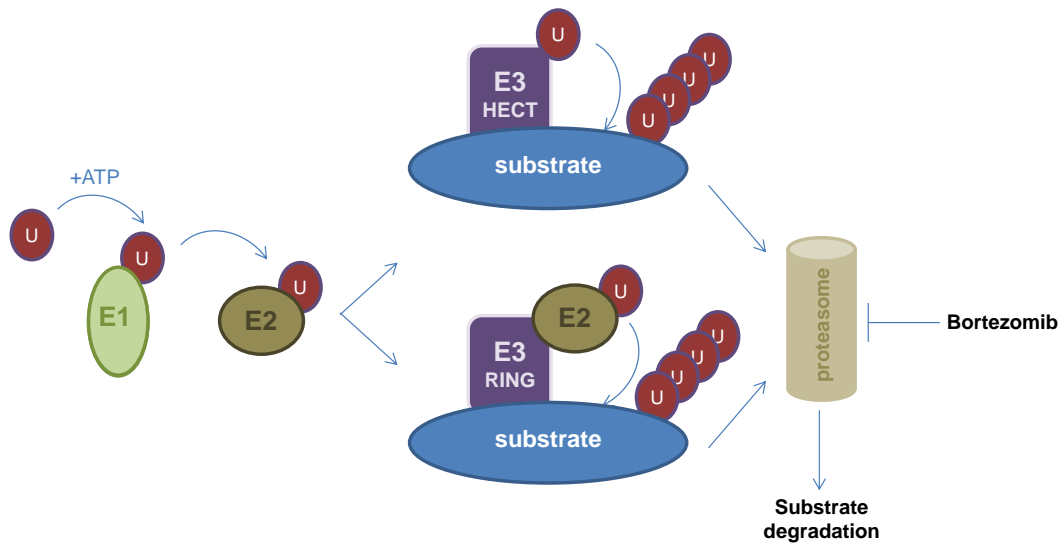
Figure 1-2 The protein ubiquitylation cascade

To activate ubiquitin, a thioester bond between its C-terminus and the active site Cysteine of the E1 is formed in an ATP-dependent manner. Ubiquitin is then transferred from the E1 to the active site Cysteine in the E2. Either the E2 then transfers ubiquitin to the HECT E3 ligase, which accepts ubiquitin onto its active site Cysteine residue and ubiquitylates the substrate directly, or the E2 binds a RING E3 ligase, which then facilitates the transfer of ubiquitin to the substrate. An isopeptide bond is formed between the C-terminus of ubiquitin and the ε-amino group of a Lysine residue in the substrate. Substrate ubiquitylation can lead to various different outcomes. K48-linked polyubiquitylation of substrates usually results in proteasomal degradation of the target protein. The proteasome can be experimentally inhibited by Bortezomib.

1.1.2.2 Deubiquitylation

The removal of ubiquitin(s) attached to target proteins is defined as deubiquitylation, catalysed by deubiquitylating enzymes (DUBs). Deubiquitylation is implicated in fine-tuning the majority of cellular signalling processes including gene expression, genome regulation, DNA repair, cell cycle progression, kinase activation, endocytic trafficking and immune responses. Hence, the malfunctioning of DUBs is often associated with various diseases ranging from cancer to neurological disorders (Clague *et al.*, 2012a, Singhal *et al.*, 2008, Clague *et al.*, 2012b, Emre and Berger, 2004, Mukai *et al.*, 2012, Reyes-Turcu *et al.*, 2009, Sun, 2008).

The DUBs encoded by the human genome are classified into five distinct functional and structural groups: the Cysteine proteases: ubiquitin-specific proteases (USPs), ovarian tumour proteases (OTUs), ubiquitin C-terminal hydrolases (UCHs) and Josephins, and the zinc metalloproteases JAB1/MPN/MOV34 (JAMM/MPN+). Similar to the DUBs that process ubiquitin, there are other ubiquitin-like proteases (ULPs) that selectively remove specific UBLs. For example, SUMO and NEDD8 are removed by ULPs that belong to the Adenain family of Cysteine proteases, whereas ISG15 is cleaved by a ULP that resembles the adenovirus protease (Komander *et al.*, 2009, Reyes-Turcu *et al.*, 2009, Nijman *et al.*, 2005, Hay, 2007).

As the human genome encodes less than 100 DUBs, it is highly likely that DUBs are intricately regulated in order to oppose the action of over 600 E3 ubiquitin ligases in diverse signalling cascades. Overall DUB specificity is achieved by a combination of substrate and target recognition. Additionally, this is regulated by conformational/post-translational changes, subcellular localisation and interactions with regulatory partners. To ensure specificity even further, DUBs also distinguish between UBLs, isopeptides, linear peptides and different types of ubiquitin linkage and chain structure as well as *exo-* versus *endo-* deubiquitylation. Enzymatic activity of DUBs might be cryptic and regulated by occluding the substrate-binding sites of certain DUBs or by inducing conformational changes that activate the catalytic site (Amerik and Hochstrasser, 2004, Clague *et al.*, 2012a, Katz *et al.*, 2010, Komander *et al.*, 2009, Nijman *et al.*, 2005, Reyes-Turcu *et al.*, 2009). Apart from these substrate-induced conformational changes and post-translational modifications, activity can also be induced by scaffold or adapter proteins and allosteric interactions as well as transcriptional regulation of DUB expression (Amerik and

Hochstrasser, 2004, Clague *et al.*, 2012a, Katz *et al.*, 2010, Komander *et al.*, 2009, Nijman *et al.*, 2005, Reyes-Turcu *et al.*, 2009).

In addition to their catalytic core, DUBs contain multiple domains that mediate protein-protein interactions. These domains include ubiquitin-binding domains (UBD), ubiquitin-like folds (UBL folds), ubiquitin-interacting motifs (UIM), ubiquitin-associated domains (UBA domain) and/or zinc finger ubiquitin-specific protease domains (ZnF-UBP domain). The ubiquitin-binding domains contribute to the binding and recognition of different ubiquitin chain linkages, although some DUBs also display direct affinity for their ubiquitylated target proteins (Amerik and Hochstrasser, 2004, Clague *et al.*, 2012a, Katz *et al.*, 2010, Komander *et al.*, 2009, Nijman *et al.*, 2005, Reyes-Turcu *et al.*, 2009).

1.1.3 Glycosylation (O-GlcNAcylation)

Glycosylation is defined as the enzymatic attachment of glycans to proteins and lipids. Five types of glycosylation are distinguished: O-linked glycosylation, N-linked glycosylation, phospho-serine glycosylation, C-mannosylation and glypiation (Varki *et al.*, 2009).

O-linked glycosylation (also known as O-GlcNAcylation) is a nutrient-sensitive sugar modification and was first discovered in 1984 as a post-translational modification by O-linked β-N-acetylglucosamine (O-GlcNAc) moiety at Serine or Threonine residues of proteins (Torres and Hart, 1984). It is one of the most abundant eukaryotic glycosyltransferase reactions and occurs in the cytoplasm and nucleus (Hanover *et al.*, 2012). O-GlcNAcylation has been shown to have extensive crosstalk with phosphorylation in several signalling cascades due to competitive site occupancy on Serine/Threonine residues. Reciprocal occupancy of phosphorylation and O-GlcNAcylation at the same

residues or at proximal sites was identified in several proteins (Hart *et al.*, 2011). The resulting diversity of O-GlcNAcylated and phosphorylated proteins contributes to the regulation of cellular processes comprising chromatin organisation, transcription, translation, proteostasis, development and signal transduction (Figure 1-3) (Hanover *et al.*, 2012).

O-GlcNAcylation can be influenced through nutrient levels, extracellular stimuli, stressors, heat shock, pathogens, cell cycle changes and development. (Hanover *et al.*, 2012). The limiting factor in the synthesis of O-GlcNAc is the availability of glucose. Nutrient concentration determines the production of uridine diphosphate N-acetylglucosamine (UDP-GlcNAc) through the metabolically controlled hexosamine biosynthetic pathway (HBP) (Figure 1-3). The HBP integrates extracellular physiological determinants such as nutrient availability with the metabolism of carbohydrates, amino acids, nucleotides and fatty acid components. Several enzymes (*cf.* Figure 1-3) aid in the ATP-dependent production of the final product (UDP-GlcNAc) of the HBP pathway (Bond and Hanover, 2013, Hanover *et al.*, 2012). UDP-GlcNAc is essential for the synthesis of glycosaminoglycans, glycolipids, membrane and secretory glycoproteins and is the substrate for O-GlcNAc transferase (OGT) (Hanover *et al.*, 2012, Love and Hanover, 2005).

OGT is an enzyme that transfers saccharides from sugar nucleotide precursors in glycosidic linkages (O-GlcNAc) to Serine/Threonine residues of target proteins (O-GlcNAcylation) (Kreppel *et al.*, 1997). The specificity of OGT for target proteins is possibly mediated by regulatory binding proteins because no strict consensus motif has been identified. However, an enrichment of O-GlcNAcylation is observed on the "PXTXA", the "PVS" and, "PPV(S/T)SATT" sequences (Hurtado-Guerrero *et al.*, 2008, Liu *et al.*, 2014b, Vosseller *et al.*,

2006). The N-terminus of OGT harbours a terminal tetratricopeptide repeat (TPR) domain, which is separated from the C-terminal catalytic and the phosphoinositide-binding domain by a bipartite nuclear localisation sequence (NLS). The *OGT* gene encodes three OGT isoforms in mammals: a nucleo-cytoplasmic OGT (ncOGT) with 12 TPRs, a mitochondrial OGT (mOGT) with 9 TPRs and short cytoplasmic form of OGT (sOGT) that contains only 2 TPRs (Vocadlo, 2012, Lazarus *et al.*, 2011, Ruan *et al.*, 2013).

O-GlcNAc can be removed by β-N-acetylglucosaminidase C (also known as O-GlcNAcase (OGA)), which then ensures efficient O-GlcNAc cycling (Lubas *et al.*, 1997). OGA is present in the cytoplasm and nucleus. Its N-terminus contains the O-GlcNAc cleavage domain and the OGT-binding region. The OGA C-terminus differs in the two splice variants OGA-L and OGA-S. OGA-L possesses a histone acetyltransferase (HAT)-like domain, which is absent from OGA-S (Vocadlo, 2012, Ruan *et al.*, 2013, Harwood and Hanover, 2014). OGT and OGA are expressed in all tissues and play major roles during vertebrate development (Harwood and Hanover, 2014, Yang *et al.*, 2012).

Changes in protein O-GlcNAcylation causes modifications in protein folding, cellular localisation, and catalytic activity of certain enzymes. The dynamic O-GlcNAc cycling regulates cellular processes in a nutrient-dependent manner. Hence, dysfunctional O-GlcNAc cycling is linked to several diseases including cancer, cardiovascular disease, neurodegeneration and diabetes (Figure 1-3) (Hart *et al.*, 2011, Bond and Hanover, 2013, Hanover *et al.*, 2012, Singh *et al.*, 2014, Harwood and Hanover, 2014, Ma and Vosseller, 2013, Zachara, 2012).

A hallmark of cancer cell energy metabolism is a shift from oxidative phosphorylation to the glycolytic pathway (Warburg effect) (Hanahan and

Weinberg, 2011). This requires enhanced glucose uptake and if combined with increased glutamine absorption, results in increased O-GlcNAc levels (Ma and Vosseller, 2013, Singh *et al.*, 2014). Cancer metabolism and survival stress signalling can be regulated by O-GlcNAcylation via regulating the stability of HIF-1α (Ferrer *et al.*, 2014). Insulin signalling is influenced by the flux of the HBP and insulin resistance is associated with type II diabetes, heart disease and obesity. O-GlcNAc is associated with direct inhibition of insulin signalling and probably contributes to its variations observed in diabetic patients (Whelan *et al.*, 2010, Bond and Hanover, 2013).
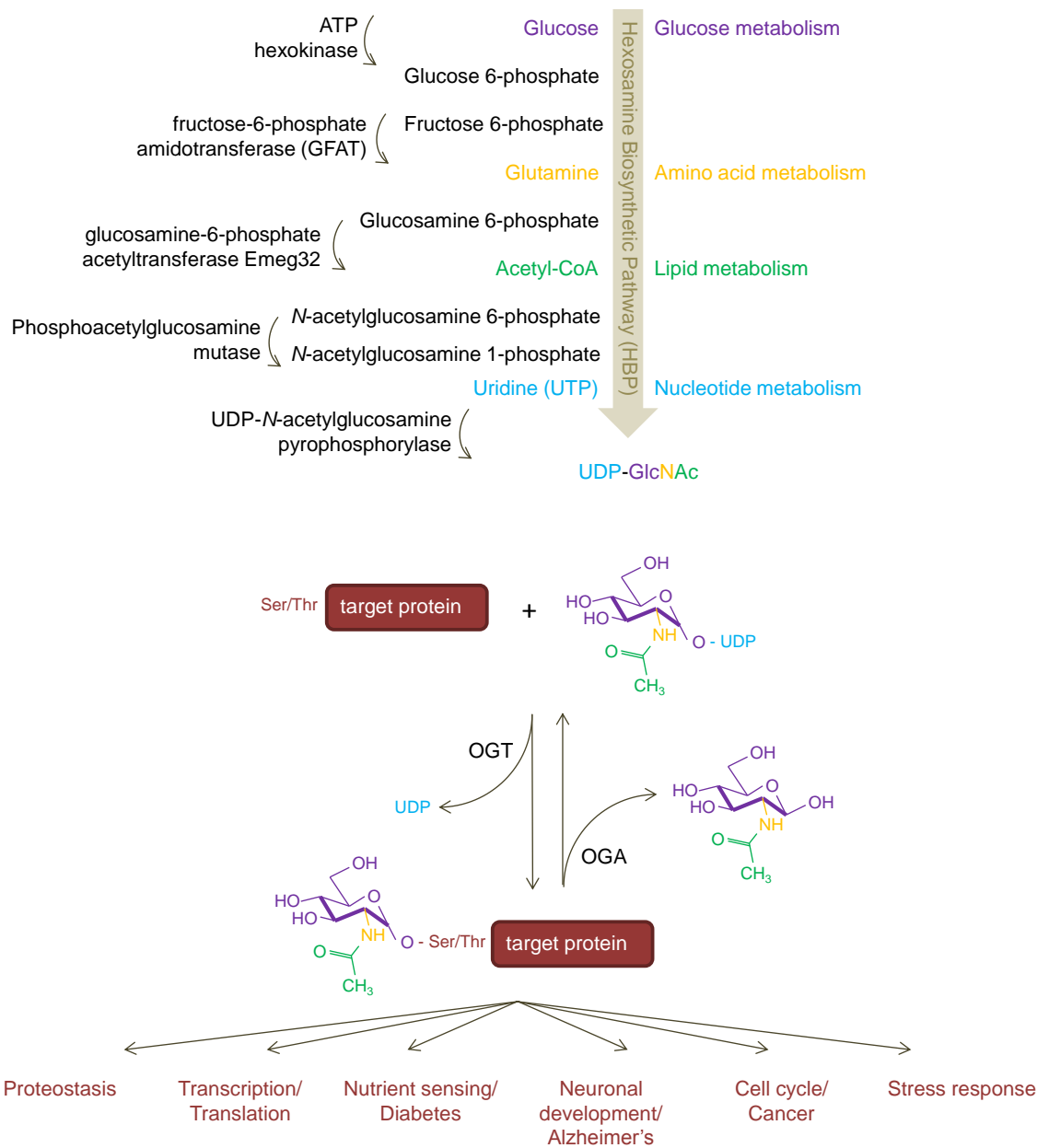
Figure 1-3 O-GlcNAc modification of proteins

The hexosamine biosynthetic pathway (HBP) provides the sugar substrate for O-GlcNAcylation as glucose is converted into UDP-N-acetylglucosamine (UDP-GlcNAc). The enzyme O-GlcNAc transferase (OGT) catalyses the addition, whereas the enzyme O-GlcNAcase (OGA) catalyses the removal of the amino sugar to/from nuclear and cytoplasmic proteins. Modified proteins are involved in multiple cellular processes, which upon misregulation can cause a variety of diseases.

1.2 <u>Transforming growth factor-β signalling</u>

The signalling pathways triggered by the transforming growth factor-β (TGFβ) family of cytokines, including bone morphogenetic proteins (BMPs), are implicated in diverse cellular functions, including differentiation, proliferation, extra-cellular matrix production, apoptosis and motility. Therefore, abnormal TGFβ signalling is associated with multiple human diseases including fibrosis, immune disorders and cancer (Akhurst and Hata, 2012, Inman, 2011, Massague, 2008, Shi and Massagué, 2003).

1.2.1 *The TGFβ ligands*

The TGFβ family of structurally related cytokines consists of at least 33 different ligands, which can be divided into two sub-families: the TGFβ subfamily comprising TGFβs, Activin and Nodal and the bone morphogenic protein (BMP) subfamily consisting of BMPs, growth and differentiation factor (GDF) and anti-Müllerian hormone (AMH). This classification is based on the difference displayed by the ligands in receptor recognition and downstream SMAD activation (Shi and Massague, 2003). Most TGFβ and BMP ligands are expressed ubiquitously, however some are expressed in a specific spatio-temporal manner. The ligands can function in an endocrine, paracrine and autocrine manner (Lin et al., 2006a, Massague, 2012, Massague, 2008).

TGFβ and BMP cytokines are expressed as large precursor polypeptides, which are subsequently cleaved by pro-protein convertases, to form active signalling molecules (Constam and Robertson, 1999, Dubois *et al.*, 1995). The endopeptidase cleavage generates the active C-terminal mature peptide (Annes *et al.,* 2003). The mature peptides subsequently form homo- or hetero-dimers within their cytokine subfamily through hydrophobic interactions and disulphide

bonds between conserved Cysteine residues (Sun and Davies, 1995). Mature TGFβ ligands are secreted and bind to latent TGFβ binding proteins (LTBPs), to form a complex in the extracellular matrix (ECM), where they remain until their release by protease- or integrin-regulated processes (Todorovic and Rifkin, 2012). The binding of mature TGFβ ligands to their cognate receptors on the cell surface initiates intracellular TGFβ signalling.

1.2.2 *TGFβ cell membrane receptors and signalling initiation*

The TGFβ cell membrane receptors can be divided into three different groups, termed type I, type II and type III receptors.

Type I and II receptors are Serine/Threonine protein kinases. Upon specific ligand dimers binding to a specific pair of type I and type II receptors, quaternary complexes are formed comprising two type I and two type II receptors. This enables the constitutively active type II receptors (ActR-IIA, ActR-IIB, BMPR-II, AMHR-II or TβR-II) to phosphorylate the type I receptors (Activin receptor like kinases (ALKs) 1-7) at the cytoplasmic GS domain, leading to their activation (*cf.* section 1.3.1.1) (Hinck, 2012, Shi and Massagué, 2003, Wrana *et al.*, 1994, Heldin *et al.*, 1997).

Activated ALKs phosphorylate the dual Serine residues at the conserved C-terminal SXS motif (also known as tail-phosphorylation) of the receptor-regulated SMAD transcription factors (R-SMADs), which transduce TGFβ signals intracellularly. The TGFβ subfamily of ligands signal through the activation of ALK4/5/7, which primarily phosphorylate SMADs 2 and 3, while the BMP ligands signal through ALK1/2/3/6, which primarily phosphorylate and activate SMAD1/5/8 (Figure 1-4) (Moustakas and Heldin, 2009, Persson *et al.*, 1998). However, TGFβ ligands can also signal through SMAD1/5/8 (Daly *et*

al., 2008) while BMPs signal through SMAD2/3 in embryonic and transformed cells (Holtzhausen *et al.*, 2014). Furthermore, TGFβ ligands can inhibit BMP-induced transcription through the formation of phosphorylated SMAD1/3/5 complexes, which bind to BMP-responsive elements on the DNA to induce TGFβ-induced transcriptional repression (Gronroos *et al.*, 2012).

Binding of SMADs to the type I receptor is enhanced upon the phosphorylation of ALKs at the GS domain. This phosphorylation also inhibits the immunophilin FKBP12 from binding to the receptors, thereby promoting R-SMAD binding (Huse *et al.*, 1999). The interaction of R-SMADs with the type I receptor can be enhanced by the scaffolds such as SMAD anchor for receptor activation (SARA) and Erbb2 interacting protein (ERBB2IP), which release R-SMADs upon phosphorylation (Sflomos *et al.*, 2011, Tsukazaki *et al.*, 1998).

TGFβ signalling can be fine-tuned by receptor-competitive cell membrane bound proteins or by ligand traps. One of the receptor-competitive proteins that binds and sequesters cytokines is BAMBI (BMP and Activin receptor membrane bound inhibitor). BAMBI exhibits homology to the type I receptor extracellular domain and thereby acts as a pseudo-receptor for BMP and Activin. Ligand traps in the ECM, such as Follistatin, Chordin and Noggin, prevent the interaction of cytokines with their respective receptors by binding to and masking the residues within ligands that are critical for receptor binding (De Robertis and Kuroda, 2004, Onichtchouk *et al.*, 1999).

The Type III receptors (TβR-III) do not possess protein kinase activity but enhance binding of ligands to type I and type II through their large extracellular domains, thereby exerting a function as co-receptors (Shi and Massagué, 2003). TβR-III is critical for epithelial cell polarity (Meyer *et al.*, 2014).
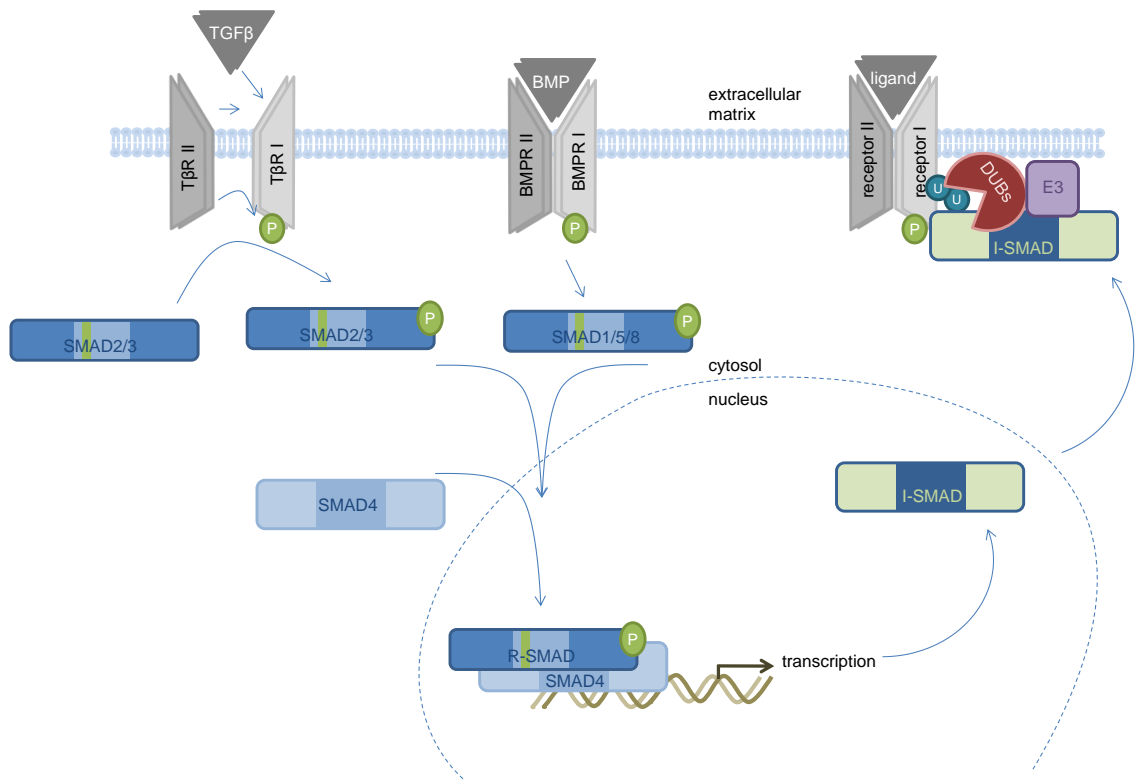
Figure 1-4 Overview of the core-components of TGFβ/BMP signalling

Ligand binding to Serine/Threonine receptor kinases induces TGFβ/BMP signalling and leads to quaternary complex formation of type I and type II receptors. In close proximity, the type II receptor is able to phosphorylate the type I receptor, which activates the kinase complex. The activated receptors can then phosphorylate R-SMADs at their conserved C-termini, which induces complex formation with SMAD4. The R-SMAD-SMAD4 complex travels to the nucleus where TGFβ/BMP-mediated target gene transcription is initiated. Inhibitory SMADs (SMAD6/7) are transcribed and act in a feedback loop, as SMAD6/7 compete with R-SMADs for receptor binding and direct E3 ubiquitin ligases and/or DUBs to the receptors.

1.2.3 SMAD proteins

The SMAD proteins are a group of transcription factors that act as the intracellular mediators of TGFβ and BMP signalling. SMADs are conserved in metazoans and are the vertebrate homologues of SMA (*Caenorhabditis elegans*) and MAD (*Drosophila melanogaster*) (Raftery *et al.,* 1995, Savage *et al.,* 1996, Sekelsky *et al.,* 1995). In humans, there are eight SMAD proteins that are classified into three distinct groups according to their structural and functional properties: the receptor regulated (R-)SMADs (SMAD1, SMAD2,

SMAD3, SMAD5 and SMAD8), the co-mediator SMAD (SMAD4/DPC4) and the inhibitory (I-)SMADs (SMAD6 and SMAD7) (Hinck, 2012, Lönn *et al.*, 2009, Moustakas and Heldin, 2009, Shi and Massagué, 2003).

SMAD proteins harbour three distinct globular domains: the conserved N-terminal MAD homology 1 (MH1) and C-terminal MAD homology 2 (MH2) domains linked by a divergent linker region. The MH1 domain of SMAD1/3/4/5/8 mediates DNA binding at promoter regions of TGFβ/BMP-target genes (Makkar et al, 2009). The MH1 domains of SMAD2/6/7 are not as well conserved, resulting in reduced DNA binding. The MH1 domain of SMAD2 contains a non-homologous insertion and SMAD7 has a truncated MH1 domain (Shi and Massagué, 2003, Dennler *et al.*, 1999).

The MH2 domain is present in all SMADs. However, the SXS phosphorylation motif at the C-terminus (tail-phosphorylation) only exists within R-SMADs. Activated ALKs phosphorylate the two Serine residues on the SXS motif to activate R-SMADs. Tail-phosphorylated R-SMADs interact with their common co-factor SMAD4 and form heterotrimeric complexes comprising SMAD4 and two R-SMADs (Figure 1-4). All pathway-specific R-SMADs employ SMAD4 as a common binding partner and the heterotrimeric complex formation is essential for SMAD function within the canonical TGFβ/BMP pathway. These ligand induced complexes then accumulate in the nucleus, where together with other transcriptional co-factors they regulate the expression of ~500 canonical TGFβ/BMP-target genes. In the absence of SMAD4, TGFβ/BMP ligands are no longer able to induce the transcription of canonical target genes (Hill, 2009, Levy and Hill, 2005, Lönn *et al.*, 2009, Moustakas and Heldin, 2009, Ross and Hill, 2008, Shi and Massagué, 2003, ten Dijke and Hill, 2004, Wang *et al.*, 2013a, Souchelnytskyi *et al.*, 1997). Additionally, the MH2 domain serves as a

protein-protein interaction platform that facilitates the interaction with cell membrane receptors, other transcription factors and regulatory proteins (Massague, 2012, Shi and Massagué, 2003).

The MH1 and MH2 domains are connected via the divergent linker region. The linker region contains several Serine/Threonine residues in close proximity to the Proline rich "PPXY" motif. In R-SMADs, this region is phosphorylated in response to TGFβ/BMP signals and serves to integrate crosstalk from other signalling pathways (*cf.* section 1.3.1.3) (Sapkota *et al.*, 2007).

Inhibitory SMADs, which are transcriptional targets of TGFβ/BMP ligands, provide a negative feedback by competing with R-SMADs for access to the receptors as well as directing E3 ubiquitin ligases and deubiquitylating enzymes to the activated receptors (Figure 1-4) (Al-Salihi *et al.*, 2012a, Zi *et al.*, 2012, Yan *et al.*, 2009, Ebisawa *et al.*, 2001, Shi *et al.*, 2004).

1.2.4 *Transcriptional control by TGFβ ligands*

TGFβ signalling can activate the transcription of certain genes while repressing others. Moreover, TGFβ signalling can control target gene transcription differentially depending on the cell type and context. These distinctive gene expression patterns are achieved through SMAD proteins interacting with unique transcriptional co-factors (Figure 1-4). DNA binding proteins that can act as SMAD co-factors include TRIM33, FOX, MIX, HOX, RUNX, E2F, AP1, C/EBPβ, CREB/ATF, Zinc-finger and other families (Massague, 2012, Massagué and Gomis, 2006, Ross and Hill, 2008, Gaarenstroom and Hill, 2014). SMAD interaction with transcriptional co-factors

serves to consolidate the otherwise weak interaction between SMADs and DNA (Chai *et al.*, 2003).

The MH1 domains of TGFβ activated SMAD2/3/4 recognise SMAD binding elements (SBE) with the 3'-CAGA-5' palindrome sequence, whereas BMP activated SMAD1/4/5/8 preferentially bind GC-rich promoter regions known as the BMP responsive element (BRE) (Zawel *et al.*, 1998, Katagiri *et al.*, 2002). The X-ray crystal structure analysis of SMAD3 MH1 domain bound to DNA revealed the SBE is recognised by a conserved 11-residue β hairpin of SMAD3, which is inserted into the major groove of DNA (Shi *et al.*, 1998). Conserved Histidine and Cysteine residues of the MH1 domain further strengthen the SMAD3-DNA binding by coordinating water molecules and a zinc atom (Chai *et al.,* 2003).

Once bound to the promoter regions, SMADs need to modulate chromatin structure in order to regulate transcription. SMADs are able to recruit components of a chromatin-remodelling complex and also interact with co-activators and co-repressors with chromatin-modifying activities (Ross *et al.*, 2006). R-SMAD-SMAD4 complexes can bind histone acetyltransferases (HATs) such as p300 and CREB. Upon histone acetylation, DNA becomes available to transcription factors as the DNA is released from histones. TGFβ signalling can induce histone acetylation through p300 and CREB-binding protein (CBP) resulting in enhanced TGFβ target gene transcription. In order to repress transcription of certain genes, SMADs can also form complexes with histone deacetylases (HDACs) or transcriptional repressors that display HDAC activity (*cf.* section 1.3.3) (Ross and Hill, 2008).

Nodal signalling can induce SMAD2/3-SMAD4 as well as SMAD2/3-TRIM33 complexes. The SMAD2/3-TRIM33 complex recognises quiescent

chromatin and binds it via the PHD-Bromo domain of TRIM33. This leads to chromatin remodelling and the SMAD2/3-SMAD4 complexes are then able to induce transcription (Massagué and Xi, 2012, Xi *et al.*, 2011, He *et al.*, 2006, Morsut *et al.*, 2010).

1.2.5 Non-canonical TGFβ signalling

The canonical TGFβ/BMP signalling pathway constitutes ligand binding to the type I and II receptor complex, which upon activation, phosphorylates R-SMADs at their conserved C-termini (*cf.* section 1.2.2). Ligand binding to the receptors can also induce non-canonical TGFβ signalling, which regulates the activity of other proteins and signalling pathways in a SMAD-independent manner. Non-canonical BMP and TGFβ signalling pathways are linked to the modulation of mitogen-activated protein kinases (MAPKs: ERK, JNK and p38 MAPK), PI3 kinase/AKT signalling pathways as well as Rho-GTPases. Thus, non-canonical signalling contributes to TGFβ-mediated physiological responses such as epithelial to mesenchymal transition (EMT), apoptosis and cytoskeleton rearrangements (Moustakas and Heldin, 2005, Zhang, 2009, Zhang *et al.*, 2013b).

BMP and TGFβ ligands can activate ERK1/2 though the ShcA/GRB2/SOS/RAS signalling cascade by binding to the cognate type I and II receptors. The activation of RAS causes the sequential phosphorylation of MEK and ERK1/2 (Lawler *et al.*, 1997, Lee *et al.*, 2007), which mediates TGFβ-induced EMT (Galliher-Beckley and Schiemann, 2008) by disassembling adherens junctions and regulating EMT-associated gene transcription (Zavadil *et al.*, 2001). Activated ERK1/2 can also phosphorylate SMAD1/2/3 in their linker region, resulting in recognition by E3 ubiquitin ligases (*cf.* sections 1.3.1.3

and 1.3.2.3). JNK and p38 MAPK are activated by TGFβ ligands through the binding of TRAF6 to the activated TGFβ cell membrane receptor complex, resulting in the activation of TAK1, MKK4, JNK and p38 MAPK (Sorrentino *et al.*, 2008, Yamashita *et al.*, 2008). However, studies performed in TAK1 knockout cells revealed that TAK1 is dispensable for the activation of p38 MAPK (Sapkota, 2013). Nevertheless, it is clear that TGFβ induced activity of JNK and p38 MAPK regulates TGFβ-mediated transcription (Sapkota, 2013), apoptosis (Edlund *et al.*, 2003) and rearrangement of the actin cytoskeleton leading to EMT (Bakin *et al.*, 2002, Yamashita *et al.*, 2008).

TGFβ ligand binding can also result in the association of the TβR-I with PI3K via its regulatory subunit p85 and induce AKT and mTORC1 activation (Bakin *et al.*, 2000, Yi *et al.*, 2005), regulating translation initiation, which results in changes in protein synthesis, increased cell size, invasion and EMT (Lamouille and Derynck, 2007, Lamouille *et al.*, 2012). BMP ligands are similarly able to induce AKT phosphorylation and PI3K-induced activation of NFκB results in the induction of migration or inhibition of Caspases with subsequent prevention of apoptosis (Sugimori *et al.*, 2005, Fong *et al.*, 2008). Moreover, AKT can influence TGFβ-target gene transcription by phosphorylating the transcription factor FoxO. This results in nuclear exclusion and hence prevention of interaction with activated R-SMADs (Seoane *et al.*, 2004). Non-canonical AKT activation can also negatively influence canonical TGFβ signalling by binding SMAD3 and restricting the type I receptor mediated SMAD3 tail-phosphorylation (Remy *et al.*, 2004, Conery *et al.*, 2004).

The TGFβ ligand-activated type I and II receptor complex binds the cell polarity protein PAR6 in tight junctions, which causes its phosphorylation by type II receptor kinase at S345. Phosphorylated PAR6 recruits SMURF1 to

induce RhoA ubiquitin-dependent proteasomal degradation, which is mediated via the C2 domain of SMURF1. Hence, in response to TGFβ ligands, RhoA dissociates from tight junctions resulting in their dissolution, which is a key step in the induction of TGFβ-induced EMT and cellular migration (Ozdamar *et al.*, 2005, Tian *et al.*, 2011, Cheng *et al.*, 2011, Wang *et al.*, 2003). BMP and the TGFβ type III receptor can also induce EMT via the PAR6/SMURF1/RhoA signalling cascade (Sanchez and Barnett, 2012, Townsend *et al.*, 2011). Furthermore, TGFβ ligands can induce RhoA-mediated cell migration via the NFκB pathway (Kim *et al.*, 2014).

RNA translation and protein synthesis is in part regulated by eEF1A1, which is phosphorylated by the type I receptor (ALK5) at S300 subsequent to TGFβ ligand binding. This phosphorylation abolishes the interaction of eEF1A1 with amino acyl-bound tRNAs resulting in reduced protein translation and cell proliferation. Hence, by altering protein production via phosphorylation of eEF1A1, TGFβ acts as a tumour suppressor exhibiting cytostatic effects (Lin *et al.*, 2010).

1.3   The regulation of TGFβ signalling by PTMs

Complex mechanisms, which are often context-dependent, have evolved to check and modulate the potency of TGFβ signalling in controlling cell behaviour (Itoh and ten Dijke, 2007). While the regulation of the TGFβ pathway occurs at multiple layers of the signalling cascade, R-SMADs, as critical mediators of TGFβ signals, are suitably primed for key regulatory inputs. Indeed, reversible phosphorylation and ubiquitylation of SMAD proteins and type I receptors are critical processes that regulate the strength and duration of TGFβ signalling (Al-Salihi et al., 2012b, Bruce and Sapkota, 2012, Lönn et al.,

2009, Massague, 2012, Xu et al., 2012, Imamura et al., 2013, Herhaus and Sapkota, 2014).

1.3.1 *Regulation of TGFβ signalling by reversible phosphorylation*

1.3.1.1 Reversible phosphorylation of TGFβ/BMP receptors

As introduced in section 1.2.2, the type II TGFβ receptor (TβR-II) is a constitutively active kinase that phosphorylates the type I receptor upon ligand binding and quaternary receptor complex formation. TβR-II phosphorylates TβR-I at several Serine residues within the GS domain in the cytoplasmic part of the receptor, immediately upstream of the kinase domain (Wrana *et al.*, 1994, Wieser *et al.*, 1995, Willis *et al.*, 1996). This phosphorylation enhances the specificity of TβR-I to C-terminal SXS motif of R-SMADs and inhibits binding to the inhibitory protein FKBP12 (Huse *et al.*, 2001).

The phosphorylation of TβR-I can be reversed by the protein phosphatase 1 (PP1). Interaction between PP1 and TβR-I can be enhanced by SARA, SMAD7 and GADD34 (Shi *et al.*, 2004, Valdimarsdottir *et al.*, 2006). Dullard is a phosphatase that acts on BMP type I receptors and its phosphatase activity is essential to promote BMPR-II degradation (Satow *et al.*, 2006).

1.3.1.2 Reversible SMAD tail-phosphorylation

The C-terminal SXS motif of R-SMADs is phosphorylated by type I BMP and TGFβ receptors as described in section 1.2.2. Although the phosphorylation motif of BMP and TGFβ activated SMADs is very similar, distinct protein phosphatases have been reported.

SCPs1-3 are reported to dephosphorylate the SMAD1 C-terminal region (Knockaert *et al.*, 2006). SCPs are nuclear phosphatases and their binding to

SMAD1 is greatly enhanced in the presence of the Proline-rich protein BAT3 (Goto *et al.*, 2011). Another SMAD1 tail phosphatase reported is the mitochondrial enzyme Pyruvate dehydrogenase (PDP) (Chen *et al.*, 2006).

The protein phosphatase Mg^{2+}/Mn^{2+} dependent 1A (PPM1A/PP2Cα) was reported to dephosphorylate both TGFβ- and BMP-induced R-SMAD tail-phosphorylation and is reported to inhibit BMP signalling by promoting the proteasomal degradation of SMAD1 (Kokabu *et al.*, 2010, Duan *et al.*, 2006, Lin *et al.*, 2006b). Two mouse models with *PPM1A* gene perturbation exist, however in these the role of PPM1A, as a SMAD2/3 C-terminal phosphatase, has not been confirmed (Dai *et al.*, 2011, Yang *et al.*, 2011). It has been reported that an interaction between protein phosphatase 2 (PP2A) and SMAD3 is induced by hypoxia and under these conditions PP2A can dephosphorylate SMAD3, but not SMAD2 (Heikkinen *et al.,* 2010). The nuclear accumulation of TGFβ-induced phospho-SMAD3 and its retention in endosomes can be caused by myotubularin related protein 4 (MTMR4). This phosphatase has been shown to promote tail-dephosphorylation of SMAD2 and 3 through binding. MTMR4 is thus another phosphatase that inhibits TGFβ signalling (Yu *et al.*, 2010).

Despite numerous reports on R-SMAD phosphatases, their precise nature of regulation remains undefined (Bruce and Sapkota, 2012, Wrighton *et al.*, 2009).

1.3.1.3 Reversible SMAD linker-phosphorylation

The divergent linker region of R-SMADs is a central platform for regulatory phosphorylation and dephosphorylation events, which alter their localisation, transcriptional ability and stability. This region can be phosphorylated in direct response to TGFβ or BMP signalling, as well as by

several other signalling pathways like the MAPKs and GSK3. Hence the linker region of R-SMADs provides a platform for crosstalk between different signalling pathways (Xu *et al.*, 2012).

MAPKs (ERK2), CDK8/9 and GSK3 sequentially phosphorylate several Proline-directed Serine/Threonine residues ("PPXY" motif) in R-SMADs. Phosphorylation of the linker region of R-SMADs by MAP kinases and GSK3 marks SMADs 1 and 3 for recognition by WW-domain containing E3 ubiquitin ligases SMURF1 and NEDD4L respectively, which mediate their polyubiquitylation and degradation (section 1.3.2.3) (Alarcón *et al.*, 2009, Sapkota *et al.*, 2007, Aragon *et al.*, 2011). CDK8/ 9 also phosphorylate SMAD1 and 3 linker region, subsequent to ligand induced tail-phosphorylation. Likewise, this primes their association with E3 ubiquitin ligases, but additionally enhances interaction of SMAD1 with YAP and of SMAD2/3 with PIN1 (Alarcón *et al.*, 2009, Gao *et al.*, 2009, Aragon *et al.*, 2011). The SMAD linker-phosphorylation-mediated SMAD degradation is however context dependent, as in contrast to epithelial cells, in mesenchymal cell types ERK-mediated linker-phosphorylation of nuclear SMAD2/3, causes increased half-life of tail-phosphorylated SMAD2/3 (Hough *et al.*, 2012). The phosphorylation of SMAD3 MH1 and linker region by CDK2/4 and SMAD2 MH1 by CDK2 inhibits TGFβ-induced transcriptional activity (Matsuura *et al.*, 2004, Baughn *et al.*, 2009). Similarly, phosphorylation of SMAD2/3 linker region by GRK2 prevents SMADs from tail-phosphorylation and nuclear shuttling, consequently inhibiting TGFβ signalling (Ho *et al.*, 2005).

The only phosphatases known to reverse R-SMAD linker phosphorylation are SCPs 1, 2 and 3. SCPs1-3 dephosphorylate SMAD2 at S245, S250 and S255 and analogous the SMAD1 and 3 linker region sites (Sapkota *et al.*, 2006, Wrighton *et al.*, 2006, Knockaert *et al.*, 2006).

1.3.2 Regulation of TGFβ signalling by reversible ubiquitylation

Reversible ubiquitylation of the type I TGFβ/BMP receptor kinases and SMADs are known to play a critical role in regulating the TGFβ pathway. The mechanisms of ubiquitin-mediated turnover of SMADs and TGFβ/BMP cell membrane receptors by distinct E3 ubiquitin ligases are generally well established (Al-Salihi *et al.*, 2012b, De Boeck and ten Dijke, 2012, Dupont *et al.*, 2012, Inoue and Imamura, 2008, Tang and Zhang, 2011, Zhang *et al.*, 2014a). However, investigations into the regulation of the TGFβ/BMP pathways by DUBs are only emerging (Herhaus and Sapkota, 2014).

1.3.2.1 Regulation of the TGFβ/BMP receptors by E3 ubiquitin ligases

Targeting the receptors for reversible ubiquitylation is very effective in modulating the TGFβ/BMP pathway, as this could inhibit (by ubiquitylation) or enhance (by deubiquitylation) signalling. SMAD6 and SMAD7 are known to direct E3 ubiquitin ligases to the receptors. The WW domains of the C2-WW HECT E3 ubiquitin ligases bind to SMAD6/7 through the Proline-rich "PPXY" motif (Rotin and Kumar, 2009). Subsequently, I-SMADs can direct HECT E3 ligases SMURF1/2, WWP1 (Tiul1) and NEDD4L to ALK5, ALK6 and TβR-II to catalyse their polyubiquitylation and subsequent degradation (Ebisawa *et al.*, 2001, Kavsak *et al.*, 2000, Murakami *et al.*, 2003, Fukasawa *et al.*, 2010, Komuro *et al.*, 2004, Kuratomi *et al.*, 2005, Seo *et al.*, 2004, Goto *et al.*, 2007). SMAD6/7-mediated SMURF-dependent receptor degradation is a negative feedback mechanism, as both SMAD6/7 and SMURFs are transcriptional targets of TGFβ signalling (Afrakhte *et al.*, 1998). Binding of the SMAD7-SMURF2 complex to the receptors can be stabilised by the TGFβ co-receptor CD109 and be destabilised by TSC22 (Bizet *et al.*, 2011, Bizet *et al.*, 2012, Yan

et al., 2011). The HECT E3 ligase ITCH (AIP4) can also inhibit TGFβ signalling by promoting the interaction of SMAD7 with the type I receptors, however this is independent of its ubiquitin ligase activity (Lallemand *et al.*, 2005).

The RING E3 ubiquitin ligase TRAF6 has been reported to polyubiquitylate the type I receptors independently of SMAD7. TRAF6 generates K63-linked chains on ALK5, leading to the recruitment of TACE, which catalyses its cleavage. The cleaved intracellular domain of ALK5 then translocates to the nucleus, where together with the transcriptional regulator p300 it induces the transcription of genes that promote cellular invasiveness such as *Snail* and *MMP2* (Mu *et al.,* 2011). TRAF4 also binds to the type I TGFβ receptor upon ligand stimulation; however, it does not polyubiquitylate the receptor complex. In fact, TRAF4 stabilises the receptor by antagonising SMURF2 and facilitating the recruitment of the DUB USP15. Receptor binding also triggers K63-polyubiquitylation of TRAF4 resulting in activation of TAK1 (Zhang *et al.*, 2013a).

The E2 enzymes involved in the ubiquitylation of TGFβ/BMP receptors have not yet been identified.

1.3.2.2 Regulation of the TGFβ/BMP receptors by DUBs

Several deubiquitylating enzymes that reverse type I receptor ubiquitylation have been identified. Among the USP family of DUBs, USP4, USP11 and USP15 are highly similar, display conserved structural domains and protein sequences (*cf.* section 5.1.1). All three of them were independently discovered as DUBs for the type I TGFβ receptors through contrasting approaches. A gain-of-function screen looking for activators of TGFβ signalling identified USP4 (Zhang *et al.*, 2012b), a proteomic approach looking at

interactors of SMAD7 identified USP11 (Al-Salihi *et al.*, 2012a), and a siRNA loss-of-function screening looking for DUBs affecting the TGFβ-induced luciferase reporter activity identified USP15 (Eichhorn *et al.*, 2012).

USP4 has been reported to enhance TGFβ signalling by directly interacting with and deubiquitylating type I TGFβ receptor (ALK5) (Zhang *et al.*, 2012b). In this study, it was reported that upon phosphorylation by AKT, USP4 translocates to the membrane, where it associates with ALK5, deubiquitylates it and protects it from degradation (Figure 1-5). The AKT-mediated phosphorylation of USP4 on S445 also affects its stability and DUB activity. Additionally, USP4 depletion inhibits TGFβ-induced EMT and AKT-induced breast cancer cell migration (Zhang *et al.*, 2012b).

USP11 was identified as an interactor of SMAD7 and ALK5 (Al-Salihi *et al.*, 2012a). When bound to ALK5, USP11 deubiquitylates and protects ALK5 from proteasomal degradation resulting in enhanced TGFβ signalling (Figure 1-5). Consequently, TGFβ-induced levels of phosphorylated SMAD2/3 and transcription were augmented. USP11 could override the negative effects of SMAD7 on the TGFβ pathway, demonstrating that a dynamic balance between ubiquitylation and deubiquitylation could determine the fate of ALK5. It was shown that depletion of USP11 resulted in inhibition of TGFβ-induced transcription as well as EMT (Al-Salihi *et al.*, 2012a).

USP15 was reported to enhance TGFβ signalling by binding to the SMAD7-SMURF2 complex and deubiquitylating ALK5 in the process (Figure 1-5) (Eichhorn *et al.*, 2012). Moreover, USP15 amplification was observed in glioblastoma, breast and ovarian cancers, which highly correlated with enhanced TGFβ signalling activity and poor prognostic outcomes in individuals with glioblastoma (Eichhorn *et al.*, 2012). Depletion of USP15 reduced the

oncogenic capacity of patient-derived glioma-initiating cells through the inhibition of TGF-β signalling, suggesting a direct role for USP15 and TGFβ signalling in glioblastoma pathogenesis (Eichhorn *et al.*, 2012). However, USP15 knockout T cells and A375 and HCT116 knockdown USP15 cells did not exhibit altered TGFβ signalling as assayed by SMAD phosphorylation levels and TGFβ-mediated gene transcription (Zou *et al.*, 2014). Hence, the function of USP15 in regulating TGFβ signalling might be cell type specific.

The UCH family of DUBs, including UCH37, are generally described as ubiquitin chain trimmers (Lee *et al.*, 2011). However, UCH37 is reported to deubiquitylate the type I receptor (ALK5) and sustain early TGFβ pathway activation (Figure 1-5) (Wicks *et al.*, 2005, Cutts *et al.*, 2011). It is directed to ALK5 via its interaction with SMAD7 (Wicks *et al.*, 2005). UCH37 influences TGFβ-mediated transcription and affects cell migration (Cutts *et al.*, 2011).

No DUBs had been known to target the type I BMP receptors, hence a proteomic study to identify novel BMP signalling regulators was performed, which identified USP15 as a deubiquitylase for ALK3 (BMPR1A). The findings of this study will be discussed in this thesis (*cf.* section 5) (Figure 1-5) (Herhaus *et al.*, 2014). Similarly, nothing is known about reversible ubiquitylation of TGFβ/BMP type II receptors. Furthermore, the precise ubiquitylation sites within the receptors and to some extent the nature of ubiquitin chain-linkages that are targeted by the different DUBs remain to be defined.
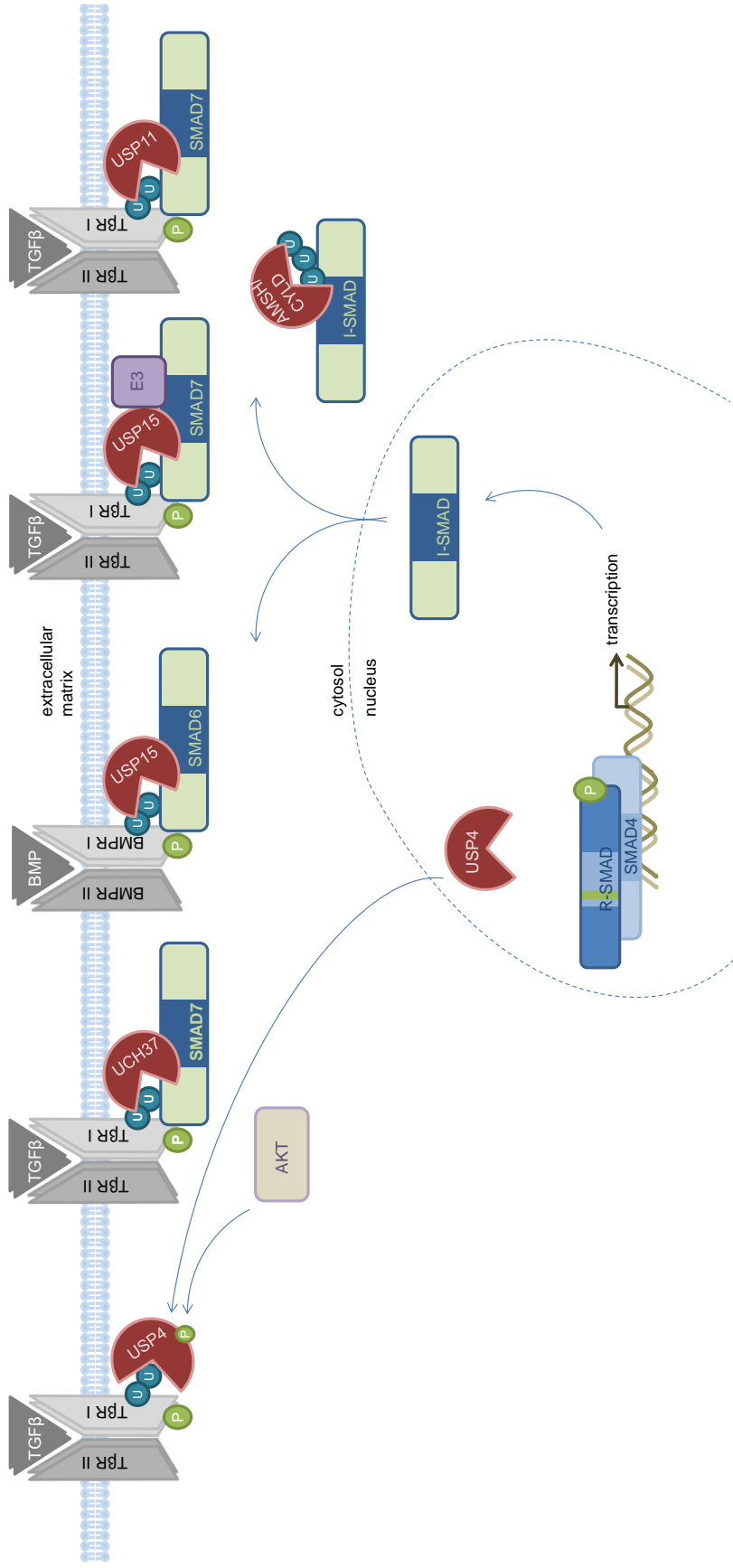
Figure 1-5 TGFβ/BMP receptor deubiquitylation

Various DUBs (USP4, UCH37, USP15, and USP11) have been identified to reverse TGFβ/BMP receptor ubiquitylation, through distinct molecular mechanisms (*cf.* text). CYLD and AMSH/AMSH-LP are DUBs that reverse ubiquitylation of I-SMADs, which in turn direct E3 ubiquitin ligases and DUBs to the receptors. Most DUBs bind the receptors through SMAD6/7. Only USP4 binds type I TGFβ receptor directly due to phosphorylation by AKT.

1.3.2.3 Regulation of R-SMADs by reversible ubiquitylation

R-SMADs, which act as transcription factors, are the key cellular mediators of the TGFβ/BMP pathways. Hence, their activity has to be tightly regulated, as it determines the strength and potency of TGFβ/BMP signalling. The regulation of R-SMADs by E3 ubiquitin ligases is well established (Al-Salihi *et al.*, 2012b, De Boeck and ten Dijke, 2012, Dupont *et al.*, 2012, Inoue and Imamura, 2008, Tang and Zhang, 2011, Zhang *et al.*, 2014a). However, no E2 enzymes have been identified to play critical roles in R-SMAD ubiquitylation and only two deubiquitylating enzymes that act on R-SMADs have been described so far (Inui *et al.*, 2011, Herhaus *et al.*, 2013).

As mentioned in section 1.3.1.3, phosphorylation of the linker region of R-SMADs primes them for recognition by WW-domain containing HECT E3 ligases, which bind the "PPXY" motif within the R-SMAD linker region, with the exception of SMAD8 that lacks the "PPXY" motif (Aragon *et al.*, 2011). The WW domain containing E3 ubiquitin ligases SMURF1 and SMURF2 have been shown to catalyse the ubiquitylation and degradation of BMP responsive SMAD1 and 5 (Sapkota *et al.*, 2007, Zhang *et al.*, 2001, Zhu *et al.*, 1999). Similarly, SMURF2, NEDD4L, WWP1 and the N-terminal isoform of WWP2 have been reported to ubiquitylate TGFβ-induced SMAD2 and 3, resulting in their proteasomal degradation (Gao *et al.*, 2009, Kuratomi *et al.*, 2005, Seo *et al.*, 2004, Lin *et al.*, 2000, Soond and Chantry, 2011).

Several non-HECT E3 ligases are also reported to target R-SMADs for ubiquitylation. The U-Box domain containing E3 ligase CHIP induces SMAD1, 2 and 3 degradation and hence inhibition of BMP and TGFβ signalling (Li *et al.*, 2004, Xin *et al.*, 2005). The RING E3 ligase ARKADIA has been reported to enhance TGFβ signalling by binding to phosphorylated SMAD2/3, thereby

ubiquitylating SMAD signal-inhibiting binding partners, such as SMAD7, SnoN and c-SKI (Koinuma *et al.*, 2003, Levy *et al.*, 2007, Nagano *et al.*, 2007, Yuzawa *et al.*, 2009). After TGFβ stimulation the RING E3 ligase ROC1-SCF-βTRCP1 has been shown to ubiquitylate SMAD3 that is bound to the transcription trans-activator p300, causing SMAD3 proteasomal degradation (Fukuchi *et al.*, 2001).

Indirect ubiquitylation machinery regulated through signalling crosstalk also affects the ubiquitylation of R-SMADs. Axin facilitates GSK3β-mediated phosphorylation of SMAD3 at T66, which promotes the degradation of non-active SMAD3 in an ubiquitin-proteasome dependent manner, however the E3 ubiquitin ligase responsible has not been identified (Guo *et al.*, 2008). CYLD indirectly inhibits TGFβ signalling by decreasing the stability of SMAD3 via the AKT-GSK3β-CHIP pathway (Lim *et al.*, 2012). CYLD deubiquitylates K63-polyubiquitylated AKT, resulting in the inhibition of AKT. This leads to the activation of GSK3β and promotes CHIP-mediated SMAD3 degradation (Lim *et al.*, 2012). Estrogen receptor α is also reported to recruit SMURFs to SMAD2/3, thereby catalysing their proteasomal degradation (Ito *et al.*, 2010).

In contrast to polyubiquitylation, monoubiquitylation in the TGFβ pathway does not result in proteasomal degradation (Dupont *et al.*, 2012). By catalysing the monoubiquitylation of SMAD2, the HECT E3 ligase ITCH enhances the interaction between SMAD2 and ALK5, which further potentiates SMAD2-tail phosphorylation (Bai *et al.*, 2004). The RING-type zinc finger E3 ligase Cbl-b might have an analogous function in T cells, as its loss reduces TGFβ-induced SMAD2 tail-phosphorylation (Wohlfert *et al.*, 2006, Adams *et al.*, 2010). SMURF2 has also been reported to result in multiple monoubiquitylation of SMAD3 MH2 domain, hindering SMAD3 from forming a complex with SMAD4

(Tang *et al.*, 2011). SMURF2 is recruited to linker-phosphorylated SMADs by another WW-domain-containing protein: PIN1 (Nakano *et al.*, 2009).

To date, the only DUB identified to deubiquitylate monoubiquitylated R-SMADs is USP15 (Figure 1-6). Monoubiquitylation of R-SMADs reportedly occurs at the DNA-binding domain of R-SMADs, thereby preventing their association with DNA at the promoters. USP15 reverses SMAD2/3-monoubiquitylation at the MH1 domain, thereby enhancing their ability to recognise the promoters (Inui *et al.*, 2011). No deubiquitylating enzymes that target activated R-SMADs to prevent their proteasomal degradation had been identified. Therefore, a proteomic screen to discover novel R-SMAD DUBs was performed and OTUB1 was as identified an interactor of TGFβ-activated SMAD3. The role of OTUB1 in the TGFβ pathway will be discussed in this thesis (*cf.* section 3) (Figure 1-6) (Herhaus *et al.*, 2013).

1.3.2.4 Regulation of I-SMADs by reversible ubiquitylation

Although I-SMADs direct E3 ubiquitin ligases and DUBs to the receptors, they can be targets of reversible ubiquitylation themselves. SMURF1/2 and WWP2 that bind to I-SMADs through their "PPXY" motif can also polyubiquitylate SMAD6/7, causing their proteasomal degradation (Soond and Chantry, 2011, Murakami *et al.*, 2003). The MH1 domain of SMAD7 also assists in E2 (UBE2L3) binding to the HECT domain of SMURF2 and thus enhances the catalytic activity of the E3 ubiquitin ligase (Ogunjimi *et al.*, 2005).

The ubiquitylation of SMAD7 on K64 and K70 by SMURF1 can be prevented by acetylation of the same sites by the histone acetyl transferase p300, which can be reversed by the deacetylase SIRT1 (Gronroos *et al.*, 2002, Kume *et al.*, 2007). The RING E3 ligases RNF12 and ARKADIA also

polyubiquitylate SMAD7, thereby increasing BMP and TGFβ signalling (Zhang *et al.*, 2012a, Koinuma *et al.*, 2003, Liu *et al.*, 2006). The E2 ubiquitin-conjugating enzyme UBE2O, which acts as an E2-E3 hybrid, interacts with and monoubiquitylates SMAD6 at K174. Monoubiquitylation of SMAD6 enhances BMP$_7$ signalling as it decreases the binding of unmodified SMAD6 to the activated type I BMP receptor (ALK2) (Zhang *et al.*, 2013c).

Several DUBs are known to deubiquitylate I-SMADs. CYLD, which only hydrolyses K63-linked polyubiquitin chains (Komander *et al.*, 2008), was shown to deubiquitylate SMAD7, thereby inhibiting TGFβ signalling in the development of Tregs (Figure 1-5) (Zhao *et al.*, 2011). CYLD targets K63-linked ubiquitin chains on SMAD7 at K360 and K374, which are shown to be required for activation of TAK1 and p38 MAP kinases in response to TGFβ (Zhao *et al.*, 2011). AMSH, a JAMM/MPN+ DUB, has been shown to bind and sequester SMAD6 upon BMP receptor activation and activate BMP signalling, however whether its catalytic activity influences BMP signalling is not known (Itoh *et al.*, 2001). Similarly, AMSH-LP is reported to sequester SMAD7, thereby exerting a positive effect on the TGFβ pathway (Figure 1-5) (Ibarrola *et al.*, 2004). Whether the catalytic activity of AMSH-LP is required is also not known. AMSH and AMSH-LP have been reported to only deubiquitylate K63-ubiquitin chains (Sato *et al.*, 2008).

1.3.2.5 Regulation of SMAD4 by reversible ubiquitylation

SMURF1/2, WWP1 and NEDD4L have been shown target SMAD4 for ubiquitin-mediated proteasomal degradation after it has formed ternary complexes with active R-SMADs or I-SMADs acting as adaptors, as SMAD4 lacks the "PPXY" motif (Morén *et al.,* 2005). Additionally, ROC1-SCF-SKP2-

βTRCP1 induces the ubiquitin-mediated degradation of SMAD4 (Liang *et al.*, 2004, Wan *et al.*, 2004). The U-Box-dependent E3 ubiquitin ligase CHIP mediates SMAD4 protein stability, but its precise role in SMAD4 ubiquitylation remains undefined (Li *et al.*, 2004).

SMAD4 can also be ubiquitylated by the RING E3 ligase TRIM33 (Ectodermin/TIF1γ), which possesses a PHD-Bromo domain that mediates chromatin binding. The PHD-Bromo domain is essential for the recruitment of TRIM33 to chromatin and chromatin binding is required for its E3 ubiquitin ligase activity (He *et al.*, 2006, Xi *et al.*, 2011, Agricola *et al.*, 2011). It has been suggested that TRIM33 directly interacts with SMAD4 and causes its polyubiquitylation (Dupont *et al.*, 2005). However, it has also been reported that SMAD4 is monoubiquitylated by TRIM33 at K519 (Dupont *et al.*, 2009). Monoubiquitylation impedes the association of SMAD4 with two other R-SMAD molecules, as the ubiquitin occupies the R-SMAD docking sides (Dupont *et al.*, 2009). In contrast, TRIM33 has also been reported to interact with tail-phosphorylated SMAD2/3 in competition with SMAD4, creating unique SMAD4-SMAD2/3 or TRIM33-SMAD2/3 complexes, each resulting in distinct cellular functions (Xi *et al.*, 2011, He *et al.*, 2006).

USP9x (FAM) is the only reported DUB that deubiquitylates SMAD4 (Figure 1-6) (Dupont *et al.*, 2009). USP9x only reverts monoubiquitylation of SMAD4 at K519. Hence, depletion of USP9x resulted in reduced TGFβ-induced transcription. It is required for TGFβ-induced growth arrest and cell migration but not phosphorylation of SMAD3. (Dupont *et al.*, 2009). Absence of USP9x has been reported to result in reduced axon length, a process that requires TGFβ signalling (Stegeman *et al.*, 2013). Studies in *Drosophila melanogaster* have also shown that fat facets (USP9x homologue) stabilises Medea (SMAD4

homologue) by deubiquitylating Medea K738 (equivalent to human SMAD4 K519) (Stinchfield *et al.*, 2012). The fat facets-mediated stabilisation of Medea is critical in regulating the zygotic Decapentaplegic (BMP$_{2/4}$ homologue) morphogen gradient that determines dorsal-ventral axis formation (Stinchfield *et al.*, 2012).
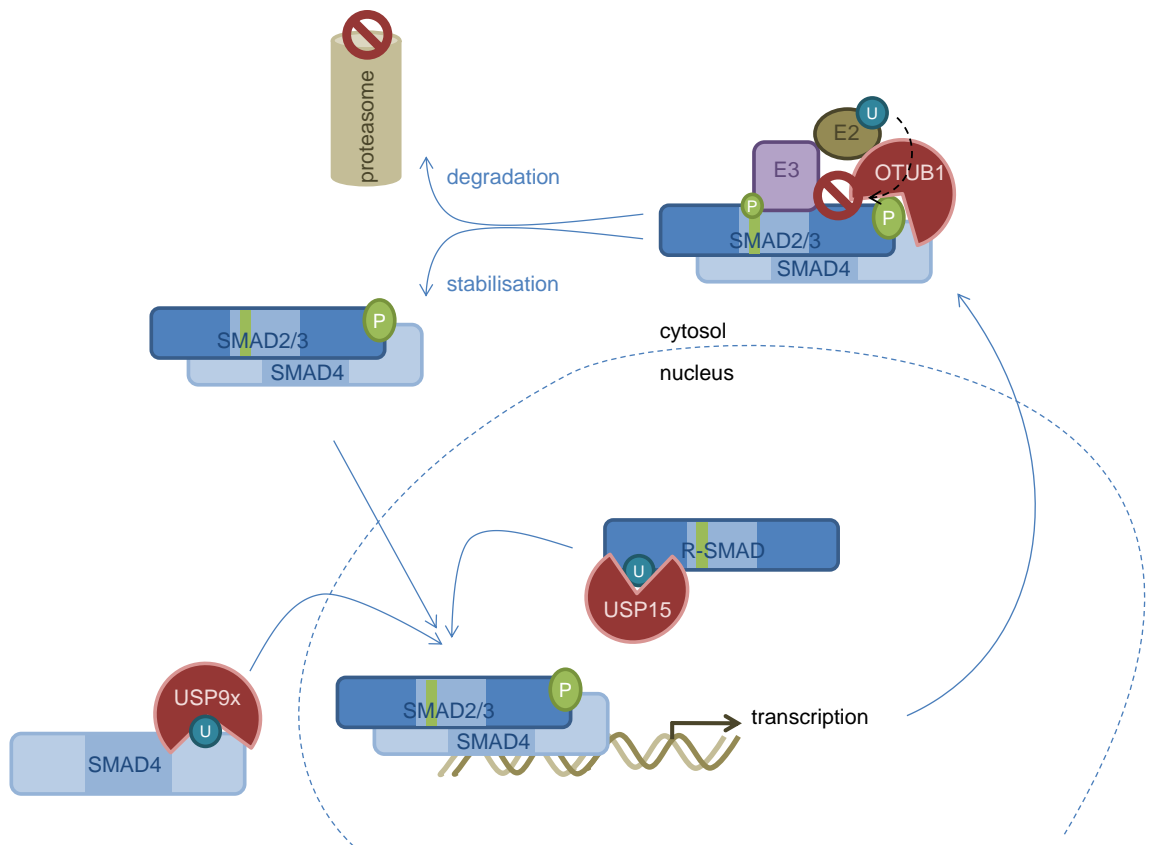
Figure 1-6 SMAD deubiquitylation

USP9x and USP15 reverse monoubiquitylation of SMAD4 and R-SMADs respectively, thereby enabling the assembly of active transcription factor complex and efficient TGFβ/BMP-mediated target gene transcription. OTUB1 recognises TGFβ-activated SMAD2/3 and inhibits their ubiquitylation, thereby stabilising the active transcriptional complex and enhancing TGFβ signalling.

1.3.2.6 Regulation of the other TGFβ pathway components by reversible ubiquitylation

Reversible ubiquitylation of proteins associated with the core TGFβ-pathway components, such as SMADs and receptors, also influences the outcome of TGFβ signalling. The transcription factor RUNX2 promotes the binding of R-SMADs to DNA. The E3 ubiquitin ligase SMURF1 can be directed by SMAD6 to RUNX2 and induce its ubiquitin-mediated degradation, resulting in decreased BMP signalling (Shen *et al.*, 2006). The negative nuclear co-factors c-SKI and SnoN, that antagonise SMAD-mediated transcriptional activity, are also targeted by E3 ubiquitin ligases. The anaphase-promoting complex (APC) is recruited to SnoN in a SMAD2-dependent manner and promotes TGFβ signalling by polyubiquitylating SnoN, leading to its degradation (Stroschein *et al.,* 2001, Wan *et al.,* 2001). In a similar TGFβ-dependent manner, SMURF2 and ARKADIA target SnoN for proteasomal degradation, causing activation of TGFβ transcriptional responses (Bonni *et al.*, 2001, Levy *et al.*, 2007, Nagano *et al.*, 2007). By binding to phosphorylated-SMAD2/3 ARKADIA can also ubiquitylate and degrade c-SKI (Yuzawa *et al.*, 2009).

Some DUBs have been implicated in the regulation of non-canonical TGFβ signalling. The deubiquitylating enzyme A20 has been shown to be recruited to TRAF6 by SMAD6 and abolish K63-linked polyubiquitylation of TRAF6, thereby inhibiting the non-canonical TGFβ signalling through the TRAF6-TAK1-p38 MAPK/JNK pathway (Jung *et al.*, 2013). Knockdown of the deubiquitylating enzyme A20 or its transporter SMAD6, both resulted in increased apoptosis, while maintaining p38 MAPK/JNK phosphorylation, indicating that SMAD6/A20 are essential for the negative regulation of non-canonical TGFβ signalling (Jung *et al.*, 2013). TAK1 is also reported to be

deubiquitylated by USP4 and USP18 (Fan *et al.*, 2011, Liu *et al.*, 2013). TNFα induces the association of USP4 and deubiquitylation of K63-polyubiquitylated TAK1. Consequently, TAK1-mediated NFκB activation is down regulated. Moreover, USP4 inhibits IL1β-, LPS- and TGFβ-induced NFκB activation (Fan *et al.*, 2011). TGFβ together with IL6 initiates T helper 17 (Th17) cell differentiation (Bettelli *et al.*, 2006). Recently, USP18 has been shown to regulate T cell activation and Th17 cell differentiation by associating with and deubiquitylating the TAK1-TAB1 complex, thereby restricting IL2 expression. USP18 knockout mice were found to be defective in Th17 generation and resistant to experimental autoimmune encephalomyelitis. Hence, the negative regulation of TAK1 activity during Th17 differentiation by USP18, led the authors to suggest USP18 as a target to treat autoimmune diseases (Liu *et al.*, 2013).

OTUD4, USP5 and USP25 have been reported to play a critical role in dorsal-ventral patterning of zebrafish embryos through the BMP pathway (Tse *et al.*, 2009). It has been reported that TSC22D3, which is crucial for dorsal-ventral patterning, segmentation and brain development, associates with USP15 and OTUD4 to impact the BMP signalling pathway (Tse *et al.*, 2013).

1.3.3 Regulation of TGFβ signalling by other PTMs

Although the focus of this thesis is primarily on reversible ubiquitylation and phosphorylation processes, it is worth noting that other PTMs of key components also play important roles in the TGFβ/BMP pathway modulation.

Sumoylation, like ubiquitylation, is attached to the Lysine residues on substrate proteins. While some sumoylation events can prime substrates for subsequent ubiquitylation (Hay, 2013, Geoffroy and Hay, 2009), in theory

ubiquitylation of a specific Lysine residue could compete with sumoylation or other ubiquitin-like modifications and acetylation. Sumoylation has been reported to alter the type I TGFβ receptor and SMAD4 functions. TβR-I is reported to be sumoylated in response to TGFβ, which results in enhanced receptor function by facilitating the recruitment and phosphorylation of SMAD3. This sumoylation event requires the kinase activities of both TβR-I and TβR-II (Kang *et al.*, 2008). SMAD4 has been reported to be sumoylated at K113 and K159 by the SUMO E2 UBC9 and members of the PIAS family of SUMO ligases. This sumoylation targets SMAD4 to subnuclear speckles and enhances TGFβ-induced transcriptional responses (Lee *et al.*, 2003, Lin *et al.*, 2003, Zhou *et al.*, 2014), whereas Medea (homologue to SMAD4) sumoylation in *Drosophila melanogaster* restricts Decapentaplegic (homologue to BMP) signalling through nuclear export (Miles *et al.*, 2008).

The RING E3 ligase c-Cbl, that harbours a Tyrosine kinase binding domain, promotes TGFβ signalling by neddylating TβR-II at K556 and K567, which stabilises TβR-II by inhibiting its ubiquitylation (Zuo *et al.*, 2013).

Acetylation of SMAD7 has been reported to compete with ubiquitylation to regulate SMAD7 stability (Gronroos *et al.*, 2002, Kume *et al.*, 2007). SMAD2 and 3 are reported to be acetylated by p300 and CBP at K19 in their MH1 domain which enhances their transcriptional activity and DNA binding (Simonsson *et al.*, 2006). Furthermore, TGFβ induces the enrichment of p300/CBP occupancies around SMAD binding sites at TGFβ target gene promoters, enhances the interaction of p300 with SMAD2/3 and increases SMAD2/3 acetylation (Yuan *et al.*, 2013). Additionally, TGFβ promotes the acetylation of histone H3 and the transcription factor Ets-1 by p300 (Kato *et al.*, 2013).

Methylation of SMAD6 by protein arginine N-methyltransferase 1 (PRMT1) has been reported to promote its dissociation from the type I BMP receptor, causing the activation of BMP-SMADs through phosphorylation (Xu *et al.*, 2013, Inamitsu *et al.*, 2006). N-linked glycosylation of the extracellular domain of TβR-II has been reported to impact TGFβ sensitivity by facilitating ligand binding (Goetschy *et al.*, 1996, Fafeur *et al.*, 1993, Kim *et al.*, 2012). Furthermore, it is suggested that glycosylation of the TGFβ ligands is necessary for their secretion (Sha *et al.*, 1989).

1.3.4 *Regulation of TGFβ signalling by non-PTM modes*

The availability of TGFβ components can further be regulated by non-PTM modes, through non-coding RNA molecules, which function in transcriptional and post-transcriptional regulation of gene and protein expression (Lee *et al.,* 1993). Regulatory RNAs include micro RNAs (which act in translational repression and transcript degradation), long non-coding RNAs (which control (post-) transcriptional gene regulation), small intronic transposable element RNAs (that mediate gene silencing), small nuclear RNAs (which control RNA splicing), small nucleolar RNAs (which chemically modify RNA), Piwi-interacting RNAs (that silence retrotransposons) and endogenous small interfering RNAs (which control post-translational gene silencing in oocytes) (Bowen *et al.*, 2013, Harding *et al.*, 2014).

Many messenger RNAs (mRNAs) of components of the TGFβ signalling pathway are reported to be targeted by microRNAs (miRNAs) for degradation (Blahna and Hata, 2012). Furthermore, the biogenesis and processing of several miRNAs is reported to be regulated by the TGFβ pathway (Blahna and Hata, 2012, Long and Miano, 2011). SMADs can modulate miRNA expression

by binding SBEs in miRNA promoter regions and by binding to SBE-like sequences of pri-miRNAs (Long and Miano, 2011, Kong *et al.*, 2008, Blahna and Hata, 2012). The 44 miRNAs that harbour the SBE-like sequence are termed TGFβ/BMP-regulated miRNAs (T/B miRNAs) (Davis *et al.*, 2010, Davis *et al.*, 2008). Moreover, miRNAs can directly interact with mRNAs of TGFβ-target genes (Butz *et al.*, 2012). Additionally, TGFβ can activate the long non-coding RNAs lncRNA-SMAD7 and lncRNA-ATB, which sequester the miRNA-200 family and stabilise IL11 mRNA, thereby promoting apoptosis or invasion, metastasis and EMT respectively (Yuan *et al.*, 2014, Arase *et al.*, 2014).

1.4 TGFβ signalling in human diseases

1.4.1 Physiological functions of TGFβ and BMP cytokines

BMP and TGFβ-dependent transcriptional activity determines cellular responses such as proliferation, apoptosis, EMT, migration, differentiation and embryonic development. TGFβ and BMP ligands are essential to maintain cell and tissue homeostasis and often act in a context dependent manner (Massague, 2012).

TGFβ cytokines inhibit cell proliferation of many cell types by repressing the transcription of c-Myc as well as the induction of CDK inhibitors including p15, p21 and p27. These inhibit CDK activities associated with the G_1 to S phase progression during cell cycle and arrest cells in G_1 (Siegel and Massague, 2003). Many other signalling cascades regulated by TGFβ cooperate with canonical TGFβ signalling in mediating TGFβ growth control (Huang and Huang, 2005, Ten Dijke *et al.*, 2002).

The induction of apoptosis by TGFβ cytokines constitutes another tumour-suppressor mechanism and plays an essential role for the maintenance of B- and T-cell homeostasis, among others. Apoptosis is initiated by TGFβ ligands in cooperation with stress signals. This leads to canonical (SMAD activation), as well as non-canonical (MAPK pathway) TGFβ signalling and induces Cytochrome c release and hence Caspase activation (Schuster and Krieglstein, 2002).

TGFβ promotes EMT, which is a fundamental process during embryogenesis and organogenesis, whereby epithelial cells undergo profound morphological and phenotypic changes to become mesenchymal cells. The acquisition of the mesenchymal phenotype is characterised by the loss of cell-cell adhesion and apical basal cell polarity, which results in enhanced cellular

plasticity, including a gain in migratory and invasive properties. All of these processes are regulated by the TGFβ-activated receptors, which signal through SMADs and the RhoA pathway, and include the rearrangement of the actin cytoskeleton and differential expressions of proteins involved in cell-cell junction formation and migration (Moreno-Bueno *et al.*, 2009, Heldin *et al.*, 2012, Heldin *et al.*, 2009, Medici *et al.*, 2011). Similarly, TGFβ family cytokines can induce endothelial to mesenchymal transition (EndoMT), which is critical during embryonic heart development and is characterised by the loss of endothelial and gain of mesenchymal phenotype (Ten Dijke *et al.*, 2012). EMT is also a hallmark of cancer and essential for tumour metastasis. Once EMT is induced and metastatic cells disseminate to a distant site, they need to undergo mesenchymal to epithelial transition (MET) regulated by BMPs, to permit colonisation and reinitiate proliferative programs necessary for the formation of secondary tumours (Jo *et al.*, 2009, Morrison *et al.*, 2013, Buijs *et al.*, 2007).

TGFβ signalling also plays a critical role in wound healing and cellular migration (Pakyari *et al.*, 2013). Cellular migration is initiated upon the TGFβ-mediated degradation of RhoA, which results in the disruption of tight junctions (section 1.2.5) (Wang *et al.*, 2003). Furthermore, increased transcription of *Snail*, down regulation of E-cadherin and inhibition of cofilin, which result in actin polymerisation, promote migratory events (Heldin *et al.*, 2009, Akhurst and Derynck, 2001). In prostate cancer cells TGFβ enhances the production of prostaglandin, which mediates cellular migration through the PI3K/AKT/mTOR pathway (Vo *et al.*, 2013).

By regulating the expression or function of tissue-specific transcription factors and growth factor cytokines, BMP and TGFβ can regulate the fate of pluripotent stem cells (Moses and Serra, 1996). TGFβ signalling also leads to

chromatin remodelling in order to transcribe genes controlling differentiation of embryonic stem cells (Gaarenstroom and Hill, 2014). TRIM33 has been shown to bind chromatin and make it accessible for SMAD2/3/4 to recruit RNA Pol II (Xi *et al.*, 2011, Massagué and Xi, 2012). TGFβ ligands inhibit myoblast, adipocyte and osteoblast differentiation, whereas BMPs promote the differentiation of mesenchymal stem cells into osteoblasts (Liu *et al.*, 2001, Derynck and Akhurst, 2007, Moses and Serra, 1996, ten Dijke *et al.*, 2003). TGFβ/BMP ligands control mesenchymal precursor cell differentiation during bone formation through canonical (SMAD dependent) and non-canonical (MAPK pathway) signalling (Chen *et al.*, 2012). In addition, TGFβ family cytokines can promote trans-differentiation via redirecting the differentiation of cells that are already partly or fully differentiated. This process of cellular plasticity is essential during embryonic development and enables BMP ligands to also convert myoblasts and pre-adipocytes into osteoblasts (Derynck and Akhurst, 2007). Apart from maintaining the pluripotent state and regulating (trans)-differentiation of stem cells, the TGFβ family of cytokines are also involved in establishing induced pluripotent stem (iPS) cells (Itoh *et al.*, 2014).

The correct induction of cellular proliferation, apoptosis and differentiation, along with EMT in a controlled temporal and spatial manner, defined by TGFβ and BMP ligands, is critical during embryonic development. *Xenopus laevis* has been employed as a model organism to study vertebrate embryogenesis and the impact of TGFβ/BMP signalling (McDowell and Gurdon, 1999, Simeoni and Gurdon, 2007, Gurdon *et al.*, 1958). During gastrulation the embryo forms three germ layers: ectoderm, mesoderm and endoderm. Each germ layer results in the formation of different tissues (De Robertis and Kuroda, 2004, Blitz *et al.*, 2006). Further organisation is achieved by two opposing

signalling centres in the ventral and dorsal sides of the mesoderm, leading to a dorsal-ventral axis formation. This axis formation is achieved by the expression of BMP cytokines in the ventral and BMP antagonists in the dorsal signalling centres creating a gradient of BMP signalling (De Robertis and Kuroda, 2004, Eivers *et al.*, 2008, McDowell *et al.*, 2001).

1.4.2 Aberrant TGFβ signalling in hereditary disease

Due to the complexity and vital function of TGFβ signalling, it is evident that aberrant signalling can cause a variety of human diseases. Most diseases are caused by mutations in key components of the signalling cascade leading to an imbalance of TGFβ/BMP signalling and resulting in somatic and hereditary diseases. These diseases comprise cardiovascular, immune and reproductive disorders as well as fibrosis and cancer (Figure 1-7) (Massague, 2008, Pardali and Ten Dijke, 2012, Hawinkels and Ten Dijke, 2011, Flavell et al., 2010, Blobe et al., 2000).

The Marfan syndrome is a connective tissue disorder that is linked to mutations in the *FBN1* gene (Dietz *et al.*, 1991). The *FBN1* gene encodes fibrillin1, which is an extracellular matrix glycoprotein that sequesters TGFβ ligands and is essential for the formation of elastic fibres in the connective tissue (Kielty *et al.*, 2002). Mutations in *FBN1* lead to decreased fibrillin1 expression, thereby increasing TGFβ signalling. This results in aortic aneurysms as well as mitral valve abnormalities and causes failure of the vascular system and lung disorders. The Marfan syndrome has also been associated with mutations in the TGFβ type I and type II receptors (Neptune *et al.*, 2003, Matyas *et al.*, 2006). Mutations in the *NOG* gene, which encodes the BMP antagonist Noggin, results in increased BMP signalling and causes

Brachydactyly Type B disease, which is characterised by skeletal defects resulting in abnormally fused finger and toe joints (Lehmann *et al.*, 2007). The insufficiency of the TGFβ family cytokine AMH can lead to the autosomal recessive congenital disorder Persistent Müllerian Duct syndrome (PMDS). PMDS is characterised by the development of female organs in genetic males. Some patients suffering from PMDS also harbour inactivating mutations in the AMH receptor (AMHR-II) that limit their interaction with AMH (Josso *et al.*, 2005, Belville *et al.*, 1999).

Inactivating mutations in ALK1 and its co-receptor endoglin are associated with the Osler-Weber-Rendu syndrome (also known as Hereditary Haemorrhagic Telangiectasia (HHT)), which is an autosomal dominant disease in which patients exhibit impaired vascular development (Govani and Shovlin, 2009, Johnson *et al.*, 1996). Inactivating mutations in ALK5 and TβR-II are associated with the Loeys-Dietz syndrome (LDS), which is a connective tissue disorder that exhibits similar symptoms as the Marfan syndrome and is characterised by impaired craniofacial development and an increased risk of aortic rupture (Loeys *et al.*, 2005, Dietz *et al.*, 2005).

Inherited mutations in intracellular TGFβ signalling components can also cause anomalous cell growth, which can predispose patients to the development of cancer. Inactivating mutations in the type I TGFβ receptor gene *TGFBR1* have been associated with the Ferguson-Smith disease (FSD), which is an autosomal dominant skin disorder that is characterised by aggressive skin tumours that invade surrounding tissue but spontaneously self-heal (Goudie *et al.,* 2011).

Autosomal dominant mutations of SMAD4 and ALK3 have been reported to drive polyp formation in patients with Juvenile polyposis, which is

characterised by the formation of spontaneous benign polyps in the gastrointestinal tract of children. These polyps predispose patients to develop colorectal, gastric and pancreatic cancers (Howe *et al.*, 2004, Latchford *et al.*, 2012, Sayed *et al.*, 2002).

Mutations in TGFβ signalling associated factors have been linked to the pathogenesis of several diseases. For example, mutations in the SMAD transcriptional co-repressor TGIF are linked to Holoprosencephaly, which causes structural defects of the developing forebrain (Gripp *et al.*, 2000).

Marfan syndrome
Brachydactyly Type B
Persitent Muellerian duct syndrome
Chondrodysplasia
Idiopathic pulmonary fibrosis
Prostate cancer

ligand

receptor II

receptor I

cytosol

nucleus

Osler-Weber-Rendu Syndrome
Persitent Muellerian duct syndrome
Loeys-Dietz syndrome
Ferguson-Smith squamous carcinoma
Marfan syndrome
Bone disorders
Pulmonary hypertension

SMAD4

Juvenile polyposis
Pancreatic and colon cancers

Holoprosencephaly

transcription co-factors

Figure 1-7 Overview of diseases caused by aberrant TGFβ/BMP signalling

Mutations in most TGFβ/BMP signalling components can cause a variety of severe human diseases.

1.4.3 The role of TGFβ signalling in cancer

In epithelial cells, TGFβ/BMP cytokines are usually regarded as tumour suppressors. Mutations and epigenetic changes, however can lead to aberrant TGFβ/BMP signalling in somatic cells, which is often associated with the development of cancer (Inman, 2011, Massague, 2008, Wakefield and Hill, 2013, Drabsch and ten Dijke, 2012). The switch from TGFβ as a tumour suppressor to tumour promoter is a critical step during cancer development. On one hand, mutations in critical signalling components can inactivate TGFβ signalling, which could result in the loss of TGFβ-induced cytostasis. On the other hand, mutations can also enhance the TGFβ-mediated tumour traits such as EMT and the induction of angiogenesis (Inman, 2011, Massague, 2008, Zhang et al., 2014b, Meulmeester and Ten Dijke, 2011, ten Dijke et al., 2008).

Inactivating mutations in the type I and II TGFβ and BMP receptors as well as SMAD4 that result in the evasion of TGFβ-dependent growth suppression are found in pancreatic, gastric and colorectal cancers (Goggins *et al.*, 1998, Hahn *et al.*, 1996, Xu and Pasche, 2007, Zhang *et al.*, 2010, Kodach *et al.*, 2007). SMAD4 is a tumour suppressor that has been reported to be mutated in ~50% of pancreatic tumours (Hahn *et al.*, 1996). Certain mutations in SMAD4 can alter its stability by priming SMAD4 for increased proteasomal degradation (Yang *et al.*, 2006, Wan *et al.*, 2005). The loss of SMAD4 promotes tumourigenesis in colon cancers and re-expression of SMAD4 is able to restore the TGFβ-mediated cytostatic effects (Zhang *et al.*, 2010, Voorneveld *et al.*, 2014). Cancer cells often exploit TGFβ signalling in order to metastasise, which is particularly evident in aggressive breast tumours (Massagué, 2008). In MDA-MB-231 breast cancer cells, SMAD4 expression is required to drive bone metastases (Deckers *et al.*, 2006). Hence, the expression of SMAD4 is an

example of how TGFβ signalling can switch from a tumour suppressor to a tumour promoter in a cell-type and context-dependent manner. Another example is the epigenetic silencing of TGFβ target genes, such as the tumour suppressors p15 and p21 (Geyer, 2010). Aberrant BMP signalling is associated with bone metastasis, which is the most common secondary tumour site in prostate and breast cancer progression (Drabsch and ten Dijke, 2011, Ye *et al.*, 2007).

Proteins regulating TGFβ/BMP signalling such as E3 ubiquitin ligases and DUBs have also been shown to influence cancer progression. Elevated TRAF4 levels, which cause increased levels of SMAD2 and TAK1 phosphorylation, correlate with poor prognosis in breast cancer patients (Zhang *et al.*, 2013a). NEDD4L and SMURF2 are significantly up regulated in prostate cancer cells (Hellwinkel *et al.*, 2011) and high SMURF2 levels, which result in TβR-II degradation, might cause the attenuation of TGFβ signalling in renal cell carcinoma (Fukasawa *et al.*, 2010). Moreover, SMURF1 amplification in pancreatic cancers decreases SMAD levels and drives tumourigenic phenotypes (Kwei *et al.*, 2011). The loss of ARKADIA is found in some cancer cell lines, resulting in the stabilisation of SnoN and c-SKI, which are transcriptional co-repressors of TGFβ signalling (Nagano *et al.*, 2010, Levy *et al.*, 2007). The DUBs USP15 and USP4, both targeting TβR-I, are also implicated in cancer progression. USP15 amplification was observed in glioblastoma, breast and ovarian cancers and correlated with high TGFβ activity and poor prognosis in individuals with glioblastoma (Eichhorn *et al.*, 2012), whereas USP4 stimulated the TGFβ-induced breast cancer invasion and metastasis (Zhang *et al.*, 2012b).

1.4.4 TGFβ-induced fibrosis

Fibrosis is caused by excessive scarring and the TGFβ signalling pathway has been implicated in orchestrating the process of fibrogenesis though excessive would healing. Fibrosis in organs like the lung, liver, kidney, skin or heart can cause organ failure and currently there is no effective treatment of fibrotic disorders as designing specific strategies for targeting the TGFβ pathway could have adverse effects on the injury response, although scarring could be reduced (Jiang *et al.*, 2014, Pakyari *et al.*, 2013, Finnson *et al.*, 2013).

The molecular mechanisms that contribute to fibrogenesis are pathological, physiological, biochemical, and physical factors including mechanical stress, myofibroblast differentiation, chemotherapy (as a result of cancer treatment), EMT, increased inflammation, ECM production (collagen deposition) and canonical as well as non-canonical TGFβ signalling (Van De Water *et al.*, 2013, Goumans *et al.*, 2008, Mancini and Sonis, 2014, Fernandez and Eickelberg, 2012). The TGFβ mediated signalling pathways involved in fibrosis are the same as those involved in the normal wound healing process, however in fibrosis, these signalling pathways escape normal cellular regulation (Choi *et al.*, 2012). TGFβ release upon injury assists in the attraction of macrophages, neutrophils and fibroblasts, which in turn release more TGFβ (Leask and Abraham, 2004). The hyperactivity of TGFβ signalling results in a disruption of ECM homeostasis and accumulation of fibrosis-associated proteins (Weiskirchen and Meurer, 2013). Pro-fibrotic protein and ECM production (e.g. collagen and fibronectin) is augmented through TGFβ, IFNγ, IL10 signalling, transcriptional activators (e.g. SMAD3), epigenetic modulators, NADPH oxidases that generate reactive oxygen species and downstream

transcription (e.g. *CTGF* and *PAI-1*) through SMAD2/3 and non-SMAD pathways (e.g. EGFR, MAP kinases, p53). PAI-1 is a potent profibrotic matricellular protein involved in wound healing, however excessive amounts contribute to scarring and organ fibrosis (Ghosh *et al.*, 2013, Samarakoon *et al.*, 2013). The constitutive overexpression of CTGF and collagen enhance the profibrotic response to TGFβ (Leask and Abraham, 2004), possibly through the ALK1/SMAD1 and ERK1/2 MAP kinase pathways but not SMAD2/3 in scleroderma fibrosis and Dupuytren's disease (Pannu *et al.*, 2007, Krause *et al.*, 2011). It has been proposed that BMP_7 could antagonise established fibrosis (Yanagita, 2012), as BMP_7 interferes with TGFβ signalling, matricellular proteins and proteins that modulate cellular proliferation, migration, adhesion and ECM production (Weiskirchen and Meurer, 2013).

1.4.5 Strategies for the treatment of TGFβ-associated diseases

The TGFβ pathway has been targeted for disruption by several therapeutic strategies, as abnormal TGFβ signalling is associated with several different diseases (section 1.4.2, 1.4.3 and 1.4.4). The strategies currently in use include antisense oligonucleotides, neutralising antibodies, ligand traps, soluble TβR-II receptors and small molecule inhibitors of type I TGFβ/BMP receptors. Numerous therapeutic strategies are tested in clinical trials and the most promising treatments to target TGFβ signalling that have progressed to Phase III clinical trials are: Trabedersen (an antisense oligonucleotide that blocks mRNA translation), Belagenpumatucel-L (an antisense gene-modified allogeneic tumour cell vaccine) and Lerdelimumab (a recombinant human IgG_4). These drugs all target $TGFβ_2$, which is produced in extreme quantities by glioblastoma and pancreatic carcinoma cells (Bogdahn *et al.*, 2011,

Schlingensiepen *et al.*, 2011, Nemunaitis *et al.*, 2009, Nemunaitis *et al.*, 2006, Cordeiro, 2003, NIH, 2014, Akhurst and Hata, 2012, Nagaraj and Datta, 2010).

Although several diseases and cancer can result from an imbalance in TGFβ signalling, there are major concerns for targeting TGFβ as a therapeutic strategy. Due to the wide-ranging physiological functions of TGFβ/BMP signalling, inactivation of the complete pathway is not a promising treatment approach. The principal apprehension is to remove the cytostatic tumour-suppressing effects of TGFβ/BMP as well as causing disturbances in the immune and cardiovascular systems. In fact, most clinical trials result in failures, possibly due to side effects (NIH, 2014). Hence, a comprehensive understanding of the TGFβ/BMP signalling pathway regulation will be essential to develop more effective therapeutic strategies. Novel regulatory components of TGFβ signalling could be exploited as potential drug targets to develop effective disease- and individually-tailored therapeutic interventions.

1.5 <u>Aims of the thesis</u>

The TGFβ and BMP pathways play critical roles during development, in adult tissue homeostasis and are intricately regulated. Malfunction of the signalling components results in severe human diseases (section 1.4). Therefore, understanding the precise molecular mechanisms by which TGFβ and BMP pathways are regulated could enable to uncover disease-specific druggable targets that modulate TGFβ/BMP signalling. Post-translational modifications of TGFβ pathway components play a key role in fine tuning TGFβ-mediated cellular responses. In particular, the post-translational regulation of the TGFβ/BMP receptors and SMAD proteins, which are the key cellular mediators of TGFβ/BMP signalling, is crucial. Much is known about E3 ligases

that ubiquitylate SMADs and the receptors to induce their proteasomal degradation (section 1.3.2). However, the deubiquitylating enzymes that could counterbalance the impact of ubiquitylation events to sustain TGFβ/BMP signalling are largely unknown.

A proteomic screen was undertaken in order to identify novel SMAD interacting partners. The deubiquitylating enzyme OTUB1 was identified as an interactor of TGFβ activated SMAD3 (section 3). Therefore, the first aim of this thesis was to characterise the role of OTUB1 in TGFβ signalling. During the course of this investigation, it was evident that OTUB1 itself could be modified by phosphorylation. Hence, the second aim of this thesis was to characterise the phosphorylation on OTUB1 (section 4).

Another proteomic screen isolated USP15 as an interactor of SMAD6. SMAD6 inhibits BMP signalling by recruiting E3 ubiquitin ligases to type I BMP receptors and causing their degradation through the proteasome. Thus, the third aim of this thesis was to characterise the role of USP15 in the BMP pathway (section 5).

Finally, O-GlcNAc transferase was isolated as an interactor of SMAD2. There are no reports of O-GlcNAc modification on SMADs in the TGFβ pathway. For this reason, the fourth aim was to establish whether SMADs are modified by OGT through O-GlcNAcylation and if so, whether this influenced TGFβ/BMP signalling (section 6).

2　**Materials and Methods**

2.1　**Materials**

2.1.1　Reagents and Instruments

Recombinant TGFβ$_1$, BMP$_2$, Activin A and macrophage colony-stimulating factor (M-CSF) were purchased from R&D Systems. The type I BMP receptor inhibitor LDN189193 (was purchased) and PI3K inhibitor LY294002 were synthesised in the DSTT. The CK2 inhibitor K66 was from Merck Millipore. The type I TGFβ receptor inhibitor SB505124, adenosine 5'-triphosphate sodium salt (ATP), Alkaline Phosphatase Detection Kit, anti-HA-agarose, anti-FLAG-agarose, ammonium persulphate (APS), ampicillin, β-mercaptoethanol (biochemical grade), Cycloheximide, benzamidine, dimethyl sulphoxide (DMSO), doxycycline, FREON, imidazole, iodoacetamide, kanamycin, Lactacystin, Nonidet P-40, phenylmethanesulphonylfluoride (PMSF), Ponceau S, polybrene, sodium dodecyl sulphate (SDS), sodium deoxycholate, tris(2-carboxyethyl)phosphine (TCEP), sodium tetraborate N, N, N', N'-tetramethylethylenediamine (TEMED), triethylammonium bicarbonate (TEAB), t-octylphenoxypolyethoxyethanol (Triton)-X-100 and polyethylene glycol sorbitan monolaurate (Tween-20) were from Sigma-Aldrich. Acetic acid, acetone, ammonium bicarbonate, ethanol, glycerol, glycine, 4-(2-Hydroxyethyl)piperazine-1-ethanesulfonic acid (HEPES), isopropanol, manganese chloride, magnesium acetate, methanol, orthophosphoric acid, potassium chloride, sodium acetate, sodium chloride, sodium ethylenediaminetetraacetic acid (EDTA), sodium ethylene glycol tetra-acetic acid (EGTA), sodium fluoride, sodium β-glycerophosphate, sodium orthovanadate, sucrose and tris(hydroxymethyl)methylamine (Tris) were from BDH. Bortezomib was purchased from LC Laboratories. MG132 was from Calbiochem. PhosphoSafe

reagent was from Novogen. Recombinant ubiquitin chains and FLAG-ubiquitin were purchased from Boston Biochem. Precision Plus Protein™ standards for SDS-PAGE (broad range), TransFectin™ lipid reagent, iScript cDNA synthesis kit, SYBR green mix for qRT-PCR, qRT-PCR plates, qRT-PCR seals, 4-20% mini-PROTEAN® TGX gels, mini trans-blot cells, gel dryer apparatus, qRT-PCR iCycler, econopac columns and mini-cell transfer tanks were from BioRad. Protein A-agarose, protein G-Sepharose, glutathione-Sepharose, Hyperfilm and $^{\gamma 32}$P-ATP were purchased from GE Healthcare. Acrylamide: bis-acrylamide (40% (w/v) 29:1) solution was from Flowgen Bioscience. GFP-TRAP® agarose was from Chromotek. Microcystin-LR, Dulbecco's modified eagle medium (DMEM), Eagle's Minimum essential medium (EMEM), RPMI-1640, Opti-MEM reduced serum media, foetal bovine serum (FBS), tissue culture grade Dulbecco's phosphate buffered saline (PBS), trypsin/EDTA solution, L-glutamine, essential amino acids, non-essential amino acids, sodium pyruvate, versene, penicillin/streptomycin, G418, blasticidin, hygromycin-B, zeocin, were from GIBCO. Mr Frosty cryo 1 °C freezing containers were from Nalgene. Pre-cast NuPAGE® Novex 4-12% Bis-Tris gels, NuPAGE® MES and MOPS running buffer (20x), 4x NuPAGE® LDS sample buffer, Colloidal Coomassie blue staining kit and the NanoDrop® spectrophotometer were from Invitrogen. ProLong Gold mounting reagent, SYBR Safe nucleotide gel stain, DNA loading dye and DNA ladder were from Life Technologies. Polyethylenimine (PEI) was from Polysciences. IgG-free BSA was from Jackson Immunoresearch. Sequencing-grade trypsin, Dual-Luciferase® reporter assay kit and passive lysis buffer were from Promega. Skimmed milk powder (Marvel) was from Premier Brands. Ni-NTA-agarose, plasmid maxi and RNeasy kits were from Qiagen. Acetonitrile (HPLC grade) and trifluoroacetic acid (TFA) were from Rathburn

Chemicals. Protease inhibitor cocktail tablets (containing aprotinin, bestatin, calpain inhibitors, chymostatin, E-64, leupeptin, α2-macroglobulin, pefabloc SC, pepstatin, PMSF, and trypsin inhibitors) were purchased from Roche. Nitrocellulose and polyvinylidene difluoride (PVDF) membranes were purchased from Whatman. Nuclease free water was from Ambion. Cryovials and Spin-X columns were from Corning. Dithiobis (succunimidyl propionate) (DSP), Coomassie protein assay reagent (Bradford reagent), SuperSignal West Pico chemiluminescent substrate, cellular fractionation kits, bench top centrifuges and the LTQ-orbitrap mass spectrometer were from Thermo Scientific. Sterile cellulose filters (0.22 μm and 0.45 μm) and steriflip columns were from Merck Millipore. Photographic developer (LX24), liquid fixer (FX40), autoradiography cassettes with intensifying screens and X-ray film were from Kodak. Tissue culture plastic-ware was from Corning, Greiner or Nunc. Cell scrapers were from Costar. Cellular migration inserts were from Ibidi. The XTT cell proliferation assay kit was purchased from ATCC. Bacterial culture medium Luria Bertani (LB) broth and LB agar plates were provided by the University of Dundee media kitchen service. Thermo mixer IP shakers, combitips and multi dispenser pipettes were purchased from Eppendorf. Self-cast polyacrylamide electrophoresis gel tanks were from ATTA. Electrophoresis power supplies from VWR. Falcon tubes and 96 well luciferase plates were from Greiner. The MicroLumat plus LB 96V luminometer was from Berthold technologies. Serological pipettes and microtubes from Sarstedt, pipettes from Gilson, pre-sterilised tips from ART and heat blocks were from Grant. Electromagnetic stirrers were from Stuart and vortexer from SLS select. CO_2 incubators were from Mackay and Lynn. Tissue culture 2nd class safety cabinets were from Medical Air Technology. The Vydac 218TP54 C_{18} reverse phase HPLC column

was from Separations Group. SpeedVacs were from CHRIST. HPLC system components were obtained from Dionex. Centrifuge tubes, rotors and centrifuges were from Beckmann. The automated capillary DNA sequencer model 3730 was from Applied Biosystems.

2.1.2 Buffers and solutions

Buffers frequently used in this thesis are listed in Table 2-1. In order to preserve the phosphorylation and expression levels of the proteins at the time of lysis, the lysis buffers were supplemented with inhibitors of proteases and phosphatases. EGTA and EDTA chelate Ca^{2+} and Mg^{2+} ions, which are essential co-factors for protein kinases respectively. To inhibit the action of Serine/Threonine protein phosphatases, sodium fluoride, sodium pyrophosphate, sodium β-glycerophosphate and microcystin-LR were supplemented. Sodium orthovanadate is a potent Tyrosine phosphatase inhibitor.

Table 2-1 Buffers and solutions

buffer	composition
5x SDS sample buffer	5% (w/v) SDS, 5% (v/v) β-ME, 50 mM Tris/HCl pH 6.8, 6.5% (v/v) glycerol and 0.02% (w/v) bromophenol blue
Ammonium chloride lysis buffer	155 mM NH4Cl, 10 mM NaHCO3, 0.1 µM EDTA, pH 7.3
Bacterial lysis buffer	50 mM Tris/HCl pH 7.5, 150 mM NaCl, 1% (v/v) Triton-X-100, 0.02 mM EDTA, 0.02 mM EGTA, 0.2 mM PMSF, 1 mM benzamidine, 0.06% β-ME
Bacterial wash buffer (GST)	50 mM Tris/HCl pH 7.5, 250 mM NaCl, 0.1 mM EGTA, 0.2 mM PMSF, 1 mM benzamidine, 0.1% β-ME, 0.03% Brij 35
Bacterial wash buffer (His-6)	50 mM Tris/HCl pH 7.5, 0.02 mM EDTA, 0.02 mM EGTA, 0.2 mM PMSF, 1 mM benzamidine, 0.06% β-ME, 20 mM imidazole, 0.03% Brij 35, 0.5 M or 150 mM NaCl
Buffer A	50 mM Tris/HCl pH 7.5, 0.1 mM EGTA and 0.1% (v/v) β-ME
Deubiquitylation assay buffer	50 mM Tris/HCl pH 7.5, 5 mM DTT, 100 mM NaCl
E2~ub loading buffer	50 mM HEPES, 150 mM NaCl, 0.5 mM TCEP, 0.2 mM ATP, 10 mM Mg-acetate
Glutathione elution buffer	20 mM glutathione, 50 mM Tris/HCl pH 7.5, 250 mM NaCl,

buffer	composition
	0.1 mM EGTA, 0.2 mM PMSF, 1 mM benzamidine, 0.1% β-ME, 0.03% Brij 35
IF blocking solution	5% (v/v) normal donkey serum, 0.01% (v/v) fish skin gelatin, 0.1% (v/v) Triton X-100, 0.05% (v/v) Tween-20 in PBS, pH 7
Kinase assay buffer	50 mM Tris/HCl pH 7.5, 0.1% β-ME, 0.1 EGTA, 10 mM MgCl2, 0.5 µM microcystin-LR
LB-plates	1% (w/v) tryptone peptone, 0.5% (w/v) yeast extract, 86 mM NaCl, 2% (w/v) bacto-agar. After autoclaving: 100 µg/ml ampicillin or 25 µg/ml kanamycin
Luria Bertani broth (LB)	1% (w/v) tryptone peptone, 0.5% (w/v) yeast extract, 86 mM NaCl. After autoclaving: 100 µg/ml ampicillin or 25 µg/ml kanamycin
Lysis buffer	50 mM Tris/HCl pH 7.4, 0.27 M sucrose, 150 mM NaCl, 1 mM EDTA pH 8.0, 1 mM EGTA pH 8.0, 1 mM sodium orthovanadate, 10 mM sodium β-glycerophosphate, 50 mM sodium fluoride, 5 mM sodium pyrophosphate, 1% (v/v) Triton X-100, 0.5% (v/v) Nonidet P-40, 0.1% (v/v) β-ME, 1 tablet of complete protease inhibitors per 25 ml lysis buffer
Lysis buffer containing DSP:	40 mM HEPES pH 7.4, 120 mM NaCl, 1 mM EDTA pH 8.0, 10 mM sodium β-glycerophosphate, 50 mM sodium fluoride, 1 mM sodium orthovanadate, 5 mM sodium pyrophosphate, 1% (v/v) Triton X-100, 1 tablet of complete protease inhibitors per 25 ml lysis buffer, 2.5 mg/ml DSP (in DMSO)
O-GlcNAcylation buffer	50 mM Tris/HCl pH 7.5, 1 mM DTT
Phosphate-buffered saline (PBS)	137 mM NaCl, 2.7 mM KCl, 4.3 mM Na2HPO4, 1.47 mM KH2PO4, pH 7.4
Polyethylenimine (PEI)	1 mg/ml PEI in 25 mM HEPES, pH 7.5
RIPA buffer	50 mM Tris/HCl pH 8.0, 150 mM NaCl, 1% Triton X-100, 0.5% sodium deoxycholate, 0.1% SDS, 0.5% Tween-20, 1 tablet of complete protease inhibitors per 25 ml lysis buffer
SDS-PAGE buffer	25 mM Tris/HCl pH 8.3, 192 mM glycine, 0.1% (v/v) SDS
Size exclusion chromatography buffer	150 mM NaCl, 50 mM Tris/HCl pH 7.5, 0.03% (v/v) Brij 35
TAE buffer	40 mM Tris-acetate pH 8.0, 1 mM EDTA
TBS-Tween (TBS-T)	50 mM Tris/HCl pH 7.5, 150 mM NaCl and 0.25% (v/v) Tween-20
tissue lysis buffer	10 mM Tris/HCl pH 8.0, 150 mM NaCl, 1 mM EDTA, 1% NP40, 0.1% SDS, 1 tablet of complete protease inhibitors per 25 ml lysis buffer
Transfer buffer	25 mM Tris/HCl pH 8.3, 192 mM glycine, 20% (v/v) methanol
Tris-buffered saline (TBS)	20 mM Tris/HCl pH 7.5, 150 mM NaCl
Ubiquitylation assay buffer	50 mM Tris/HCl pH 7.4, 5 mM MgCl2, 2 µM ATP

2.1.3 Plasmids

All plasmids encoding mammalian expression constructs were cloned into

pCMV5, pBABE-puro or pcDNA/Frt/TO vectors with N-terminal FLAG,

haemagglutinin (HA) or green fluorescent protein (GFP) tags. pcDNA-Frt/TO plasmids (Invitrogen) were used to generate stable tetracycline-inducible HEK293 cell lines following manufacturer's protocol. pBABE-puro constructs were used to generate protein expressions similar to endogenous protein levels. Rescue constructs harbouring resistance against *OTUB1* siRNAs *(#1+3)* and *OTUB1 shRNA* were generated by adding silent mutations. For bacterial expression, constructs were cloned into pGEX6p or pET vectors with N- or C-terminal GST- or His$_6$- tags. For baculoviral expression, constructs were cloned into pFB- GST-expression vectors. Baculovirus was expressed in insect cells in order to produce post-translationally modified, biologically active recombinant proteins.

pGL2.11 3TP-Lux luciferase reporter construct was a kind gift from Joan Massagué. The pGL4.11 LUC2p-BRE (BMP-Response Element) and pGL4.11 LUC2p-CAGA (SMAD-Response Element) reporter constructs were constructed based on SMAD-binding sequences within *ID-1* (BMP-target gene) and *PAI-1* (TGFβ target gene) promoters respectively. All plasmids used in this thesis are listed in Table 2-2 and were generated by the DSTT cloning team.

All DNA constructs used were verified by DNA sequencing, performed by DNA Sequencing & Services using Applied Biosystems Big-Dye Ver 3.1 chemistry on an Applied Biosystems model 3730 automated capillary DNA sequencer. The details of all plasmids used in this thesis, which are publicly available to the research community worldwide, can be found on the following website: http://mrcppureagents.dundee.ac.uk/reagents-cdna-clones.

Table 2-2 Plasmids

Plasmid	DU number	Plasmid	DU number
pBABE puro ALK5	DU47035	pCMV-FLAG CK2α	DU42995
pBABE puro ALK5 K232R	DU47042	pCMV-FLAG CK2α D156A	DU47033
pBABEhygroFLAG-OTUB1 47-end sprot 1+3	DU42293	pCMVFLAG1-UBE2D1	DU42180
pBABEhygroFLAG-OTUB1 C91S sprot 1+3	DU42272	pCMVFLAG-UBC13	DU42326
pBABEhygroFLAG-OTUB1 sprot 1+3	DU42270	pCMV-HA-1 OTUB2	DU32797
pcDNA5-FRT/TO-GFP OTUB1	DU20859	pCMVHA-OTUB1 S16/18A	DU42530
pcDNA5-FRT/TO-GFP SMAD1	DU19336	pCMV-HA-OTUB1 S16/18E	DU42496
pcDNA5-FRT/TO-GFP SMAD3	DU19337	pet156P UBC13	DU15705
pcDNA5-FRT/TO-GFP SMAD6	DU19606	pET156P UBCH6	DU12803
pcDNA5-FRT/TO-GFP USP15	DU33581	pET156P UBCH7	DU12798
pCMV 3xFLAG ALK2	DU42353	pET28A OTUB1	DU19744
pCMV 3xFLAG ALK6	DU42354	pET28a(+) UBE2D1	DU4315
pCMV5 FLAG DU	DU44060	pET28-UBE2D2	DU20184
pCMV5 GFP DU	DU44062	pFBHTb Ube1	DU32888
pCMV5 HA DU	DU44059	pFBHTc Nedd4-2	DU4004
pCMV5-ALK3	DU42988	pGEX6P-1-ALK5 T204D	DU33585
pCMV5-FLAG PIM1	DU1453	pGEX6P-1-OTUB1	DU19741
pCMV5-FLAG PIM1 D277A	DU5245	pGEX6P-1-OTUB1 47-271	DU20885
pCMV5-FLAG SMAD3 S423A S425A	DU37860	pGEX6P-1-OTUB1 C91S	DU20873
pCMV5-FLAG SMAD3 S423D S425D	DU37862	pGEX6P-1-OTUB1 D88A	DU41084
pCMV5-FLAG SMAD3 T179A S/204/208/213/423/425/A	DU37861	pGEX6P-1-OTUB1 D88A H265A	DU41086
pCMV5-FLAG SMAD3 T179E S/204/208/213/423/425/D	DU37885	pGEX6P-1-OTUB1 H265A	DU41065
pCMV5-FLAG-1 SMAD1	DU19264	pGEX6P-1-OTUB1 K71R	DU41360

Plasmid	DU number	Plasmid	DU number
pCMV5-FLAG-1 SMAD2	DU19306	pGEX6P1-OTUB1 S16/18A	DU42396
pCMV5-FLAG-1 SMAD3	DU19307	pGEX6P1-OTUB1 S16/18A	DU42396
pCMV5-FLAG-1 SMAD4	DU19309	pGEX6P1-OTUB1 S16A	DU42397
pCMV5-FLAG-1 SMAD6	DU19599	pGEX6P1-OTUB1 S18A	DU42398
pCMV5-FLAG-1 SMAD7	DU19221	pGEX6P1-OTUB1 T134R	DU42189
pCMV5-FLAG-2xFlag-ALK3	DU42276	pGEX6P-1-SMAD1	DU19269
pCMV5-FLAG-CK2 α'	DU24467	pGEX6P-1-SMAD2	DU19418
pCMV5-HA ALK3	DU19704	pGEX6P-1-SMAD2d3	DU19371
pCMV5-HA ALK3 D380A	DU19717	pGEX6P-1-SMAD3	DU19399
pCMV5-HA OTUB1	DU19616	pGEX6P-1-SMAD4	DU19398
pCMV5-HA OTUB1 C91S	DU41008	pGeX6P1-SMAD4 S221A	DU42764
pCMV5-HA OTUB1 D88A	DU41054	pGEX6P1-SMAD4 S221A S483A	DU42804
pCMV5-HA OTUB1 D88A C91S H265A	DU37473	pGeX6P1-SMAD4 S483A	DU42765
pCMV5-HA OTUB1 D88A H265A	DU41055	pGEX6P-1-SMAD6	DU12813
pCMV5-HA OTUB1 H265A	DU41021	pGEX6P-1-SMAD7	DU12443
pCMV5-HA OTUB1 K71R	DU41333	pGEX6P-1-UBE2D1/UBCH5a	DU4151
pCMV5-HA Ubiquitin	DU3650	pGEX6P-1-USP15	DU19772
pCMV5-HA USP11	DU19619	pGEX6P-2-NEDD4.2b1	DU8073
pCMV5-HA USP15	DU19760	pGL4.11 LUC2p-BRE	DU19945
pCMV5-HA USP15 C269S	DU33767	pGL4.11 LUC2p-SRE	DU19948
pCMV5-HA-1 OTUB1 47-end	DU37633	pSUPER.retro.puro-OTUB1 siRNA.2	DU19913
pCMV5-HA-2 NEDD4-2B	DU19847		

2.1.4 qRT-PCR primers

Human qRT-PCR primers were designed using PerlPrimer® with a melting temperature between 58-62 °C. For each primer the integrity and melting curve were determined. All primers are 20-24 bases long with an overlap of seven bases at the intron/exon boundary, producing an amplicon of 100-300 bases. The primers were ordered from Invitrogen. All DNA oligonucleotides used in this thesis are listed in Table 2-3.

Table 2-3 qRT-PCR primers

Target	Sequence (5'-3')
CTGF	forward: GGAGATTTTGGGAGTACGG reverse: TACCAATGACAACGCCTCCT
FoxO4	forward: TTGGAGAACCTGGAGTGTGACA reverse: AAGCTTCCAGGCATGACTCAG
GAPDH	forward: TGCACCACCAACTGCTTAGC reverse: GGCATGGACTGTGGTCATGAG
H4	forward: CGGGATAACATTCAGGGTATCACT reverse: ATCCATGGCGGTAATGTCTTCCT
HPRTI	forward: TGACACTGGCAAAACAATGCA reverse: GGTCCTTTTCACCAGCAAGCT
ID-1	forward: AGGCTGGATGCAGTTAAGGG reverse: GACGATCGCATCTTGTGTCG
OTUB1	forward: ACAGAAGATCAAGGACCTCCA reverse: CAACTCCTTGCTGTCATCCA
PAI-1	forward: AGCTCCTTGTACAGATGCCG reverse: ACAACAGGAGGAGAAACCCA
RPLI3A	forward: CTGGAGGAGAAGAGGAAAGAGA reverse: TGAGGACCTCTGTGTATTTGTCAA
SMAD6	forward: CCATCAAGGTGTTCGACTTC reverse: TTGTTGAGGAGGATCTCCAG
USP11	forward: GTGTTCAAGAACAAGGTTGG reverse: CGATTAAGGTCCTCATGCAG
USP15	forward: GACCCATTGATAACTCTGGAC reverse: TGTTCAACCACCTTTCGTG
xVENT1	forward: TTCCCTTCAGCATGGTTCAAC reverse: GCATCTCCTTGGCATATTTGG

2.1.5 siRNA oligonucleotide sequences

siRNA oligonucleotides were purchased from Sigma-Aldrich or Dharmacon and the sequences are listed in Table 2-4.

Table 2-4 siRNA oligonucleotides

Target	Sequence (5'-3')
CK2 (#1)	human: GCUGGUCGCUUACAUCACU
CK2 (#2)	human: GGAAGUGUGUCUUAGUUAC
CK2 (#3)	human: AACAUUGUCUGUACAGGUU
CK2 (#4)	human: GCAUUUAGGUGGAGACUUC
FoxO4	human: CCCGACCAGAGAUCGCUAA mouse: GCAAGUUCAUCAAGGUUCA
OTUB1 (#1)	human: GCAAGUUCUUCGAGCACUU mouse: GAACCCAUGUGCAAGGAGA
OTUB1 (#3)	human: CCGACUACCUUGUGGUCUA mouse: CAAUUGAAGACUUCCACAA
OTUB1 shRNA	human and mouse: GCAAGTTCTTCGAGCACTT
USP11	human: GAUUCUAUUGGCCUAGUAU
USP15 (#1)	human: CUCUUGAGAAUGUGCCGAU mouse: GAACUACUGGCUUUCCUGU
USP15 (#2)	human: CACAAUAGAUACAAUUGAA mouse: CCUUAUUGAUGAGUUGGAU
USP15 (#3)	human: CACAUUGAUGGAAGGUCAA mouse: GGUAUUGUCCAAAUUGUAA
USP15-MO	*Xenopus*: CGCCCTCCGCCATCTTACTCACTT-Lissamine
Control-MO	*Xenopus:* CCTCTTACCTCAGTTACAATTTATA-Lissamine

2.1.6 Proteins

For recombinant protein expression in bacteria, plasmids listed in Table 2-2 were transformed into BL21 *Escherichia coli* cells and most of the N-or C-terminal GST or His$_6$-tagged proteins were expressed and purified by the Protein Production Team (DSTT) or Knebel group. Free ubiquitin and FLAG-ubiquitin, as well as polyubiquitin chains of different linkages were purchased from Boston Biochem. ALK2, ALK3 and ALK6 were purchased from Carna Biosciences.

2.1.7 Antibodies

All primary antibodies employed in this thesis are listed in Table 2-5. In-house antibodies raised in sheep or rabbit were purified by the DSTT using standard protocols. Human recombinant SMAD1 (aa 141-268) polypeptide,

ALK3 (aa 200-end) polypeptide, ALK5 (aa 142-172) polypeptide, full length OTUB1, full length USP15, full length GFP, or OTUB1 (aa 10-22) polypeptide (KQEPLG<u>S</u>DSEGVN) were used as immunogens to generated the respective antibodies.

For production of phospho-specific antibodies, the phospho-peptides were first conjugated to bovine serum albumin (BSA) and keyhole limpet haemocyanin (KLH), whereas for the production of antibodies against total proteins, bacterially expressed GST tag proteins, emulsified in Freund's adjuvant, were injected into sheep. A pre-immune bleed was taken on the same day as the first injection of antigen. Each animal was immunised every 28 days up to four times. Seven days after the injections, a blood sample was collected. Each blood sample was allowed to clot at 4 °C for 16 hours, was then centrifuged for 1 hour at 1500 g at 4 °C and decanted though glass wool. For serum purification, the blood sample was heated for 20 min at 56 °C and filtered (0.45 μm). The anti-serum was subsequently diluted 1:1 in 50 mM Tris/HCl pH 7.5, 2% Triton X-100. In order or minimise the cross reactivity of the antibodies present in the anti-serum with GST, the GST antibodies were depleted using activated CH Sepharose beads coupled to GST. The GST cleared flow-through was affinity purified against the relevant antigen. For the purification of phospho-specific antibodies, the antibodies purified on the column containing the phosphopeptide immunogen were passed through a peptide column made with the non-phosphorylated form of the peptide immunogen. The antibodies that did not bind to the non-phosphorylated peptide column were collected and used. Antibodies were eluted with 50 mM glycine pH 2.5 and were then dialyzed for 16 hours in PBS.

The phospho-antibodies stated in Table 2-5 are specific to the following residues: anti-phospho-S463/465 SMAD1 (SMAD1-TP), anti-phospho-S465/467 SMAD2 (SMAD2-TP), anti-phospho-S423/425 SMAD3 (SMAD3-TP), anti-phospho-T179 SMAD3 (SMAD3-LP), anti-phospho-S16 OTUB1.

Species-specific HRP-coupled secondary antibodies (1:5000) were obtained from Thermo Scientific and HRP-coupled light chain specific secondary antibodies (1:10000) were purchased from Jackson Immuno Research. Rabbit anti-sheep IRDye 800CW and goat anti-mouse IRDye 680LT were from LI-COR. Alexa Fluor® 488 donkey anti-sheep IgG (A11015) and Alexa Fluor® 594 goat anti-rabbit IgG (A11012) were used 1:1000 for immunofluorescence and purchased from Invitrogen.

Table 2-5 Antibodies

Antibody	Product reference	Source	Conditions	
ALK3	DSTT S985C	sheep	1:1000	Milk
ALK5	DSTT S426D	sheep	1:1000	Milk
BIRC6	Cell Signalling #8756	rabbit	1:1000	Milk
Caspase 3	Cell Signalling #9662	rabbit	1:1000	Milk
CK2	Abcam ab10466	rabbit	1:1000	Milk
E-cadherin	Cell Signalling #3195	rabbit	1:1000	Milk
Fibronectin	Sigma-Aldrich F3648	rabbit	1:2000	Milk
FLAG-M2 HRP	Sigma-Aldrich A 8592	mouse	1:2000	Milk
GAPDH	Cell Signalling #2118	rabbit	1:5000	Milk
GFP	DSTT S268B	sheep	1:2000	Milk
GST HRP	Abcam ab3416	rabbit	1:5000	Milk
HA HRP	Roche 12 013 819 001	rat	1:2000	Milk
Histone 2B-ub	Cell Signalling #5546	rabbit	1:1000	Milk
LAMIN A/C	Cell Signalling #2032	rabbit	1:1000	Milk
Na$^+$/K$^+$-ATPase	Cell Signalling #3010	rabbit	1:1000	Milk
O-GlcNAc	Abcam ab2739	mouse	1:1000	BSA
OGT	Santa Cruz sc-32921	rabbit	1:1000	Milk
OTUB1	DSTT S104D, S300D, S499D	sheep	1:1000	Milk
OTUB1	Abcam ab82154	goat	1:1000	Milk
OTUB1 pS16	DSTT R3383	rabbit	1:1000	BSA
PARP	Cell Signalling #9542	rabbit	1:1000	Milk
Phalloidin	Invitrogen A12379	-	1: 50 used for IF	
SMAD1	DSTT S618C	sheep	1:1000	Milk

Antibody	Product reference	Source	Conditions	
SMAD1/5/8-TP	Cell Signalling #9511	rabbit	1:1000	Milk
SMAD2/3	Cell Signalling #8658	rabbit	1:2000	Milk
SMAD2-TP	Cell Signalling #3101	rabbit	1:1000	Milk
SMAD3-LP	Rockland 600-401-C48S	rabbit	1:1000	Milk
SMAD3-TP	Rockland 600-401-919	rabbit	1:2000	Milk
SMAD4	Cell Signalling #9515	rabbit	1:1000	BSA
SMAD7	R&D Systems MAB2029	mouse	1:1000	Milk
tubulin	Calbiochem DM1A	mouse	1:2000	Milk
Ub K-48	Millipore 05-1307	rabbit	1:1000	BSA
Ub K-63	Millipore 05-1313	mouse	1:1000	BSA
UBE2D	Santa Cruz sc-15000	goat	1:1000	Milk
UBE2N	Cell Signalling #6999	rabbit	1:1000	Milk
Ubiquitin	Dako Z 0458	rabbit	1:1000	Milk
USP15	DSTT S844C	sheep	1:1000	Milk

2.2   Methods

2.2.1 Mammalian cell culture

2.2.1.1 Cell Culture

HaCaT, HEK293, U2OS, C2C12, A172, HeLa, MDA-MB-231, COS-1, G361, U87, RPE-1, NMuMG, LoVo and SW620 cells were cultured in Dulbecco's modified Eagle's medium (DMEM) supplemented with 10% fetal bovine serum (FBS), 2 mM L-glutamine, 100 units/ml penicillin and 100 µg/ml streptomycin. G361 and U87 cells were supplemented with 1 mM sodium pyruvate and 0.1 mM non-essential amino acids (NEAA). NMuMG cells were supplemented with 5 µg/ml insulin. LoVo and SW620 cells were supplemented with 4.5 g/L glucose. HT29 and MCF7 cells were grown in Eagle's Minimum essential medium (EMEM) supplemented with 2 mM L-glutamine, 100 units/ml penicillin, 100 µg/ml streptomycin, 1% NEAA, 1 mM sodium pyruvate and 10% FBS. NCI-H727, NCI-H441, HCT15, Ramos, ZR-75-1 and T47D cells were grown in RPMI-1640 supplemented with 10% FBS, 2 mM L-glutamine, 100 units/ml penicillin and 100 µg/ml streptomycin. ZR-75-1 were supplemented with 1 mM sodium pyruvate and 25 mM HEPES. T47D cells were

supplemented with 4.5 g/L glucose. RPE-1, ARPE-19, SW480 and BT-474 cells were grown in DMEM:Ham's F12 (1:1) medium supplemented with 2 mM L-glutamine, 10% FBS, 100 units/ml penicillin and 100 µg/ml streptomycin. BT-474 cells were supplemented with 5 µg/ml insulin. All cells were maintained at 37 ^{o}C in a humidified atmosphere with 5% CO_2.

Stable cell lines infected with pBABE-puro retroviral constructs or pSUPERIOR-puro retroviral shRNA constructs were supplemented with 2 µg/ml puromycin. Stable CAGA (TGFβ responsive) or BRE (BMP responsive) luciferase reporter C2C12 cells were selected in 0.7 mg/ml G418.

Cells were passaged at 80-90% confluency. For passaging, cells were washed once with sterile PBS and then incubated with trypsin/EDTA to facilitate cell disassociation. Cells were returned to a 37 ºC incubator for 5-15 min, depending on the adherence of the cell line. Detached cells were resuspended in their corresponding culture media to a final volume of 10 ml in a 10 cm culture dish. All procedures were carried out in aseptic conditions meeting biological safety category 2 regulations.

2.2.1.2 Generation of primary cells

Primary cells (mouse embryonic fibroblasts (MEFs) and bone marrow derived macrophages (BMDMs)) were generated from animals that were housed under specific pathogen free conditions in accordance with UK and EU regulations.

Wild type MEFs were isolated from decapitated embryos with red organs removed. The embryo was minced and resuspended in 1 ml trypsin and incubated at 37 °C for 15 min before the addition of 10 ml growth medium (DMEM supplemented with 10% heat-inactivated FBS (56 °C for 30 min), 2 mM

L-glutamine, 100 units/ml penicillin and 100 µg/ml streptomycin). Cells were plated and allowed to attach overnight before being washed with fresh medium to remove debris. Growth media was additionally supplemented with 1 mM sodium pyruvate and 0.1 mM NEAA. ALK5-/- MEF cells were a kind gift of G. Inman (Dundee).

BMDMs were generated by flushing femurs from female mice with PBS. Red blood cells were lysed in ammonium chloride lysis buffer (155 mM NH_4Cl, 10 mM $NaHCO_3$, 0.1 µM EDTA, pH 7.3). Cells were then pelleted by centrifugation and cultured on bacterial grade plastic plates for 7 days in DMEM supplemented with 10% heat-inactivated FBS (56 °C for 30 min), 2 mM L-glutamine, 100 units/ml penicillin, 100 µg/ml streptomycin media and 5 ng/ml recombinant M-CSF (macrophage colony-stimulating factor). Cells were then detached by scraping in versene and re-plated on tissue culture treated petri dishes. All procedures were carried out in accordance with University of Dundee and United Kingdom Home Office regulations (Pattison *et al.*, 2012, Wiggin *et al.*, 2002).

2.2.1.3 Freezing/thawing of cell lines

Sub-confluent cells were trypsinised and centrifuged at 800 rpm for 5 min prior to resuspension in freezing media (90% FBS, 10% DMSO). 1 ml aliquots were stored in cryovials in a Mr Frosty freezing container at -80 °C prior to long-term storage in liquid nitrogen. To thaw the cells, cryovials were placed in a 37 °C water bath for 2 min and cells were transferred to a T25 flask containing 5 ml of appropriate culture medium.

2.2.1.4 Mouse tissue isolation

Tissues from mice were snap frozen in liquid nitrogen and ground with mortar and pestle. Pulverised tissues were resuspended in tissue lysis buffer (10 mM Tris/HCl pH 8, 150 mM NaCl, 1 mM EDTA, 1% NP40, 0.1% SDS, 1 tablet of complete protease inhibitors per 25 ml lysis buffer) and incubated on ice for 30 min before centrifugation. The cleared extracts were processed as described for cell extracts.

2.2.1.5 Treatment of cells with inhibitors and cytokines

The inhibitors used in this thesis are listed in Table 2-6. All compounds were resuspended in DMSO and used as indicated in Table 2-6 or figure legends. Human recombinant BMP_2, $TGF\beta_1$ or Activin A (R&D Systems) were resuspended in 4 mM HCl, 0.1% BSA. Cells were serum starved for 16 hours at 37 ^{o}C prior to ligand treatment with BMP_2 (6.25 ng/ml or 25 ng/ml), $TGF\beta_1$ (50 pM) or Activin A (20 ng/ml) for 1 hour (or indicated time points).

Table 2-6 Inhibitors

Inhibitor	Molecular target	Dose	Source
4Ac-5S-glcNAc	OGT	10 µM, 16 h	S. Pathak, Dundee, UK
Bafilomycin A1	V-ATPase	100 nM, 3 h	Sigma-Aldrich
Bortezomib	proteasome	10 µM, 3 h	LC laboratories
Cycloheximide	80S ribosome	20 µM, 21 h	Sigma-Aldrich
GlcNAcstatin G	OGA	2 µM, 16 h	S. Pathak, Dundee, UK
Iodoacetamide	DUBs	50 mM	Sigma-Aldrich
K66	CK2	10 µM, 4 h	Merck Millipore
Lactacystin	proteasome	10 µM, 3 h	Sigma-Aldrich
LDN189193	ALK2/3/6	100 nM, 1 h	DSTT
LY294002	PI3K	10 µM, 4 h	DSTT
MG132	proteasome	10 µM, 3 h	Calbiochem
Quinalizarin	CK2	10 µM, 4 h	G. Cozza, Padova, Italy
SB505124	ALK4/5/7	1 µM, 1 h	Sigma-Aldrich
TDB	CK2	10 µM, 4 h	G. Cozza, Padova, Italy

2.2.1.6 Cell transfections

For plasmid transfections, cells were grown to 50-60% confluence and were transfected using 25 µl of 1 mg/ml polyethylenimine (PEI, Polysciences) in 1 ml DMEM up to 10 µg of plasmid DNA. The mixture was vortexed, left at room temperature for 15 minutes and added drop-wise to cells in a 10 cm dish containing 9 ml media. The media was replaced 16 hours post-transfection and the cells were lysed after 48 hours. Plasmids used for transfections are stated in Table 2-2.

For siRNA oligonucleotide transfections, the cells were transfected during attachment. 30 µl TransFectin^{TM} (BioRad) and 300 pM of siRNA (per 10 cm dish) were mixed in 2 ml OptiMEM (Invitrogen). After incubating for 15 min the solution was added to the cells and cells were lysed 48 hours post-transfection. *FoxO4* siRNA was used as a control as it is known not to interfere with the TGFβ/BMP pathway (Sapkota *et al.*, 2006, Al-Salihi *et al.*, 2012a). The oligonucleotide sequences of the siRNAs are listed in Table 2-4.

2.2.1.7 Luciferase reporter assays

C2C12 cells, stably expressing CAGA or BRE luciferase reporter constructs were seeded onto 12-well plates in triplicate and transfected with appropriate siRNA or pCMV5-HA constructs. 36 hours post-transfection, cells were stimulated with TGFβ$_1$ (50 pM) or BMP$_2$ (25 ng/ml) for 6 hours and lysed in passive lysis buffer (Promega). To assay the luciferase reporter activity, the lysates (10 µl) were mixed with luciferase assay substrate (50 µl) (Dual-Luciferase™ kit, Promega) and luciferase activity was measured on a MicroLumat plus LB 96V luminometer (Berthold technologies). The Luciferase counts were normalised to the protein concentration and averaged.

2.2.1.8 Retroviral infection

A retroviral system was used to generate cell lines that stably express proteins at comparable to their levels to endogenous expression, or to introduce shRNA. H29 cells (stably integrated with CMV-Gag/Pol and CMV-VSVG) were cultured in growth media supplemented with 20 ng/ml doxycycline, 2 µg/ml puromycin and 0.3 mg/ml G418. The cells were grown to sub-confluency in a 15 cm dish and transfected using 75 µl PEI in 2 ml DMEM and 25 µg of plasmid DNA: pRetro SUPERIOR shRNA control or OTUB1 shRNA, as well as pBABE constructs (pBABE-puro control, OTUB1 or mutant constructs harbouring silent mutations for protection against human *iOTUB1#1* and *#3* siRNAs, or pBABE-puro ALK5 and pBABE-puro ALK5 K232R). Cells were transfected in 10 ml of growth media supplemented with 1% sodium pyruvate. After 48 hours, the virus containing media was filtered (20 µm) and added to 60% confluent target cells in the presence of 8 µg/ml polybrene. Target cells were selected in growth media containing 2 µg/ml puromycin 24 hours post-viral infection.

2.2.1.9 Generation of tetracycline-inducible Flp-IN® HEK293 cells

FlpIN TRex HEK293 cell lines (Invitrogen) were maintained in growth media supplemented with blasticidin (15 µg/ml) and zeocin (100 µg/ml). Zeocin and blasticidin were added to select for the FLP recombination target (Frt/TO) sites and tetracycline repressor sequence respectively. To generate stably expressing tetracycline-inducible GFP-constructs (GFP, GFP-SMAD1, GFP-SMAD3, GFP-SMAD6, GFP-OTUB1 and GFP-USP15) the cells were transfected with the plasmid of interest (pcDNA/Frt/TO, 1 µg) and pOG44 (9 µg), which encodes the FLP recombinase that leads to site specific recombination of the sequence of interest, using PEI. The cells were selected in

growth media containing blasticidin (15 µg/ml) and hygromycin B (100 µg/ml) 48 hours post-transfection. Hygromycin B selection was used to ensure the correct integration of the sequence of interest. GFP-protein expression was induced with 20 ng/ml doxycycline for 16 hours prior to lysis.

2.2.1.10   Cell lysis

For lysis, PBS washed cells were scraped on ice in lysis buffer (50 mM Tris/HCl pH 7.5, 0.27 M sucrose, 150 mM NaCl, 1 mM EGTA, 1 mM EDTA, 1 mM sodium orthovanadate, 1 mM sodium β-glycerophosphate, 50 mM sodium fluoride, 5 mM sodium pyrophosphate, 1% Triton X-100, 0.5% Nonidet P-40) supplemented with complete protease inhibitors (1 tablet per 25 ml) and 0.1% β-mercaptoethanol, or 50 mM iodoacetamide.

For apoptosis assays, cells were lysed in RIPA lysis buffer (50 mM Tris/HCl pH 8.0, 150 mM NaCl, 1% Triton X-100, 0.5% sodium deoxycholate, 0.1% SDS, 0.5% Tween-20, 1 tablet of complete protease inhibitors per 25 ml lysis buffer).

When the chemical cross-linking agent Dithiobis (succinimidyl propionate) (DSP) was used, cells were lysed in HEPES lysis buffer (40 mM HEPES pH 7.4, 120 mM NaCl, 1 mM EDTA pH 8.0, 10 mM sodium pyrophosphate, 50 mM sodium fluoride, 1 mM sodium orthovanadate, 5 mM sodium pyrophosphate, 1% (v/v) Triton X-100, complete protease inhibitors) containing 2.5 mg/ml DSP. Cell extracts were incubated at 4 °C for 30 min before cross-linking was quenched with Tris/HCl pH 7.5 at a final concentration of 0.2 M. Extracts were further incubated for 30 min at 4 °C. Lysates were then centrifuged for 10 min at 4 ºC, 14000 rpm and processed immediately or snap frozen in liquid nitrogen and stored at -80 ºC.

For mRNA isolation, cells were processed using an RNA extraction kit according to the manufacturer's instructions (Qiagen RNeasy kit).

2.2.1.11 XTT Cell proliferation assay

The XTT cell proliferation assay kit from ATCC was used to monitor HaCaT cell proliferation. HaCaT cells (5000 cells/ml) were seeded into low evaporation 96 well tissue culture plates. Growth media, supplemented with 2 µg/ml puromycin to select for HaCaT control (puromycin empty vector) or HaCaT shRNA OTUB1 cells, was exchanged daily and supplemented with or without 50 pM TGFβ$_1$. Every 24 hours one set of cells was incubated for 4 hours with XTT dye to detect differences in cellular metabolic activities and the absorbance measured at 480 nm on a microtiter plate reader. Cell proliferation was measured for 8 days and performed in triplicate.

2.2.1.12 Alkaline phosphatase assay

C2C12 cells were transfected with siRNAs against mouse *USP15* or mouse *FoxO4* (300 pM each) using transfectin reagent and grown in DMEM with 5% FBS. 48 hours post-transfection 100 ng/ml BMP$_2$ was added for 48 or 96 hours and cells were lysed using CelLytic reagent. The protein concentration was determined using Bradford and equal protein amounts were used to detect alkaline phosphatase activity. Alkaline phosphatase activity detection was carried out in accordance with the manufacturer's protocol (Sigma). In brief, cell extracts were diluted in assay buffer and fluorescent substrate (4-methylumbelliferyl phosphate disodium salt) was added. Fluorescence was detected using a fluorescent plate reader (PHERAstar) at 350 nm excitation and 460 nm emission.

2.2.1.13   Epithelial to mesenchymal transition (EMT) assay

NMuMG cells were grown on glass cover slips or in 6 cm cell culture dishes. SB505124 (1 μM) was added 1 hour prior to TGFβ$_1$ (75 pM) stimulation for 24 or 48 hours. Cells were either lysed and analysed by immunoblotting (section 2.2.3.8) or fixed and evaluated via immunofluorescence microscopy (section 2.2.3.9) using antibodies against known markers of EMT.

2.2.1.14   Cell migration assay

HaCaT cells stably expressing control shRNA or OTUB1 shRNA were seeded to near confluency into migration inserts (Ibidi) and transfected with *FoxO4* or *OTUB1* siRNAs respectively. After 24 hours the inserts were removed, the cells were serum starved for 4 hours and stimulated with TGFβ$_1$ (50 pM). Cellular migration was monitored and pictures taken every 24 hours.

2.2.1.15   *Xenopus* studies

Xenopus laevis embryos were obtained by *in vitro* fertilisation and staged according to Nieuwkoop and Faber (Niewkoop and Faber, 1975). Lissamine coupled USP15 (xUSP15-*MO*) and control antisense morpholino (control-*MO*) oligonucleotides (Table 2-4) were obtained from GeneTools. The oligonucleotides were dissolved in distilled water and stored at 4 °C. Animal cap assays were carried out as described previously (Smith, 1993).

For *Xenopus laevis* experiments, embryos were cultured in 0.1x Normal Amphibian Medium (Slack, 1984) for indicated times. Ten embryos per time point were lysed in 100 μl of PhosphoSafe reagent supplemented with complete protease inhibitors and extracted with an equal volume of FREON to remove yolk proteins. Samples were reduced by adding 4x SDS sample buffer with 10%

β-mercaptoethanol and boiled for 5 min. Samples were separated on 7.5% TGX gels and then transferred to PVDF membranes. Membranes were blocked for 1 hour and then incubated in primary antibody in PBS-T (PBS, 0.1% Tween 20) overnight at 4 °C. Blots were washed 3x in PBS-T then incubated with a combination of IRDye 680LT and 800CW labelled secondary antibodies (1:15000 in PBS-T supplemented with 0.02% SDS) for 1 hour. Washed blots were imaged with a LI-COR Odyssey scanner followed by image analysis using Image Studio. All *Xenopus laevis* studies were carried out by K. Dingwell at NIMR London.

2.2.2 General molecular biology

2.2.2.1 DNA and RNA concentration measurement

The absorbance of isolated DNA or mRNA in aqueous solution was measured at 260 nm with a NanoDrop® spectrophotometer, after calibration with nuclease-free water, according to the manufacturer's instructions.

2.2.2.2 Plasmid transformation, amplification and isolation

For each transformation, competent *E. coli* DH5α or BL21 cells from -80 °C glycerol stocks were thawed on ice. Plasmid DNA (10 ng) was added to the cells and incubated on ice for 2 min. Cells were heat-shocked at 42 °C for 1 min to facilitate DNA uptake. After 2 min incubation on ice, cells were plated onto LB agar plates containing 100 µg/ml ampicillin and incubated for 16 hours at 37 °C. For plasmid amplification, one transformed colony was used to inoculate 250 ml LB media containing 100 µg/ml ampicillin. Cultures were grown to stationary phase overnight at 37 °C in a shaking incubator. The transformed cells were pelleted by centrifugation (3000 rpm, 10 min, 4 °C). The plasmid DNA was

isolated using Qiagen DNA Maxi Kit according to the manufacturer's instructions.

2.2.2.3 Restriction enzyme digests of plasmid DNA

Restriction digests were carried out using 0.5 μg of DNA with 1 unit of restriction enzyme in the presence of the appropriate digestion buffer. Reactions were incubated at 37 °C for 3 hours and analysed by agarose gel electrophoresis.

2.2.2.4 Agarose gel electrophoresis

The size and the purity of DNA products were assessed by electrophoresis on 1% agarose gels. Each gel contained a 1:1000 dilution of SYBR Safe nucleotide gel stain. Gels were submerged in 1x TAE (40 mM Tris-acetate pH 8.0, 1 mM EDTA) running buffer. DNA (0.5 μg) was loaded onto a gel together with 1x DNA loading dye. 0.5 μg of a 1 kbp DNA ladder was used as a marker. Gels were run at 100 V for 30 min. The stained nucleotide complexes were visualised using a UV transilluminator.

2.2.2.5 DNA mutagenesis

DNA mutagenesis of all plasmids (Table 2-2) was performed by the DSTT cloning team using the QuikChange site directed mutagenesis method (Stratagene) with KOD polymerase (Novagen). DNA constructs were verified by DNA sequencing.

2.2.2.6 Real time quantitative reverse transcription PCR (qRT-PCR)

Cells were seeded in 6-well plates, transfected with siRNAs and serum starved for 16 hours prior to TGFβ$_1$ (50 pM) treatment. cDNA was made from 1 µg of the isolated RNA using the I-Script cDNA kit (BioRad) according to the manufacturer's protocol. qRT-PCR reactions were performed in quadruplicate according to the manufacturer's protocol in a CFX 384 Real time System qRT-PCR machine (BioRad). Each reaction included cDNA (2.5% of reverse transcriptase reaction) with forward and reverse primers (0.5 µM each) and 50% SYBR Green (BioRad). All primers were designed using PerlPrimer and purchased from Invitrogen (Table 2-3). The primer efficiency was determined and taken into account when evaluating the qRT-PCR data. The data was normalised to the geometrical mean of two housekeeping genes (GAPDH, HPRTI or RPLI3A) and the Pfaffl method (Pfaffl, 2001) was used to analyse the qRT-PCR data.

2.2.3 General biochemistry

2.2.3.1 Protein concentration measurement

The protein concentration was determined by the Bradford method (Bradford, 1976) with a spectrophotometer using Bradford protein assay reagent (Thermo Scientific). When Coomassie dye binds to proteins in acidic medium, the absorbance maximum shifts from 465 nm to 595 nm resulting in a colour change from brown to blue. A standard curve was prepared from a BSA standard solution at serial dilutions ranging from 0.125 mg/ml to 2 mg/ml. 5 µl of standard BSA solution or diluted cell extract were added to 200 µl Bradford reagent in a 96 well plate. This mixture, including a blank probe, was incubated

for 5 min at RT and the absorbance was measured with a spectrophotometer at 595 nm. All Bradford measurements were performed in triplicate.

2.2.3.2 Immunoprecipitation

Cleared cell extracts were further pre-cleared to minimise unspecific binding of proteins to the solid phase resins by incubating with agarose or protein-G Sepharose beads for 1 hour at 4 °C prior to immunoprecipitation (IP). The cleared extracts (2 mg for WB or 50 mg for mass spectrometry analysis) were then mixed with FLAG- or HA-agarose beads (Sigma-Aldrich), GFP-Trap agarose beads (Chromatek) or antibody/IgG-coupled protein G-Sepharose or Agarose beads for 2 hours at 4 ºC on a rotating platform. The flow-through was retained for Western blot analysis and the beads were washed twice in lysis buffer containing 0.4 M NaCl, and twice in buffer A (50 mM Tris/HCl pH 7.5, 0.1 mM EGTA). IP samples, as well as flow-through and input samples, were reduced in sodium dodecyl sulphate (SDS) sample buffer (62.5 mM Tris/HCl pH 6.8, 10% (v/v) glycerol, 2% (w/v) SDS, 0.02% (w/v) bromophenol blue) containing either 50 mM dithiothreitol (DTT) or 1% (v/v) β-mercaptoethanol and heated at 95 ºC for 5 min.

Where appropriate, lambda phosphatase (1 µM) was added to OTUB1 IPs resuspended in 50 µl buffer (50 mM HEPES, 100 mM NaCl, 0.01% Brij-35, 2 mM DTT, 1 mM $MnCl_2$, pH 7.5) and agitated at 30 °C for 30 min. IPs were then washed and processed as stated above.

2.2.3.3 Conjugation of antibodies to protein-G/A Agarose or Sepharose

The required volumes of protein G-Agarose/Sepharose beads were washed twice in PBS (1 ml) and the final volume was adjusted to 50% (v/v)

slurry before addition of antibodies. For each IP, 5 µg of antibody or IgG were added to 20 µl of protein G Agarose or Sepharose beads. This mixture was left on a shaker at 4 °C to allow conjugation of the antibodies to the beads. After 1 hour, the beads were washed twice in PBS and resuspended as 50% (v/v) slurry. The antibody-coupled beads were then ready to be used for IPs.

2.2.3.4 Subcellular fractionation

Subcellular fractionation was performed using the NE-PER (nuclear and cytoplasmic) kit or subcellular protein fractionation kit for cultured cells (Thermo Scientific) according to the manufacturer's instructions. The lysis buffers were supplemented with protease inhibitors (Roche). Fractions were reduced in SDS sample buffer as stated above.

2.2.3.5 Size exclusion chromatography

Unstimulated and TGFβ treated (50 pM, 1 hour) HaCaT cells were lysed in the presence of 50 mM iodoacetamide and filtered using Spin-X columns. The AKTA Explorer was operated according to manufacturer's instructions using Unicorn 4.1 software. 7 mg of protein extracts were injected into a Superdex S200 column (GE Health Care) which was equilibrated overnight with degassed and filtered buffer (50 mM Tris/HCl pH 7.5, 150 mM NaCl, 0.03% (v/v) Brij35). The samples were collected in 56 separate fractions (0.2 ml) at a flow rate of 0.15 ml/min. The fractions were reduced with SDS sample buffer and analysed by SDS-PAGE and immunoblotting.

2.2.3.6 Separation of proteins by SDS-PAGE

Three different sodium dodecyl sulphate polyacrylamide gel electrophoresis (SDS-PAGE) systems were used in this thesis. NuPAGE 4-12% Bis-Tris pre-cast gels (Invitrogen) were used for mass spectrometry applications and 4-20% TGX pre-cast gels (BioRad) were used to resolve ubiquitin chains. For all other experiments, the ATTO self-assemble gel system for gel electrophoresis was employed (ATTO). The SDS-PAGE gels were made by pouring the SDS-PAGE gel mix (0.375 M Tris/HCl pH 8.8, 0.1% (w/v) SDS, 10% (w/v) acrylamide and 0.075% (w/v) ammonium persulphate, 0.1% (v/v) TEMED) and allowing it to polymerise with 100% isopropanol on top (to level the surface). After 20 min, the isopropanol was removed and a stacking gel (0.125 M Tris/HCl pH 6.8, 0.1% (w/v) SDS, 4% (w/v) acrylamide, 0.075% (w/v) ammonium persulphate, 0.1% (v/v) TEMED) was poured on top of the set SDS-PAGE gel and a comb inserted. NuPAGE 4-12% Bis-Tris gels were run using MOPS or MES running buffer. BioRad 4-20% TGX pre-cast gels and ATTO gels were run using running buffer, which contained 25 mM Tris/HCl pH 8.3, 192 mM glycine and 0.1% (v/v) SDS. 5 µl of Precision Plus Protein Standards (BioRad) and 20 µg (or 80 µg for the detection of endogenous OTUB1 pS16) of protein extracts in SDS sample buffer were loaded for gel electrophoresis. Gel electrophoresis was performed at a constant voltage of 180 V for 1 hour for the NuPAGE Novex gels and 1 hour and 25 min for ATTO gels. BioRad 4-20% TGX pre-cast gels were run at 300 V for 20 min.

2.2.3.7 Coomassie staining of protein gels

Following SDS-PAGE, protein separation was visualised by in gel staining of the proteins using colloidal Coomassie Blue staining solution (Invitrogen)

according to the manufacturer's instructions. Gels were stained for 3 hours at RT with continual agitation on a rocking platform. Destaining was performed with deionised water until the background staining was reduced.

2.2.3.8 Immunoblotting (Western blots)

Reduced protein extracts or IPs were separated on 10% SDS-PAGE gels, 4-20% TGX gels or 4-12% NuPAGE bis-tris gels by electrophoresis (section 2.2.3.6) and transferred to methanol-activated polyvinylidene fluoride (PVDF) membranes (Whatmann). Protein transfer was performed in a Mini-Cell (BioRad) transfer system at 90 V for 1.5 hours in 1x transfer buffer (25 mM Tris/HCl pH 8.3, 192 mM glycine, 20% (v/v) methanol). Efficiency of the transfer was assessed by staining the membranes with Ponceau S solution. Membranes were blocked in 5% (w/v) non-fat milk in TBS-T (50 mM Tris-HCl pH 7.5, 150 mM NaCl, 0.2% Tween-20) for 1 hour at RT. The appropriate primary antibodies (Table 2-5) were diluted in 5% milk-TBS-T or 3% BSA-TBS-T and incubated for 16 hours at 4 °C. Membranes were washed in TBS-T three times for 10 min, before being incubated with the HRP-conjugated secondary antibodies in 5% milk-TBS-T for 1 hour at RT. After washing, detection was performed by enhanced chemiluminescence reagent (ECL luminescence, Thermo Scientific) followed by exposure to Medical X-Ray Film in the dark and development of the film using an SRX-101A automatic film processor (Konica Minolta).

2.2.3.9 Immunofluorescence microscopy (IF)

Cells were seeded onto poly-L-lysine treated glass cover slips in 6-well culture dishes and treated as described (starved for 16 hours and treated with TGFβ$_1$ (50 pM) or BMP$_2$ (6.25 ng/ml) treated for 1 hour, or for EMT 75 pM

TGFβ$_1$ for 24 or 48 hours). Cells were washed in PBS before fixation with 3.7% paraformaldehyde for 20 min at RT and washed a further three times in PBS before permeabilisation with 0.2% Triton X-100 in PBS for 12 min at RT. Cells were rinsed with PBS before being incubated for 1 hour in blocking solution (5% (v/v) normal donkey serum, 0.01% (v/v) fish skin gelatin, 0.1% (v/v) Triton X-100, 0.05% (v/v) Tween-20 in PBS). Primary antibodies (Table 2-5) were incubated for 16 hours in a humidified chamber at 4 °C. After thorough washes in PBS, cells were incubated with AlexaFluor® or Cyanine Cy5 secondary antibodies for 1 hour in the dark. Cells were washed three more times in PBS and once with deionised water before being mounted onto glass slides using ProLong® Gold mounting reagent (Life Technologies), which contained the nuclear stain 4',6-diamidino-2-phenylindole (DAPI). Slides were viewed using a Nikon Eclipse Ti microscope fitted with a 20x, 40x and 60x lens and a cooled charge-coupled device camera.

2.2.3.10 Purification of GST-tagged proteins from bacteria

Bacterial expression vectors (pGEX6P) encoding GST-tagged proteins were transformed into BL21 *E. coli* cells. To generate a starter culture, a single colony of the transformed BL21 bacteria was added to 50 ml LB/100 µg/ml ampicillin media and incubated overnight at 37 °C in a shaking incubator. The starter culture was then added to 1 L LB/100 µg/ml ampicillin media, and bacterial growth was monitored by measuring the optical density (OD) at 600 nm. Once the OD$_{600}$ reached 0.5, the expression of the GST-tagged protein was induced using 0.1 mM isopropyl β-D-1-thiogalactopyranoside (IPTG) for 16 hours at 16 °C. Bacteria were harvested by centrifugation in a Beckman J6 rotor (5000 rpm, 30 min, 4 °C). The pellet was resuspended in 30 ml bacterial lysis

buffer (50 mM Tris/HCl pH 7.5, 150 mM NaCl, 1% (v/v) triton-X-100, 0.02 mM EDTA, 0.02 mM EGTA, 0.2 mM PMSF, 1 mM benzamidine, 0.06% β-ME) sonicated (8x15 s bursts at 4 °C) and centrifuged (15000 rpm, 30 min, 4 °C). To immunoprecipitate the GST-tagged proteins, 1 ml equilibrated glutathione-Sepharose beads were added to the cleared extract and incubated for 1 hour at 4 °C with constant agitation. Beads were collected by centrifugation at 3000 rpm for 15 min at 4 °C. The beads were washed five times with bacterial wash buffer (50 mM Tris/HCl pH 7.5, 250 mM NaCl, 0.1 mM EGTA, 0.2 mM PMSF, 1 mM benzamidine, 0.1% β-ME, 0.03% Brij 35). GST-proteins were eluted from glutathione-Sepharose by adding an equal volume of glutathione elution buffer (20 mM glutathione, 50 mM Tris/HCl pH 7.5, 250 mM NaCl, 0.1 mM EGTA, 0.2 mM PMSF, 1 mM benzamidine, 0.1% β-ME, 0.03% Brij 35) for 5 min at 4 °C. The elution was repeated, both eluates combined and dialysed in 1 L buffer A using a Slide-A-Lyzer Cassette (Thermo Scientific) for 16 hours at 4 °C. The protein concentration was determined and the purity was verified by SDS-PAGE and Coomassie staining. Purified proteins were stored at -80 °C.

2.2.3.11 Purification of His$_6$-tagged proteins from bacteria

Bacterial expression vectors (pET) encoding His$_6$-tagged proteins were transformed into BL21 *E. coli* cells, expressed and lysed as described in (section 2.2.3.10). To immunoprecipitate the His$_6$-tagged proteins, 1 ml equilibrated Ni-NTA-agarose (Qiagen) beads were added to the clarified lysate and incubated for 1 hour at 4 °C with constant agitation. Beads were collected by centrifugation. The beads were washed five times with bacterial wash buffer (50 mM Tris/HCl pH 7.5, 0.02 mM EDTA, 0.02 mM EGTA, 0.2 mM PMSF, 1 mM benzamidine, 0.06% β-ME, 20 mM imidazole, 0.03% Brij 35) containing 0.5 M

NaCl and twice with bacterial wash buffer containing 150 mM NaCl. His$_6$-tagged proteins were eluted from Ni-NTA-agarose with bacterial wash buffer containing 150 mM NaCl and 300 mM imidazole. The eluted proteins were dialysed in 1 L buffer A using a Slide-A-Lyzer Cassette (Thermo Scientific) for 16 hours at 4 °C. The protein concentration was determined and protein purity was verified by SDS-PAGE and Coomassie staining. Purified proteins were stored at -80 °C.

2.2.4 *In vitro assays*

2.2.4.1 Peptide binding assay

Biotin-C6-RQTVTSTPCWIELHLNGPLQWLDKVLTQMGSPSVRCS$\underline{S}$M$\underline{S}$ (SMAD2-TP) (3 µg) was incubated with purified GST-OTUB1 (5 µg) or pre-cleared HaCaT cell lysate (150 µg) (with or without pre-treatment with TGFβ (50 pM, 1 hour)) in lysis buffer for 30 min, 30 °C, 900 rpm. As a control the phospho-peptide was additionally treated with lambda phosphatase (18 µM) in buffer (50 mM HEPES, 100 mM NaCl, 0.01% Brij-35, 2 mM DTT, 1 mM MnCl$_2$, pH 7.5). Streptavidin-Sepharose High Performance beads (GE Healthcare) were equilibrated in lysis buffer and 20 µl of 50% (v/v) slurry beads were added for 15 min, 30 °C, 1300 rpm. IPs were washed 6 times in lysis buffer with 0.4 M NaCl and twice in buffer A. Proteins were resolved by SDS-PAGE and immunoblotted.

2.2.4.2 *In vitro* ubiquitylation assays

In-cell ubiquitylation assays were performed in HEK293 cells by co-transfection as described in section 2.2.1.6.

In vitro ubiquitylation assays were performed with human recombinant E1 ubiquitin activating enzyme, E2 ubiquitin conjugating enzyme, E3 ubiquitin

ligase and SMAD proteins. Ubiquitylation assays of recombinant SMAD2 or FLAG-SMAD2/3/4 (immunoprecipitated from HEK293 cells treated with 50 pM TGFβ for 1 hour prior to lysis) were performed in ubiquitylation assay buffer (50 mM Tris-HCl pH 7.5, 5 mM $MgCl_2$, 2 µM ATP) with His_6-UBE1 (0.1 µM), the appropriate E2 (1 µM, or indicated concentrations), His_6-NEDD4L (1 µM) and ubiquitin (50 µM) in a total reaction volume of 20 µl for 1 hour at 30 °C on an IP-shaker. Ubiquitylation assays were stopped by adding SDS sample buffer containing 1% β-mercaptoethanol and heating at 95 °C for 5 min. Proteins were resolved by SDS-PAGE and immunoblotted.

2.2.4.3 *In vitro* E2~ub loading assays

For E2~ub loading assays, reactions were performed in 25 µl buffer (50 mM HEPES, 150 mM NaCl, 0.5 mM TCEP) using His_6-UBE1 (0.5 µg), UBE2D1/UBE2N (2 µg), FLAG-ubiquitin (2 µg), GST-OTUB1 (5.5 µg), His_6-NEDD4L (1.4 µg), SMAD3 (0.55 µg) and 2 µl Mg-ATP solution (2 mM ATP, 100 mM Mg-acetate). Protein solutions were mixed on an IP shaker before the addition of ATP for 10 minutes at 30 °C. After ATP addition protein mixtures were agitated for a further 10 min at 30 °C before terminating the reaction with 4x LDS sample buffer (not containing any reducing agents). 10 µl of each reaction was separated by SDS-PAGE. The gels were stained with Coomassie and imaged.

2.2.4.4 *In vitro* deubiquitylation assays

In-cell deubiquitylation assays were performed in HEK293 cells by co-transfection as described in section 2.2.1.6.

In vitro deubiquitylation assays were performed with human recombinant wild type or mutant GST-OTUB1 and GST-USP15. For chain-cleavage assays, DUBs (30 ng/µl) were incubated in DUB buffer (50 mM Tris/HCl pH 7.5, 5 mM DTT, 100 mM NaCl) with the indicated ubiquitin chains (0.13 µg/µl, K48 ub_{2-7}, K63 ub_{2-7}, K48 ub_2) on an IP-shaker for 1 hour at 30 °C.

In vitro DUB assays of *in vivo* polyubiquitylated FLAG-ALK3 or FLAG-SMAD2/3/4 (FLAG- SMAD2/3/4 were co-expressed with HA-NEDD4L and HA-ubiquitin in HEK293 cells, treated with 50 pM TGFβ and 10 µM Bortezomib for 3 hours and FLAG was immunoprecipitated) or *in vitro* polyubiquitylated SMAD2, SMAD3 or FLAG-SMAD2/3/4 were performed with indicated DUBs in DUB assay buffer at 30 °C on an IP-shaker. GST-USP15 or GST-OTUB1 (30 ng/µl) were added for 1 hour post substrate ubiquitylation. To monitor the ability of OTUB1 to inhibit ubiquitylation, it was added at the start of the ubiquitylation assay (time 0) (30 ng/µl, or at increasing concentrations (8-60) . The DUB assays were quenched by adding SDS sample buffer containing 1% β-mercaptoethanol and heating at 95 °C for 5 min Proteins were resolved by SDS-PAGE and immunoblotted.

2.2.4.5 *In vitro* kinase assays

To phosphorylate OTUB1 *in vitro,* 200 ng of kinase and 2 µg substrate were incubated in a total volume of 20 µl kinase assay buffer (50 mM Tris/HCl pH 7.5, 0.1% β-mercaptoethanol, 0.1 mM EGTA, 10 mM $MgCl_2$, 0.5 µM Microcystin-LR and 0.1 mM ($^{\gamma 32}$P-)ATP (500 cpm/pmole)) at 30 °C for 30 min. The kinase assay was stopped by adding SDS sample buffer containing 1% β-mercaptoethanol and heating at 95 °C for 5 min. The samples were resolved by SDS-PAGE and the gels were stained with Coomassie and dried. The

radioactivity was analysed by autoradiography and exposed to Hyperfilm for different lengths of time. For long exposures, the cassette was placed in -80 °C to enhance the autoradiographic signal. Films were developed using a Konica automatic developer. For identification of OTUB1 phosphorylation sites by mass spectrometry, wet gels were autoradiographed before excision of the bands (see section 2.2.5.4).

2.2.4.6 *In vitro* O-GlcNAcylation assay

In vitro O-GlcNAcylation assays of TAB1 or SMAD proteins (4 µM) were carried out in 20 µl assay volumes containing 1 µM O-GlcNAc transferase, 2 mM UDP-GlcNAc and the buffer (50 mM Tris/HCl pH 7.5, 1 mM DTT). Bacterially expressed O-GlcNAcase (cpOGA) (1 µM) was added as a negative control. The reactions were incubated for 90 min at 37 °C, 700 rpm, quenched by adding SDS sample buffer containing 1% β-mercaptoethanol and heated at 95 °C for 5 min. The samples were resolved by SDS-PAGE and the gels were stained with Coomassie or immunoblotted.

2.2.5 Mass spectrometry

2.2.5.1 Preparation of samples for mass spectrometry

For mass spectrometry analysis HEK293 cells expressing the protein of interest were lysed in HEPES lysis buffer (40 mM HEPES pH 7.4, 120 mM NaCl, 1 mM EDTA, 10 mM sodium pyrophosphate, 50 mM sodium fluoride, 1.5 mM sodium orthovanadate, 1% Triton X-100) supplemented with 0.5 µM microcystin-LR, 2.5 mg/ml DSP (in DMSO) and complete protease inhibitors (1 tablet per 25 ml). The lysate was incubated for 30 min on ice and DSP cross-linking reaction quenched by the addition of Tris/HCl pH 7.5 (200 mM final).

Lysates were then cleared by centrifugation (15000 rpm, 30 min) and filtration (0.45 µm). Subsequently, the lysates were incubated with Protein A-agarose beads (1 hour on a rotating platform at 4 ⁰C) to limit nonspecific binding. The cleared lysate (50 mg) was incubated with GFP-Trap beads (50 µl) for 4 hours on a rotating platform at 4 ⁰C. The beads were washed 4 times in complete lysis buffer containing 0.4 M NaCl and twice in 10 mM Tris/HCl pH 7.4. The beads were reconstituted in 1x LDS containing 0.1 M DTT, incubated at 37 ⁰C for 1 hour and heated at 95 ⁰C for 5 min. The samples were separated by gel electrophoresis and stained with Colloidal Coomassie.

2.2.5.2 In-gel digestion of proteins for mass spectrometry analysis

To minimise contamination, preparation steps for mass spectrometry were performed under a laminar flow hood (Model A3VB, Bassaire Limited). Disposable scalpels were used to excise the protein bands of interest from Coomassie-stained SDS-PAGE gels. Gel pieces were cut into 1 mm cubes and sequentially washed on a vibrating platform for 10 min in 0.5 ml with water, 50% acetonitrile (ACN), 100 mM NH_4HCO_3 and 50% acetonitrile/50 mM NH_4HCO_3. Disulphide bonds were reduced by incubation with 10 mM DTT/100 mM NH_4HCO_3 for 45 min at 65 °C, followed by alkylation with 50 mM iodoacetamide/100 mM NH_4HCO_3 for 30 min at RT in the dark. Gel pieces were repeatedly washed with 100 mM NH_4HCO_3 and 50% ACN /50 mM NH_4HCO_3 until colourless. Gel pieces were incubated in 0.3 ml ACN for 15 min at RT, the ACN was removed and the dehydrated gel pieces were completely dried in a SpeedVac. To digest the proteins in the gel pieces, 30 µl of 25 mM Triethylammonium bicarbonate (TEA) containing Trypsin (5 µg/ml) was added and the gel pieces incubated for 16 hours at 30 °C with constant agitation. 200

µl of ACN was added to the digest for 15 min at RT. Supernatants were transferred to clean Eppendorf tubes and subsequently dried using a SpeedVac. To maximise the peptide recovery, 100 µl 50% ACN/ 2.5% formic acid was added to the remaining gel pieces. The supernatant was combined with the first dried extract and the samples were vacuum-trap evaporated to complete dryness. Peptide samples were stored at -20 °C prior to analysis by mass spectrometry.

2.2.5.3 Peptide analysis by liquid chromatography-tandem mass spectrometry

The digested peptides were reconstituted in 5% ACN and 0.1% formic acid and injected into a nano liquid chromatography system coupled to a LTQ-orbitrap mass spectrometer. Data files were converted to MSM files and submitted to the in-house Mascot server. Data was searched against the International Protein Index human database with variable modifications allowing for phosphorylation of Serine/Threonine or Tyrosine residues and for Methionine oxidation, dioxidation or carboxy modification. Liquid chromatography-tandem mass spectrometry (LC-MS-MS) analysis was performed by Dr David Campbell and Robert Gourlay. Data analysis was performed using OLMAT (http://www.proteinguru.com/MassSpec/OLMAT).

2.2.5.4 Identification of phosphorylated peptides

Phosphorylated OTUB1 (see section 2.2.4.5) was digested as described above (section 2.2.5.2). The dried peptides were reconstituted in 5% ACN/ 0.1% TFA and injected into a 218TP5215 C_{18} column equilibrated in 0.1% TFA, with a linear ACN gradient at a flow rate of 0.2 ml/min and fractions of 100 µl

were collected. The major eluting peptides were analysed by LTQ-orbitrap mass spectrometer. To determine the phosphorylated residue in each $^{\gamma 32}$P-labelled peptide, the peptides were immobilised on a Sequelon-AA membrane and subjected to solid-phase Edman degradation as previously described (Campbell and Morrice, 2002). HPLC, LTQ-orbitrap mass spectrometry and Edman degradation was performed by Robert Gourlay.

2.2.6 Statistical analysis

All experiments have a minimum of three biological replicates. Luciferase experiments additionally have three and qRT-PCR experiments four technical repeats for each biological replicate. Data are presented as the mean with error bars indicating the standard deviation. Statistical significance of differences between experimental groups was assessed with Student's t-test or ANOVA with Bonferroni Correction. Differences in means were considered significant if $p<0.05$. Differences with $p<0.05$ were annotated as *, $p<0.01$ were annotated as ** and $p<0.001$ were annotated as ***. All Western blots shown are representatives.

3 OTUB1 enhances TGFβ signalling by inhibiting the ubiquitylation and degradation of active SMAD2/3

3.1 Introduction

Post-translational modifications of TGFβ pathway components play a critical role in fine tuning TGFβ-mediated cellular responses. SMAD proteins are the key cellular mediators of TGFβ signalling; hence, their activity has to be tightly regulated in order to control the potency of TGFβ signalling. A proteomic screen was performed in order to identify novel SMAD interactors that could regulate the TGFβ pathway (Figure 3-1). OTUB1 was identified as an interactor of TGFβ stimulated SMAD3 (Figure 3-4). Previously, nothing was known about the role of OTUB1 in the regulation of SMAD3 and the TGFβ pathway. Hence, the aim of this chapter was to characterise the role of OTUB1 in the TGFβ pathway and achieve a better understanding of the molecular mechanisms by which it regulated TGFβ signalling.
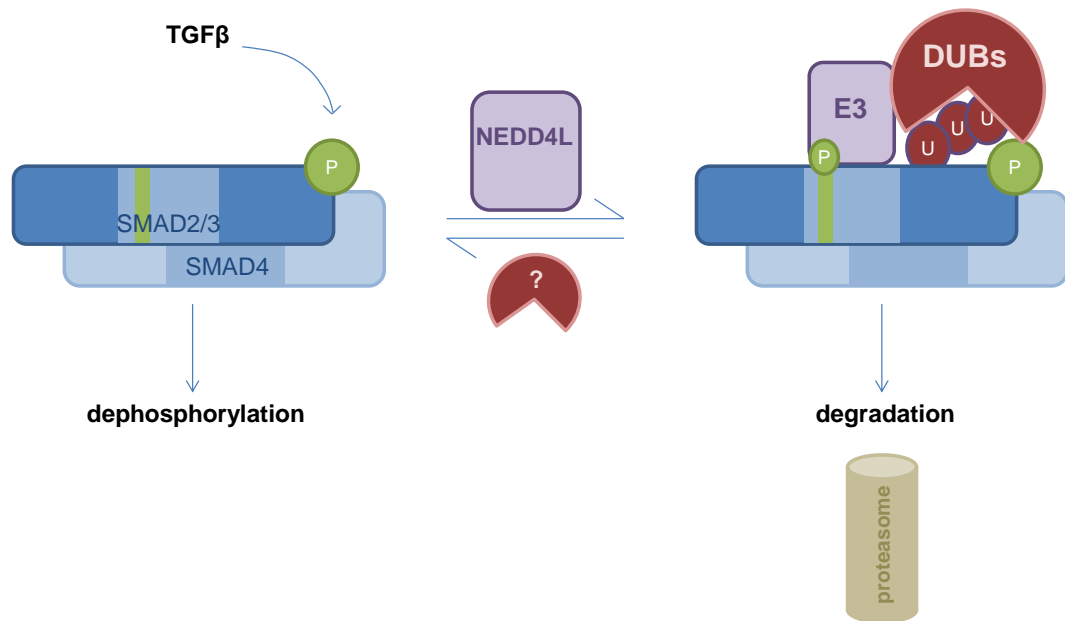
Figure 3-1 Regulation of R-SMADs by post-translational modifications

R-SMADs are activated through TGFβ induced tail-phosphorylation. R-SMAD activity can be curtailed either by dephosphorylation (section 1.3.1.2) or by ubiquitin mediated proteasomal degradation (section 1.3.2.3). Upon nuclear localisation, R-SMADs are linker-phosphorylated through CDKs (section 1.3.1.3), which triggers their recognition by E3 ubiquitin ligases leading to their polyubiquitylation and proteasomal degradation. Because ubiquitylation is reversible, the ubiquitylation of SMAD2/3 by NEDD4L or other E3 ubiquitin ligases can be reversed by DUBs, thereby balancing the outcome of the TGFβ/BMP pathway. The turnover of active SMADs is likely to be regulated either by removal of the polyubiquitin chains by selective DUBs or prevention of polyubiquitylation to produce a dynamic fine-tuning of signalling.

3.1.1 The OTU family of DUBs

OTUB1 belongs to the ovarian tumour domain protease (OTU) family of DUBs that comprises 18 members, of which 14 are catalytically active (Komander *et al.*, 2009, Mevissen *et al.*, 2013). The OTU DUBs can be further classified into four subfamilies according to phylogenetic analysis: the OTUD subfamily (OTUD1, OTUD2, OTUD3, OTUD4, OTUD5, OTUD6A, OTUD6B, ALG13, and HIN1L), the A20-like subfamily (A20, Cezanne, Cezanne2, TRABID and VCPIP), the OTUB subfamily (OTUB1 and OTUB2) and the OTULIN subfamily (OTULIN and FAM105A) (Figure 3-2) (Mevissen *et al.*, 2013).

All mammalian OTU DUBs are ubiquitin specific (Mevissen *et al.*, 2013), although viral OTU domains also target ISG15 (Frias-Staheli *et al.*, 2007). Most human OTU DUBs are linkage specific and only cleave one to four chain types (Figure 3-2) (Mevissen *et al.*, 2013). For cleavage, both linked-ubiquitins have to interact with the catalytic domain of the DUB. Hence, they have to be positioned in such a manner that the isopeptide linkage enters the catalytic site. To achieve this, the distal ubiquitin binds the S1 site (see footnote[1]) in order to position its C-terminus in the catalytic triad (Mevissen *et al.*, 2013, Schechter and Berger, 1967). The proximal ubiquitin is the ubiquitin that contributes the Lysine residue to the isopeptide bond and determines the diubiquitin chain linkage type. Hence, positioning of the proximal ubiquitin that binds to the S1' site (see footnote[1]) determines the chain specificity of the DUB. Additionally, OTU DUBs harbour distinct ubiquitin binding motifs (UBDs) (Figure 3-2). Together these features enable OTU DUB specificity and lead to the regulation of chain cleavage via four distinct mechanisms. Chain cleavage specificity can be achieved (1) by positioning the proximal ubiquitin via the S1' site of a UBD *in cis*, or (2) by positioning the proximal ubiquitin via a conserved S1' UBD in the OTU domain itself, (3) by the use of an S2 site enabling DUBs to bind longer chains in a linkage-specific manner and (4) by specific recognition of a ubiquitylated sequence (Mevissen *et al.*, 2013). It is not yet established whether all active OTU DUBs can hydrolyse the ubiquitin-linkage between the substrate and proximal ubiquitin and cleave branched polyubiquitin chains. Only OTUB1 and OTUD3 are known to cleave mixed and branched chains (Hospenthal *et al.*, 2013, Nakasone *et al.*, 2013).

---

[1] The active site of an enzyme is composed of subsites (S1-Sn and S1'-Sn'), which are located on both sites of the catalytic Cysteine (C) (S1-Sn C S1'-Sn'). The positions (P) on the peptide substrate have the same numbering as the subsites they occupy (P1-Pn and P1'-Pn') (Schechter and Berger, 1967).
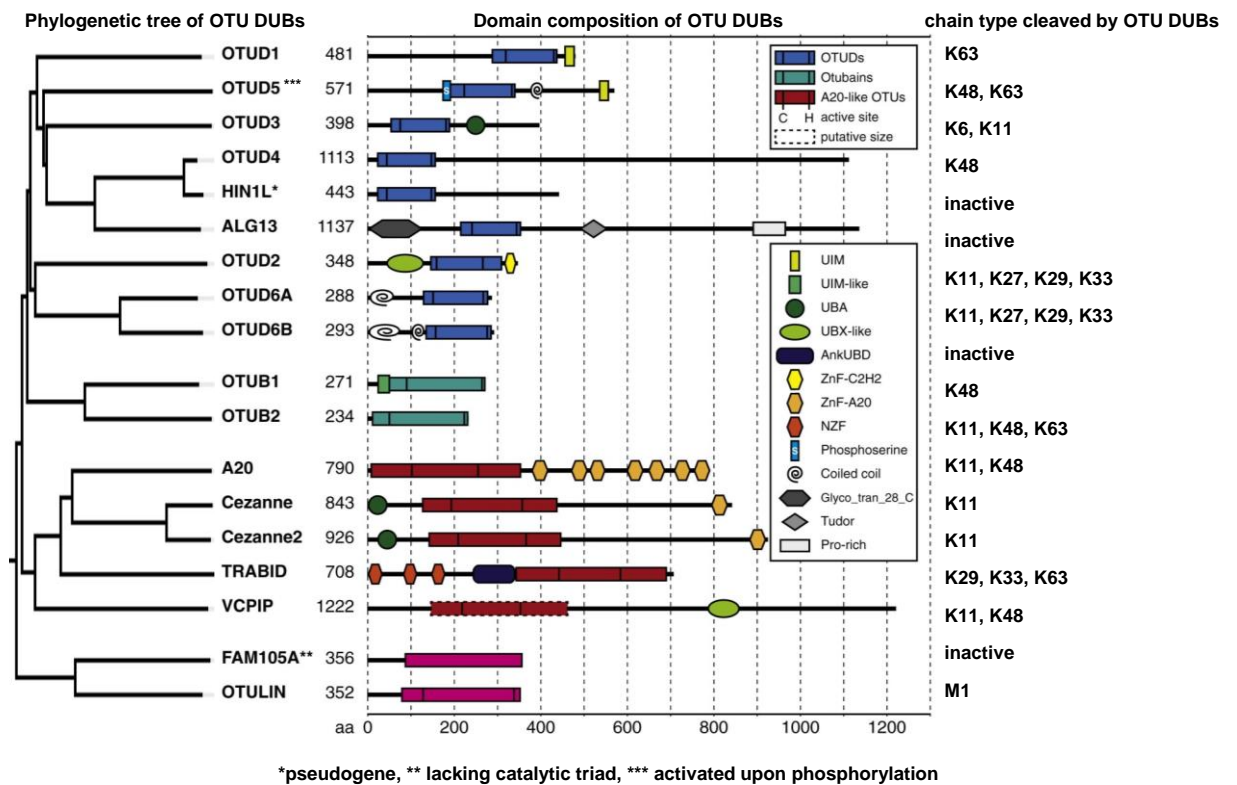
Figure 3-2 Overview of OTU domain family DUBs

The OTU domain family DUBs are displayed on a phylogenetic tree, their domain structures are indicated and the type of ubiquitin chain linkage cleaved by each OTU DUB is listed. This Figure was adapted from Mevissen *et al.*, 2013.

3.1.2 *OTUB1 structure and canonical mode of action*

OTUB1 functions as a cysteine protease that hydrolyses the isopeptide bond between K48-linked ubiquitin chains (canonical mode of action) (Edelmann *et al.*, 2009). The catalytic triad of OTUB1 is composed of D88/C91/H265 within the OTU domain, which come into close contact upon protein folding (Figure 3-3A). OTUB1 preferentially cleaves isopeptide bonds over ubiquitin C-terminal fusions due to a bulky side chain (P87) in close proximity to the catalytic Cysteine. P87 sterically restricts the P1' site (see footnote[1]) of OTUB1, favouring its specificity for K48-linked ubiquitin chains over K6-, K11-, K29-, K63-, or M1-linked polyubiquitin chains via bidentate

substrate binding (Figure 3-3) (Balakirev *et al.*, 2003, Edelmann *et al.*, 2009, Messick *et al.*, 2008, Wang *et al.*, 2009).

The N-terminal domain of OTUB1 harbours a UIM-like (ubiquitin interacting motif-like) which acts as a S1' site, hence the N-terminal helix, which forms following ubiquitin binding, helps to position the proximal ubiquitin relative to the active site (OTU DUB ubiquitin cleavage mechanism (1) see section 3.1.1) (Figure 3-3B). In addition to the UIM-like, OTUB1 function also requires an extensive proximal ubiquitin-binding site in the OTU domain itself (Figure 3-3B) (Balakirev *et al.*, 2003, Juang *et al.*, 2012, Wiener *et al.*, 2012, Edelmann *et al.*, 2009). OTUB1 binds proximal and distal ubiquitins in an orientation that positions the isopeptide linkage of K48-diubiquitin in close proximity to the OTUB1 catalytic site for cleavage (Figure 3-3B). According to this bidentate binding model, free ubiquitin is likely to reduce OTUB1 catalytic activity by binding to one or both ubiquitin-binding sites of OTUB1. The N-terminus of OTUB1 forms an interaction surface between the I44 patch of proximal ubiquitin upon ubiquitin binding to OTUB1. This interaction surface created by the amino terminal α-helix is absent in the *apo* (unbound) structure of OTUB1. Ligand-free OTUB1 is auto-inhibited, as it bears a unique structure of the catalytic triad, not observed in other Cysteine proteases. Thus, upon ubiquitin binding OTUB1 undergoes a conformational change. It is suggested that specific substrates (or interactors) are required for OTUB1 activation, possibly through an induced fit mechanism (Edelmann *et al.*, 2009, Messick *et al.*, 2008, Wang *et al.*, 2009, Wiener *et al.*, 2012, Juang *et al.*, 2012, McGouran *et al.*, 2013). Indeed, the catalytic activity of OTUB1 can be regulated by the UBE2D family, UBE2E1, UBE2N and UBE2W. The E2 stimulates the binding of K48-linked ubiquitin to

OTUB1 by stabilising the folding of the N-terminal ubiquitin binding helix of OTUB1 (Wiener *et al.*, 2013).

The amino acid sequence of OTUB1 is highly similar to OTUB2 (Edelmann *et al.*, 2009). The major difference between OTUB1 and OTUB2 is the N-terminal extension in OTUB1. Additionally, their molecular modes of action are distinct. While both cleave ubiquitin chains, OTUB1 also acts in a non-canonical mode through the inhibition of E2 enzymes (section 3.1.3).

3.1.3 Non-canonical mode of OTUB1 action: inhibition of E2 enzymes

In addition to its ability to cleave K48-linked ubiquitin chains, OTUB1 has been reported to act in a catalytically independent manner (non-canonical). Several studies have described the non-canonical mode of OTUB1 action in which OTUB1 inhibits the ubiquitylation of target proteins by binding to and inhibiting E2 ubiquitin conjugating enzymes, independently of its catalytic activity (Wiener *et al.*, 2012, Nakada *et al.*, 2010, Juang *et al.*, 2012, Sato *et al.*, 2012).

The non-canonical mode of action relies on OTUB1 binding to ubiquitin charged-E2 enzymes (E2~ub) through the ubiquitin-binding motif in the N-terminus. The charged E2~ub and free ubiquitin bind OTUB1 in a way that mimics K48-linked cleaved chains (Figure 3-3B,C). Therefore, OTUB1 can inhibit E2s that generate any ubiquitin-linkage type on substrate proteins. The ubiquitin that is bound to the E2, is positioned at the S1' ubiquitin-binding (proximal) site of OTUB1, forming a pseudo-substrate complex (Figure 3-3C) (Messick *et al.*, 2008, Wiener *et al.*, 2012, Wang *et al.*, 2009, Nakada *et al.*, 2010, Juang *et al.*, 2012, Sato *et al.*, 2012).

The binding of OTUB1 to the UBE2N~ub conjugate is allosterically regulated by free ubiquitin, which binds to the distal ubiquitin-binding region of OTUB1 (Figure 3-3). Hence, in the absence of free ubiquitin, OTUB1 binds charged and uncharged E2s with similar affinity. The binding of conjugated donor ubiquitin to OTUB1 is encouraged by conformational changes in the OTU domain, which maximises contacts with the ubiquitin bound at the OTUB1 proximal site. Furthermore, the formation of a 20-amino acid ubiquitin-binding helix at the N-terminus of OTUB1, which is disordered in the *apo* enzyme, contacts the donor ubiquitin in the distal site favouring binding (Messick *et al.*, 2008, Wiener *et al.*, 2012, Wang *et al.*, 2009, Nakada *et al.*, 2010, Juang *et al.*, 2012, Sato *et al.*, 2012). The N-terminal region of OTUB1 possibly disrupts the interaction between UBE2N and its co-factor UBE2V1, thereby disrupting the donor ubiquitin-E2 interaction. A similar mechanism is possible for the interaction between OTUB1 and UBE2D2, whereby the OTUB1 N-terminus might interfere with acceptor ubiquitin binding to the E2 (Wiener *et al.*, 2012).

The OTUB1-interacting surface on UBE2D2 or UBE2N is in vicinity to the interface that mediates E2-E3 interaction and is conserved among the UBE2E/D families, leading to the prediction that the interaction mode of all OTUB1-interacting E2s is universal (Juang *et al.*, 2012). Interestingly, uncharged E2 binding increases OTUB1 affinity for K48-diubiquitin by stabilising the N-terminus of OTUB1. Hence, the ratio of charged and uncharged E2s in cells as well as the amount of K48-linked ubiquitin present could regulate OTUB1 activity. Furthermore, OTUB1 could coexist in E2-OTUB1 and E2~ub-OTUB1 complexes (Wiener *et al.*, 2013).

In summary, for the non-canonical mode of action, OTUB1 inhibits the ubiquitin transfer from the E2 to the E3. OTUB1 occludes the E3 binding site on

the E2 and binds donor ubiquitin with its N-terminus so that it cannot interact with the E2 enzyme. Hence, OTUB1 also inhibits substrate ubiquitylation in a non-catalytic manner (Wiener *et al.*, 2012, Nakada *et al.*, 2010, Juang *et al.*, 2012).
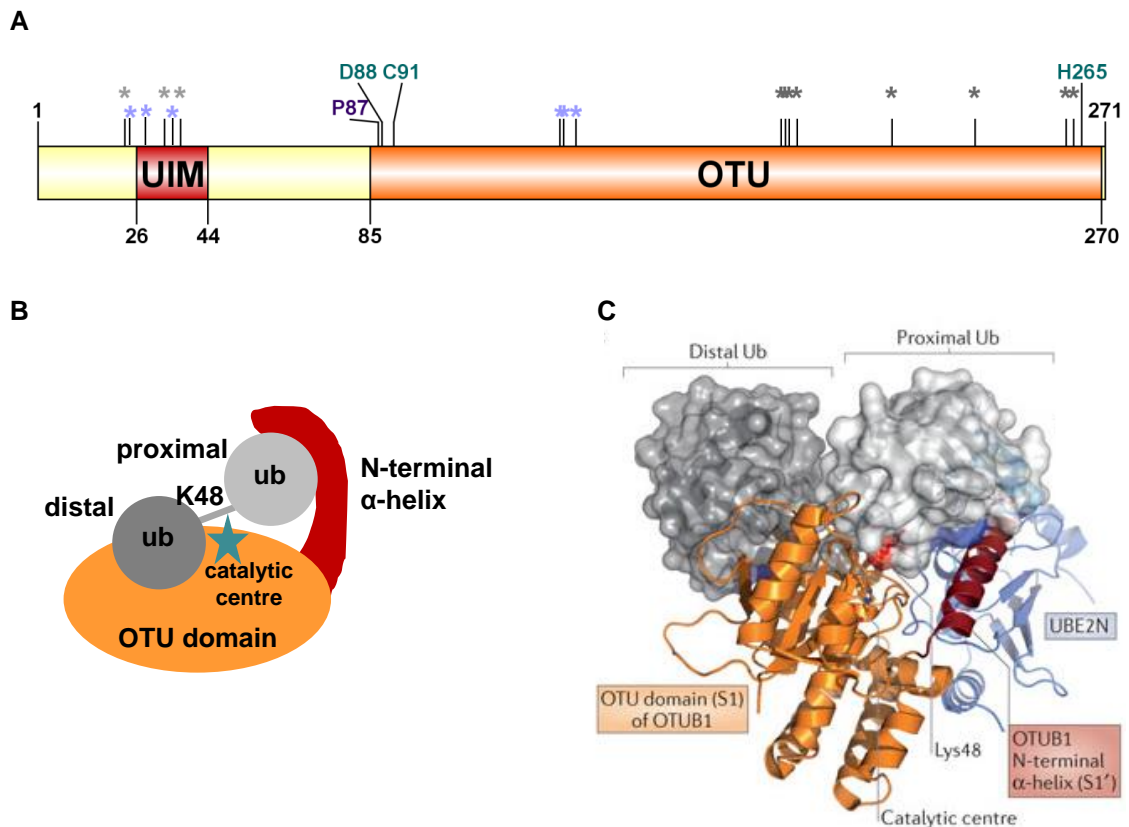
Figure 3-3 Mechanisms of OTUB1 cleavage of K48-linked ubiquitin chains and the inhibition of ubiquitylation

A) Schematic representation of human OTUB1 indicating the domain structures (UIM in red, OTU in orange), catalytic residues (in green), P1' site (P87 in purple), the E2 interface (* in light blue), the proximal ubiquitin binding interface (S1') (* in light grey) and the distal ubiquitin interface (S1) (* in dark grey). **B)** OTUB1 binds K48-linked ubiquitin in a bidentate manner using its distal ubiquitin-binding site in the OTU domain and the proximal ubiquitin binding site, which is formed upon substrate binding, by the N-terminal region. **C)** Crystal structure of OTUB1 bound to ubiquitin in complex with ubiquitin charged UBE2N (taken from Kulathu and Komander, 2012). Binding of ubiquitin-charged E2 (E2~ub) to OTUB1 positions the proximal ubiquitin (which is bound by the E2) into the S1' binding site of OTUB1 and distal ubiquitin binds OTUB1 at its S1 site. This conformation mimics the canonical substrate binding as in B.

3.1.4 Cellular functions of OTUB1

Both canonical and non-canonical roles of OTUB1 have been implicated in the regulation of several cellular processes (Zhang *et al.*, 2012c, Xia *et al.*, 2008, Rumpf and Jentsch, 2006, Peng *et al.*, 2014, Li *et al.*, 2014), including immune response (Li *et al.*, 2010, Soares *et al.*, 2004, Goncharov *et al.*, 2013), estrogen signalling (Stanisic *et al.*, 2009) and DNA damage response (Nakada *et al.*, 2010).

The catalytic activity of OTUB1 is required for its function in apoptosis and pathogen invasion. By regulating the E3 ubiquitin ligase cellular inhibitor of apoptosis (c-IAP1) via deubiquitylation, OTUB1 regulates the assembly of tumour necrosis factor (TNF) receptor signalling complexes and regulates apoptosis (Goncharov *et al.*, 2013). OTUB1 was found to stabilise active RhoA through deubiquitylation, thereby influencing the susceptibility of host cells to bacterial invasion by *Yersinia* (Edelmann *et al.*, 2010).

OTUB1 has been reported to deubiquitylate TRAF3 and 6, thereby negatively regulating the virus induced type I interferon production and cellular antiviral response (Li *et al.*, 2010). Furthermore, it was suggested that HSCARG recruits OTUB1 to TRAF3 (Peng *et al.*, 2014). However, whether the catalytic activity of OTUB1 is required for cellular responses was not assessed in either of the studies. Furthermore, OTUB1 has been reported to act as a specific receptor for the ubiquitylated E3 ligase GRAIL, enhancing its degradation and thereby regulating CD4$^+$ T cell clonal anergy and promoting IL2 production (Soares *et al.*, 2004). OTUB1 function in the regulation of T cell anergy can be antagonised by ARF-1, a longer isoform of OTUB1 resulting from an alternative splicing and start codon. The OTUB1 mediated degradation of GRAIL, which is opposite to the expected function of a DUB, is independent of its catalytic

activity (Soares *et al.*, 2004). OTUB1 has been reported to deubiquitylate and stabilise Estrogen receptor alpha (ERα) in chromatin, but surprisingly resulting in the inhibition of ERα-regulated transcription (Stanisic *et al.*, 2009).

OTUB1 has been shown to inhibit E2 enzymes (non-canonical mode of action) and thereby regulate the cellular responses to DNA damage and stability of p53 (Nakada *et al.*, 2010, Sun *et al.*, 2011). OTUB1 can inhibit DNA-damage-induced RNF168-mediated K63-linked polyubiquitylation on chromatin at DNA double-strand breaks. This is independent of its DUB activity but requires the N-terminal UIM-like, as OTUB1 sequesters the RNF168 cognate E2, UBE2N (Nakada *et al.*, 2010). This was the first report of the non-canonical mode of action for OTUB1, in which OTUB1 directly inhibits RNF168-UBE2N dependent K63-linked ubiquitin chain elongation by preventing the isopeptide bond formation between a donor ubiquitin on UBE2N and an acceptor ubiquitin coordinated by its co-factor UBE2V1. Furthermore, OTUB1 was also found to interact with and inhibit the UBE2D and UBE2E subfamilies (Nakada *et al.*, 2010). OTUB1 has been reported to regulate the activity and stability of p53 and induce p53-mediated apoptosis and cell growth inhibition through its non-canonical mode of action. OTUB1 inhibits MDM2-mediated ubiquitylation of p53 by sequestering its cognate E2, UBE2D1 (Sun *et al.*, 2011). Recently, it was suggested that OTUB1 is monoubiquitylated by UBE2D1, which in turn enhances binding between OTUB1 and UBE2D1 and could disrupt UBE2D1~ub complexes (Li *et al.*, 2014).

3.2 <u>Results</u>

3.2.1 Identification of OTUB1 as an interactor of GFP-SMAD3

In order to uncover novel modes of regulation of the TGFβ pathway, a proteomic approach was employed to identify interactors of SMAD1 and SMAD3, key mediators of the BMP and TGFβ ligands respectively. HEK293 cells stably expressing GFP alone and N-terminally GFP-tagged SMAD1 or SMAD3 under the control of a tetracycline-inducible promoter were generated. GFP-immunoprecipitates (IPs) were resolved by SDS-PAGE and the interacting proteins excised, digested with trypsin and identified by mass spectrometry (Figure 3-4A). As expected, BMP and TGFβ treatment resulted in the phosphorylation of GFP-SMAD1 and GFP-SMAD3 respectively (Figure 3-4B). Previously reported R-SMAD interactors, including SMAD4, LEMD3, TRIM33 and c-SKI were identified in GFP-SMAD1 and GFP-SMAD3 IPs as indicated (Figure 3-4A) (Zhang *et al.*, 1996, Lagna *et al.*, 1996, Luo *et al.*, 1999, Osada *et al.*, 2003, Pan *et al.*, 2005). OTUB1 was identified as a novel interactor of GFP-SMAD3 only when cells were treated with TGFβ (Figure 3-4A). Four OTUB1 tryptic peptides, representing ~ 8% sequence coverage, were identified.
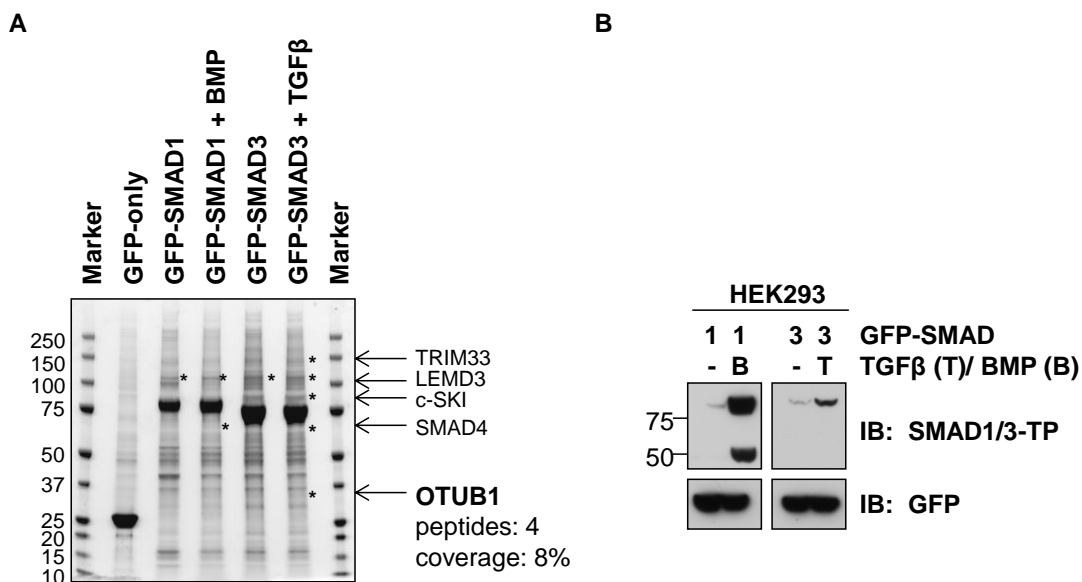
Figure 3-4 Identification of OTUB1 as an interactor of GFP-SMAD3 upon TGFβ stimulation

A) HEK293 cells stably expressing GFP-only, GFP-SMAD1 or GFP-SMAD3 were treated with 50 pM TGFβ or 25 ng/ml BMP as indicated for 1 hour prior to lysis. GFP-immunoprecipitates (IPs) were separated by SDS-PAGE and the interacting partners identified by mass spectrometry. **B)** HEK293 cells stably expressing GFP-SMAD1 or GFP-SMAD3 were treated with BMP (25 ng/ml) or TGFβ (50 pM) respectively for 1 hour prior to lysis. Extracts were resolved by SDS-PAGE and immunoblotted with the indicated antibodies. Abbreviations used: SMAD-TP= tail-phosphorylated SMAD.

3.2.2 Assessment of interactions between OTUB1 and SMADs at the endogenous level

To verify the ligand-inducible nature of interaction between OTUB1 and SMAD3 (Figure 3-4A) at the endogenous level, OTUB1 was immunoprecipitated from HaCaT cell extracts. OTUB1 was efficiently immunoprecipitated with the anti-OTUB1 antibody but not with the pre-immune IgG (Figure 3-5A). TGFβ induces formation of the active phospho-SMAD2/3-SMAD4 transcription factor complex (Lagna *et al.*, 1996, Zhang *et al.*, 1996). Tail (TP)- and linker (LP)-phosphorylated SMAD3, total SMAD3, tail-phosphorylated SMAD2 and total SMAD2 were all detected in OTUB1 IPs from cells stimulated with TGFβ but not from BMP or unstimulated controls (Figure 3-5A). SMAD4 was also detected in OTUB1 IPs only upon TGFβ stimulation (Figure 3-5A), indicating that OTUB1 binds to the active SMAD2/3/4 complex. Endogenous tail-phosphorylated SMAD1 and SMAD4 were not detected in OTUB1 IPs from control or BMP treated extracts (Figure 3-5A), suggesting that OTUB1 selectively recognises the TGFβ-induced SMAD complexes. Similarly, SMAD7 was not detected in OTUB1 IPs (Figure 3-5A). None of the SMADs were detected in pre-immune sheep IgG IPs, employed as control (Figure 3-5A). SMAD2-TP and total SMAD2/3 were also detected in OTUB1 IPs from primary bone marrow derived macrophages (BMDMs) and mouse embryonic fibroblasts (MEFs) only when cells were treated with TGFβ (Figure 3-5B). Next, the kinetics of OTUB1-SMAD2/3 interaction upon TGFβ stimulation in HaCaT cells was investigated. The binding of endogenous OTUB1 to the active SMAD2/3/4 complex occurred within 30 minutes of TGFβ stimulation and persisted through 6 hours of continuous stimulation, closely mirroring the levels of SMAD2/3-tail phosphorylation (Figure 3-5C).
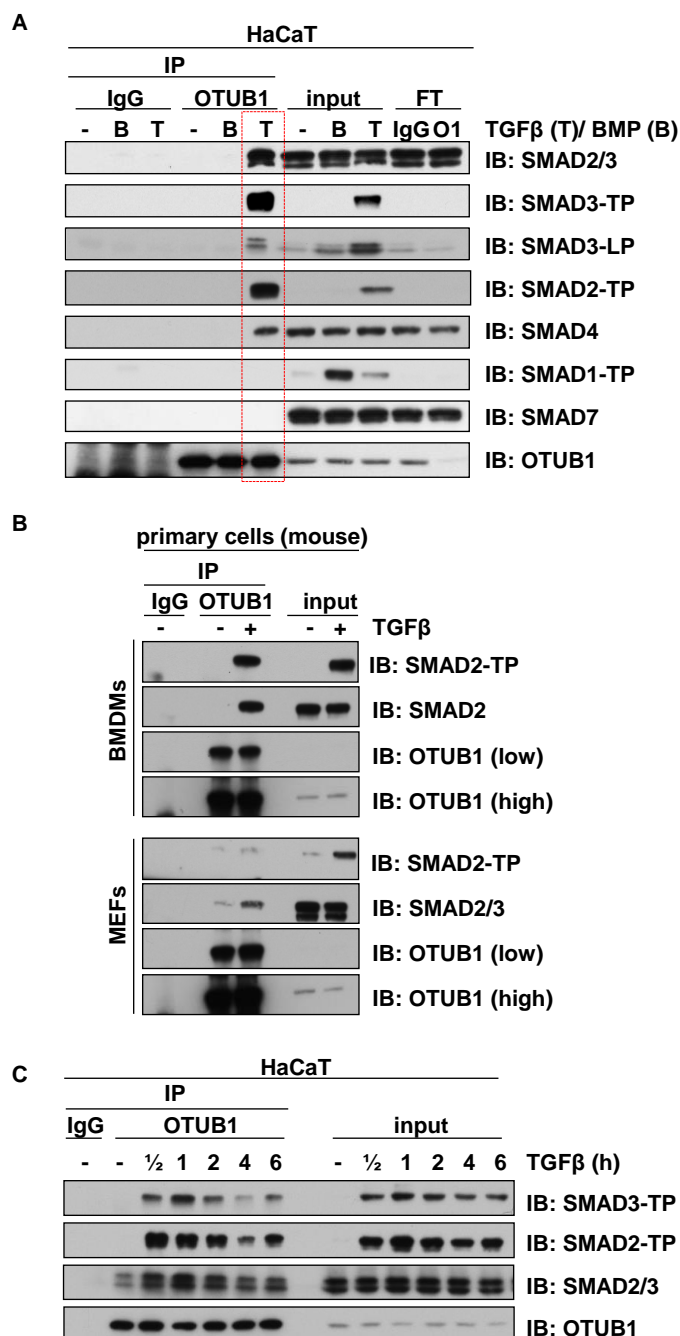
Figure 3-5 Endogenous interactions between OTUB1 and TGFβ activated SMADs

A) An endogenous IP with anti-OTUB1 antibody or pre-immune sheep IgG was performed in HaCaT cell extracts, stimulated without or with 50 pM TGFβ or 25 ng/ml BMP for 1 hour. Cell extracts (input), IgG or anti-OTUB1 IPs and the corresponding immune-depleted flow-through extracts (FT) (O1=OTUB1-depleted untreated HaCaT extract) were resolved by SDS-PAGE and immunoblotted with the indicated antibodies. **B)** An endogenous IP with anti-OTUB1 antibody or pre-immune sheep IgG was performed in extracts from BMDMs and MEFs stimulated with or without 50 pM TGFβ for 1 hour. Prior to TGFβ stimulation BMDMs were serum starved for 2 hours, whereas MEFs were not starved. Cell extracts (input) or IPs were resolved by SDS-PAGE and immunoblotted with the indicated antibodies. **C)** As in A, except that a time course of TGFβ treatment was performed for up to 6 hours prior to lysis. Abbreviations used: SMAD-LP: linker-phosphorylated SMAD.

3.2.3 OTUB1 and phospho-SMAD2/3 co-elute in size exclusion chromatography

To visualise the co-elution of possible OTUB1 and SMAD2/3/4 macromolecular complexes, size exclusion chromatography was performed on untreated or TGFβ treated HaCaT cell extracts (Figure 3-6). While most of OTUB1 eluted in lower molecular weight fractions under both unstimulated or TGFβ stimulated conditions, some OTUB1 eluted in a high molecular weight fraction only upon TGFβ stimulation (Figure 3-6). Tail-phosphorylated SMAD2/3 and SMAD4 also co-elute in this fraction (fraction 17), indicating the potential existence of an OTUB1/SMAD2/3/4 macromolecular complex (Figure 3-6).
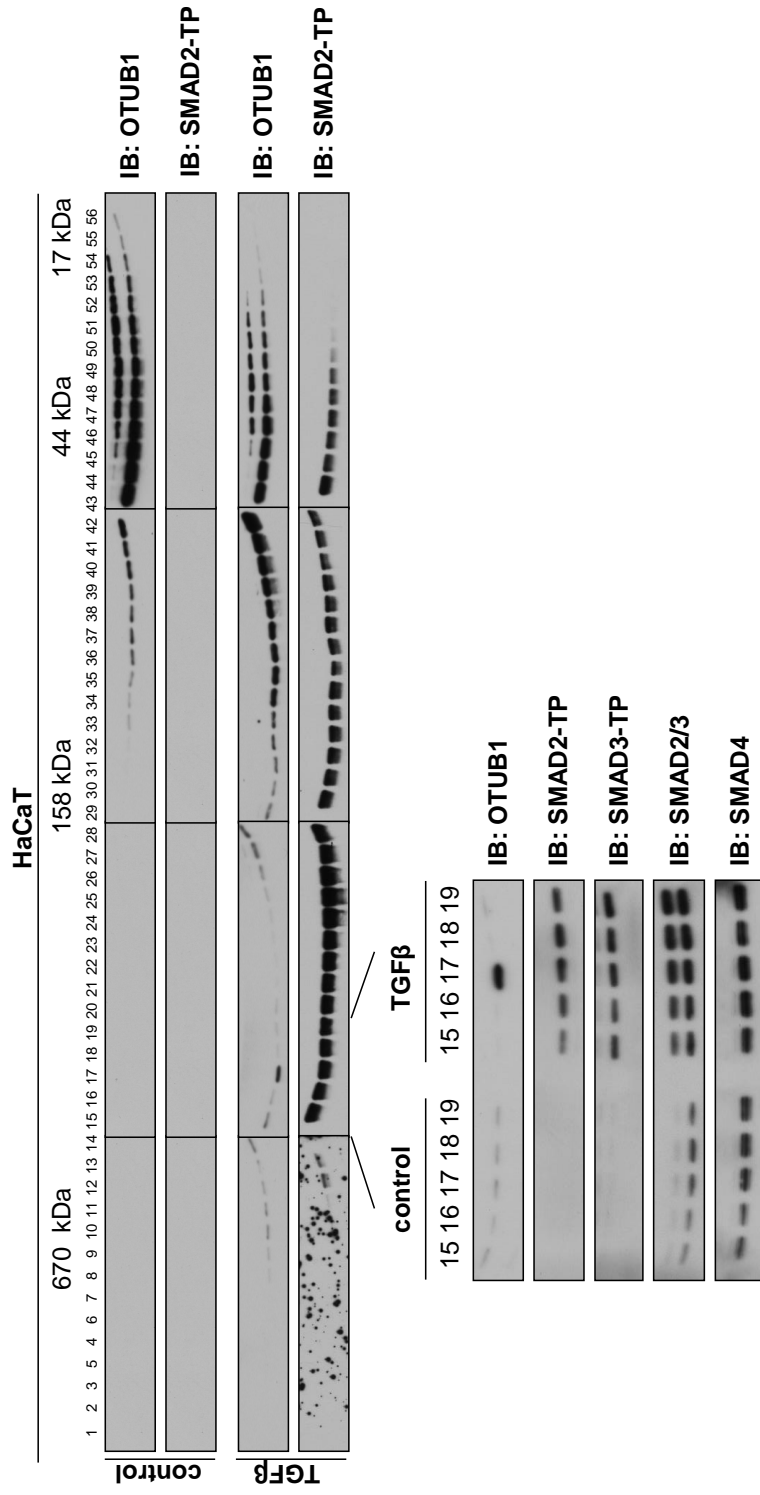
Figure 3-6 Elution profile of OTUB1 and SMADs in size exclusion chromatography

HaCaT cells left untreated or treated with 50 pM TGFβ for 1 hour were lysed in the presence of 50 mM iodoacetamide. The extract was subjected to size exclusion chromatography on a Superdex S200 column and 56 fractions were collected. The fractions were resolved by SDS-PAGE and immunoblotted with the indicated antibodies. Upon TGFβ treatment, OTUB1 and phospho-SMAD2 were observed in high molecular weight fractions, with significant overlap surrounding fraction 17. These fractions were re-analysed on the bottom panel and immunoblotted with OTUB1, SMAD2-TP, SMAD3-TP, total SMAD2/3 and SMAD4 antibodies.

3.2.4 *Phosphorylation of SMAD2/3 is necessary for OTUB1 binding*

As shown in Figure 3-5, OTUB1 selectively bound components of the active phospho-SMAD2/3-SMAD4 complex; however, it was not clear whether SMAD4 was required for this interaction. Therefore, the SW480 colon cancer cell line, which lacks SMAD4 expression (Calonge and Massague, 1999), was employed. In both HaCaT and SW480 cells, TGFβ induced the phosphorylation of SMAD2/3 (Figure 3-7). Phospho-SMAD2/3 proteins were detected in OTUB1 IPs upon TGFβ stimulation in both cell types (Figure 3-7). SW480 cells displayed elevated basal levels of phospho-SMAD2/3 over HaCaT cells (Figure 3-7). Consistent with this, even in the absence of TGFβ stimulation, phospho-SMAD2/3 was detected in OTUB1 IPs in SW480 cells (Figure 3-7). These observations imply that SMAD4 is not required for the interaction between OTUB1 and phospho-SMAD2/3.

To establish whether the phosphorylation of SMAD2/3 in response to TGFβ is critical for its interaction with OTUB1, OTUB1 IPs from TGFβ-treated HaCaT extracts were lambda (λ) phosphatase treated (Figure 3-8A). This resulted in a dissociation of SMAD2 from OTUB1 IPs indicating that phosphorylation of SMAD2 in response to TGFβ is necessary for its interaction with OTUB1. As expected, λ phosphatase efficiently dephosphorylated TGFβ-induced phospho-SMAD2 in extracts (Figure 3-8A; input). Furthermore endogenous OTUB1 IPs were capable of interacting with wild type FLAG-SMAD3 and a phospho-mimetic mutant of FLAG-SMAD3 but not a phospho-deficient mutant of FLAG-SMAD3 overexpressed in U2OS cells (Figure 3-8B). To definitively establish whether the interaction of OTUB1 with SMAD2 is tail-phosphorylation dependent, a biotin-tagged SMAD2 tail-peptide (incorporating residues 428-467 of hSMAD2) phosphorylated at the "S<u>MS</u>" motif (SMAD2

phospho-peptide) was generated. When the SMAD2 phospho-peptide was incubated with purified GST-OTUB1 protein *in vitro,* a robust OTUB1 interaction was observed (Figure 3-8C; lane 2). This interaction was abolished upon λ phosphatase treatment to dephosphorylate the SMAD2 phospho-peptide (Figure 3-8C; lane 3). These observations suggest that the interaction between OTUB1 and phospho-SMAD2 is direct. Furthermore, only SMAD2 phospho-peptide but not the λ phosphatase treated phospho-peptide was able to pull down endogenous OTUB1 from HaCaT cell extracts independent of TGFβ treatment (Figure 3-8D). Similarly, as expected, SMAD2 phospho-peptide pulled down SMAD4, which is known to interact with tail-phosphorylated SMAD2 (Lagna *et al.*, 1996) (Figure 3-8D).
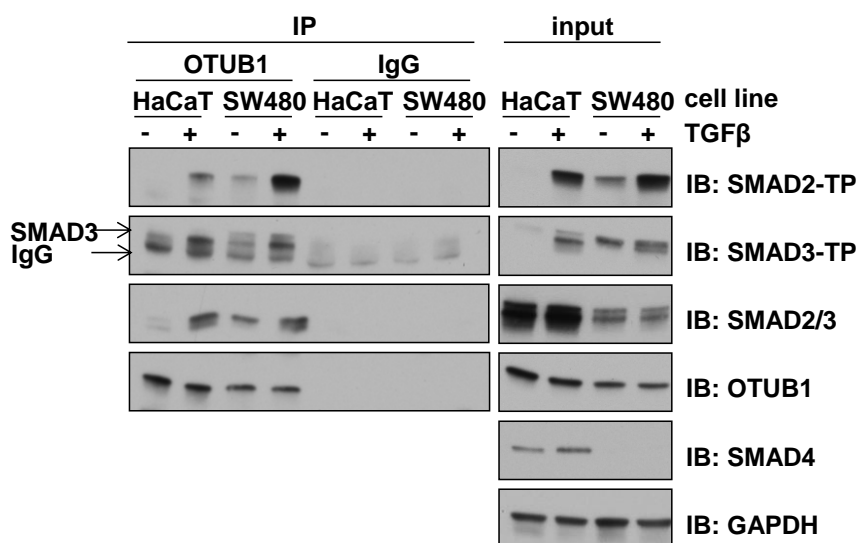
Figure 3-7 SMAD4 is dispensable for the interaction between OTUB1 and tail-phosphorylated SMAD2/3

An endogenous IP with anti-OTUB1 antibody or pre-immune sheep IgG was performed in HaCaT and SW480 cell extracts, stimulated with or without 50 pM TGFβ for 1 hour prior to lysis. Extracts (input) and endogenous anti-OTUB1 or IgG IPs were resolved by SDS-PAGE and immunoblotted with the indicated antibodies.
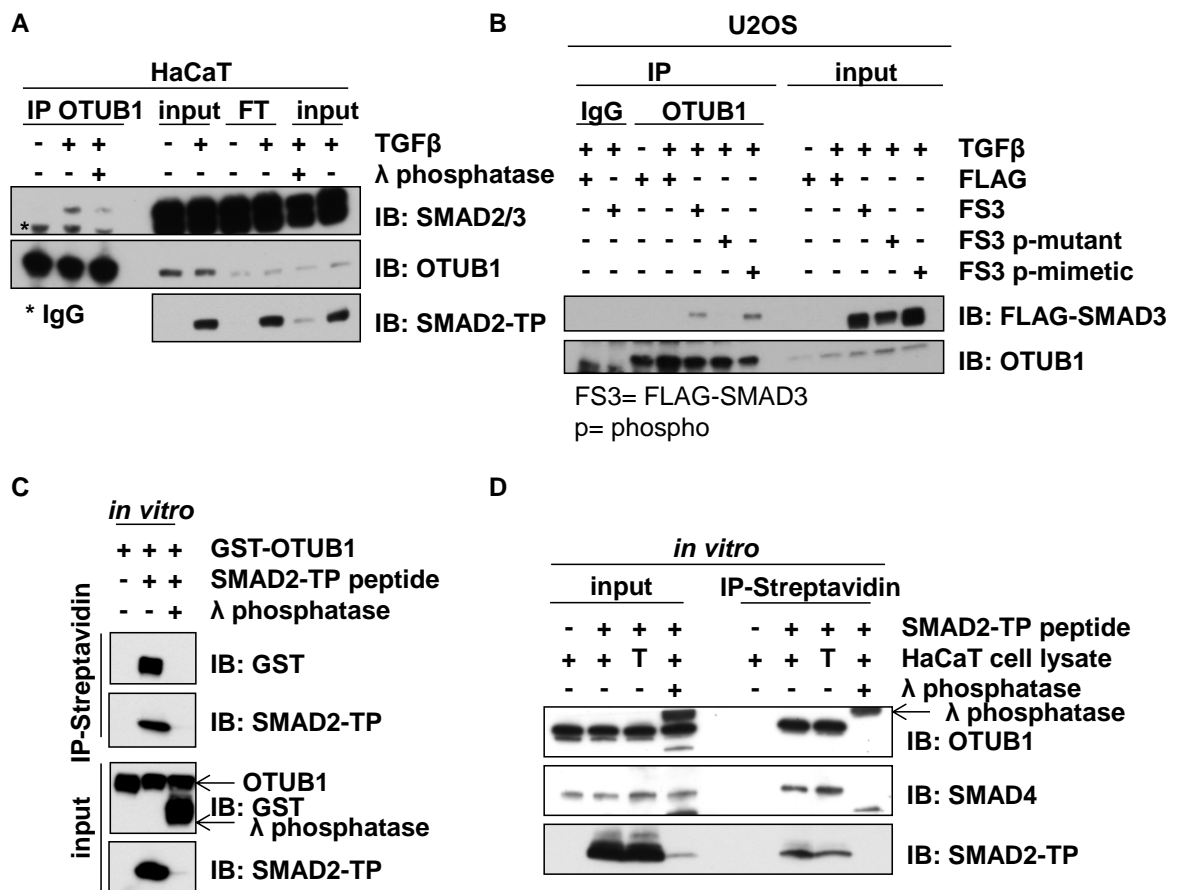
Figure 3-8 OTUB1 binding to SMAD2/3 is phosphorylation dependent

A) Endogenous OTUB1 was immunoprecipitated from HaCaT cells treated with or without TGFβ (50 pM; 1 h) prior to lysis. After washing, the IPs were treated with or without lambda (λ) phosphatase for 30 min at 30 °C and washed 4 times. As a control, an aliquot of TGFβ-treated cell extract was incubated with lambda (λ) phosphatase for 30 min at 30 °C. Cell extracts, IPs and flow-through extracts were resolved by SDS-PAGE and immunoblotted with the indicated antibodies. **B)** U2OS cells were transfected with vectors encoding wild type FLAG-SMAD3, FLAG-SMAD3 phospho-mutant or FLAG-SMAD3 phospho-mimetic mutant and were treated with TGFβ (50 pM; 1 h) prior to lysis. Extracts or IPs with pre-immune IgG or anti-OTUB1 antibody were resolved by SDS-PAGE and immunoblotted with the indicated antibodies. **C)** Purified GST-OTUB1 was incubated with biotin-tagged phospho-SMAD2 peptide in the presence or absence of lambda (λ) phosphatase for 30 min at 30 °C. The SMAD2 peptide was immunoprecipitated with Streptavidin beads and washed 6 times. Input and IP samples were resolved by SDS-PAGE and immunoblotted with the indicated antibodies. **D)** As in D, however the SMAD2-peptide was incubated with untreated HaCaT (+) or TGFβ (T) (50 pM; 1 h) treated cell lysate. SMAD4 antibody was used as a positive control.

- 111 -

3.2.5 Expression of OTUB1 in different tissues and cell lines

To further investigate the function of OTUB1, mouse tissues and different cancer cell lines were probed for the expression of OTUB1 protein. Mouse spatial tissue distribution of OTUB1 revealed that it was ubiquitously expressed, with high expression levels observed in the brain (Figure 3-9A). Moreover, OTUB1 was ubiquitously expressed across many human cell lines, with relatively high expressions observed in breast cancer cells (Figure 3-9B).
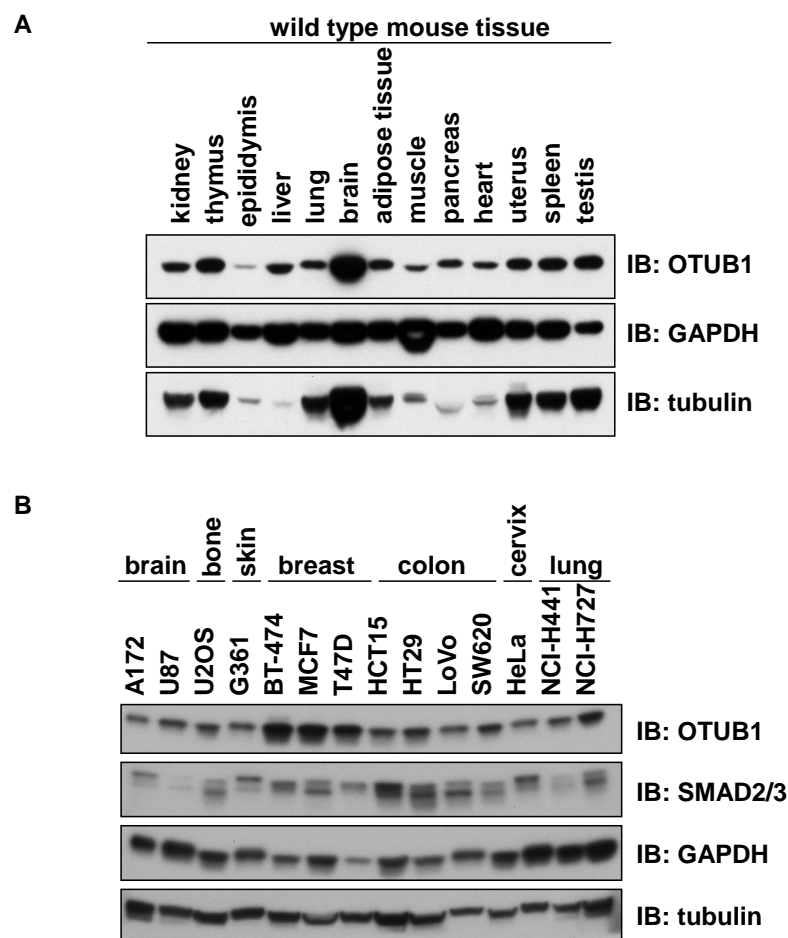
Figure 3-9 OTUB1 is ubiquitously expressed

A) Indicated mouse tissues were homogenised in lysis buffer, and 20 µg of protein lysate were resolved by SDS-PAGE and immunoblotted with antibodies against OTUB1, GAPDH and tubulin (the latter ones used as loading controls). **B)** Different cancer cell lines were lysed and extracts resolved by SDS-PAGE and immunoblotted with the indicated antibodies. GAPDH and tubulin immunoblots were used as loading controls.

3.2.6 Subcellular localisation of OTUB1

The intracellular distribution of OTUB1 was also investigated. Immunofluorescence microscopy was employed to investigate if TGFβ treatment affected the intracellular distribution of OTUB1 and if OTUB1 and tail-phosphorylated SMADs co-localised. Control or OTUB1 depleted (*iOTUB1*) HaCaT cells were left untreated or treated with TGFβ. TGFβ treatment resulted in nuclear accumulation of tail-phosphorylated SMAD3 (Figure 3-10A). Depletion of OTUB1 weakened the OTUB1 signal but did not eradicate it completely (Figure 3-10B), suggesting that the OTUB1 antibody was not completely suitable for IF applications. Nevertheless, OTUB1 was mainly cytosolic. This was confirmed by subcellular fractionation in HaCaT and MDA-MB-231 cells (Figure 3-11A). Endogenous OTUB1 was detected mainly in the cytosolic fraction and TGFβ/BMP treatment did not appear to significantly alter its localisation. In contrast, tail-phosphorylated SMADs1 and 3 were mainly detected in the nuclear fractions (Figure 3-11A). Efficient fractionation was indicated by the presence of Lamin A/C and GAPDH in nuclear and cytosolic fractions respectively (Figure 3-11A). When fractionating HaCaT cells into five compartments (cytoplasm, membrane, nucleus, chromatin, cytoskeleton), OTUB1 was detected primarily in the cytosol with some detected at the membrane (Figure 3-11B). To assess whether OTUB1 might sequester tail-phosphorylated SMAD2 from entering the nucleus, HaCaT cells were fractionated and the amount of SMAD2-TP in the presence or absence of OTUB1 in the nucleus compared. There was no significant difference in the amount of SMAD2 entering the nucleus upon TGFβ stimulation in the absence or presence of OTUB1 (Figure 3-12).
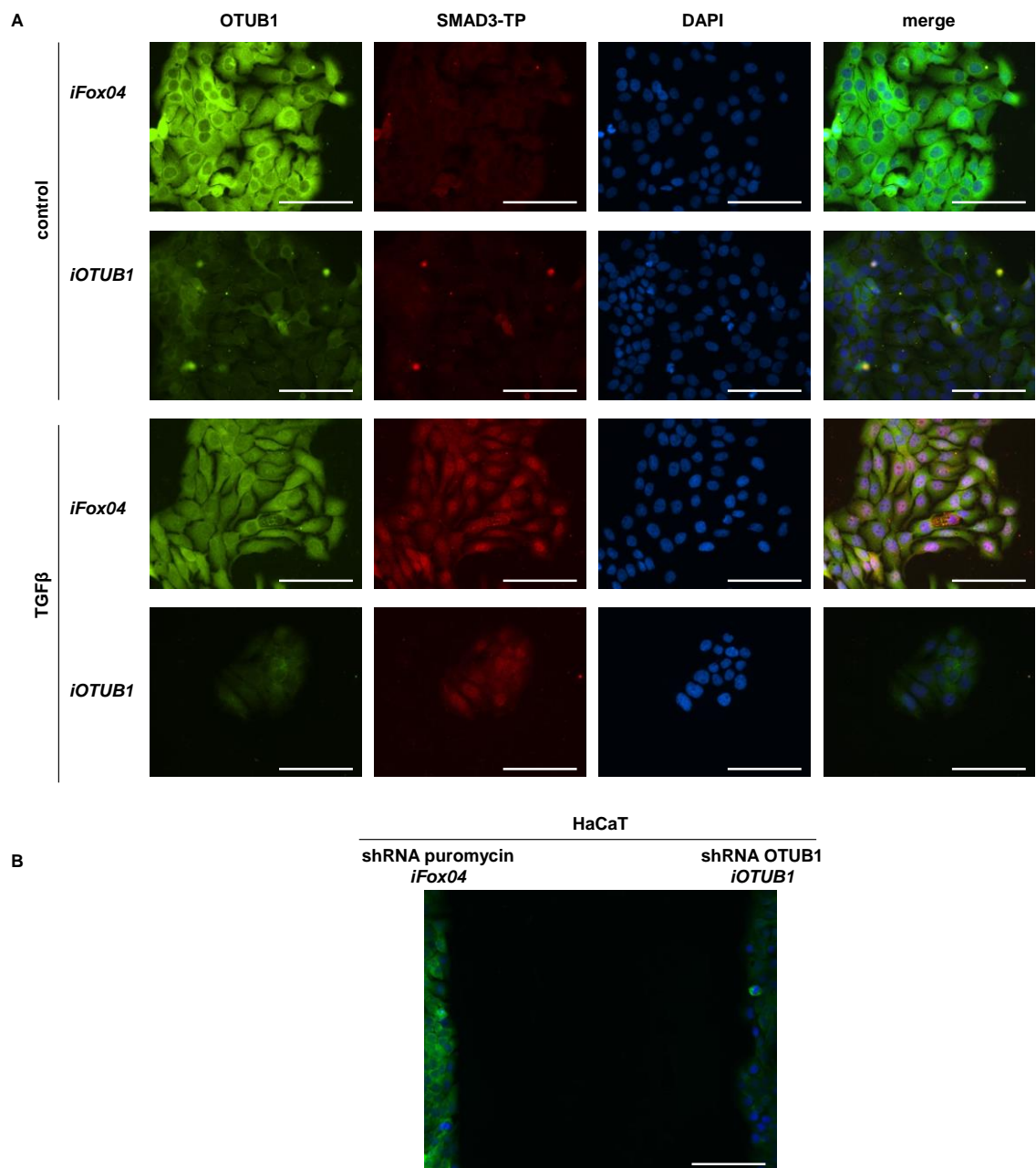
Figure 3-10 Immunofluorescence microscopy indicates that OTUB1 is cytosolic

A) Fixed cell immunofluorescence was performed on HaCaT cells transfected with *FoxO4* control siRNA or *OTUB1* siRNA and treated with 50 pM TGFβ for 1 hour or left untreated. Individual and merged pictures are shown, indicating localisation of OTUB1 mainly in the cytosol and upon TGFβ stimulation SMAD3-TP in the nucleus. Pictures were taken using a 40x lens, scale bars represent 50 μm. **B)** HaCaT cells transfected with *FoxO4* control siRNA and control shRNA or *OTUB1* siRNA and shRNA were seeded onto an Ibidi cellular migration chamber and fixed cell immunofluorescence was performed. Pictures were taken using a 20x lens, scale bar represents 100 μm.
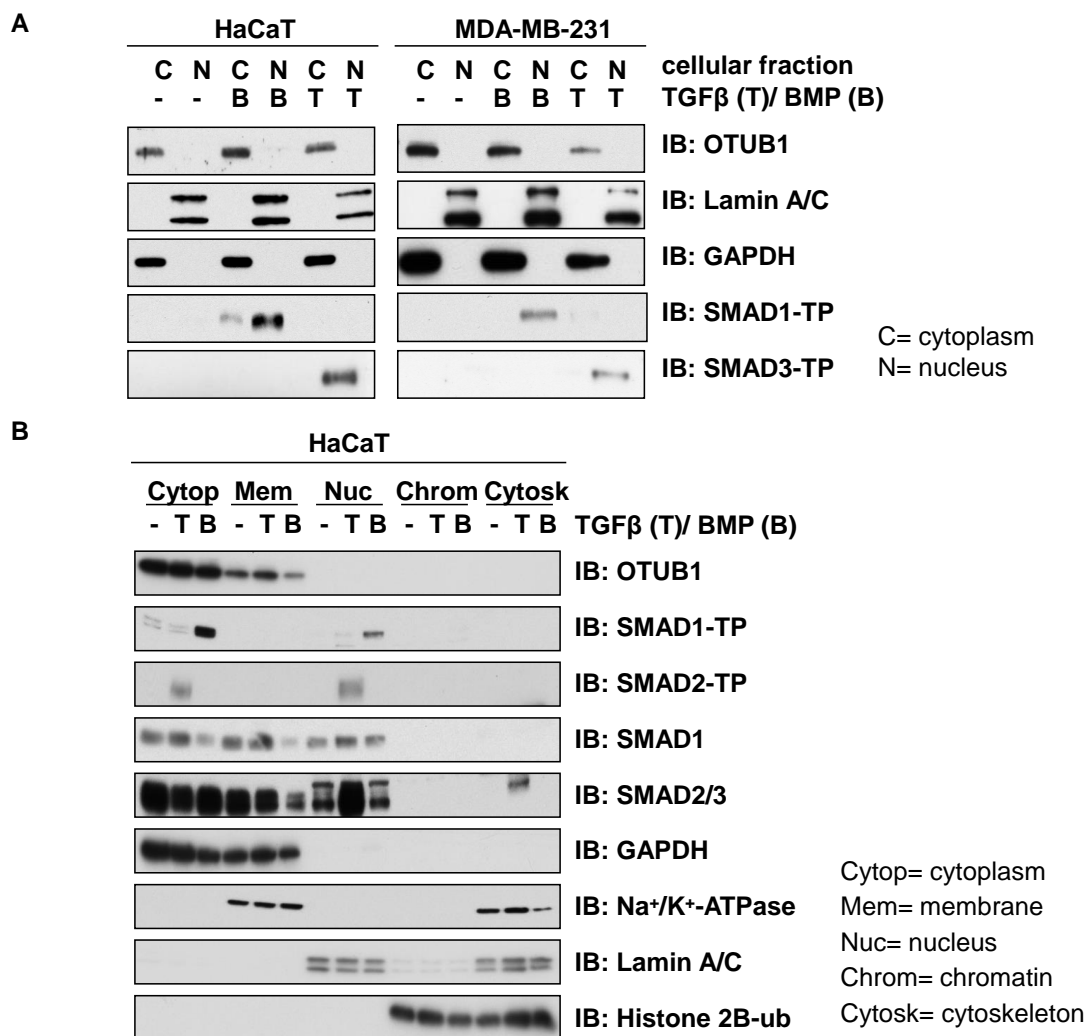
Figure 3-11 Cellular fractionation confirms cytosolic localisation of OTUB1

A) HaCaT and MDA-MB-231 cells were treated with or without 25 ng/ml BMP or 50 pM TGFβ for 1 hour prior to lysis and separated into nuclear and cytosolic fractions. The fractions were resolved by SDS-PAGE and immunoblotted with the indicated antibodies. **B)** As in A, however HaCaT cells were fractioned into cytoplasm, membrane, nucleus, chromatin and cytoskeleton.
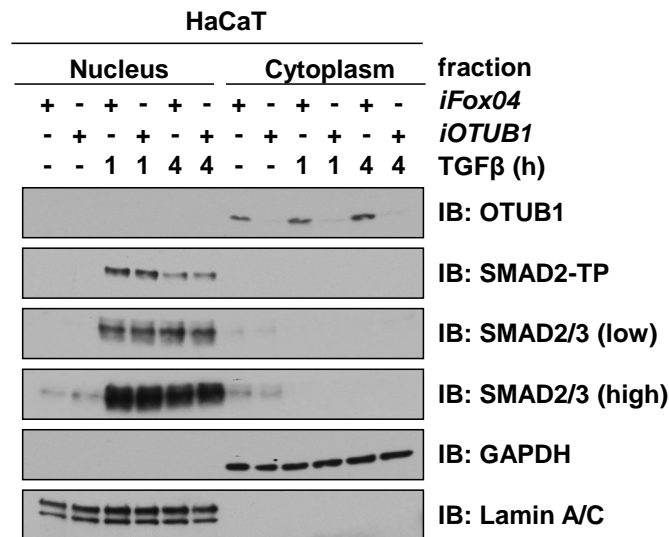
Figure 3-12 OTUB1 does not affect SMAD2/3 nuclear entry

HaCaT cells were treated with *FoxO4* or *OTUB1* siRNA for 48 hours prior to TGFβ stimulation (50 pM) for indicated times and cells were separated into nuclear and cytosolic fractions. The fractions were resolved by SDS-PAGE and immunoblotted with the indicated antibodies.

3.2.7 *OTUB1 enhances TGFβ-mediated gene transcription*

The ligand-inducible interaction between OTUB1 and phospho-SMAD2/3 indicated that OTUB1 could play a regulatory role in the TGFβ pathway. Therefore, depleting OTUB1 expression from cells might promote the ubiquitylation of active phospho-SMAD2/3 and thus result in the inhibition of TGFβ signalling.

OTUB1 was depleted from mouse myoblast C2C12 cells stably integrated with a TGFβ-responsive CAGA-luciferase reporter construct using multiple siRNAs (Figure 3-13A). Depletion of OTUB1 with mouse *iOTUB1#1,* yielded >90% knockdown of OTUB1 protein levels (Figure 3-13A) resulting in significant inhibition of TGFβ-induced CAGA-luciferase reporter activity compared to control siRNA (mouse *iFoxO4*) (Figure 3-13B). Similar results were obtained with mouse *iOTUB1#3* (Figure 3-13C)*,* which yielded >80%

depletion in OTUB1 expression (Figure 3-13A). These results suggested that OTUB1 enhances TGFβ-induced transcriptional responses.

In order to confirm the repression of TGFβ-mediated transcription upon OTUB1 depletion in human cells, HaCaT cells were transiently transfected with a control siRNA (human *iFoxO4)*, human *iOTUB1#1* siRNA or a stable shRNA against *OTUB1* (Figure 3-14A) and the endogenous expression of TGFβ-target genes was tested by qRT-PCR (Figure 3-14B). Upon depletion of OTUB1 by both transient and stable knockdown methods, TGFβ-induced PAI-1 mRNA expression was significantly inhibited (Figure 3-14B). The expression of another TGFβ-target gene, *CTGF*, was also significantly inhibited upon siRNA-mediated depletion of OTUB1 (Figure 3-14C). These results demonstrated that depletion of OTUB1 by two independent RNAi oligonucleotides in mouse and human cells caused inhibition of TGFβ-induced transcriptional activity.

OTUB1 did not interact with SMAD1 upon BMP-stimulation (Figure 3-5A). To confirm that OTUB1 only affects the TGFβ pathway, BMP-mediated gene transcription was monitored in the presence or absence of OTUB1 (Figure 3-15). No difference in luciferase activity was observed in C2C12 cells stably expressing a SMAD1-dependent BMP-responsive BRE luciferase reporter construct, transfected with *iFoxO4* control or *iOTUB1#1* siRNAs (Figure 3-15A). Similarly, the overexpression of HA-control, HA-OTUB1 or HA-OTUB1 C91S did not alter the BMP-dependent luciferase activity (Figure 3-15B).
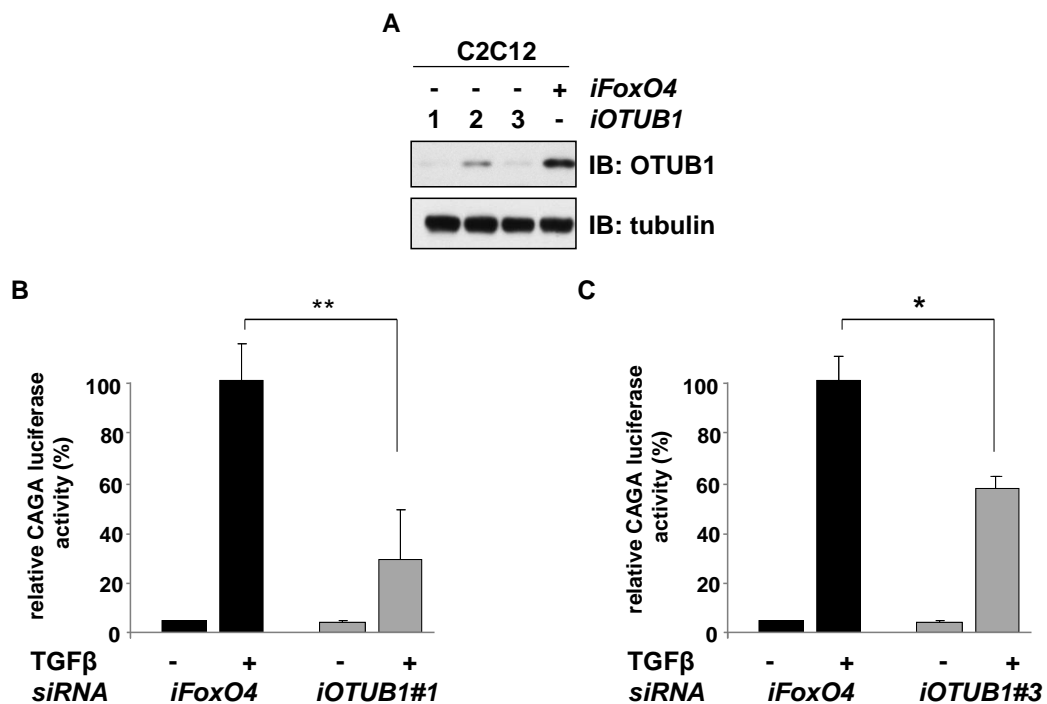
Figure 3-13 Depletion of OTUB1 represses TGFβ-induced transcription in mouse cells

A) C2C12 cells were transfected with three different siRNAs (#1, #2, #3) targeting mouse *OTUB1* (300 pM/10-cm dish each) and lysed 48 hours post-transfection. Extracts were resolved by SDS-PAGE and immunoblotted with the indicated antibodies. **B)** C2C12 cells stably expressing a SMAD3-dependent TGFβ-responsive CAGA luciferase reporter construct were transfected with *iFoxO4* or *iOTUB1#1*. Cells were treated with or without 50 pM TGFβ for 6 hours prior to lysis and luciferase activity was measured. Data are represented as mean and error bars indicate standard deviation (n=3). Differences with p<0.01 were annotated as **. **C)** As in C, however cells were transfected with *iFoxO4* and *iOTUB1#3*. Data are represented as mean and error bars indicate standard deviation (n=3). Differences with p<0.05 were annotated as *.
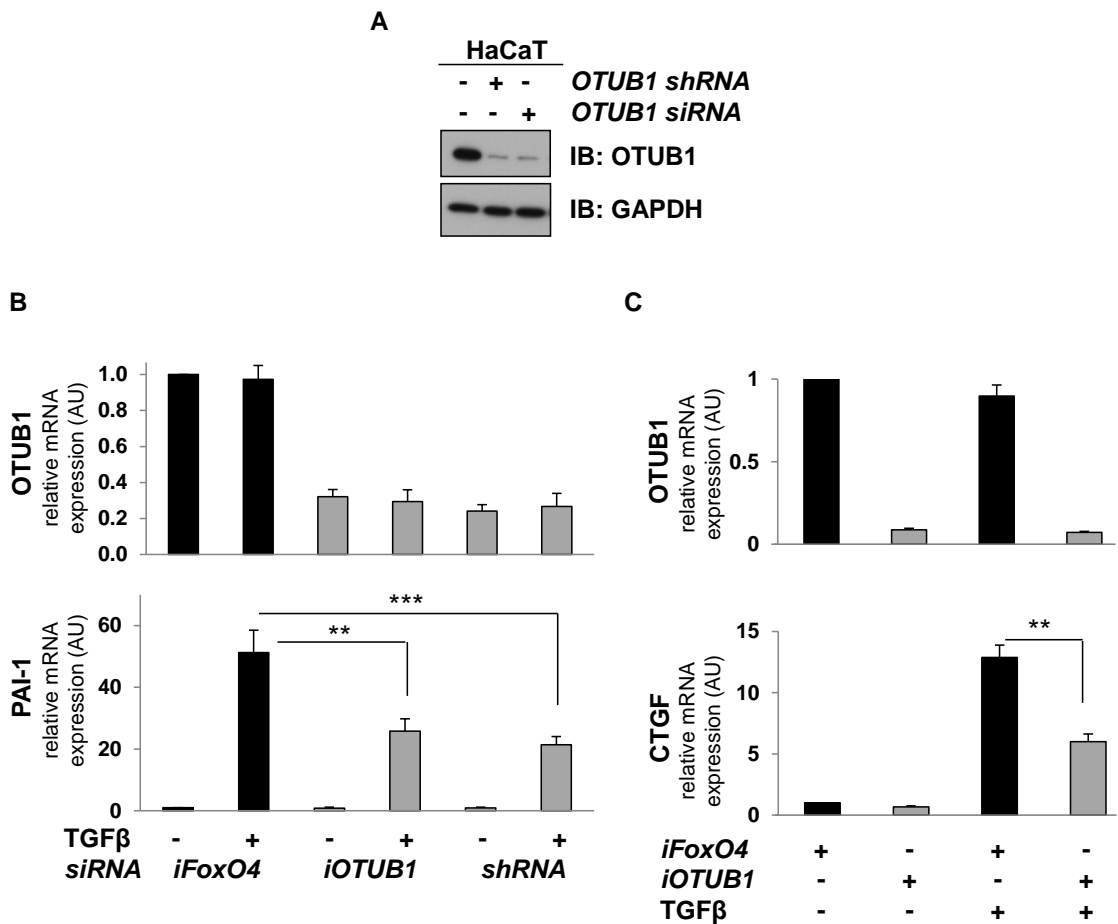
Figure 3-14 Depletion of OTUB1 represses TGFβ-induced transcription in human cells

A) HaCaT cells stably expressing shRNA against *OTUB1* or transfected with control (-) or *OTUB1* siRNA (300 pM/10-cm dish each) for 48 hours were lysed and extracts resolved by SDS-PAGE and immunoblotted with the indicated antibodies. **B)** HaCaT cells, transfected with human *OTUB1* siRNA, human *FoxO4* siRNA, or stably expressing OTUB1 shRNA, were treated with 50 pM TGFβ for 4 hours prior to RNA isolation. Relative expression levels of indicated mRNAs were analysed by qRT-PCR. Data are represented as mean and error bars indicate standard deviation (n=6). Differences with p<0.01 were annotated as ** and p<0.001 were annotated as ***. **C)** HaCaT cells depleted of human *OTUB1* or *FoxO4* by RNAi were treated with 50 pM TGFβ for 1 hour. TGFβ was then washed off and SB505124 (1 µM) added. mRNA was isolated 45 min post TGFβ removal. Relative expression levels of *OTUB1* and *CTGF* mRNAs were analysed by qRT-PCR. Data are represented as mean and error bars indicate standard deviation (n=6). Differences with p<0.01 were annotated as **.
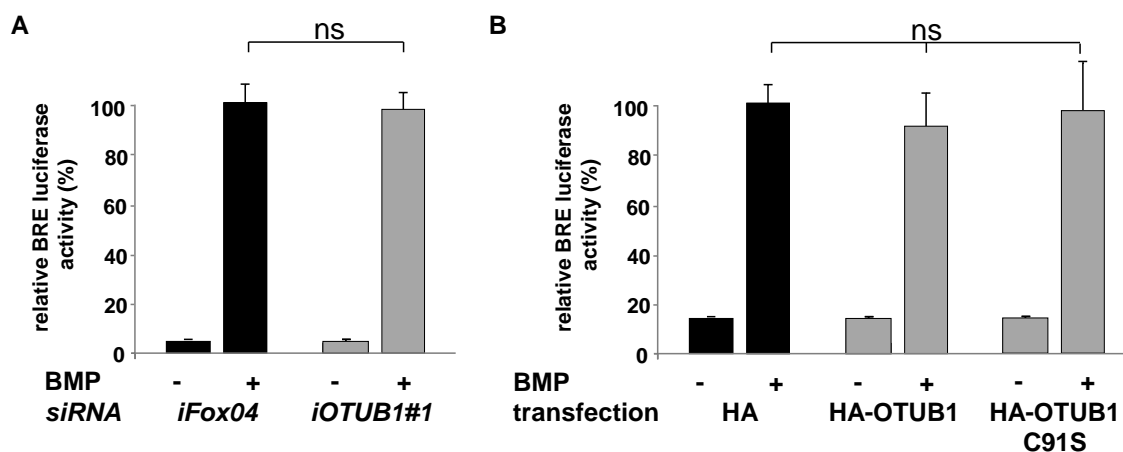
Figure 3-15 OTUB1 does not affect BMP-induced gene transcription

A) C2C12 cells stably expressing a SMAD1-dependent BMP-responsive BRE luciferase reporter construct were transfected with *iFoxO4* or *iOTUB1#1*. Cells were treated with or without 25 ng/ml BMP for 6 hours prior to lysis and luciferase activity was measured. Data are represented as mean and error bars indicate standard deviation (n=3). **B)** Same as in A, except that cells were transfected with HA-OTUB1 or HA-OTUB1 C91S. Data are represented as mean and error bars indicate standard deviation (n=3). Differences with p>0.05 were annotated as ns (not significant).

3.2.8 OTUB1 cleaves K48-linked ubiquitin

In order to investigate the molecular mechanisms by which OTUB1 regulates SMAD2/3 function in the TGFβ pathway, several OTUB1 mutants were generated. Mutants were selected to either abolish OTUB1 catalytic activity or disrupt the interaction of OTUB1 with phospho-SMAD2/3. The catalytic Cysteine of OTUB1, C91, is present in the OTU domain of OTUB1 and forms a catalytic triad with D88 and H265 (Messick *et al.*, 2008). These three residues were targeted for mutagenesis to potentially disrupt the catalytic activity of OTUB1. The N-terminus of OTUB1 harbours the UIM-like, which is deleted in the OTUB1 ΔN mutant (Balakirev *et al.*, 2003, Nakada *et al.*, 2010). Several other point mutants of OTUB1 were also generated. The relative locations of the key residues mutated and employed in this thesis are indicated in a schematic representation of OTUB1 (Figure 3-16A).

To assess the catalytic activity of OTUB1 and mutants described above, *in vitro* deubiquitylation assays on di- or polyubiquitin chains were performed (Figure 3-16B-E). Wild type OTUB1 cleaved K48-linked diubiquitin (Figure 3-16B,C) as well as longer K48-linked polyubiquitin chains (Figure 3-16D), but not K63-linked polyubiquitin chains (Figure 3-16E). The OTUB1 ΔN mutant exhibited slightly reduced catalytic activity *in vitro* against K48-linked ubiquitin chains (Figure 3-16B,D). All the other mutants of OTUB1: D88A, C91S, H265A, D88A/H265A (D/H), D88A/C91S/H265A (D/C/H) (Figure 3-16B,D) and K71R (Figure 3-16C) did not cleave K48-linked ubiquitin chains, indicating that these mutants were catalytically inactive. The addition of phosphorylated (SIRCS<u>S</u>V<u>S</u>) or unphosphorylated (SIRCSSVS) SMAD3 peptide (aa 418-425) to the DUB assay did not significantly alter the catalytic activity of OTUB1 (Figure 3-17).
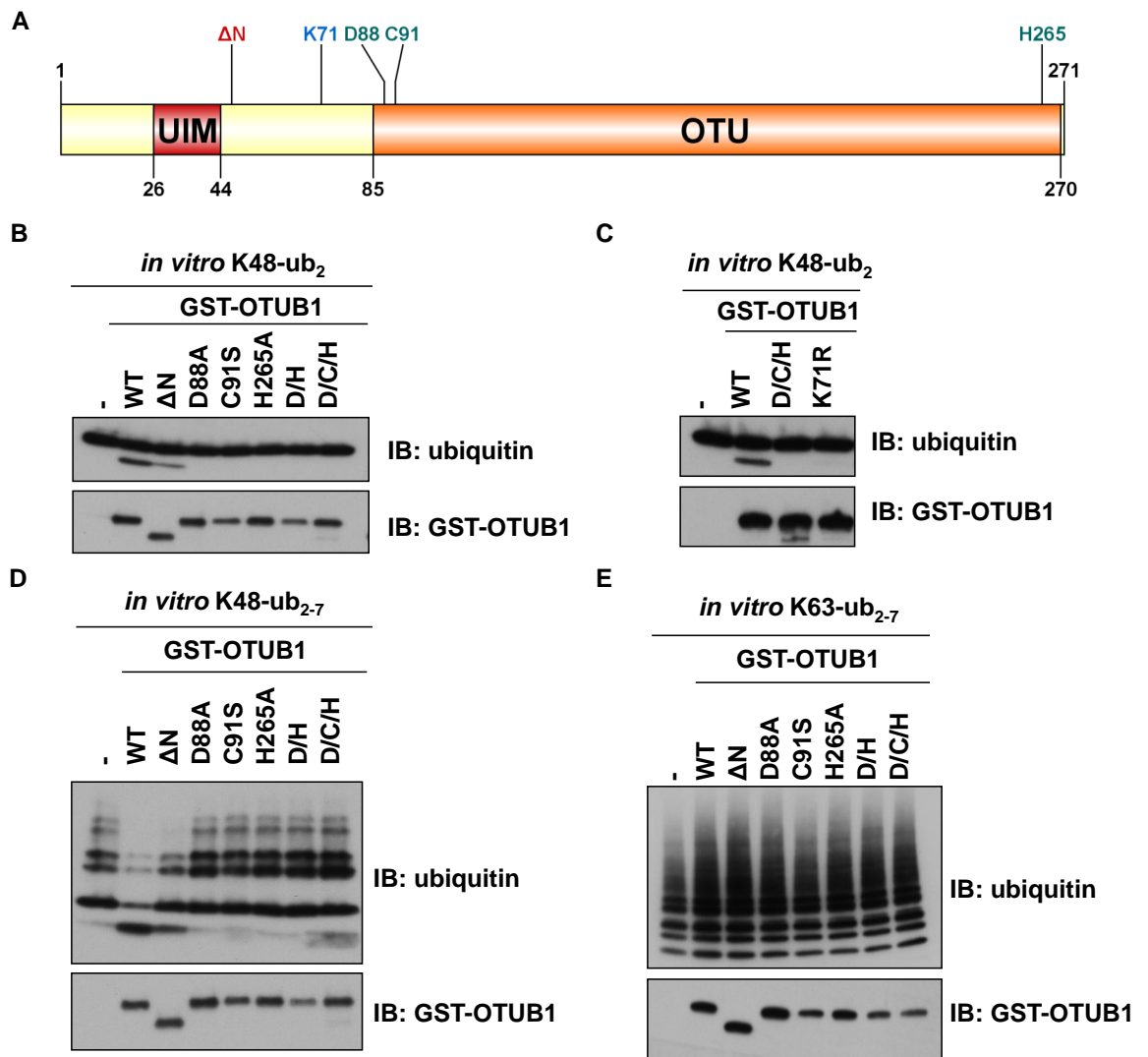
Figure 3-16 Characterisation of OTUB1 activity *in vitro*

A) A schematic representation of OTUB1 indicating the positions of key residues and domains. **B&C)** Human recombinant GST-OTUB1 or indicated GST-OTUB1 mutants were incubated with K48-linked diubiquitin chains in a DUB assay buffer for 1 hour at 30 °C. The reaction was stopped by the addition of 1x SDS sample buffer, the assay mix was resolved by SDS-PAGE and immunoblotted with GST or ubiquitin antibodies as indicated. **D)** As in B&C, however GST-OTUB1 was incubated with K48-linked 2-7 polyubiquitin chains. **E)** As in D, however GST-OTUB1 was incubated with K63-linked 2-7 polyubiquitin chains.
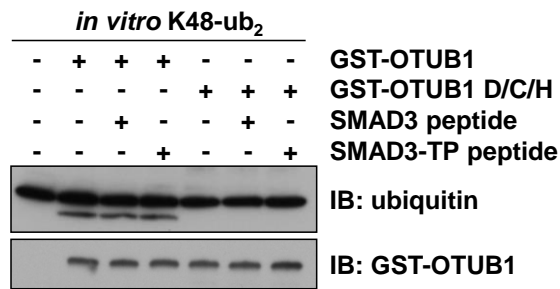
Figure 3-17 The catalytic activity of OTUB1 is not influenced by SMAD3

Human recombinant GST-OTUB1 or GST-OTUB1 D/C/H were incubated with K48-linked diubiquitin in the presence or absence of tail-phosphorylated or unphosphorylated SMAD3 peptide in a DUB assay buffer for 1 hour at 30 °C. The reaction was stopped by the addition of 1x SDS sample buffer, the assay mix was resolved by SDS-PAGE and immunoblotted with GST or ubiquitin antibodies as indicated.

3.2.9 SMAD2/3 are polyubiquitylated by NEDD4L

NEDD4L had previously been described as the E3 ubiquitin ligase that polyubiquitylates SMAD2/3 (Gao *et al.*, 2009, Kuratomi *et al.*, 2005), however the type of ubiquitin chain linkages on SMAD2/3 have not been identified. To verify that NEDD4L polyubiquitylates SMAD3, both proteins were overexpressed in HEK293 cells and SMAD3 immunoprecipitated (Figure 3-18A). In the presence of NEDD4L, the polyubiquitylation of SMAD3 intensifies and probing with K48-ubiquitin specific antibody indicates that part of the ubiquitin chains formed on SMAD3 are K48-linked (Figure 3-18A). K48-linked polyubiquitylation leads to proteasomal degradation (Pickart, 1997), which can be blocked by the proteasomal inhibitor Bortezomib (Adams *et al.*, 1999). NEDD4L mediated degradation of endogenous SMAD2/3 (Figure 3-18B, lane 2) can be rescued by the addition of Bortezomib (Figure 3-18B, lane 4).
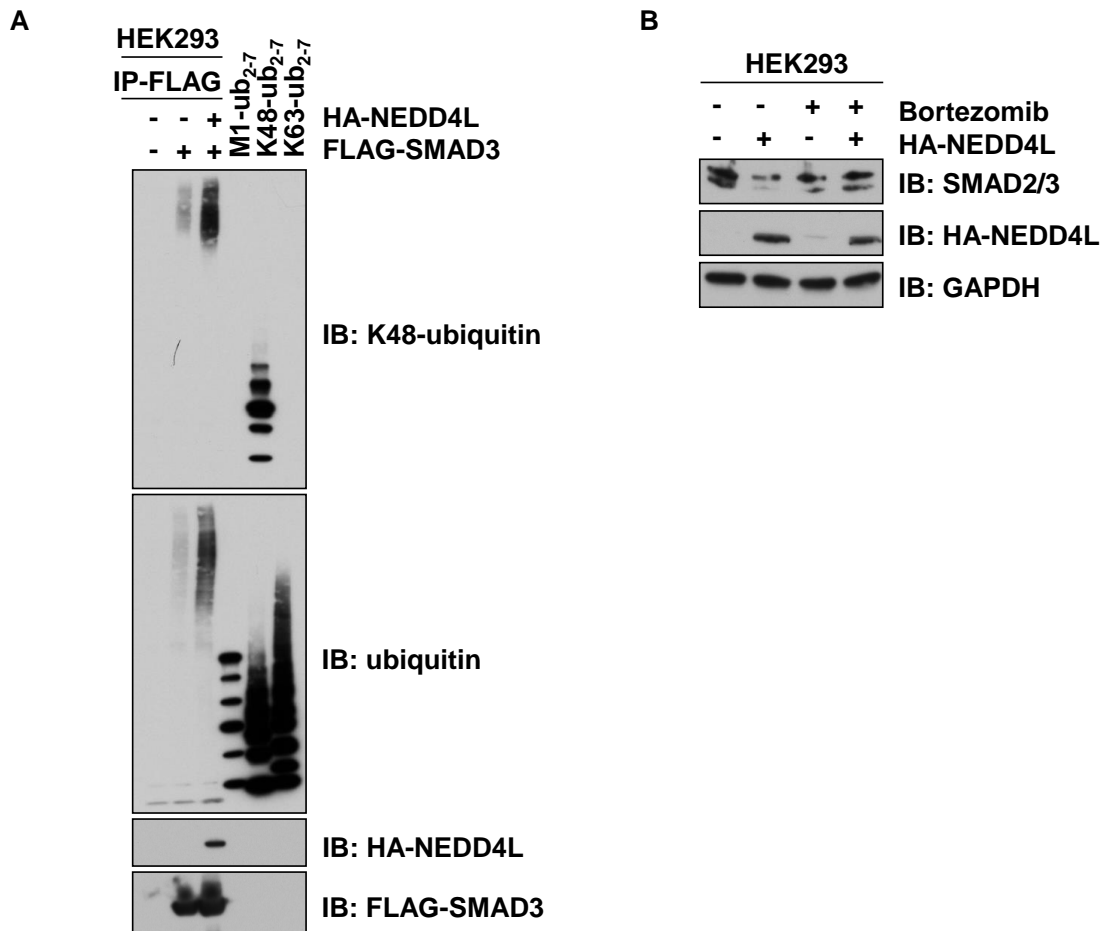
Figure 3-18 NEDD4L polyubiquitylates SMAD2/3

A) HEK293 cells were co-transfected with vectors encoding HA-NEDD4L and FLAG-SMAD3. Prior to lysis (in the presence of iodoacetamide) cells were treated with 50 pM TGFβ for 1 hour and 10 µM Bortezomib for 3 hours. FLAG-IPs and linear-, K48- or K63-linked ubiquitin (2-7 molecules) chains were resolved by SDS-PAGE and immunoblotted with K48-linkage specific and total ubiquitin antibodies. **B)** HEK293 cells were transfected with HA-NEDD4L. Prior to lysis, cells were treated with 50 pM TGFβ for 1 hour and with or without 10 µM Bortezomib for 3 hours. Extracts were resolved by SDS-PAGE and immunoblotted with the indicated antibodies.

3.2.10 OTUB1 affects SMAD3 ubiquitylation

After establishing the catalytic activity of various OTUB1 mutants, their ability to interact with and deubiquitylate SMAD3 was assayed. To test this, HEK293 cells were transfected with HA-OTUB1 or mutant constructs together with FLAG-SMAD3 and HA-ubiquitin. Full-length HA-OTUB1, as well as HA-OTUB1 ΔN, HA-OTUB1 H265A and HA-OTUB1 K71R interacted with FLAG-SMAD3 while HA-OTUB1 C91S, HA-OTUB1 D/C/H mutants and OTUB2 did not (Figure 3-19A,C). Overexpression of FLAG-SMAD3 in HEK293 cells resulted in a spontaneous tail-phosphorylation of FLAG-SMAD3 even in the absence of TGFβ (Figure 3-19B). This potentially caused the interaction between HA-OTUB1 and FLAG-SMAD3 under overexpression conditions even in the absence of TGFβ. When co-expressed with HA-ubiquitin in HEK293 cells, efficient polyubiquitylation was observed in FLAG-SMAD3 IPs independent of TGFβ stimulation (Figure 3-19A,D). Upon co-expression with wild type OTUB1, the polyubiquitylation of FLAG-SMAD3 IPs was reduced (Figure 3-19A,D). However, this reduction could due to the general reduction in polyubiquitin chains observed in extracts when OTUB1, or catalytically inactive mutants of OTUB1 (C91S & H265A), were overexpressed (Figure 3-19A,D). Overexpression of the OTUB1 K71R mutant, which is also catalytically inactive but still interacts with SMAD3, only caused a moderate decrease in FLAG-SMAD3-polyubiquitylation levels (Figure 3-19D).

Overexpression of OTUB1 also led to a general reduction in global endogenous polyubiquitylation seen in extracts (Figure 3-20A). This loss was not rescued completely by proteasomal inhibitors Bortezomib and Lactacystin (Figure 3-20B).
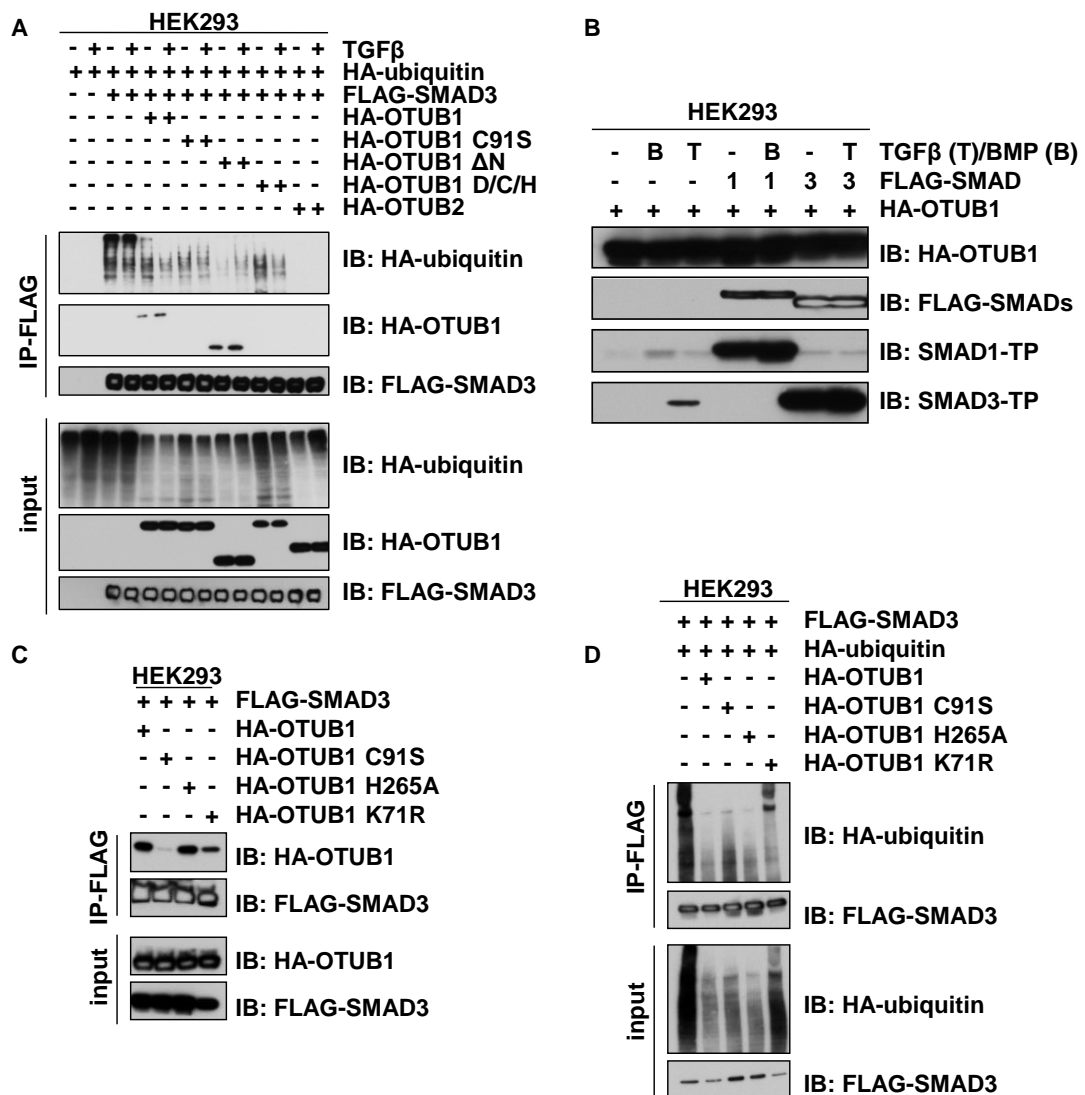
Figure 3-19 OTUB1 affects SMAD3 ubiquitylation

A) HEK293 cells were co-transfected with vectors encoding N-terminal HA-tagged OTUB1 or indicated HA-OTUB1 mutants (C91S, ΔN, D88A/C91S/H265A (D/C/H) or HA-OTUB2), HA-ubiquitin and N-terminal FLAG-tagged SMAD3. Prior to lysis (in the presence of iodoacetamide) cells were treated with or without 50 pM TGFβ and 10 µM Bortezomib for 3 hours. FLAG-immunoprecipitates or extracts were resolved by SDS-PAGE and immunoblotted with the indicated antibodies. **B)** HEK293 cells were co-transfected with vectors encoding N-terminal HA-tagged OTUB1 and N-terminal FLAG-tagged SMAD1 or SMAD3. Prior to lysis cells were treated for 1 hour with 25 ng/ml BMP or 50 pM TGFβ respectively. Extracts were resolved by SDS-PAGE and immunoblotted with the indicated antibodies. **C)** As in A, except that HA-OTUB1 C91S, H265A and K71R mutants but no HA-ubiquitin was transfected. **D)** As in A, except that HA-OTUB1 C91S, H265A and K71R mutants were transfected.
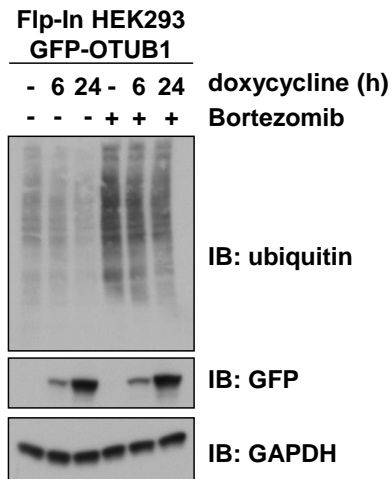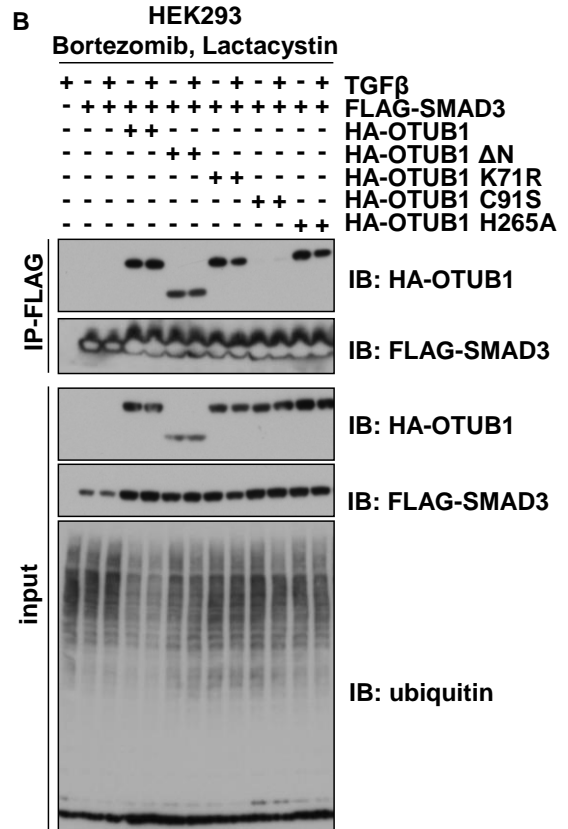
Figure 3-20 OTUB1 inhibits ubiquitylation in cells

A) HEK293 Flp-In cells expressing GFP-OTUB1 under a tetracycline inducible promoter were treated with tetracycline for 6 or 24 hours in the presence or absence of Bortezomib (10 µM, 3 hours). Extracts were resolved by SDS-PAGE and immunoblotted with the indicated antibodies. **B)** HEK293 cells were co-transfected with vectors encoding N-terminal HA-tagged OTUB1 or indicated HA-OTUB1 mutants (ΔN, K71R, C91S, and H265A) and N-terminal FLAG-tagged SMAD3. Prior to lysis (in the presence of iodoacetamide) cells were treated with or without 50 pM TGFβ for 1 hour, 10 µM Bortezomib and 10 µM Lactacystin for 3 hours. FLAG-IPs or extracts were resolved by SDS-PAGE and immunoblotted with the indicated antibodies.

3.2.11 OTUB1 does not appear to deubiquitylate polyubiquitylated SMAD2/3 in vitro

As OTUB1 overexpression in cells lead to a general loss of overall polyubiquitylation in whole cell extracts (Figure 3-20), an *in vitro* approach was chosen to test whether OTUB1 deubiquitylates polyubiquitylated SMAD2/3. FLAG-SMAD2/3 and 4 overexpressed in HEK293 cells together with HA-ubiquitin and HA-NEDD4L were immunoprecipitated and used as substrate for an OTUB1 *in vitro* deubiquitylation assay. Prior to lysis cells were treated with TGFβ and Bortezomib to induce SMAD2/3/4 complex formation and inhibit proteasomal degradation respectively (Figure 3-21A). Wild type OTUB1 and the ΔN mutant, both capable of cleaving K48-linked di- or polyubiquitin chains *in vitro* (Figure 3-16B,D), along with all the catalytically inactive mutants (D88A, C91S, H265A, D/H, D/C/H, K71R) were unable to deubiquitylate the polyubiquitylated FLAG-SMAD2/3/4 complex (Figure 3-21A). Identical results were obtained when *in vitro* polyubiquitylated recombinant SMAD3 was used as a substrate for OTUB1 (Figure 3-21B), indicating that OTUB1 does not deubiquitylate polyubiquitylated SMAD3.
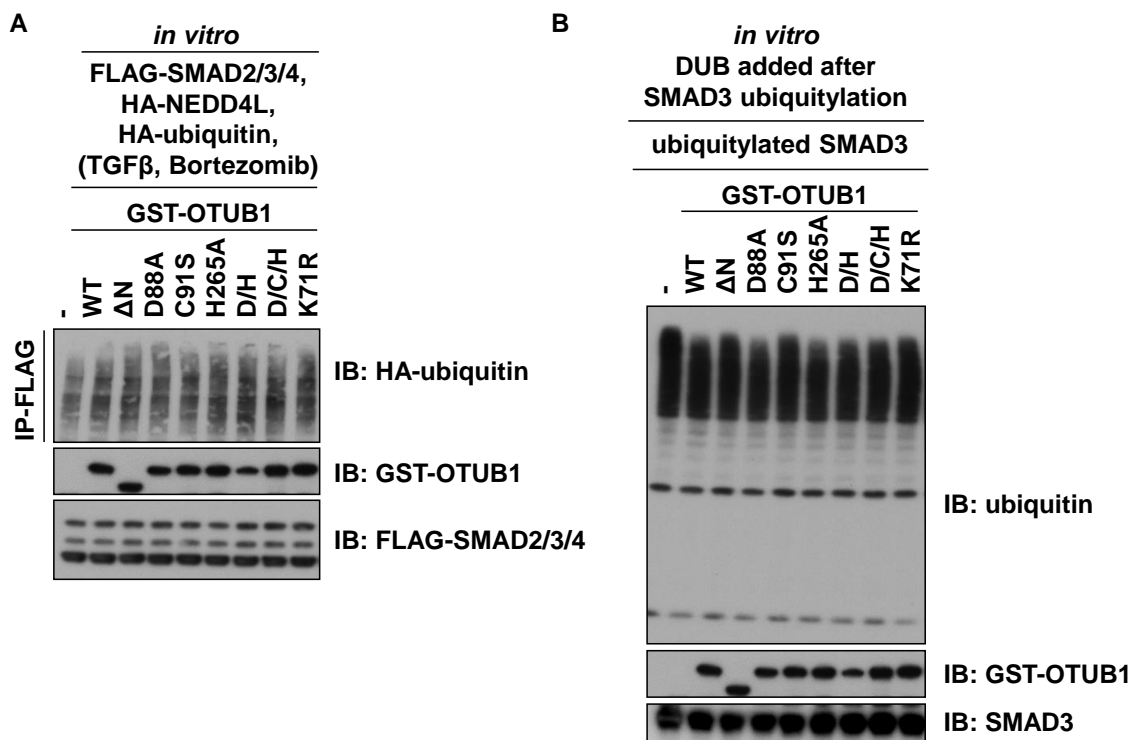
Figure 3-21 OTUB1 does not deubiquitylate polyubiquitylated SMAD2/3

A) For *in-cell* polyubiquitylation of FLAG-SMAD2/3/4, vectors encoding FLAG-SMAD2/3/4 were co-transfected with HA-NEDD4L and HA-ubiquitin in HEK293 cells and treated with 50 pM TGFβ and 10 µM Bortezomib for 3 hours prior to lysis and FLAG-SMAD2/3/4 were immunoprecipitated. An *in vitro* DUB assay of *in-cell* polyubiquitylated FLAG-SMAD2/3/4 was performed with GST-OTUB1 and the indicated GST-OTUB1 mutants in DUB assay buffer for 1 hour at 30 °C. The assay mix was resolved by SDS-PAGE and immunoblotted with the indicated antibodies. **B)** SMAD3 was ubiquitylated *in vitro* in ubiquitylation assay buffer for 1 hour at 30 °C with His-UBE1 (E1), UBE2D1 (E2), His-NEDD4L (E3) and FLAG-ubiquitin. An *in vitro* DUB assay of polyubiquitylated SMAD3 was performed with GST-OTUB1 and the indicated GST-OTUB1 mutants in DUB assay buffer for 1 hour at 30 °C and proteins were resolved by SDS-PAGE and immunoblotted with indicated antibodies.

3.2.12 OTUB1 inhibits polyubiquitylation of SMAD2/3

The decrease in SMAD2/3 polyubiquitylation in cells (Figure 3-19) but no deubiquitylation *in vitro* (Figure 3-21) suggested that OTUB1 possibly inhibits the ubiquitylation of SMAD2/3. Such mode of action had been reported for other substrates of OTUB1 (Nakada *et al.*, 2010, Sun *et al.*, 2011). Therefore, it was tested whether OTUB1 could inhibit the polyubiquitylation of SMAD2/3. Recombinant SMAD2 was polyubiquitylated *in vitro* using UBE1 (E1), UBE2D1 (E2) and NEDD4L (E3) (Alarcón *et al.*, 2009, Kuratomi *et al.*, 2005) (Figure 3-22A). OTUB1 or OTUB1 C91S were added at increasing concentrations at the start of the reaction. In the absence of SMAD2, no autoubiquitylation of E2 or E3 was detected (Figure 3-22A, lane 1). In the presence of SMAD2, robust polyubiquitylation was observed (Figure 3-22A, lane 2). Adding increasing amounts of wild type OTUB1 or catalytically inactive OTUB1 C91S mutant at the start of the assay inhibited the polyubiquitylation of SMAD2 in a dose-dependent manner (Figure 3-22A, lanes 3-10). Likewise, OTUB1 could inhibit the polyubiquitylation of FLAG-SMAD2/3/4 *in vitro* when added at the start of the reaction (Figure 3-22B). As seen with recombinant SMAD2, TGFβ-treated FLAG-SMAD2/3/4 IPs were polyubiquitylated in the presence of E1, E2 & E3 (Figure 3-22B, lane 3) and no autoubiquitylation occurred (Figure 3-22B, lane 2). Polyubiquitylation was significantly inhibited when OTUB1 and most of the OTUB1 mutants (D88A, C91S, H265A, D/H) were added at the start of the ubiquitylation assay (Figure 3-22B, lanes 4, 6-9). These results implied that OTUB1 inhibits the ubiquitylation of SMAD2/3 rather than directly deubiquitylating them. However, OTUB1 ΔN, D/C/H and K71R mutants were unable to inhibit polyubiquitylation (Figure 3-22B, lanes 5, 10, 11, discussed in

section 3.3.2). A summary of the ability of each OTUB1 mutant to bind SMAD3, deubiquitylate or inhibit ubiquitylation are outlined in Table 3-1.
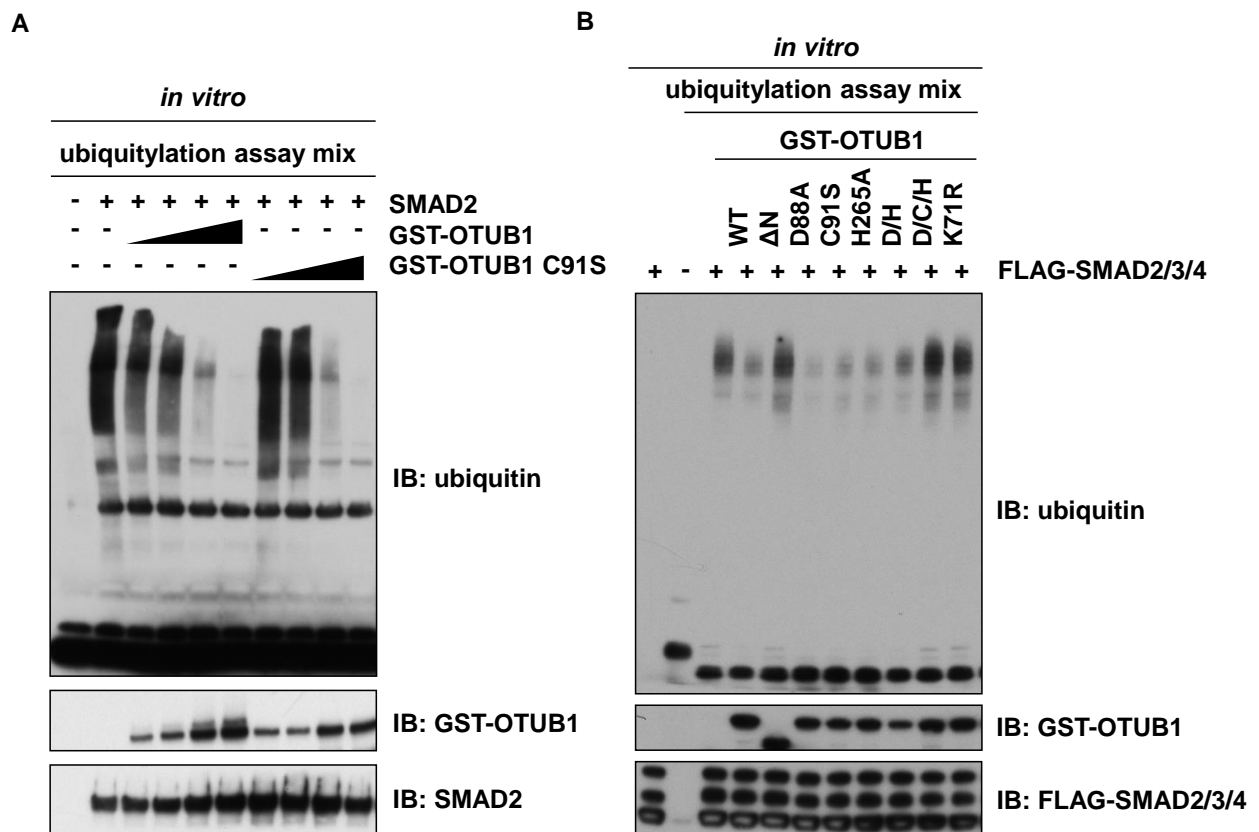
Figure 3-22 OTUB1 prevents SMAD2/3 ubiquitylation *in vitro*

A) An *in vitro* ubiquitylation assay was performed with human recombinant SMAD2. SMAD2 was incubated with His-UBE1 (E1), UBE2D1 (E2), His-NEDD4L (E3) and ubiquitin in ubiquitylation assay buffer for 1 hour at 30 °C. Increasing concentrations of GST-OTUB1 and GST-OTUB1 C91S (8-60 ng/µl) were added at the start of the ubiquitylation assay (time 0). Proteins were resolved by SDS-PAGE and immunoblotted with the indicated antibodies. **B)** FLAG-SMAD2/3/4 IPs (from HEK293 cells expressing FLAG-SMAD2/3/4 treated with 50 pM TGFβ for 1 hour prior to lysis) were ubiquitylated *in vitro* in ubiquitylation assay buffer for 1 hour at 30 °C using His-UBE1 (E1), UBE2D1 (E2), His-NEDD4L (E3) and ubiquitin. The indicated DUBs were added at the start of the ubiquitylation assay (time 0) and proteins were resolved by SDS-PAGE and immunoblotted with the indicated antibodies.

Table 3-1 Assessment of OTUB1 mutants

Outline of the ability of OTUB1 mutants to bind SMAD3, cleave K48-linked ubiquitin or inhibit ubiquitylation of SMAD3.

mutant	binds SMAD3	cleaves K48-ub chains *in vitro*	inhibits SMAD3 ubiquitylation
WT	+	+	+
ΔN	+	+	-
D88A	-	-	+
C91S	-	-	+
H265A	+	-	+
D/H	-	-	+
D/C/H	-	-	-
K71R	+	-	-

3.2.13 Effects of OTUB1 mutations on TGFβ-induced transcription

The previous results suggested that OTUB1 inhibits ubiquitylation of SMAD2/3, possibly stabilising the complex. As SMADs are transcription factors, the impact of OTUB1 mutations on TGFβ-induced target gene transcription was investigated. The impact of OTUB1 catalytic activity, its ability to inhibit ubiquitylation of SMAD2/3 and its ability to interact with SMAD3 on TGFβ-induced transcription were investigated. The loss in expression of the TGFβ-target gene *PAI-1* caused by siRNA-mediated depletion of *OTUB1* was efficiently rescued by the re-introduction of siRNA-resistant *OTUB1* (Figure 3-23A). However, neither OTUB1 C91S (catalytically inactive, inhibits polyubiquitylation of SMAD3 *in vitro* but does not interact with SMAD3) nor OTUB1 ΔN (catalytically active and interacts with SMAD3 but does not inhibit polyubiquitylation of SMAD3 *in vitro*) were able to rescue *PAI-1* expression (Figure 3-23A). These results suggested that the ability of OTUB1 to both interact with and prevent the ubiquitylation of SMAD3 independent of its

catalytic activity were essential for the regulation of TGFβ-induced transcription. The expression levels of OTUB1 mutant proteins were confirmed by immunoblotting (Figure 3-23).
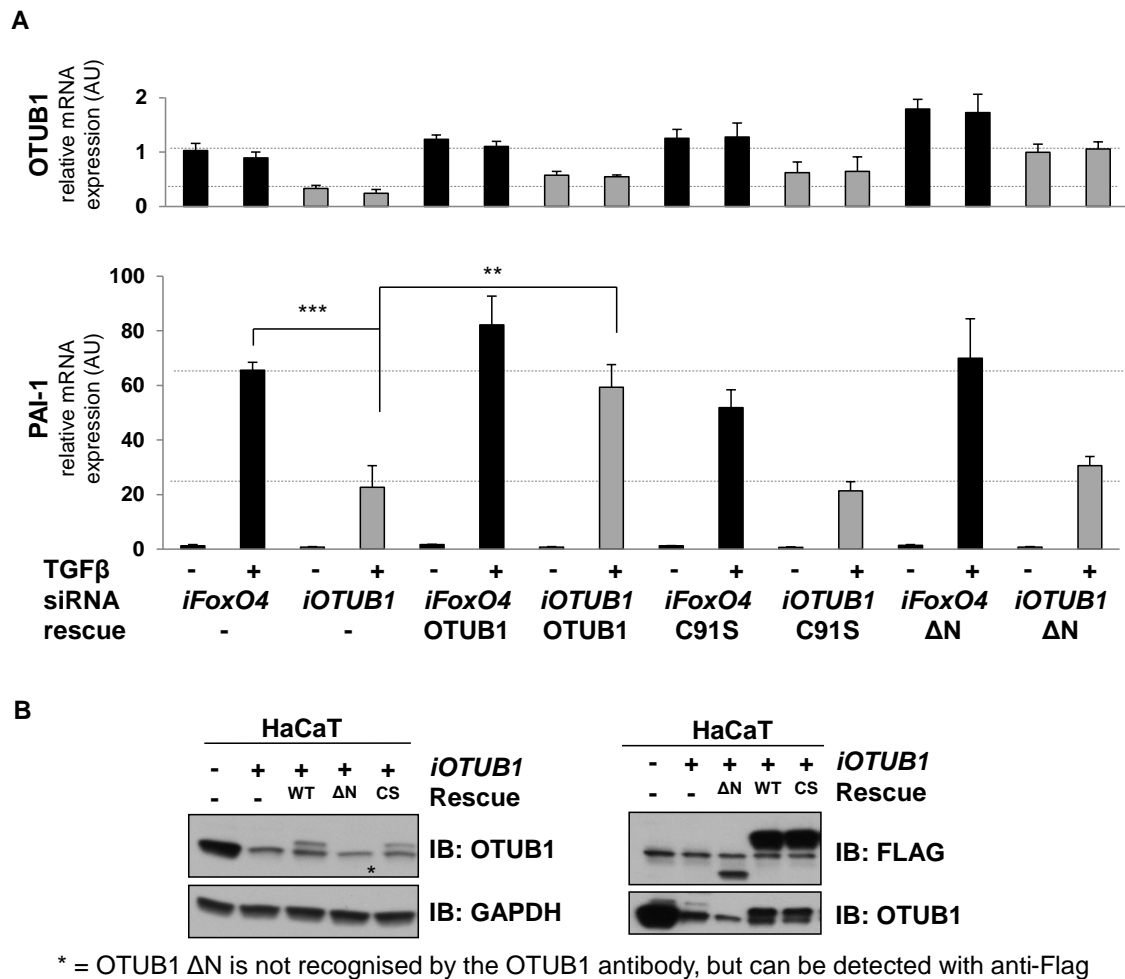
Figure 3-23 Only wild type OTUB1 rescues *iOTUB1* phenotype

A) HaCaT cells were stably transfected with vectors encoding siRNA-resistant silent mutations (rescue) of the indicated OTUB1 constructs. These cells were then transfected with control *FoxO4* or *OTUB1* siRNA for 48 hours and treated with or without TGFβ for 4 hours prior to RNA isolation. Relative expression levels of indicated mRNAs were analysed by qRT-PCR. Data are represented as mean and error bars indicate standard deviation (n=6). Differences with *p*<0.01 were annotated as ** and *p*<0.001 were annotated as ***. **B)** Extracts from A were resolved by SDS-PAGE and immunoblotted with the indicated antibodies.

3.2.14 OTUB1 binds E2 enzymes

OTUB1 had previously been reported to inhibit ubiquitylation of target proteins by interacting with and inhibiting E2 ubiquitin conjugating enzymes (Nakada *et al.*, 2010, Juang *et al.*, 2012, Sato *et al.*, 2012, Wiener *et al.*, 2012). Consistent with the reported findings, several members of E2 ubiquitin conjugating enzymes, including UBE2N, all members of the UBE2D and UBE2E family of E2s and BIRC6, were identified as major interactors of GFP-OTUB1 by mass spectrometry (Table 3-2, Figure 3-24A,B). In OTUB1 IPs, endogenous UBE2D and UBE2N were identified as interactors independent of TGFβ signalling (Figure 3-24C). Additionally, the endogenous interaction between OTUB1 with BIRC6 was verified (Figure 3-24D).
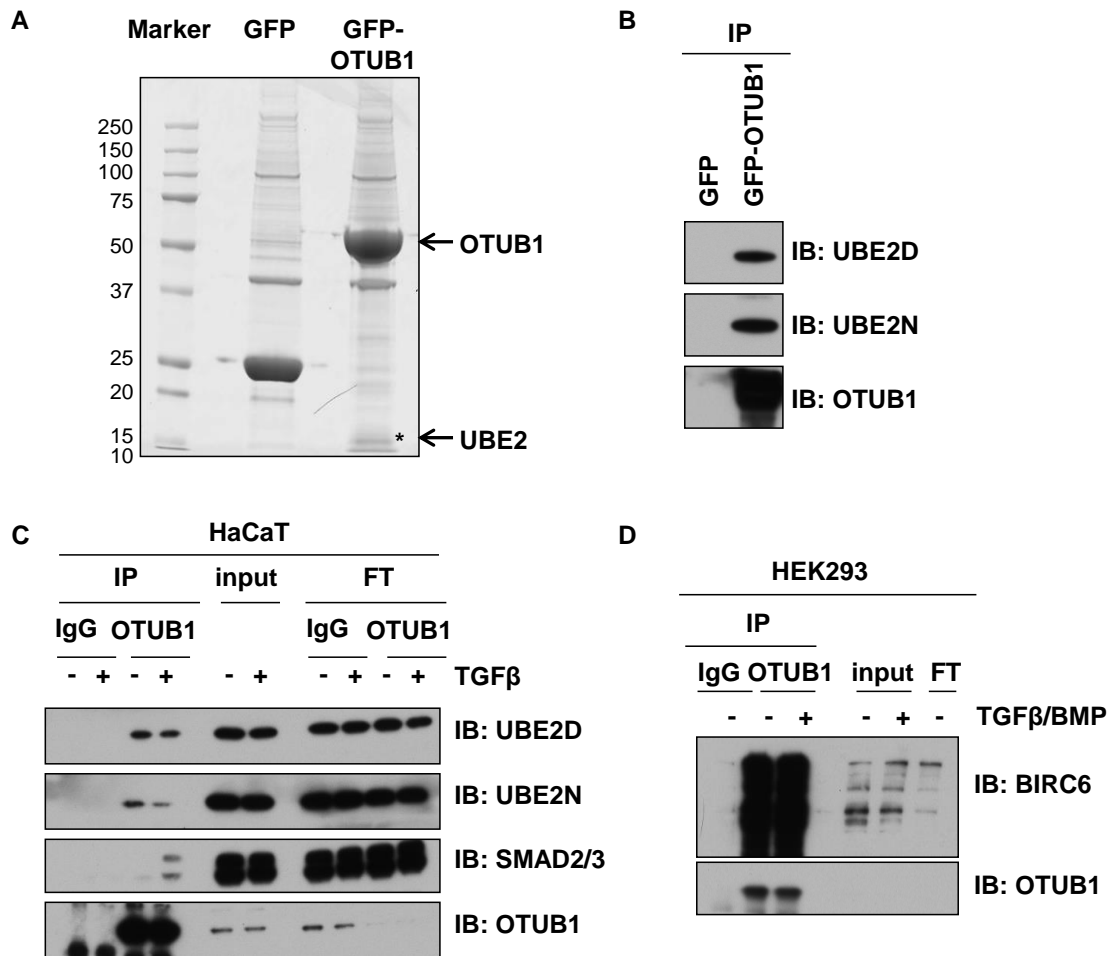
Figure 3-24 OTUB1 binds E2 enzymes

A) GFP and GFP-OTUB1 immunoprecipitates from HEK293 cells stably expressing these proteins were lysed in the presence of DSP and GFP-IPs were separated by SDS-PAGE and interacting proteins identified by mass spectrometry (*cf.* Table 3-2). **B)** Same as in A, but samples were immunoblotted with the indicated antibodies. **C)** An endogenous IP with OTUB1 antibody or pre-immune sheep IgG was performed in HaCaT cell extracts stimulated with or without 50 pM TGFβ for 1 hour prior to lysis in the presence of DSP. Cell extracts, endogenous IgG or anti-OTUB1 IPs and the corresponding immune-depleted flow-through extracts were resolved by SDS-PAGE and immunoblotted with the indicated antibodies. **D)** An endogenous IP with OTUB1 antibody or pre-immune sheep IgG was performed in HEK293 cell extracts stimulated with or without 50 pM TGFβ and 25 ng/ml BMP for 1 hour prior to lysis in the presence of DSP. Cell extracts, endogenous IgG or anti-OTUB1 IPs and immune-depleted flow-through extracts were resolved by SDS-PAGE and immunoblotted with the indicated antibodies.

Table 3-2 OTUB1 binds E2 enzymes

List of E2 enzymes that were identified as interactors of GFP-OTUB1 but not GFP. UBE2D1 was used for the ubiquitylation assays.

Gene	Protein Name	MW (Da)	score	peptide	coverage
UBE2N	Ubiquitin-conjugating enzyme E2 N	17184	1171	50	79%
UBE2E1	Ubiquitin-conjugating enzyme E2 E1	21676	872	37	65%
UBE2E2	Ubiquitin-conjugating enzyme E2 E2	22526	756	34	59%
UBE2E3	Ubiquitin-conjugating enzyme E2 E3	23184	685	24	58%
UBE2D2	Ubiquitin-conjugating enzyme E2 D2	16953	582	34	87%
UBE2D3	Ubiquitin-conjugating enzyme E2 D3	16904	577	34	91%
UBE2V2	Ubiquitin-conjugating enzyme E2 variant 2	16409	390	17	55%
UBE2V1	Ubiquitin-conjugating enzyme E2 variant 1	16598	348	15	59%
UBE2NL	Putative ubiquitin-conjugating enzyme E2 N-like	17366	296	21	35%
UBE2D1	Ubiquitin-conjugating enzyme E2 D1	16819	272	19	46%
UBE2D4	Ubiquitin-conjugating enzyme E2 D4	16866	219	19	25%
UBE2L3	Ubiquitin-conjugating enzyme E2 L3	18021	105	3	24%
BIRC6	Baculoviral IAP repeat-containing protein 6	536192	9560	454	55%

3.2.15 OTUB1 inhibits the transfer of ubiquitin from E2~ub to the E3 ligase

To investigate if OTUB1 inhibits SMAD3 polyubiquitylation by binding to and thereby inhibiting E2 enzymes and whether this step is the rate-limiting step, an *in vitro* ubiquitylation assay with ubiquitin, UBE1 (E1), varying concentrations of UBE2D1 (E2), NEDD4L (E3) and recombinant human SMAD3 in the presence or absence of 0.5 µM GST-OTUB1 was set up (Figure 3-25A). In the absence of OTUB1, increasing concentrations of UBE2D1 resulted in enhanced polyubiquitylation of SMAD3 in a dose dependent manner (Figure 3-25A). As observed previously (Figure 3-22), the presence of OTUB1 in the reaction resulted in a significant inhibition of polyubiquitylation, especially at lower concentrations of UBE2D1 (Figure 3-25A). Higher concentrations of UBE2D1 substantially rescued this inhibition, suggesting that binding of OTUB1 to UBE2D1 is likely to be the rate-limiting step in the inhibition of

polyubiquitylation of SMAD3 (Figure 3-25A). Next, it was investigated whether OTUB1 inhibits UBE2D1 by preventing the conjugation of ubiquitin or the transfer of ubiquitin from UBE2D1 to NEDD4L. In the presence of ubiquitin, ATP and UBE1, almost every molecule of UBE2D1 was loaded with ubiquitin (UBE2D1~ub) (Figure 3-25B; compare lane 1 vs. 2). This ubiquitin-loading of UBE2D1 was not inhibited when wild type OTUB1, OTUB1 C91S or OTUB1 K71R mutants were present. When E3 ubiquitin ligase NEDD4L and its substrate SMAD3 were added to the reaction, in the absence of OTUB1 most of the ubiquitin at the predicted molecular weight disappeared (Figure 3-25B; compare lane 2 vs. 7). Under these conditions, consistent with an efficient transfer of ubiquitin from UBE2D1~ub to NEDD4L and substrate, UBE2D1 was mostly observed in a non-ubiquitin loaded native molecular weight state (Figure 3-25B). However, when wild type OTUB1 was added to the reaction at the start, some ubiquitin was observed at its native molecular weight while a significant amount of ubiquitin-loaded UBE2D1 was also observed, suggesting that OTUB1 inhibited the transfer of ubiquitin from UBE2D1~ub complex to NEDD4L (Figure 3-25B). OTUB1 C91S, a catalytically inactive mutant that did not interact with SMAD3 but prevented its ubiquitylation, mimicked wild type OTUB1. However, OTUB1 K71R, a catalytically inactive mutant, did not appear to inhibit the transfer of ubiquitin from UBE2D1-ub complex to NEDD4L (Figure 3-25B, *cf.* bottom line monoubiquitin). This was consistent with the inability of OTUB1 K71R mutant to inhibit the ubiquitylation of SMAD3 (Figure 3-22B). These results suggested that by binding to E2 ubiquitin conjugating enzymes, OTUB1 inhibited the transfer of ubiquitin from the E2-ub complex onto E3 ubiquitin ligases.
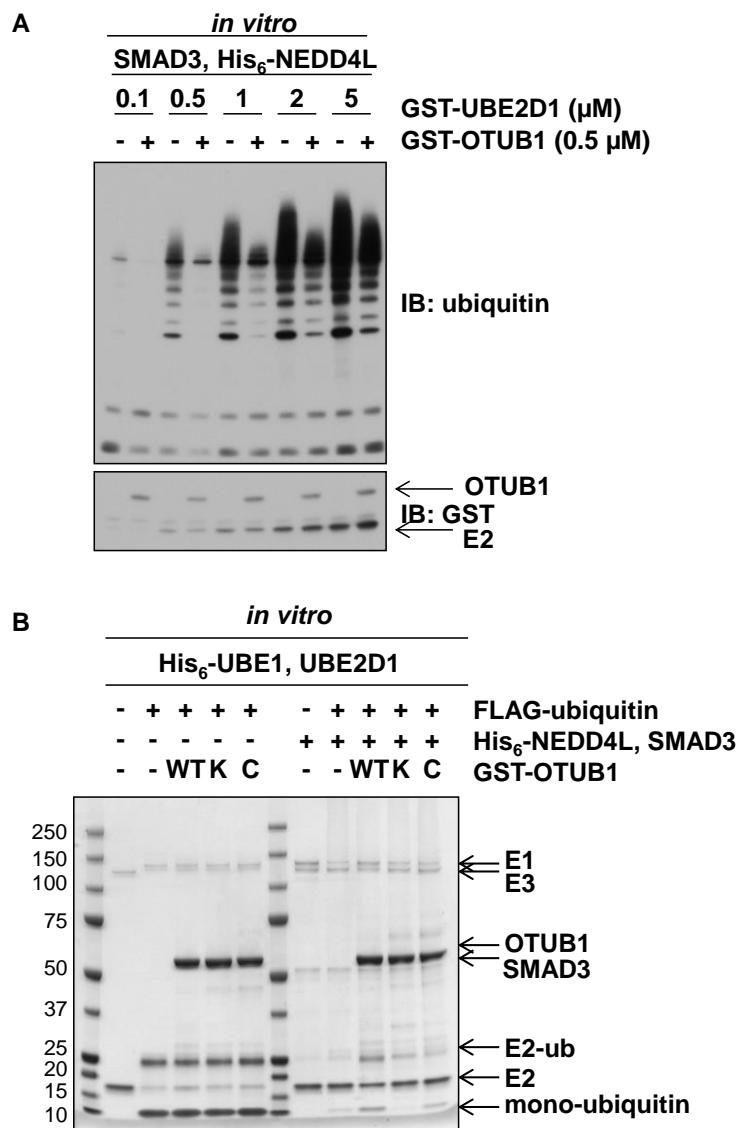
Figure 3-25 OTUB1 inhibits ubiquitin transfer from E2~ub to E3

A) An *in vitro* ubiquitylation assay was performed with human recombinant SMAD3, His-UBE1 (0.1 µM), ubiquitin, His-NEDD4L (1 µM) and increasing concentrations of GST-UBE2D1 (0.1-5 µM) in ubiquitylation assay buffer for 1 hour at 30 °C. GST-OTUB1 was added at the start of the ubiquitylation assay (time 0). Proteins were resolved by SDS-PAGE and immunoblotted with the indicated antibodies. **B)** His-UBE1, UBE2D1, FLAG-ubiquitin, GST-OTUB1 and mutants were mixed with or without His-NEDD4L and SMAD3 prior to the addition of ATP. After 10 min at 30 °C, proteins were separated by SDS-PAGE and visualised with Coomassie staining (performed by M. Al-Salihi). Abbreviations used: WT= wild type, K=K71R, C=C91S.

3.2.16 OTUB1 rescues phospho-SMAD2/3 from proteasomal degradation

OTUB1 bound to phospho-SMAD2/3 (Figure 3-5) and E2 ubiquitin conjugating enzymes (Figure 3-24), thereby inhibiting the polyubiquitylation of SMAD2/3 *in vitro* (Figure 3-22). Therefore, OTUB1 potentially enhanced the TGFβ-induced transcriptional responses (Figure 3-14) via the stabilisation of the active phospho-SMAD2/3 pool in cells by protecting it from polyubiquitin-mediated proteasomal degradation. To demonstrate that the turnover of active phospho-SMAD2/3 was mediated in part by proteasomal degradation, HaCaT cells were treated with 26S proteasome inhibitors (Bortezomib or MG132) and TGFβ for 3 hours. Bortezomib, and to a lesser extent MG132, treatment resulted in enhanced levels of TGFβ-induced phospho-SMAD2/3 as well as polyubiquitylated proteins (Figure 3-26A). Bortezomib stabilised phospho-SMAD2/3 levels for up to 16 hours following ligand removal (Figure 3-26B). When TGFβ and Bortezomib were added to the cells for 1 hour, the increase in the levels of TGFβ-induced phospho-SMAD2/3 caused by Bortezomib were only slight. Additionally, early induction of phospho-SMAD2/3 by TGFβ were unaffected by siRNA-mediated depletion of OTUB1 (Figure 3-26C).

As polyubiquitylation and degradation of phospho-SMAD2/3 occur subsequent to the assembly of the active SMAD2/3/4 complex at the transcription sites (Alarcón *et al.*, 2009), a pulse-chase experiment was performed (Figure 3-27). Control or OTUB1-depleted HaCaT cells were stimulated with TGFβ for 1 hour to induce maximal phosphorylation of SMAD2/3, after which the TGFβ ligand was removed. In addition to ligand removal, SB505124 (1 μM) was added to the samples in order to block any further TGFβ receptor activity, with or without Bortezomib (10 μM). The levels of phospho-SMAD2/3 were tracked at fixed time points thereafter in the

presence or absence of Bortezomib. The cells depleted of OTUB1 expression exhibited lower levels of phospho-SMAD2/3 after ½ and 1 hour of TGFβ removal compared to control cells (Figure 3-27A, lanes 2 and 6). This effect appeared to be a result of rapid proteasomal degradation, as the levels of phospho-SMAD2/3 were stabilised in the presence of Bortezomib (Figure 3-27A, lanes 4, 8). The levels of total SMAD2/3 or SMAD4 did not change significantly (Figure 3-27A). The reduction in the levels of phospho-SMAD2 caused by depletion of OTUB1 was rescued by a siRNA-resistant wild type FLAG-OTUB1 construct, suggesting that the results obtained were unlikely to be due to off-target effects (Figure 3-27B).
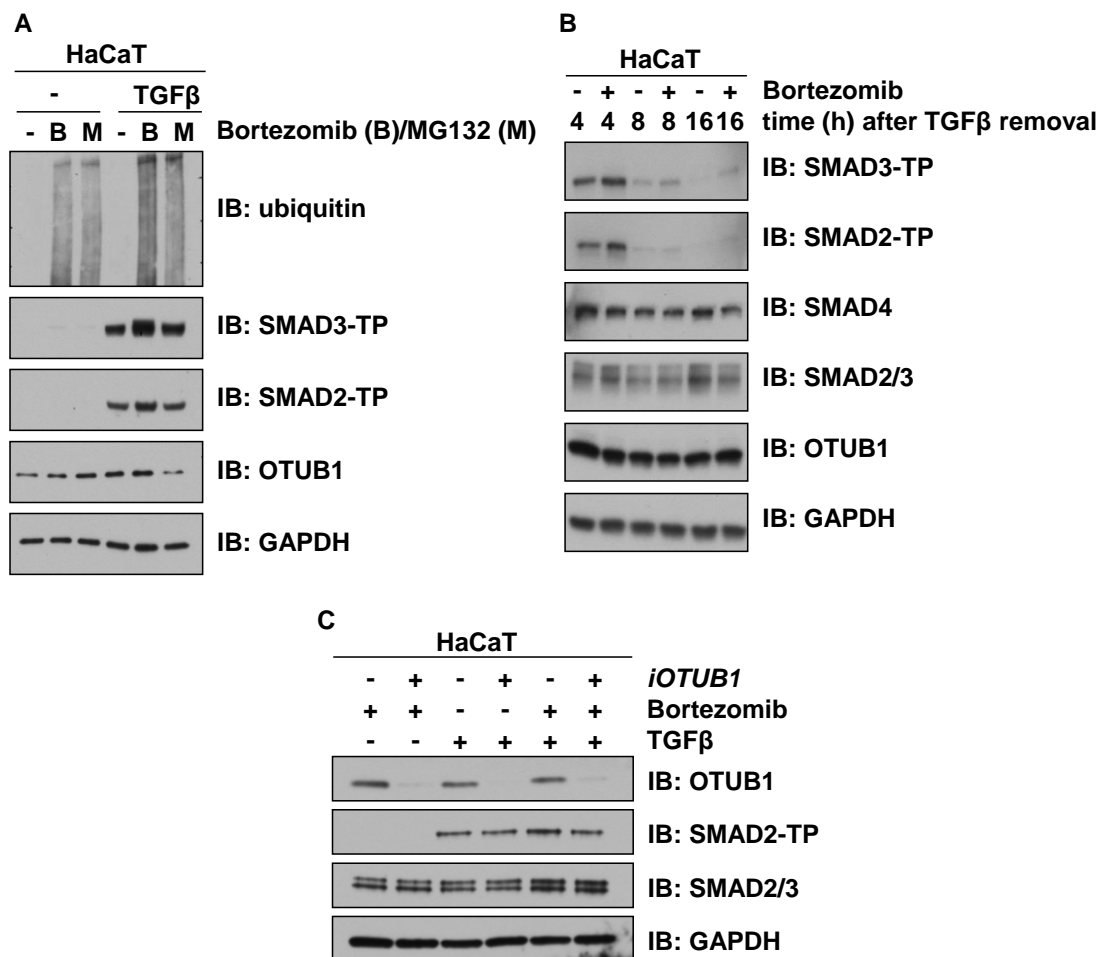
Figure 3-26 OTUB1 does not affect tail-phosphorylated SMAD2/3 stability during early pathway activation

A) HaCaT cells were treated with TGFβ (50 pM) and Bortezomib or MG132 (10 µM) for 3 hours. Extracts were resolved by SDS-PAGE and immunoblotted with the indicated antibodies. **B)** HaCaT cells were treated with TGFβ (50 pM) for 1 hour and the media was replaced with serum free media, supplemented with SB505124 (1 µM) in the presence or absence of Bortezomib (10 µM). Cells were lysed at the indicated times after removal of TGFβ, extracts resolved with SDS-PAGE and immunoblotted with the indicated antibodies. **C)** HaCaT cells transfected with *FoxO4* (-) or *OTUB1* siRNAs were treated with TGFβ (50 pM) and Bortezomib (10 µM) for 1 hour. Extracts were resolved by SDS-PAGE and immunoblotted with the indicated antibodies.

A

HaCaT

-	+	-	+	-	+	-	+	*iOTUB1*
-	-	+	+	-	-	+	+	Bortezomib
½	½	½	½	1	1	1	1	time (h) after TGFβ removal

IB: SMAD2-TP (low)

IB: SMAD2-TP (high)

IB: SMAD3-TP

IB: SMAD2/3

IB: SMAD4

IB: OTUB1

IB: GAPDH

B

HaCaT

-	+	+	*iOTUB1*
-	-	+	Rescue
45	45	45	time (min) after TGFβ removal

IB: SMAD2-TP

IB: OTUB1

IB: GAPDH
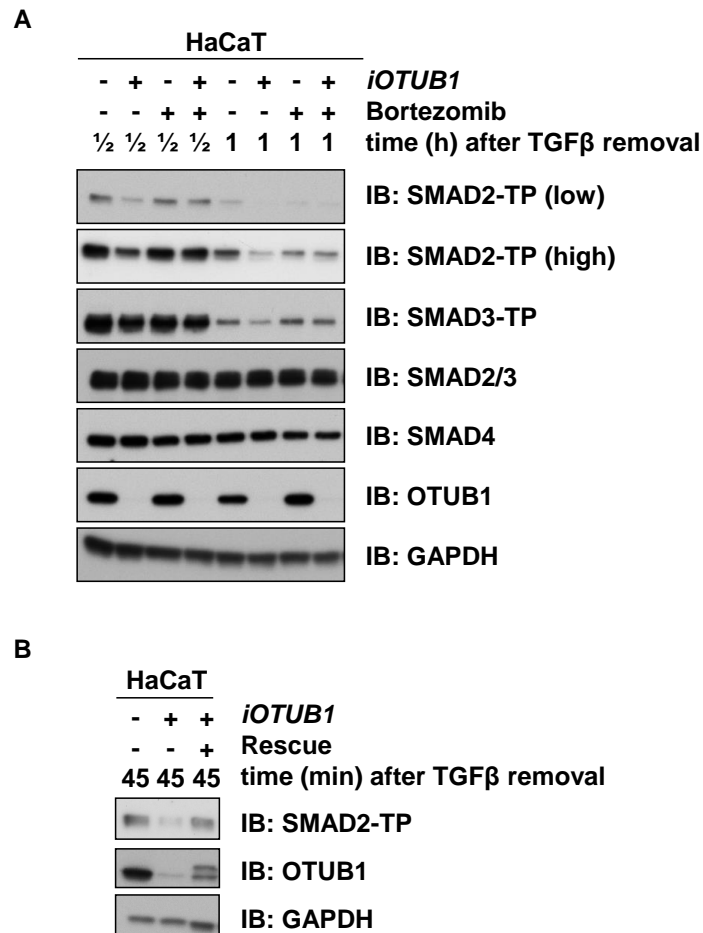
Figure 3-27 OTUB1 protects TGFβ-activated SMAD2/3 from proteasomal degradation

A) HaCaT cells, expressing control shRNA (-) or *OTUB1* shRNA were transfected with *FoxO4* (-) or *OTUB1* siRNAs respectively, 48 hours prior to cell lysis. Cells were serum starved for 16 hours and stimulated with TGFβ (50 pM) and Bortezomib (10 μM) for 1 hour. The cells were then washed in PBS and media was replaced with starvation media supplemented with SB505124 (1 μM) (to block any further TGFβ receptor activity), with or without Bortezomib (10 μM). The cells were lysed at ½ or 1 hour time points and cell extracts resolved by SDS-PAGE and immunoblotted with the indicated antibodies. **B)** As in A, except cells were transfected with vector encoding FLAG-tagged full length OTUB1 resistant to *OTUB1* shRNA and siRNA (rescue).

3.2.17 OTUB1 does not have an effect on TGFβ-induced apoptosis

TGFβ cytokines can act as tumour suppressors by inducing apoptosis which is critical during tissue formation and remodelling (Schuster and Krieglstein, 2002). In order to investigate whether OTUB1 had an effect on TGFβ-induced apoptosis, several cell lines were tested for their susceptibility to apoptosis by a 24-hour treatment with 50 pM of TGFβ (Figure 3-28A). Induction of apoptosis can be monitored by the cleavage of Caspase3 or PARP via immunoblotting (Fernandes-Alnemri *et al.*, 1994, Nicholson *et al.*, 1995). NMuMG and RAMOS cells underwent apoptosis upon prolonged TGFβ treatment (Figure 3-28A). As RAMOS cells were inefficient at RNAi or cDNA transfections (data not shown), NMuMG cells were employed to investigate whether OTUB1 perturbations influence TGFβ-mediated apoptosis (Figure 3-28B). Neither overexpression of HA-OTUB1 nor siRNA mediated depletion of OTUB1 changed the levels of cleaved Caspase3 upon TGFβ stimulation, indicating that OTUB1 does not influence TGFβ-dependent apoptosis (Figure 3-28B).
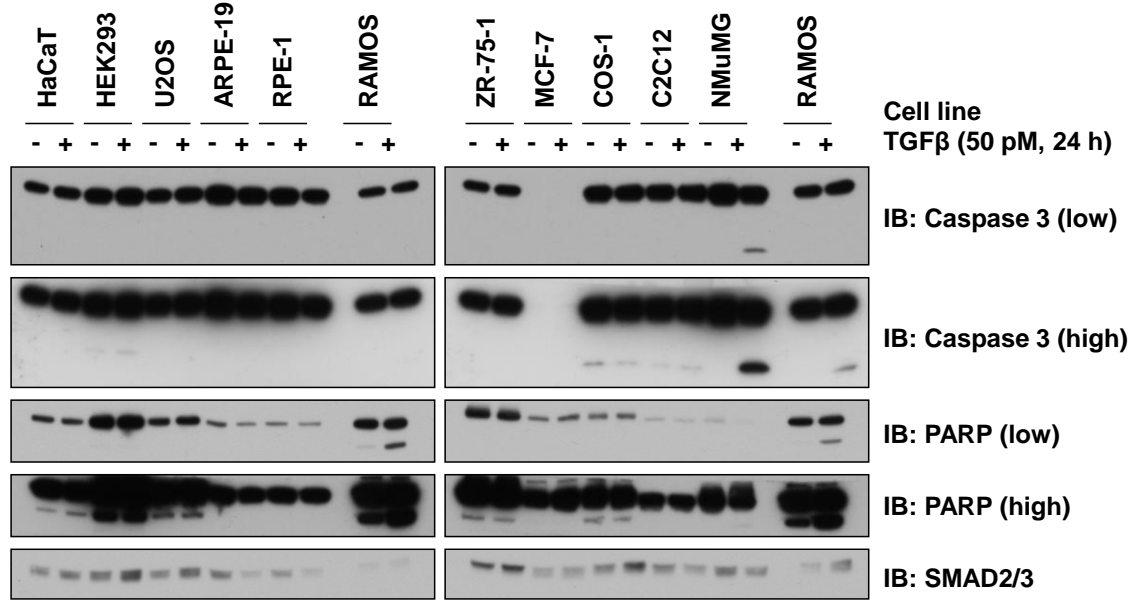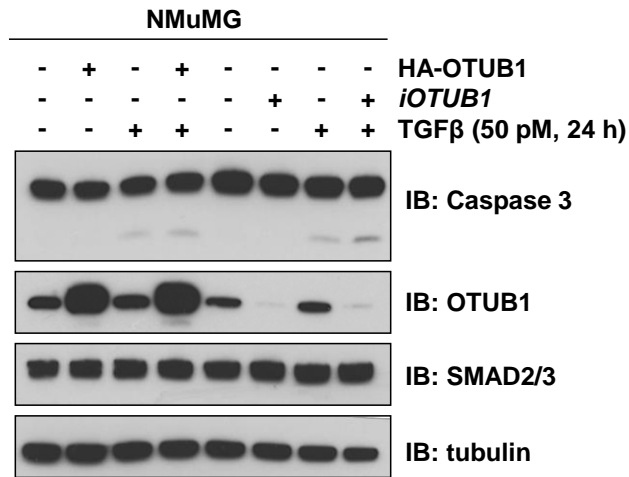
Figure 3-28 OTUB1 does not influence TGFβ-induced apoptosis

A) Different cell lines were treated with 50 pM TGFβ for 24 hours. Extracts were resolved by SDS-PAGE and immunoblotted with the indicated antibodies. **B)** NMuMG cells transfected with HA-OTUB1 or *OTUB1* siRNAs were treated with 50 pM TGFβ for 24 hours. Extracts were resolved by SDS-PAGE and immunoblotted with the indicated antibodies.

3.2.18 OTUB1 does not have an effect on TGFβ-regulated cell proliferation

Another tumour suppressor function of TGFβ cytokines relies on the inhibition of cell proliferation (Siegel and Massague, 2003). To test whether the absence of OTUB1 from cells influences TGFβ-mediated growth inhibition, a proliferation assay was performed using HaCaT cells transfected with OTUB1 or control siRNAs. The XTT assay, which is a colorimetric assay that makes use of the ability of live cells to metabolically reduce tetrazolium salt into coloured formazans, was employed to assess proliferation (Scudiero *et al.*, 1988). As expected, the addition of TGFβ in HaCaT cells decreased their proliferation (Huang and Huang, 2005) (Figure 3-29, Table 3-3). The depletion of OTUB1 also resulted in a slight, but not significant, reduction of cell growth. Importantly, the difference in proliferation between control cells and OTUB1-depleted cells both treated with TGFβ was not significant (Table 3-3, Figure 3-29). Hence, OTUB1 does not appear to influence TGFβ-mediated inhibition of HaCaT cell proliferation.
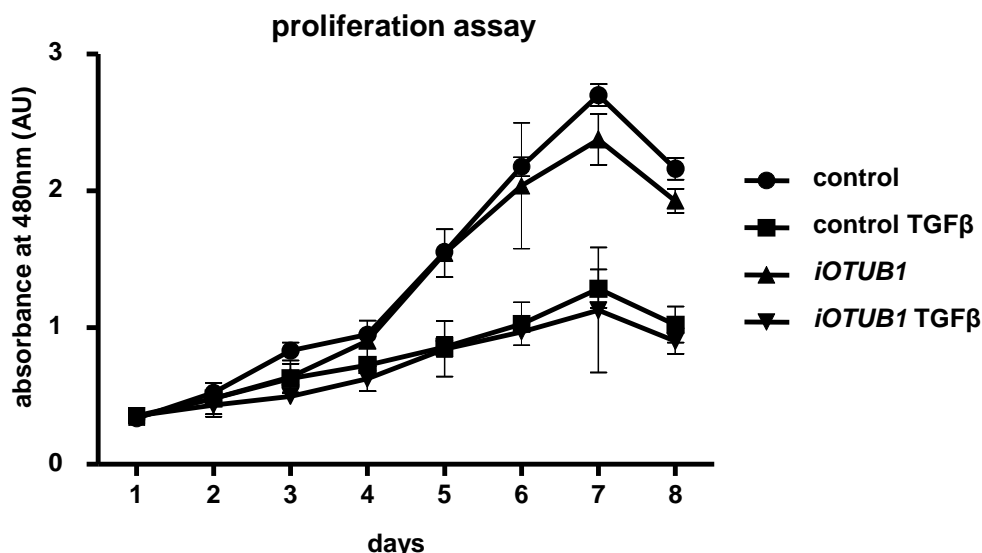
Figure 3-29 OTUB1 does not affect TGFβ-regulated cell proliferation

Control HaCaT cells or *OTUB1* depleted HaCaT cells were seeded into 96-well plates. Every 24 hours a pool of cells was incubated for 4 hours with XTT dye to detect differences in cellular metabolic activities and the absorbance measured at 480 nm. Cell proliferation was monitored for 8 days. Data are represented as mean and error bars indicate standard deviation (n=3).

Table 3-3 Statistical analysis of the proliferation assay

The statistical significance of the data obtained in Figure 3-29 was calculated using ANOVA with Bonferroni Correction. Differences with $p>0.05$ were annotated as ns (not significant), $p<0.05$ were annotated as *, $p<0.01$ were annotated as ** and $p<0.001$ were annotated as ***. *vs= versus*

	statistical significance			
day	control *vs* control TGFβ	*iOTUB1 vs* *iOTUB1* TGFβ	control *vs* *iOTUB1*	control TGFβ *vs* *iOTUB1* TGFβ
1	ns	ns	ns	ns
2	ns	ns	ns	ns
3	*	ns	ns	ns
4	*	ns	ns	ns
5	***	**	ns	ns
6	***	***	ns	ns
7	***	***	ns	ns
8	***	***	ns	ns

3.2.19 OTUB1 does not impact TGFβ-induced EMT

EMT is characterised by the loss of cell adhesion, apical-basal polarity and the acquisition of fibroblastic characteristics as well as increased cell migration. These morphological changes are regulated by actin cytoskeleton rearrangements and differential protein expressions of E-cadherin, which is highly expressed in epithelial cells, whereas mesenchymal cells express N-cadherin, fibronectin and vimentin. TGFβ is a potent inducer of EMT during development, would healing and potentially metastasis (Moreno-Bueno *et al.*, 2009, Heldin *et al.*, 2012). To test whether the absence or presence of OTUB1 influences TGFβ-induced EMT, NMuMG cells were transfected with control or *OTUB1* siRNA and EMT induced with 75 pM TGFβ for 24 or 48 hours (Figure 3-30). In the absence of TGFβ, cells display epithelial morphology, characterised by the low expression of fibronectin (Figure 3-30A,B), robust E-cadherin staining at cell-cell junctions (Figure 3-30A,B) and a cuboidal shape visualised by actin staining and phase contrast microscopy (Figure 3-30A). The addition of TGFβ resulted in an EMT response, as demonstrated by elongated cell shape and increased expression of fibronectin by immunofluorescence (Figure 3-30A) and immunoblotting (Figure 3-30B) in control (*iFoxO4*) and *iOTUB1* cells to similar extent but not in cells treated with the TGFβ inhibitor SB505124 (Figure 3-30A,B). Therefore, OTUB1 does not influence TGFβ-induced EMT.
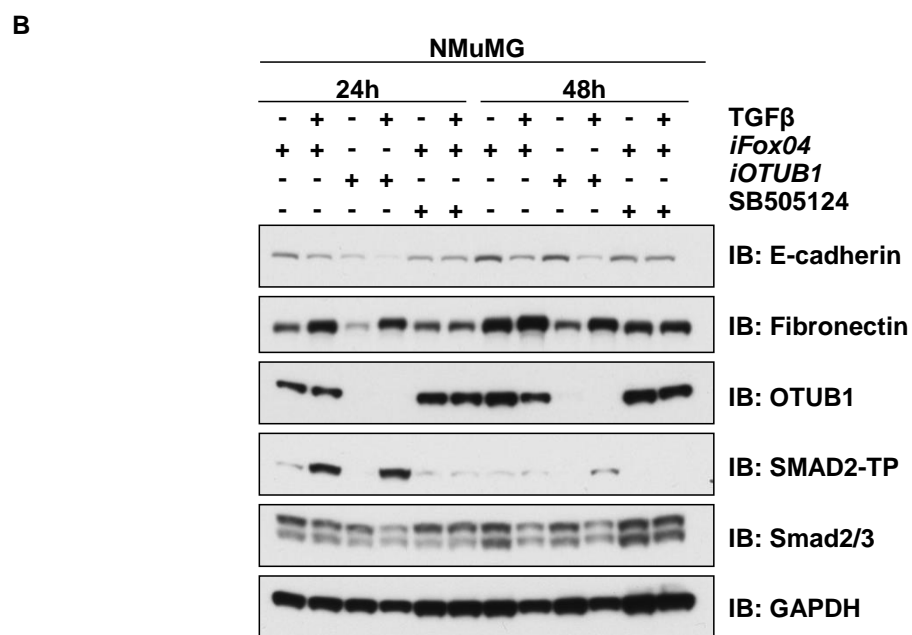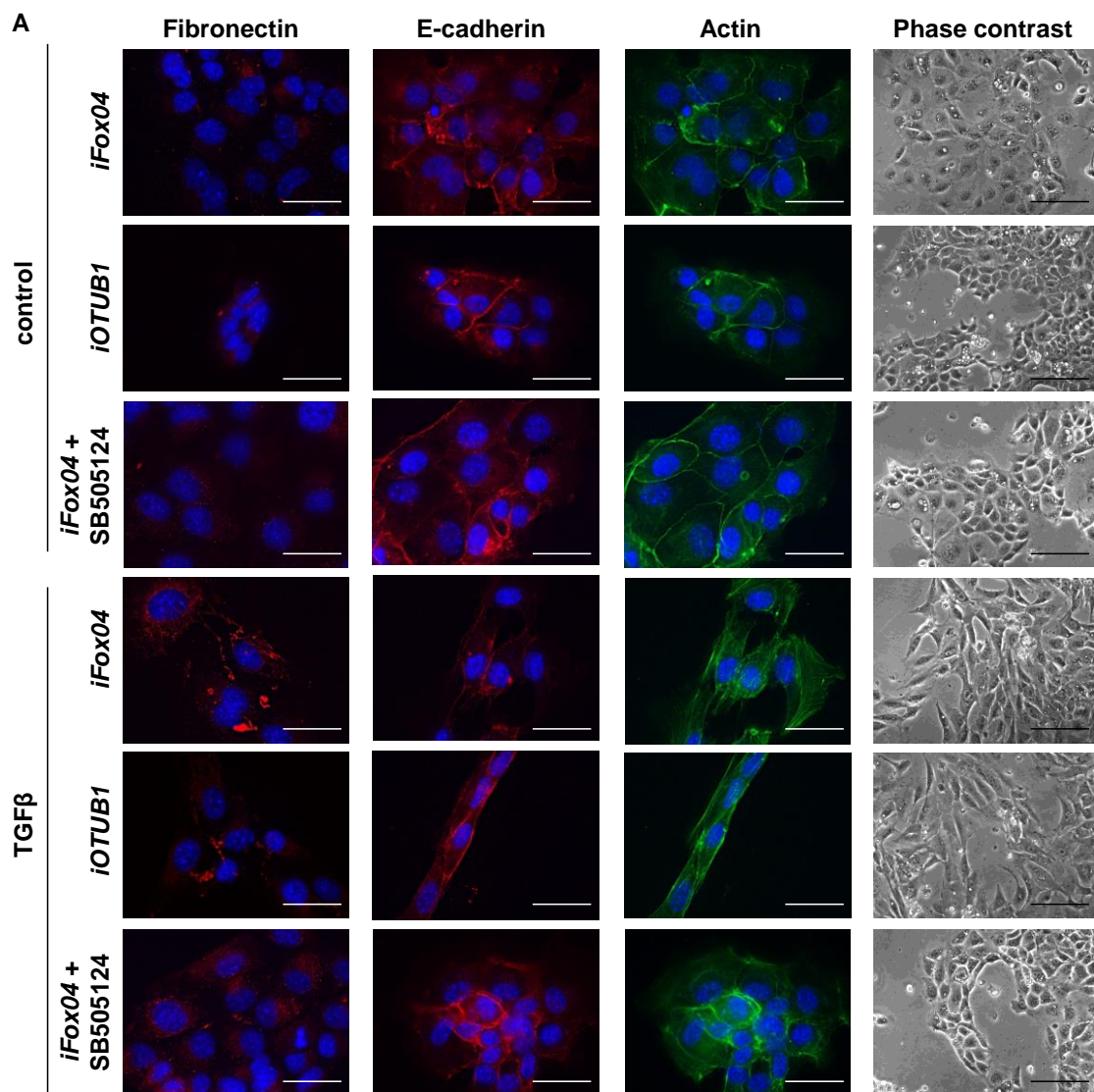
Figure 3-30 OTUB1 depletion does not influence TGFβ-mediated epithelial to mesenchymal transition (EMT)
(Figure legend on next page)

Figure 3-30 OTUB1 depletion does not influence TGFβ-mediated epithelial to mesenchymal transition (EMT)

A) NMuMG cells, transfected with *FoxO4* (control) or *OTUB1* siRNAs, were treated with 75 pM TGFβ for 24 hours in the presence or absence of 1 µM SB505124. Light microscopy or immunofluorescence microscopy (with the indicated antibodies) were performed to analyse EMT. White scale bar = 30 µm, black scale bar = 100 µm. **B)** Same as in A, except that cells were lysed for Western Blot analysis after 24 and 48 hours. Extracts were resolved by SDS-PAGE and immunoblotted with the indicated antibodies.

3.2.20 *OTUB1 influences TGFβ-induced cellular migration*

TGFβ signalling also regulates wound healing and migration (Heldin *et al.*, 2009, Medici *et al.*, 2011, Akhurst and Derynck, 2001). The induction of cellular migration by TGFβ is in part implicated in cancer progression and metastasis (Akhurst and Derynck, 2001, Massagué 2008). In order to assess the impact of OTUB1 on TGFβ-induced cellular migration, a wound healing "scratch assay" was employed. Control or *OTUB1*-depleted HaCaT cells were cultured to confluency in adjacent chambers of an insert separated by a small fixed-size spacer. Upon the removal of the insert, a uniform gap was formed. Cellular migration onto the gap was monitored for up to 48 hours (Figure 3-31A). In control cells, TGFβ treatment induced migration of cells within 24 hours and by 48 hours the gap was completely covered with cells. Depletion of *OTUB1* substantially inhibited the migration of HaCaT cells onto the gap after TGFβ treatment (Figure 3-31A). Efficient knockdown of OTUB1 was confirmed by immunoblotting (Figure 3-31B).
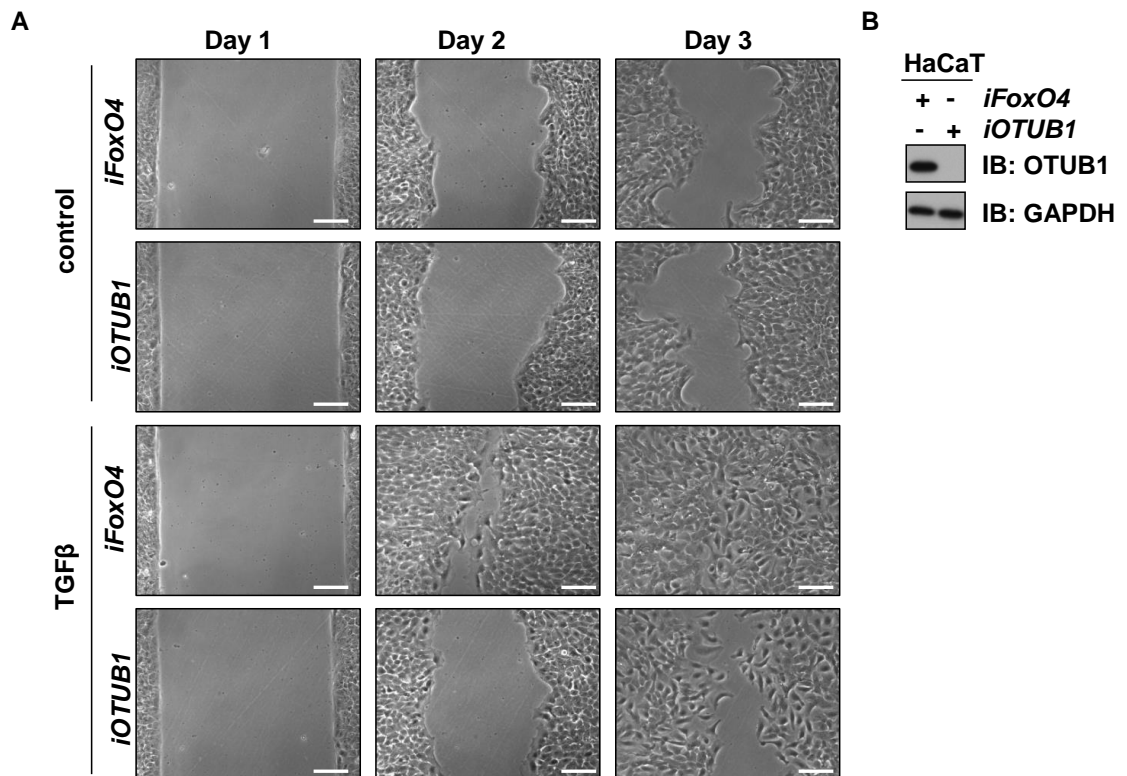
Figure 3-31 OTUB1 depletion reduces TGFβ-induced cellular migration

A) HaCaT cells stably expressing control shRNA and *FoxO4* siRNA or *OTUB1* shRNA and *OTUB1* siRNA were seeded onto migration inserts (Ibidi). After 24 hours the inserts were removed and cells were serum starved for 4 hours and stimulated without or with TGFβ (50 pM). Cell migration was tracked by taking images of the gaps every 24 hours. Scale bars = 100 μm. **B)** HaCaT cells used in A were lysed after 48 hours and extracts were resolved by SDS-PAGE and immunoblotted with the indicated antibodies, confirming a knockdown of OTUB1.

3.3 <u>Discussion</u>

This thesis describes a new regulatory role for OTUB1 in recognising phospho-SMAD2/3 upon TGFβ induction, controlling their turnover and consequently influencing downstream signalling (Figure 3-32). The results reveal a novel interplay between phosphorylation and the recruitment of OTUB1 to its target in the TGFβ pathway.
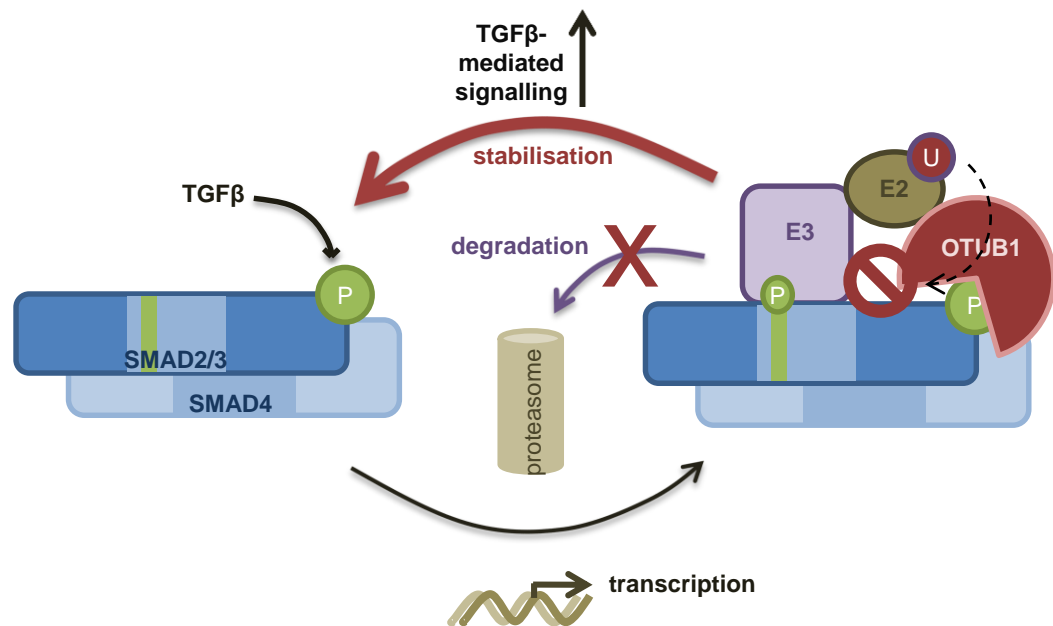
Figure 3-32 Summary of OTUB1 function within the TGFβ signalling pathway

TGFβ induces SMAD2/3 tail-phosphorylation, association with SMAD4 and entry into the nucleus, where SMADs act as transcription factors. Following linker phosphorylation, the E3 ubiquitin ligase NEDD4L recognises the SMAD2/3/4 complex and polyubiquitylates SMAD2/3, leading to proteasomal degradation. OTUB1 interacts with and thereby chaperones the active SMAD2/3 complex by inhibiting its ubiquitylation, through its interactions with and inhibition of the cognate E2. Proteasomal degradation of active SMAD2/3 is thus prevented and the complex can recycle, which leads to sustained TGFβ signalling.

3.3.1 *Phospho-dependent interaction between OTUB1 and SMAD2/3*

The TGFβ-induced phosphorylation of SMAD2/3 by the type I TGFβ receptor kinases is the central event for intracellular transduction of TGFβ signals. This triggers the formation of an active SMAD2/3/4 transcriptional

complex, their translocation to the nucleus and transcriptional control of target genes (Shi and Massague, 2003). OTUB1 was isolated from a proteomic screen as an interactor of SMAD3 upon stimulation of cells with TGFβ. Importantly, endogenous OTUB1 interacts with SMAD2/3 only in TGFβ treated cells and the levels of phospho-SMAD2/3 upon TGFβ stimulation directly correlate with the ability of OTUB1 to pull down endogenous SMAD2/3. Additionally, OTUB1 co-elutes with tail-phosphorylated SMAD2/3 and SMAD4 in a molecular weight fraction, indicating possible complex formation.

Although SMAD4 was detected in OTUB1 immunoprecipitates upon TGFβ stimulation, it is not an essential component for the recruitment of OTUB1 to TGFβ-induced phospho-SMAD2/3. Consistent with the concept that OTUB1 interaction could be phospho-SMAD2/3-dependent, dephosphorylation of OTUB1 IPs by lambda phosphatase (to dephosphorylate phospho-SMAD2/3) partially abolished OTUB1-SMAD2/3 interaction. Furthermore, recombinant OTUB1 was able to interact with a SMAD2 tail-phospho-peptide, indicating that tail-phosphorylation of SMAD2 is sufficient for its interaction with OTUB1.

Despite the phospho-dependent nature of OTUB1 interaction with SMAD2/3, no phospho-interaction motifs within OTUB1 have been reported. Moreover, whether OTUB1 is recruited to other targets in a phosphorylation dependent manner is not known or reported. Although the published crystal structures of OTUB1 exhibit a few positively charged pockets, none are predicted to be phospho-binding pockets. A phospho-SMAD2-OTUB1 structural analysis might shed new light into the molecular basis of their interaction. In order to achieve the phospho-SMAD2-OTUB1 structure, crystallisation screens with the phospho-SMAD2 peptide and OTUB1 can be

set up. The N-terminus of OTUB1 (at least aa 1-24) is disordered and has been omitted for previous crystal structure analysis (Edelmann *et al.*, 2009, Sato *et al.*, 2012, Juang *et al.*, 2012, Wiener *et al.*, 2012). Because the N-terminal domain of OTUB1 is not critical for the interaction with SMAD3, OTUB1 ΔN can be employed for crystallisation trials. The solved crystal structure might give molecular insights into how OTUB1 recognises only phosphorylated-SMAD2/3. By mutating key residues in OTUB1 that mediate the binding to phospho-SMAD2/3, it will be possible to investigate the overall contribution of OTUB1 in the regulation of the TGFβ pathway.

The identification of a phospho-binding pocket within OTUB1 has the potential to unravel a unique mode of action by which OTUB1 recognises its targets in response to different environmental cues. With the limited number of DUBs and multiple substrates they are expected to target, the substrate specificity of DUBs probably relies on signal-induced target modifications. The fact that OTUB1 interacts with tail-phosphorylated SMAD2/3 upon TGFβ stimulation signifies a unique interplay between phosphorylation and the recruitment of a DUB to its target in the TGFβ pathway.

3.3.2 A non-canonical mode of OTUB1 action in the TGFβ pathway

The TGFβ-dependent recruitment of the deubiquitylating enzyme OTUB1 to active phospho-SMAD2/3 complex combined with its impact on TGFβ-induced transcription, suggested that OTUB1 might impact TGFβ signalling by deubiquitylating and stabilising phospho-SMAD2/3 in cells. *In vitro* OTUB1 cleaves K48-linked polyubiquitin chains, which in cells direct target proteins for proteasomal degradation (Thrower *et al.*, 2000). NEDD4L catalyses the attachment of K48-linked polyubiquitin chains on SMAD3.

However, OTUB1 was unable to deubiquitylate polyubiquitylated SMAD2/3 *in vitro*. Furthermore, *in-cell* SMAD3 deubiquitylation assays demonstrated that some of the catalytically inactive mutants of OTUB1 were still able to reduce polyubiquitylation on SMAD3. Further investigations revealed that the action of OTUB1 predominantly relies on its ability to inhibit the ubiquitylation of SMAD2/3 independently of its catalytic activity.

Recent reports demonstrate that the catalytic activity of a DUB is not always essential in order to regulate the function of its substrate (Sarkari *et al.*, 2010, Hanna *et al.*, 2006). The ability of OTUB1 to inhibit the polyubiquitylation of chromatin upon DNA-damage independent of its catalytic activity has been reported previously (Nakada *et al.*, 2010). This and other studies have reported that OTUB1 inhibits ubiquitylation by binding to and inhibiting E2 enzymes (Juang *et al.*, 2012, Nakada *et al.*, 2010, Sato *et al.*, 2012, Sun *et al.*, 2011, Wiener *et al.*, 2012). In agreement with these reports, several E2 enzymes, including UBE2D1 and UBE2N, bound to OTUB1 at the endogenous level. By binding to UBE2D1, OTUB1 inhibits the transfer of ubiquitin from the UBE2D1~ub conjugate to the E3 ubiquitin ligase NEDD4L and subsequently to SMAD3.

OTUB1 is likely to undergo conformational changes upon substrate binding (Edelmann *et al.*, 2009, Messick *et al.*, 2008). The addition of SMAD3 peptides to OTUB1 did not alter its catalytic activity. Nevertheless, it is possible that SMAD3 binding to OTUB1 could induce conformational changes that may influence its ability to inhibit ubiquitylation or the recruitment of other co-factors. Mutations in the catalytic centre of OTUB1 could also result in conformational changes (Edelmann *et al.*, 2009, Stanisic *et al.*, 2009). These changes might account for the inability of OTUB1 C91S to interact with SMAD3. In the pursuit

of mutations in OTUB1 that are catalytically inactive but still interact with SMAD3, K71R, a previously uncharacterised mutant, was identified. Although K71 lies upstream of the OTU domain, the K71R mutation renders the DUB catalytically inactive, possibly through conformational changes within the catalytic domain. OTUB1 K71R cannot inhibit SMAD2/3 ubiquitylation *in vitro*, possibly because OTUB1 K71R is unable to inhibit the ubiquitin transfer from the E2~ub to the E3.

The ability of OTUB1 to inhibit E2 enzymes, thereby leading to the prevention of SMAD ubiquitylation, is in accordance with recent reports on OTUB1 function in cells (Nakada *et al.*, 2010, Sun *et al.*, 2011). Furthermore, overexpression of OTUB1 in cells can inhibit global polyubiquitylation, which cannot be completely rescued by Bortezomib and Lactacystin, suggesting that OTUB1 can inhibit the formation of various polyubiquitin chains. Nevertheless, due to the regulation of OTUB1 activity through the balance of ubiquitin-charged E2s, uncharged E2s and K48-linked ubiquitin (Wiener *et al.*, 2013), OTUB1 can still act as a classic deubiquitylating enzyme for some targets, such as c-IAP and active RhoA (Goncharov *et al.*, 2013, Edelmann *et al.*, 2010).

3.3.3   OTUB1 could target phosphorylated SMAD2/3 in the cytosol

OTUB1 was mostly found in the cytosol, partly at the membrane and not in the nucleus, as assessed by immunofluorescence microscopy and cellular fractionation. Still, it is possible that small amounts of OTUB1 reside in the nucleus, which could not be detected by the employed methods. Furthermore, the OTUB1 antibody did not prove suitable for high-resolution microscopy; hence, no definitive co-localisation studies of OTUB1 and phospho-SMAD2/3 could be performed.

OTUB1 could be protecting phospho-SMAD2/3 from ubiquitylation either by binding phospho-SMAD2/3 in the cytosol or through a sustained (and hardly detectable) interaction in both cytosolic and nuclear compartments. At 1 hour post TGFβ stimulation, some linker phosphorylated SMAD3 is also present in OTUB1 IPs. It has been reported that tail-phosphorylated SMAD2/3 are targeted for polyubiquitylation by NEDD4L upon further phosphorylation at the linker region by CDK8/9 and nuclear export, which then leads to their proteasomal degradation in the cytosol (Gao *et al.*, 2009). Although, tail-phosphorylation of SMAD2/3 is sufficient for their interaction with OTUB1, SMAD2/3 linker phosphorylation could play a regulatory role of SMAD recognition by E3s and DUBs. Linker phosphorylation-mediated recruitment of E3 ligases to SMADs in the cytosol is consistent with accelerated proteasomal degradation of phospho-SMAD2/3 in the absence of OTUB1. Hence, it is possible that OTUB1 protects SMAD2/3 in the cytosol.

3.3.4 *The ability of OTUB1 to bind to SMAD2/3 and inhibit ubiquitylation is necessary to impact TGFβ signalling*

The activation of TGFβ signalling results in the transcription of target genes, which ultimately determines the nature of cellular responses. The results obtained indicate that OTUB1 modulates TGFβ-induced transcription of some target genes. The inhibition of TGFβ-induced transcription of *PAI-1* upon *OTUB1* depletion can be rescued by siRNA-resistant wild type OTUB1. However, neither siRNA-resistant OTUB1 C91S mutant (catalytically inactive, SMAD3-interaction deficient but able to inhibit SMAD3 ubiquitylation) nor OTUB1 ΔN mutant (catalytically active, interacts with SMAD3 but unable to

inhibit SMAD3 ubiquitylation) was able to rescue the TGFβ-induced transcription caused by OTUB1 depletion.

Together these results imply that binding to SMAD2/3 as well as the ability to inhibit SMAD2/3 ubiquitylation are essential for OTUB1 to impact the TGFβ pathway. Therefore, the association of OTUB1 with phospho-SMAD2/3 would be predicted to prevent SMAD2/3 from being polyubiquitylated and degraded, thereby enhancing TGFβ signalling. Consistent with this notion, the depletion of OTUB1 from cells leads to a rapid loss in levels of tail-phosphorylated SMAD2/3 but this reduction can be rescued upon treatment of cells with proteasomal inhibitor Bortezomib or the expression of siRNA-resistant OTUB1.

3.3.5 OTUB1 influences TGFβ-mediated cellular migration

The TGFβ pathway controls multiple cellular processes and is implicated in carcinogenesis, in part through the induction of cellular migration (Akhurst and Derynck, 2001, Massagué, 2008). OTUB1 has been shown to inhibit cellular growth and induce cell death (Goncharov et al., 2013, Sun et al., 2011). However, in the cell types tested in this thesis, the perturbation of OTUB1 expression does not influence apoptosis or proliferation in the presence or absence of TGFβ stimulation. Similarly, OTUB1 depletion does not impact TGFβ-induced EMT. However, the depletion of OTUB1 from HaCaT cells significantly inhibits lateral migration induced by TGFβ. TGFβ-mediated cellular migration is in part controlled through RhoA (section 1.2.5), which is also a reported target of OTUB1 (Edelmann et al., 2010). The disparity in TGFβ-dependent cellular effects of OTUB1 depletion above could be because OTUB1 only influences a small pool of phosphorylated-SMAD2/3 and thus controls a

subset of TGFβ-mediated genes. Consistent with this possibility, only a small portion of OTUB1 co-elutes with phospho-SMAD2/3 in size exclusion chromatography, whereas most of the activated SMAD2/3 is still observed in high molecular weight fractions that exclude OTUB1. Furthermore, it could be that the siRNA-mediated depletion of OTUB1 is below the threshold needed to observe OTUB1 depletion phenotypes. In order to test these possibilities and study the effect of complete OTUB1 depletion on cellular responses of TGFβ signalling, it would be beneficial to obtain OTUB1 knockout cells. Attempts to generate OTUB1 knockout cells via homologous recombination in KBM7 cells and CRISP/CAS9 in U2OS cells did not lead to OTUB1 knockout clones, while the integration of the targeting vectors was verified and positive controls of other targeted genes resulted in their knockout. This indicates that the OTUB1 gene could be essential for cellular survival.

3.3.6 Possible other targets of OTUB1 in the TGFβ signalling pathway

The specific binding of OTUB1 to phosphorylated SMADs2/3, does not exclude the possibility that OTUB1 could also act on other proteins that signal in the TGFβ pathway. The membrane localisation of OTUB1 and its ability to interact with overexpressed ALK5 indicate that OTUB1 could potentially also target the receptors for deubiquitylation and thereby enhance TGFβ mediated responses. This possibility should be further investigated. It could be tested whether OTUB1 co-localises with ALK5 upon TGFβ treatment by employing Fluorescence Resonance Energy Transfer (FRET) or Proximity Ligation Assay (PLA). Additionally it could be tested whether OTUB1 deubiquitylates ALK5 in cells or *in vitro*, or if OTUB1 possibly inhibits the polyubiquitylation of ALK5 and stabilises receptor levels. By binding phosphorylated-SMADs2/3, OTUB1 could

also be present in complexes that include other transcription factors or SMAD-binding proteins. In close proximity OTUB1 could possibly also deubiquitylate or inhibit the ubiquitylation of other SMAD-binding proteins. The physiological effects of OTUB1 perturbation were limited to a few TGFβ target genes and cellular migration. This indicates that OTUB1 only targets a small pool of phosphorylated-SMAD2/3 and that there have to be additional mechanisms in place to regulate the specific effects of OTUB1 on TGFβ signalling. This could possibly be regulated by specific complex formations that include OTUB1, activated SMAD2/3 and additional regulatory proteins. These other regulatory proteins could then specifically induce the transcription of a small set of TGFβ target genes or assist in TGFβ-mediated cellular migration. Moreover, OTUB1 could enhance the presence of these other regulatory proteins by rescuing them from proteasomal degradation.

3.3.7 OTUB1 as a potential drug target

Various diseases have been linked to the TGFβ pathway malfunction (section 1.4) (Akhurst and Hata, 2012). Hence, the development of new small molecule inhibitors that fine tune TGFβ signalling is desirable. The discussed properties, modes of action and cellular functions of OTUB1, make it a promising target for the development of small molecule inhibitors to specifically target the OTUB1-SMAD2/3 interaction. This could result in the inhibition of TGFβ signalling and consequently be useful against diseases, such as cancer and fibrosis, where TGFβ signalling is abnormal.

In order to avoid the targeting of multiple signalling pathways that OTUB1 impacts (Edelmann et al, 2009; Li et al, 2012; Soares et al, 2004; Stanisic et al, 2009; Sun et al, 2011; Zhang et al, 2012), inhibitors that specifically target the

OTUB1-SMAD2/3 interaction are desirable. The generation of an OTUB1-phospho-SMAD2 crystal structure might reveal novel opportunities to develop small molecule inhibitors that disrupt their interaction by targeting the binding interface (although other substrates could potentially interact with OTUB1 through the same binding pocket). These molecules could dampen context-dependent TGFβ-signalling in specific pathological disorders. In order to test these molecules and study the effect of OTUB1-interaction deficient mutations on TGFβ signalling, it would be beneficial to obtain OTUB1 knockout mice. No OTUB1 knockout mice have been generated yet. Conditional OTUB1 knockout mice or conditional OTUB1-SMAD2/3 interaction-deficient knockin mice would be useful to study the effects of OTUB1 in TGFβ-induced disorders, especially as the impact of OTUB1 on TGFβ signalling has also been demonstrated in cells derived from mice.

RNAi-mediated depletion of OTUB1 from HaCaT cells resulted in inhibition of TGFβ-induced expression of the *PAI-1* and *CTGF* transcripts, both known TGFβ target genes (Igarashi *et al.*, 1993, Lund *et al.*, 1987). CTGF (connective tissue growth factor) is a cysteine-rich matricellular secreted protein that regulates diverse cellular functions (Mann *et al.*, 2011). TGFβ-induced CTGF expression can lead to ECM accumulation, vascular remodelling and result in glomerular disease, vascular fibrosis or carcinogenesis (Cheng *et al.*, 2014, Lan *et al.*, 2013, Lee, 2012). The TGFβ-target gene *PAI-1* (plasminogen activator inhibitor 1, member of the Serine protease inhibitor family) is a contributor to fibrogenesis in numerous organ systems. In the progression of several clinically important fibrotic disorders, PAI-1 is found to be highly up regulated and is causatively linked to disease severity (Samarakoon *et al.*, 2012, Mann *et al.*, 2011, Samarakoon *et al.*, 2013). Furthermore, PAI-1 is

a causative factor in the progression of vascular disorders as well as a biomarker for cardiovascular-disease associated mortality. PAI-1 has also been reported to be a regulator of ECM accumulation impacting smooth muscle cell migration via the EGFR/ERK/RhoA/SMAD signalling cascade (Samarakoon and Higgins, 2008). As OTUB1 potentiates TGFβ signalling via SMAD2/3 stabilisation, OTUB1 might serve as a potential drug target for fibrotic disorders.

Furthermore, recent reports imply that certain DUBs are themselves modified or misexpressed in cancers (Eichhorn *et al.*, 2012), thereby affecting TGFβ signalling. OTUB1 is expressed in most mouse tissues and across many human cell lines, but was found to be slightly up regulated in human breast, larynx, prostate and colon cancers (Luise *et al.*, 2011). The increased expression of OTUB1 in colon cancer correlates with tumour size, differentiation and lymph node metastasis (Liu *et al.*, 2014a).

4   Phosphorylation of OTUB1 by ALKs and CK2

4.1   Introduction

Deubiquitylating enzymes impact many cellular signalling pathways and are highly regulated enzymes (Komander *et al.*, 2009, Kessler and Edelmann, 2011). Although some recent reports have shed light into the molecular functions of OTUB1 (Mevissen *et al.*, 2013, Nakada *et al.*, 2010, Wiener *et al.*, 2013), its regulation *in vivo* remains to be defined. While investigating the role of OTUB1 in TGFβ signalling, it was discovered that OTUB1 itself could be post-translationally modified by phosphorylation. The aim of the following chapter was to characterise the phosphorylation of OTUB1 at S16 and S18.

4.1.1   Post-translational modifications on OTUB1

PTMs, such as phosphorylation, monoubiquitylation, sumoylation and acetylation, have been reported to alter DUB functions in cells (Kessler and Edelmann, 2011). Global mass spectrometry approaches have revealed several phosphorylation and ubiquitylation sites on OTUB1 (Figure 4-1) (Edelmann *et al.*, 2010, Li *et al.*, 2014, Wagner *et al.*, 2011, Kim *et al.*, 2011, Pozuelo Rubio *et al.*, 2004). It has been reported that monoubiquitylation of OTUB1 by UBE2D1 mainly on K59 and K109 is critical for its ability to suppress UBE2D1, as the E2 preferentially binds ubiquitylated OTUB1 (Li *et al.*, 2014). OTUB1 phosphorylation at S16 and S18, among others, has been reported to be essential for cellular susceptibility to *Yersinia enterocolitica* and *Yersinia pseudotuberculosis* invasion (Edelmann *et al.*, 2010). Although Yersinia protein kinase A (YpkA) can phosphorylate OTUB1 *in vitro*, OTUB1 phosphorylation in cells was observed independently of *Yersinia* invasion (Juris *et al.*, 2006,

Edelmann *et al.*, 2010). Therefore, the mechanism and kinase(s) that mediate the phosphorylation of OTUB1 at S16 and S18 remain elusive.
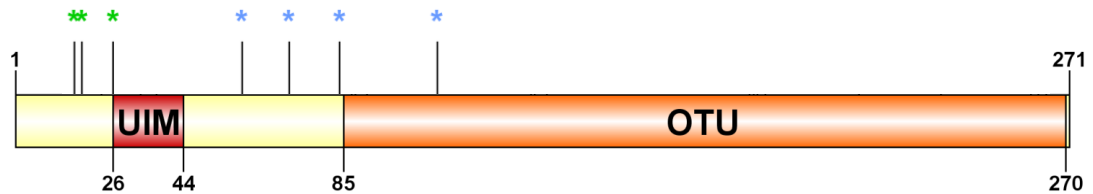
Figure 4-1 Post-translational modifications on OTUB1

Schematic representation of human OTUB1 domain structure indicating the ubiquitin interaction motif (UIM) in red and the OTU domain in orange. Putative OTUB1 phosphorylation sites S16, S18 and Y26 are indicated in green and reported OTUB1 ubiquitylation sites K59, K71, K84, K109 are indicated in light blue.

4.1.2 *Non-SMAD substrates of type I TGFβ/BMP receptors*

Type I TGFβ/BMP receptors (ALKs; Activin-receptor-Like-Kinases) are Serine/Threonine protein kinases (*cf.* section 1.2.2). In the canonical TGFβ pathway, the activated ALKs phosphorylate R-SMADs at their conserved C-terminal "SXS" motif (Shi and Massague, 2003). S16 and S18 of OTUB1 conform to the "SXS" motif, although they are separated by an Aspartic acid residue instead of Valine or Methionine in R-SMADs and do not lie at the extreme C-terminus as in R-SMADs. However, a non-SMAD substrate PAWS1 has been reported to be phosphorylated at an intrinsic "SXS" motif by ALK3 in response to BMP (Vogt *et al.*, 2014). Therefore, it was tested if OTUB1 could be phosphorylated by type I TGFβ/BMP receptors.

4.1.3 S16 of OTUB1 is a putative substrate for protein kinase CK2

The residues surrounding S16 of OTUB1 "G**SD**S**E**GVN", with acidic residues at +1 and +3, make it an optimal site for phosphorylation by protein kinase CK2 (Meggio and Pinna, 2003, Battistutta and Lolli, 2011, Montenarh, 2010). Furthermore, the phosphorylation of S18 at +2 would be predicted to prime and improve the phosphorylation of S16 by CK2. CK2 (derived from the misnomer Casein Kinase 2) is a ubiquitously expressed and highly pleiotropic dual-specificity protein kinase. The CK2 holoenzyme is a tetrameric complex comprising two regulatory β-subunits and two catalytic (α, α' or α'') subunits in a homomeric or heteromeric conformation. In cells, the subunits can occur individually or as the holoenzyme and the catalytic subunits of CK2 are active combined or not with a dimer of its non-catalytic β-subunits (Meggio and Pinna, 2003, Battistutta and Lolli, 2011, Pinna, 2002). The crystal structure of the CK2 holoenzyme has been solved and indicates that the regulatory β-subunits form a stable dimer that links both catalytic α-subunits (Niefind *et al.*, 2001, Niefind and Issinger, 2010). CK2 is a constitutively active kinase and the basal catalytic activity is not influenced by specific ligands, extracellular stimuli or metabolic conditions. Furthermore, fluctuations in the protein levels of the subunits or the holoenzyme of CK2 have not been observed, thus excluding acute regulation through transcription/translation or degradative pathways. The phosphorylation of CK2 substrates is individually regulated through different conformations and regulated assembly of the holoenzyme and subunits, regulatory interactions with CK2 inhibitors or activators and most importantly through protein-protein interactions (Pinna, 2003, Montenarh, 2010, Litchfield, 2003).

CK2 has been shown to phosphorylate over 300 substrates and therefore regulates many cellular processes (Meggio and Pinna, 2003, Ruzzene

and Pinna, 2010). Several targets of CK2 have been reported to regulate ubiquitylation and deubiquitylation processes. CK2 phosphorylation of the E2 ubiquitin conjugating enzyme UBE2R1 (CDC34) at S203 and S222 regulates the substrate recognition of βTRCP1 (Semplici *et al.*, 2002) and stimulates SCF-mediated ubiquitylation (Block *et al.*, 2005). Furthermore, CK2 phosphorylation of UBE2R1 at S130 and S167 stimulates UBE2R1 ubiquitin charging (Coccetti *et al.*, 2008) by opening the catalytic cleft and promoting ubiquitin access (Papaleo *et al.*, 2011). Moreover, CK2 mediates the regulation of deubiquitylating enzymes Ataxin-3 and OTUD5 through phosphorylation. Phosphorylation of Ataxin-3 by CK2 at S340 and S352 within its third UIM promotes its nuclear localisation, aggregation and stability (Mueller *et al.*, 2009). OTUD5 is catalytically activated upon phosphorylation by CK2 at S177 by positioning the ubiquitin substrate through interactions of the phosphate group with the C-terminal tail of distal ubiquitin (Huang *et al.*, 2012).

The phosphorylation of OTUB1 at S16 and S18 could influence its activity, subcellular localisation, substrate specificity and/or function in cells. Hence, the aim of this chapter was to characterise the phosphorylation of OTUB1 in cells and identify the upstream kinases mediating the phosphorylation.

4.2 <u>Results</u>

4.2.1 OTUB1 is phosphorylated by ALK5 in vitro

During the investigation on the role of OTUB1 in the TGFβ pathway (section 3), a mass spectrometry analysis of GFP-OTUB1 immunoprecipitated from HEK293 cells identified a tryptic phospho-peptide of OTUB1 (Figure 4-2) that was two-fold more abundant upon TGFβ stimulation. The identified phospho-peptide (QEPLG<u>S</u>D<u>S</u>EGVNCLA<u>Y</u>DEAIMAQQDR), revealed three possible phosphorylation sites at S16, S18 and Y26. S16 and S18 constitute a "SXS" motif, which in R-SMADs is phosphorylated by ALKs. To determine if the type I TGFβ receptor ALK5 was able to phosphorylate OTUB1, an *in vitro* kinase assay was set up (Figure 4-3A). GST-ALK5 T204D was used for all kinase assays. The T204D mutation mimics ALK5 phosphorylation by the type II receptor and activates ALK5 in its absence. ALK5 phosphorylates wild type recombinant GST-OTUB1 *in vitro* (Figure 4-3A), to a similar extent as it phosphorylates SMAD2 and SMAD3 (Figure 4-3A). To test whether ALK5 preferentially phosphorylates OTUB1 or SMAD3, both SMAD3 and OTUB1 were phosphorylated by ALK5 in the same assay. Under these conditions, ALK5 preferentially phosphorylated SMAD3 over OTUB1, although when phosphorylated individually both SMAD3 and OTUB1 are phosphorylated to a similar extent (Figure 4-3B). The specific ALK5 inhibitor SB505124 was able to inhibit OTUB1 and SMAD3 phosphorylation in a dose dependent manner (Figure 4-3B,C), suggesting that ALK5 rather than a contaminating kinase phosphorylated these proteins.

In order to confirm that S16 and S18 were targeted for phosphorylation by ALK5, an *in vitro* kinase assay was performed on wild type, as well as S16A, S18A and S16/18A mutant of GST-OTUB1 (Figure 4-3D). GST-OTUB1 was

phosphorylated by ALK5 (Figure 4-3D) and the mutation of S16A did not significantly impact the ability of ALK5 to phosphorylate OTUB1 (Figure 4-3D). The mutation of S18A decreased the phosphorylation of OTUB1 by ALK5 (Figure 4-3D). When both Serine 16 and 18 were mutated to Alanine, the ALK5-mediated phosphorylation of OTUB1 was lost, indicating that *in vitro* ALK5 could phosphorylate S16 and S18 of OTUB1, however primarily phosphorylated S18 (Figure 4-3D).
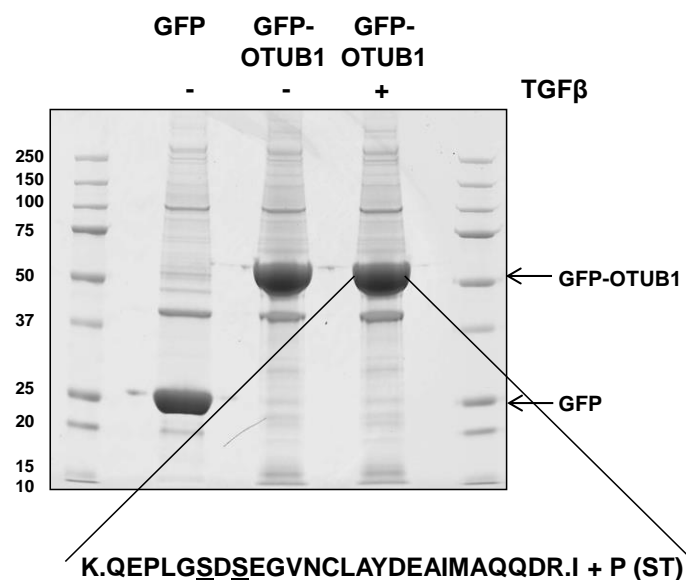
Figure 4-2 Identification of an OTUB1 phospho-peptide

HEK293 cells stably expressing GFP-only or GFP-OTUB1 were stimulated with 50 pM TGFβ for 1 hour and lysed in the presence of DSP. GFP-immunoprecipitates (IPs) were separated by SDS-PAGE, bands excised and processed for mass spectrometry. One OTUB1 peptide (QEPLGSDSEGVNCLAYDEAIMAQQDR) was phosphorylated *in vivo*, with a two-fold increase in the presence of TGFβ.
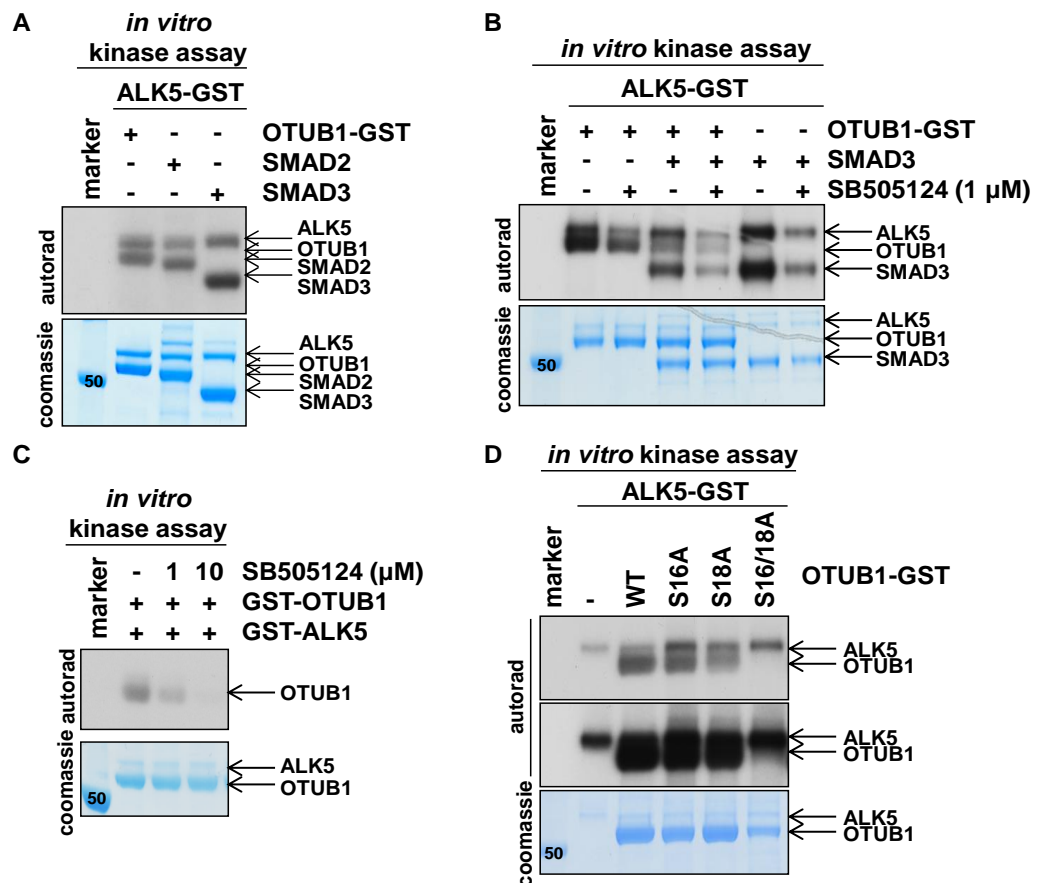
Figure 4-3 OTUB1 is phosphorylated by ALK5 *in vitro*

A) An *in vitro* kinase assay with GST-ALK5 was set up, using SMAD2, SMAD3 and GST-OTUB1 as substrates in the presence of $^{\gamma 32}$P-ATP (500 cpm/pmole). The reaction was stopped after 30 min at 30 °C and the samples were resolved by SDS-PAGE, the gel was Coomassie stained and radioactivity was analysed by autoradiography. **B)** As in A, however ALK5 phosphorylation of SMAD3 and/or GST-OTUB1 was performed in the presence or absence of the SB505124 (1 µM). **C)** As in A, however increasing amounts of ALK5 inhibitor SB505124 were used to inhibit ALK5-mediated GST-OTUB1 phosphorylation. **D)** As in A, however GST-ALK5 was used with GST-OTUB1 and GST-OTUB1 point mutants as substrates.

4.2.2 Assessment of OTUB1 phosphorylation by ALKs in cells

To assess the role of ALK5 in OTUB1 phosphorylation, it was tested whether ALK5 and OTUB1 physically interact. FLAG-ALK5 and HA-OTUB1 were co-expressed in HEK293 cells. FLAG-ALK5 IPs pulled down HA-OTUB1 and HA-OTUB1 S16/18A mutants in the presence or absence of SB505124 (Figure 4-4A).

Phospho-specific antibodies recognising OTUB1 pS16, pS18 or pS16/18 were generated. Both pS16 and pS16/pS18 antibodies only recognised OTUB1 phosphorylated at S16. The antibody against pS18 did not recognise OTUB1 phosphorylated at S18, which was challenging in terms of characterising S18 as a substrate for ALK5 in cells. Nonetheless, the phosphorylation of S16 in response to TGFβ was characterised. To investigate whether TGFβ treatment induces OTUB1 phosphorylation at S16 in a time and dose dependent manner, HA-OTUB1 or HA-OTUB1 S16/18 were overexpressed in cells (Figure 4-4B). OTUB1 was constitutively phosphorylated at S16 in U2OS (Figure 4-4B) and HEK293 (Figure 4-4C) cells independently of TGFβ, BMP and Activin treatment or ALK inhibitors SB505124 and LDN198193 (Figure 4-4B,C) (Vogt *et al.*, 2011). This could be due to other constitutively active kinases phosphorylating OTUB1 under basal conditions. ALK5 knockout MEF cells were used to definitively establish the involvement of ALK5 in endogenous OTUB1 phosphorylation at S16 (Figure 4-4D). Wild type, ALK5-/- and ALK5-/- cells restored with ALK5 or catalytically inactive ALK5 K232R (Wieser *et al.*, 1995) were used to assess endogenous phosphorylation of OTUB1 at S16. The phosphorylation of the *bona fide* ALK5 substrate SMAD2 in response to TGFβ was detected only in wild type and ALK5-/- MEFs restored with wild type ALK5 but not in ALK5-/- MEFs or those restored with catalytically inactive ALK5 K232R. OTUB1 S16 phosphorylation was detected in all cells regardless of ALK5 activity or expression (Figure 4-4D), suggesting that ALKs are unlikely to mediate the phosphorylation of S16.

Although S18 was identified as the key *in vitro* ALK5 phosphorylation site of OTUB1, it has not been possible to characterise this in cells due to the lack of a suitable antibody to detect OTUB1 pS18.
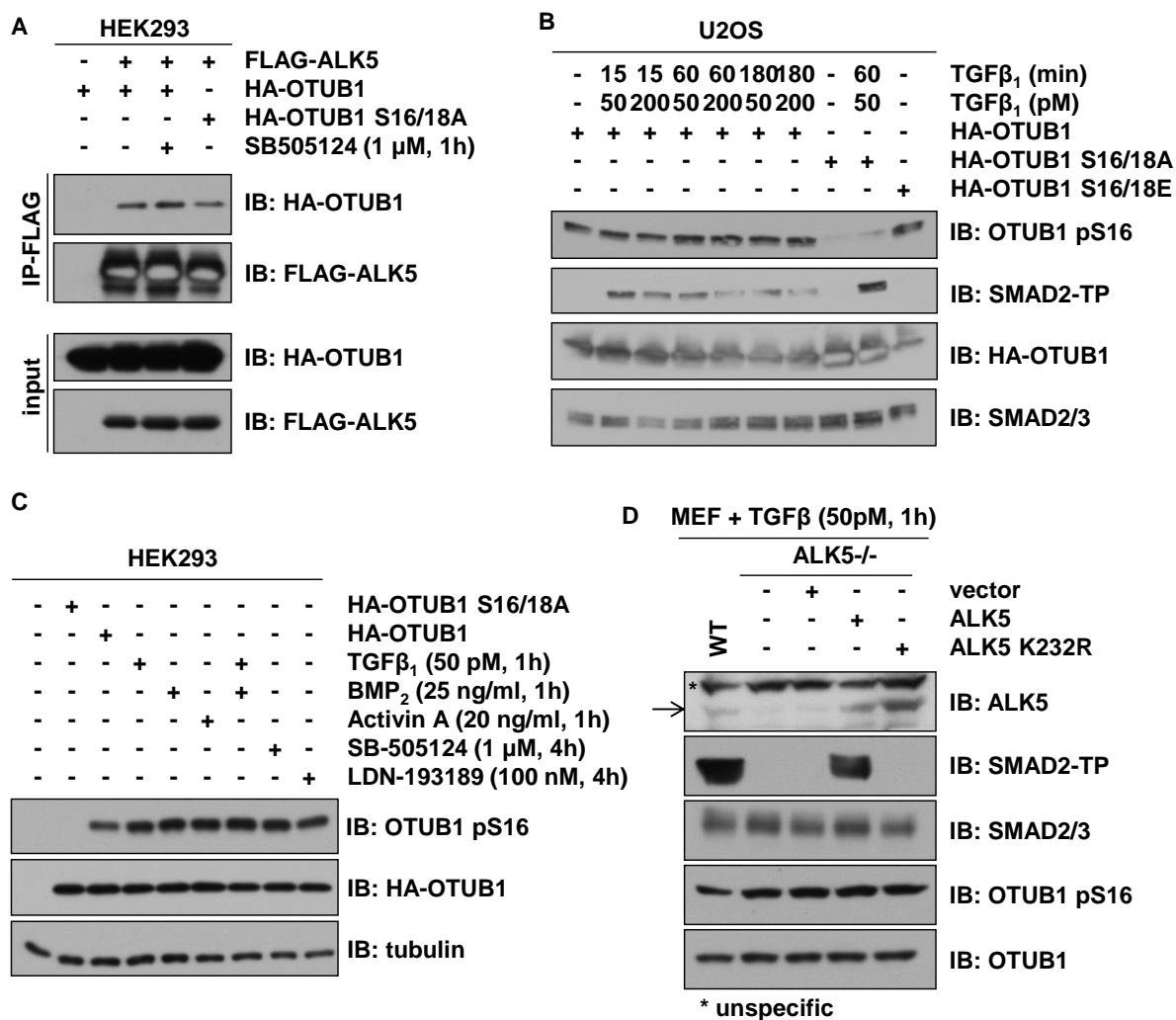
Figure 4-4 Assessment of *in vivo* OTUB1 phosphorylation by ALKs

A) HEK293 cells were co-transfected with vectors encoding N-terminal HA-tagged OTUB1 or HA-OTUB1 S16/18A and N-terminal FLAG-tagged ALK5. Prior to lysis cells were treated with or without SB505124 (1 µM, 1 hour). FLAG-immunoprecipitates (IP) or extracts were resolved by SDS-PAGE and immunoblotted with the indicated antibodies. **B)** U2OS cells were transfected with vectors encoding N-terminal HA-tagged OTUB1 or indicated HA-OTUB1 mutants (S16/18A, S16/18E). Prior to lysis cells were treated with indicated amounts (pM) of TGFβ for indicated time points (min). Extracts were resolved by SDS-PAGE and immunoblotted with the indicated antibodies. **C)** HEK293 cells were transfected with vectors encoding N-terminal HA-tagged OTUB1 or HA-OTUB1 S16/18A. Prior to lysis cells were treated with indicated amounts of stimuli for indicated time points. Extracts were resolved by SDS-PAGE and immunoblotted with the indicated antibodies. **D)** MEF cells (wild type, ALK5-/- and ALK5-/- putback with vector, ALK5 or ALK5 kinase inactive (K232R)) were treated with TGFβ (50 pM, 1 hour). Cells were lysed and extracts resolved by SDS-PAGE and immunoblotted with the indicated antibodies.

4.2.3 OTUB1 is phosphorylated in vitro by ALKs2-6 and CK2α

The observation that S16 is unlikely to be phosphorylated by ALKs suggested that other kinases might be involved. To test whether other kinases were able to phosphorylate OTUB1 *in vitro*, a panel of kinases that potentially phosphorylate a similar motif that surrounds OTUB1 S16 (Figure 4-5) were selected with ALKs to phosphorylate OTUB1 *in vitro*. The TGFβ-regulated ALKs4 and 5 phosphorylate OTUB1 more efficiently than the BMP-regulated ALKs2, 3 and 6. Of the other selected kinases assayed, only CK2α was able to robustly phosphorylate OTUB1 (Figure 4-5).

Figure 4-5 OTUB1 is phosphorylated *in vitro* by ALK2-6 and CK2α

An *in vitro* kinase assay was set up with various kinases and GST-OTUB1 as substrate in the presence or absence of $^{\gamma 32}$P-ATP (500 cpm/pmole). The reaction was stopped after 30 min at 30 °C and the samples were resolved by SDS-PAGE, the gel was Coomassie stained and radioactivity was analysed by autoradiography.

4.2.4 CK2α phosphorylates OTUB1 on S16 in vitro

Having established that CK2α phosphorylates OTUB1 *in vitro* (Figure 4-5), the CK2 phosphorylation site on OTUB1 was determined by a combination of mass spectrometry and solid-phase Edman sequencing (Figure 4-6). OTUB1 was phosphorylated by CK2α using $^{\gamma 32}$P-ATP *in vitro,* the phospho-OTUB1 band excised, trypsin digested and the resulting peptides were separated by chromatography on a C_{18} column. One $^{\gamma 32}$P-labelled peak eluting at 25% acetonitrile was identified (Figure 4-6A). Analysis of this peptide by mass spectrometry resulted in m/z of 2975.2314, which is identical to the OTUB1 tryptic peptide QEPLGSDSEGVNCLAYDEAIMAQQDR with an additional single phospho-modification. To determine the precise phosphorylated residue in the $^{\gamma 32}$P-labelled peptide, the peptide was subjected to solid-phase Edman degradation. $^{\gamma 32}$P radioactivity was released after the sixth cycle of Edman degradation, suggesting that CK2α could phosphorylate OTUB1 on S16 (Figure 4-6B).

An *in vitro* kinase assay on wild type, as well as S16A, S18A and S16/18A GST-OTUB1 was performed to confirm the phosphorylation sites identified by mass spectrometry and Edman degradation. Mutation of S16A or S16/18A, but not S18A, abolished the phosphorylation of OTUB1 by CK2 (Figure 4-6C).
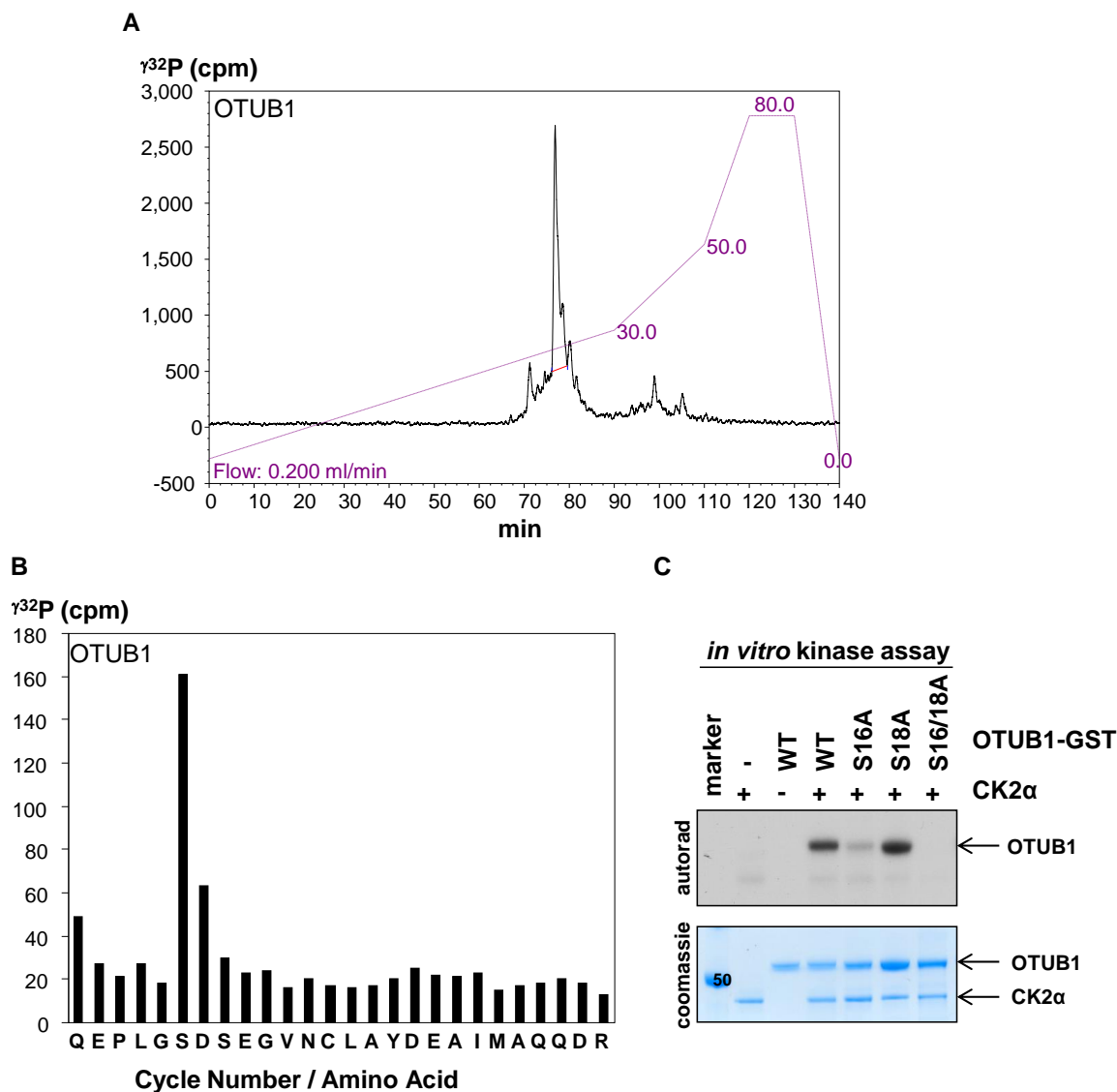
Figure 4-6 CK2 phosphorylates OTUB1 on S16 *in vitro*

A) GST-OTUB1 phosphorylated by CK2α *in vitro* was excised, digested with trypsin and resolved by HPLC on a C_{18} column on an increasing acetonitrile gradient. One peak of $^{\gamma 32}P$ release was observed after 76 minutes. **B)** Solid-phase sequencing of the peak revealed the release of $^{\gamma 32}P$ radioactivity after the sixth cycle of Edman degradation (performed by R. Gourlay). **C)** An *in vitro* kinase assay with CK2α was set up, using GST-OTUB1 and the indicated mutants of GST-OTUB1 as substrates in the presence of $^{\gamma 32}P$-ATP (500 cpm/pmole). The reaction was stopped after 30 min at 30 °C and the samples were resolved by SDS-PAGE, the gel was Coomassie stained and radioactivity was analysed by autoradiography**.**

4.2.5 CK2α phosphorylates OTUB1 on S16 in vivo

The phosphorylation of OTUB1 at S16 was further investigated by employing several chemical inhibitors of CK2 and ALK5 in cells. First, the specificity of CK2 and ALK inhibitors was tested in HEK293 cells (Figure 4-7A). SB505124 inhibits ALK5 activity and thereby abolishes SMAD2 phosphorylation (Vogt *et al.*, 2011). Moreover, it did not affect the phosphorylation of known CK2 substrates AKT1 pS129 and CDC37 pS13 (Figure 4-7A) (Di Maira *et al.*, 2005, Miyata and Nishida, 2004). Several inhibitors of CK2 have been developed (Battistutta, 2009, Cozza *et al.*, 2010, Pagano *et al.*, 2008). Non-selective inhibitors of CK2 LY294002 and K66 (Pagano *et al.*, 2008) did not significantly impact AKT1 or CDC37 phosphorylation at the CK2 sites and were discarded for further use (Figure 4-7A). In contrast, TDB (Cozza *et al.*, 2013) efficiently inhibited the CK2-mediated phosphorylation of AKT1 at S129 (Di Maira *et al.*, 2005) and partially inhibited the phosphorylation at S13 (Miyata and Nishida, 2004) (Figure 4-7A).

To test whether OTUB1 is a *bona fide* substrate of CK2 in cells, wild type or the OTUB1 S16/18A mutant were overexpressed in HEK293 cells and the extracts immunoblotted with anti-OTUB1 pS16 antibody (Figure 4-7B). OTUB1 S16 phosphorylation was detected in cells transfected with wild type OTUB1 but not OTUB1 S16/18A mutant. The CK2 inhibitor TDB (Cozza *et al.*, 2013) blocked the S16 phosphorylation of OTUB1 in cells (Figure 4-7B, last lane). OTUB1 S16 phosphorylation was also detected in endogenous OTUB1 immunoprecipitates of U2OS, HeLa and HEK293 cells in the absence of TDB (Figure 4-7C). By probing untreated cell extracts for phosphorylation of OTUB1 at S16, it was discovered that endogenous OTUB1 was constitutively phosphorylated, which was blocked by the CK2 inhibitor TDB (Figure 4-7D),

suggesting that CK2 is a constitutively active kinase upstream of OTUB1 (Pinna, 2003). For endogenous detection of OTUB1 pS16, TDB and OTUB1 siRNA were employed as controls to verify the specificity of the anti-OTUB1 pS16 antibody (Figure 4-7D).

Several cell permeable CK2 inhibitors are available, however many of them also target a wide range of other kinases (Battistutta, 2009, Cozza *et al.*, 2010, Pagano *et al.*, 2008). To date, TDB is the most potent and specific CK2 inhibitor to be reported, although it also inhibits 3 other kinases: PIM1, CLK2 and DYRK1A (Cozza *et al.*, 2014). An *in vitro* kinase assay was set up to test whether PIM1, DYRK1A and CLK2 were also able to phosphorylate OTUB1. Under the conditions where CK2α phosphorylates OTUB1, PIM1, DYRK1A and CLK2 failed to phosphorylate OTUB1 (Figure 4-8A). To verify the *in vitro* results, PIM1 and its catalytically inactive mutant PIM1 D277A were overexpressed in HEK293 cells (Figure 4-8B). PIM1 did not alter the levels of endogenous OTUB1 phosphorylation at S16 (Figure 4-8B). To further verify that the inhibition of OTUB1 phosphorylation mediated by TDB is specific to CK2, another potent and specific CK2 inhibitor (Quinalizarin) was employed (Cozza *et al.*, 2009). Quinalizarin also inhibited OTUB1 phosphorylation at S16, however not as efficient as TDB (Figure 4-8C).

To verify that CK2α expression and activity mediated the OTUB1 phosphorylation at S16, wild type CK2α or the catalytically inactive CK2α D156A mutant (Korn *et al.*, 1999) were overexpressed in HEK293 cells (Figure 4-9A). Wild type CK2α enhances phosphorylation of OTUB1 S16 over the basal levels (Figure 4-9A, lane 2), whereas the catalytically inactive CK2α did not alter basal OTUB1 S16 phosphorylation (Figure 4-9A, lane 4). TDB was less efficient at inhibiting OTUB1 S16 phosphorylation when CK2α was

overexpressed (Figure 4-9A, lane 3). Catalytically active CK2α (42 kDa) or CK2α' (38 kDa) were both able to phosphorylate endogenous OTUB1 at S16 (Figure 4-9B). To further confirm that CK2 was the main mediator for OTUB1 S16 phosphorylation *in vivo*, a loss-of-function experiment was employed using 4 different siRNAs against CK2α (Figure 4-9C). All four CK2 siRNAs target CK2α and CK2α', however the anti-CK2 antibody only recognises CK2α (Figure 4-9C). siRNAs *#1* and *#3* were selected for further investigation and in both cases robust CK2α knockdowns were achieved (Figure 4-9D). Under these conditions, a significant reduction in S16 phosphorylation of OTUB1 was achieved (Figure 4-9D), indicating that OTUB1 is a new *bona fide* substrate for CK2 in cells.
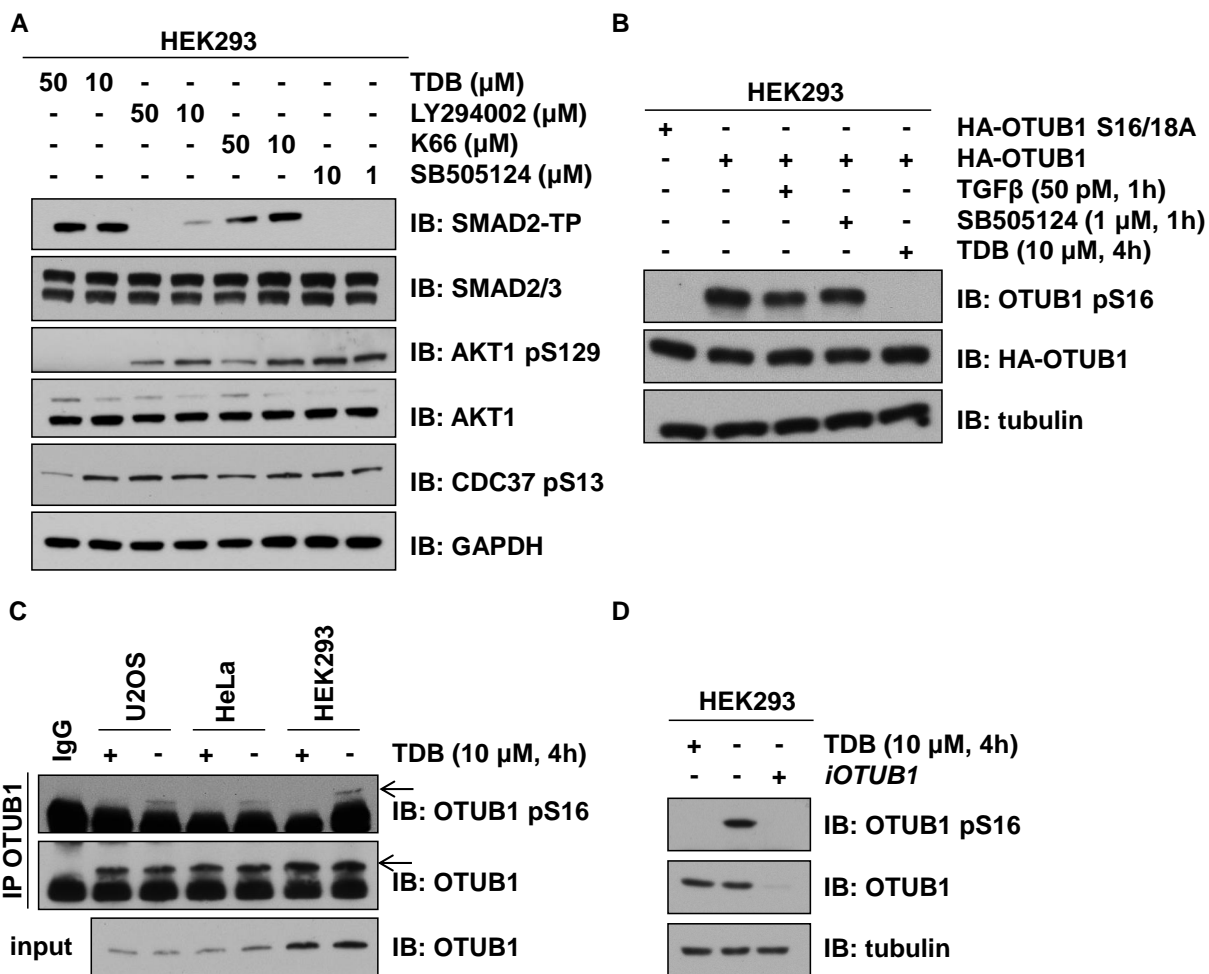
Figure 4-7 OTUB1 is constitutively phosphorylated at S16 *in vivo*

A) HEK293 cells were treated with the indicated amounts of inhibitors for 4 hours. Extracts were resolved by SDS-PAGE and immunoblotted with the indicated antibodies. **B)** HEK293 cells were transfected with vectors encoding N-terminal HA-tagged OTUB1 or HA-OTUB1 S16/18A. Prior to lysis cells were treated with the indicated inhibitor or cytokines for the indicated time points. Extracts were resolved by SDS-PAGE and immunoblotted with the indicated antibodies. **C)** An endogenous IP with anti-OTUB1 antibody or pre-immune sheep IgG was performed in HeLa, HEK293 or U2OS cell extracts, treated with or without 10 µM TDB for 4 hours. Endogenous IgG or anti-OTUB1 IPs were resolved by SDS-PAGE and immunoblotted with the indicated antibodies. **D)** HEK293 cells were left untreated, treated with TDB (10 µM, 4 h) or were transfected with siRNA against *OTUB1* (300 pM/10-cm dish each) and lysed 48 hours post-transfection. Extracts (80 µg) were resolved by SDS-PAGE and immunoblotted with the indicated antibodies.
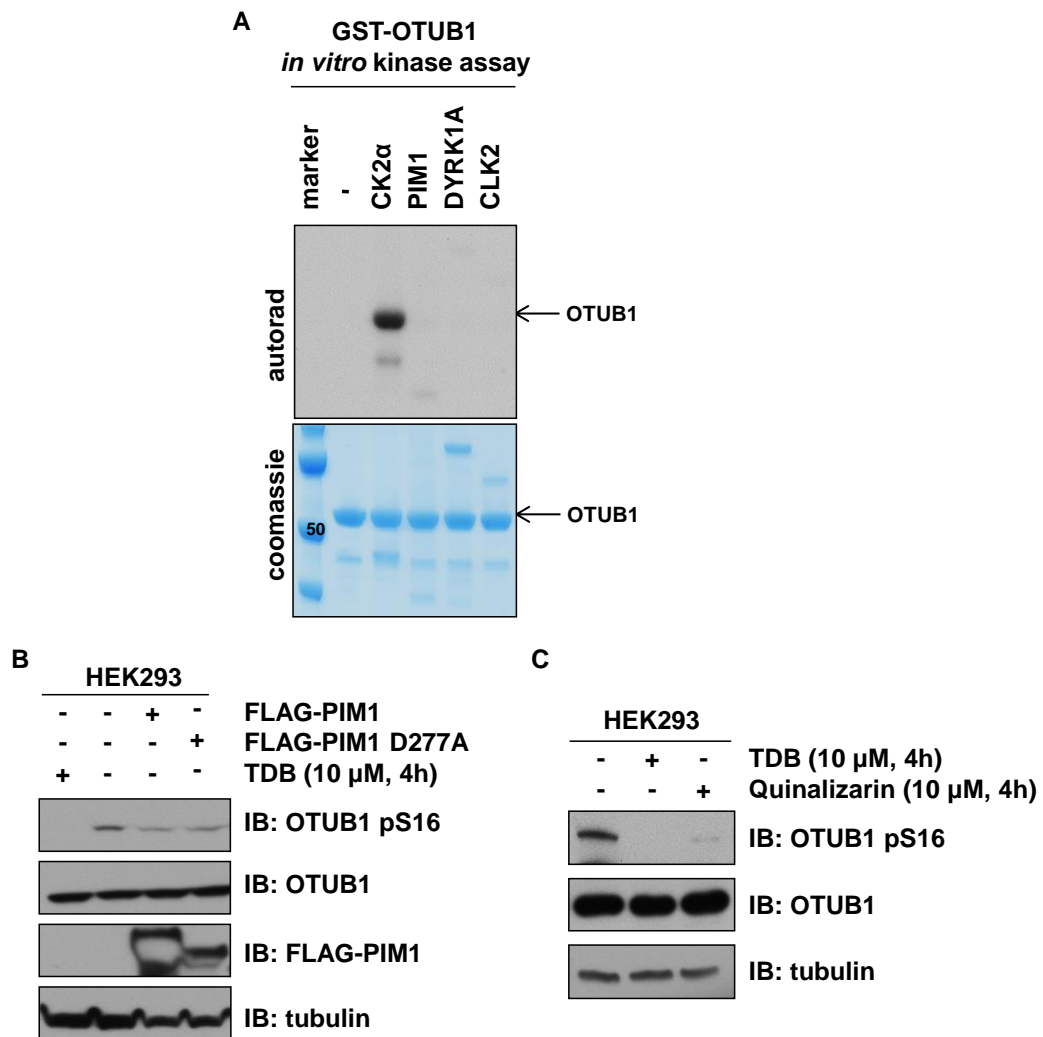
Figure 4-8 Phosphorylation of OTUB1 at S16 is specific to CK2

A) An *in vitro* kinase assay was set up with various kinases using GST-OTUB1 as substrate in the presence of $^{\gamma 32}$P-ATP (500 cpm/pmole). The reaction was stopped after 30 min at 30 °C and the samples were resolved by SDS-PAGE, the gel was Coomassie stained and radioactivity was analysed by autoradiography. **B)** HEK293 cells were transfected with vectors encoding N-terminal FLAG-tagged PIM1 or FLAG-PIM1 D277A. Prior to lysis cells were treated with or without TDB (10 μM, 4 hours). Extracts were resolved by SDS-PAGE and immunoblotted with the indicated antibodies. **C)** HEK293 cells were left untreated, treated with TDB (10 μM, 4 h) or Quinalizarin (10 μM, 4 h) prior to lysis. Extracts (80 μg) were resolved by SDS-PAGE and immunoblotted with the indicated antibodies.
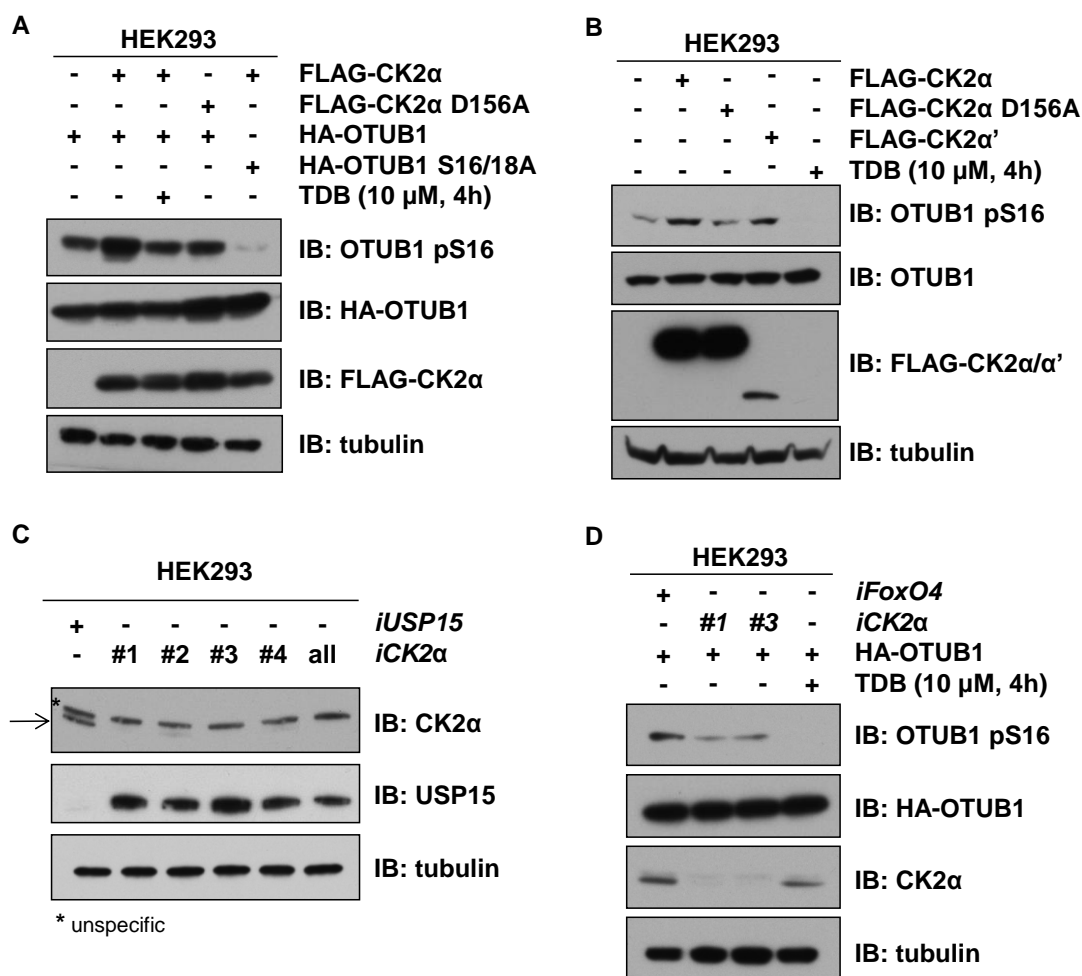
Figure 4-9 CK2 phosphorylates OTUB1 *in vivo*

A) HEK293 cells were co-transfected with vectors encoding N-terminal HA-tagged OTUB1 or HA-OTUB1 S16/18A and N-terminal FLAG-tagged CK2 or FLAG-CK2 D156A. Prior to lysis cells were treated with or without TDB (10 µM, 4 hours). Extracts were resolved by SDS-PAGE and immunoblotted with the indicated antibodies. **B)** HEK293 cells were transfected with vectors encoding N-terminal FLAG-tagged CK2α, FLAG-CK2α D156A or FLAG-CK2α'. Prior to lysis cells were treated with or without TDB (10 µM, 4 hours). Extracts were resolved by SDS-PAGE and immunoblotted with the indicated antibodies. **C)** HEK293 cells were transfected with *USP15* siRNA or four siRNAs against *CK2α/α' (#1, #2, #3, #4)* (300 pM/10-cm dish each) and lysed 48 hours post-transfection. Extracts were resolved by SDS-PAGE and immunoblotted with the indicated antibodies. **D)** HEK293 cells were transfected with HA-OTUB1 and siRNAs against *CK2α/α' (#1, #3)* or *FoxO4* (control) (300 pM/10-cm dish each) and lysed 48 hours post-transfection. Prior to lysis cells were treated with or without 10 µM TDB for 4 hours. Extracts were resolved by SDS-PAGE and immunoblotted with the indicated antibodies.

4.3 <u>**Discussion**</u>

In this study, two residues on OTUB1, S16 and S18, were identified as potential phosphorylation sites. Further investigations on these residues have revealed that CK2 phosphorylates OTUB1 at S16 *in vivo*, making OTUB1 a *bona fide* substrate for CK2. The regulation of OTUB1 by phosphorylation remains to be investigated.

4.3.1 *Identification of the kinases responsible for OTUB1 phosphorylation at S16 and S18*

It had been suggested previously that OTUB1 could be phosphorylated by the *Yersinia* encoded kinase YpkA, which phosphorylates OTUB1 *in vitro*. However, in the absence of *Yersinia* infection OTUB1 is still phosphorylated in cells (Juris *et al.*, 2006, Edelmann *et al.*, 2010), suggesting a host kinase mediates the phosphorylation of OTUB1. In this study, type I TGFβ/BMP receptors (ALKs2-6) were identified as kinases that are able to phosphorylate OTUB1, primarily at S18, *in vitro*. However, currently no suitable tools are available to assess whether S18 of OTUB1 is phosphorylated by these kinases in response to TGFβ or BMP. In the absence of a phospho-specific antibody recognising OTUB1 phosphorylated at S18, SRM (selected reaction monitoring) could be used to establish whether activated ALKs could phosphorylate OTUB1 at S18 in cells.

The activation of ALKs through TGFβ/BMP/Activin did not enhance the phosphorylation of OTUB1 at S16 in cells. In order to identify the kinase(s) that mediates OTUB1 S16 phosphorylation, several kinases that phosphorylate residues in a motif similar to the one that surrounds OTUB1 S16 were selected. From this kinase panel, only CK2α was able to phosphorylate OTUB1 *in vitro*.

CK2 is an acidophilic Serine/Threonine kinase that targets "SXX(E/D/pS/pT)" and prefers acidic amino acids at positions n+1 and n+3 (Meggio and Pinna, 2003). OTUB1 is phosphorylated by CK2 at S16 ("SDSE"), which is followed by two acidic residues (at n+1 and n+3). Moreover, the preference for CK2 towards OTUB1 at S16 could potentially be further enhanced by phosphorylation of S18 by ALKs or other unknown kinase(s). An *in vitro* phosphorylation assay using OTUB1 S18 or pS18 peptides could be employed to further test whether phosphorylation at S18 primes OTUB1 for recognition and phosphorylation by CK2. However, preliminary data suggests that CK2 phosphorylates OTUB1 independently of S18 phosphorylation. If S18 phosphorylation would prime OTUB1 for recognition by CK2, then it would be unlikely that S18 is phosphorylated in response to TGFβ/BMP because, in ALK5-/- MEFs the CK2-mediated phosphorylation of S16 was not affected.

CK2 phosphorylates OTUB1 at S16 in different cell lines. Through overexpression and loss of function experiments, OTUB1 has been verified as a *bona fide* substrate of CK2 (Figure 4-10). Furthermore, inhibitors of CK2 abolish the phosphorylation of OTUB1. The phosphorylation of OTUB1 S16 in cells is constitutive, which is consistent with CK2 being a constitutively active kinase (Meggio and Pinna, 2003, Battistutta and Lolli, 2011, Pinna, 2003, Montenarh, 2010). Although the phosphorylation of OTUB1 might not be induced through extracellular stimuli, the dephosphorylation of OTUB1 could be. Potential phosphatase(s) that target OTUB1 are not known. OTUB1 is phosphorylated by CK2; however it is possible that not every molecule of OTUB1 is phosphorylated in cells. A balance between phosphorylated and unphosphorylated OTUB1 could be created by phosphatases, other OTUB1 binding proteins that restrict access to CK2, or differential pools of OTUB1 and

CK2 in subcellular compartments. CK2 only phosphorylates OTUB1 on S16, as assessed by mass spectrometry and Edman degradation.
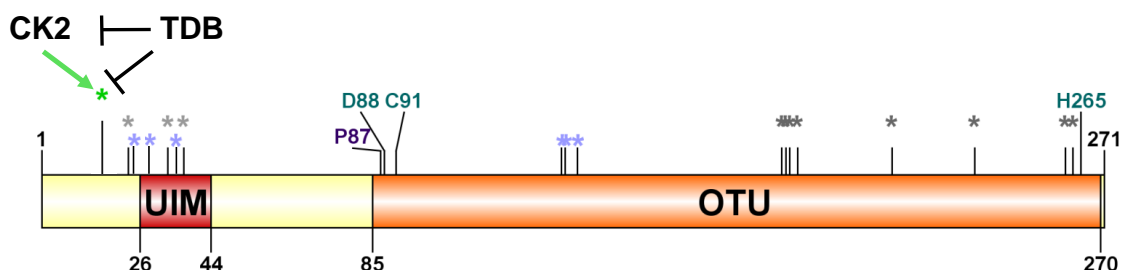
Figure 4-10 OTUB1 is phosphorylated by CK2 at S16

Schematic representation of human OTUB1 indicating the domain structures (UIM in red, OTU in orange), catalytic residues (in dark green), P1' site (P87 in purple), the E2 interface (* in light blue), the proximal ubiquitin binding interface (S1') (* in light grey), the distal ubiquitin interface (S1) (* in dark grey) and the OTUB1 CK2-mediated phosphorylation site S16 (light green), which can be blocked by the CK2 inhibitor TDB.

4.3.2 The potential impact of OTUB1 phosphorylation

Phosphates introduce a change in the local charge of proteins, thereby causing conformational changes in the modified protein, which could alter their affinity or activity towards ligands, substrates or binding partners (Manning *et al.*, 2002). The phosphorylation sites of OTUB1 (S16 and S18) are present in its N-terminus (Figure 4-10). The N-terminus of OTUB1 harbours a UIM-like motif and folds into an α-helix upon ubiquitin binding (section 3.1.2 and 3.1.3). S16 and S18 are in proximity to the E2 and proximal ubiquitin-binding interface and their phosphorylation could change the conformation of OTUB1. Hence, phosphorylation of S16 and S18 could potentially alter the K_M of OTUB1 catalytic activity or the affinity for the specific chain linkage types (Figure 4-11). It has been reported that the E2 stimulated catalytic activity of OTUB1 is affected by a deletion of the first 30 N-terminal OTUB1 residues, while a

deletion of the first 15 amino acids of OTUB1 had no effect (Wiener *et al.*, 2013). Therefore, it is tempting to speculate that the phosphorylation of S16 and S18 could potentially influence the E2 stimulated catalytic activity of OTUB1.

The binding of OTUB1 to ubiquitin, K63-linked polyubiquitin chains, E2 or E2~ub could be altered through the negative charge of S16 and S18 phosphorylation and influence its non-canonical function (Figure 4-11). The first 23 amino acids preceding the α-helix of the OTUB1 N-terminus are disordered (Wiener *et al.*, 2013) and absent from all reported crystal structures (Wiener *et al.*, 2013, Wiener *et al.*, 2012, Juang *et al.*, 2012, Sato *et al.*, 2012). S16 and S18 phosphorylation could alter protein folding (Figure 4-11) or assist in protein-protein interactions that mediate the transition from intrinsically unstructured to ordered state. Apart from E2s and ubiquitin, the phosphorylation of OTUB1 could also attract the binding of other regulatory proteins such as 14-3-3s or influence its affinity towards substrates, such as phosphorylated SMAD2/3 (section 3.1.4) (Figure 4-11). It has been reported that phosphorylated OTUB1 displays increased affinity towards YpkA, which modulates susceptibility to *Yersinia* invasion (Edelmann *et al.*, 2010). Small molecule inhibitors that inhibit the CK2 mediated phosphorylation of OTUB1 in cells could potentially decrease the uptake of *Yersinia* into host cells and be employed as therapeutic strategies.

OTUB1 is mainly observed in the cytosol. However, upon phosphorylation a small pool of OTUB1 could potentially translocate to the nucleus or other organelles (Figure 4-11), as has been reported for Ataxin-3 (Mueller *et al.*, 2009). CK2 localises to DNA double strand breaks and is implicated in the DNA damage repair (Olsen *et al.*, 2012, Blaydes and Hupp, 1998, Loizou *et al.*, 2004, Ghavidel and Schultz, 2001). The mechanism of

OTUB1 displacement from DNA damage sites is still unknown (Nakada *et al.*, 2010), but could potentially be regulated by CK2 mediated phosphorylation.

The generation of OTUB1 knockout cells will be helpful to decipher the physiological roles of OTUB1 phosphorylation, as these cells could be employed to generate stable OTUB1 phosphorylation deficient or mimetic mutant cell lines. Furthermore, the generation of bacterially purified OTUB1 pS16 would be a versatile tool for functional *in vitro* studies of OTUB1. Small amounts of phosphorylated OTUB1 at S16 have been purified using the amber-stop codon technique to incorporate phospho-Serines at desired sites during translation (Park *et al.*, 2011). However, initial trials of this technique have failed to yield homogeneous pS16 and pS18 OTUB1 and further optimisation is needed.

The possibility of OTUB1 regulation in cells through phosphorylation should be taken into account when designing small molecule inhibitors of OTUB1. By modulating the amount of phosphorylated OTUB1 in cells, distinct physiological functions of OTUB1 could be altered. The precise mechanisms and interplay between phosphorylation and ubiquitylation in the regulation of OTUB1 should be further investigated and could open new avenues of research.
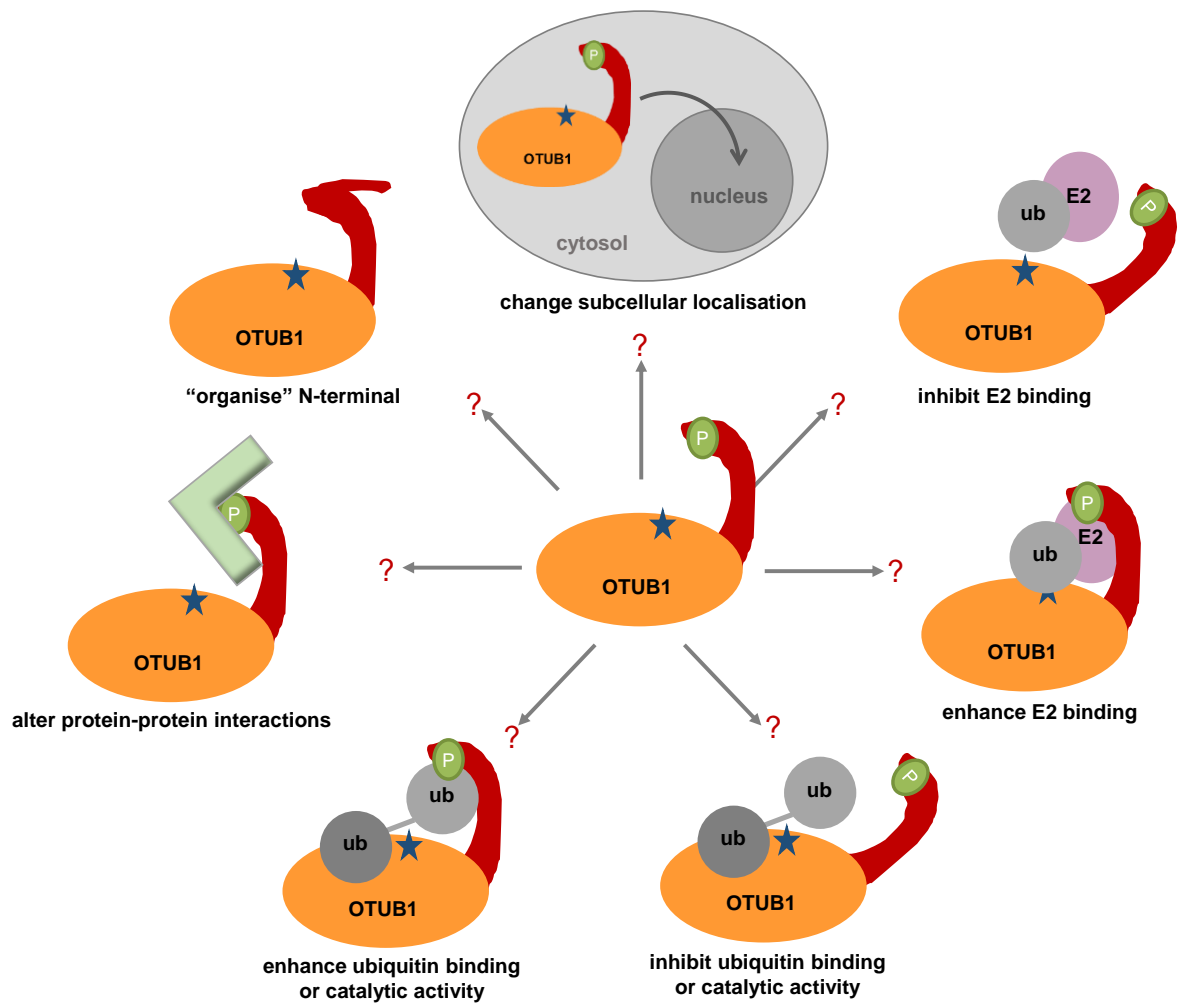
Figure 4-11 Possible functions of OTUB1 phosphorylation

The phosphorylation of OTUB1 could result in a change of OTUB1 function. It could enhance or inhibit E2, E2~ub or ubiquitin binding, alter OTUB1 catalytic activity, protein-protein interactions or subcellular localisation or change the organisation structure of the disordered first 24 amino acids of the N-terminus.

5 <u>USP15 targets ALK3 for deubiquitylation to enhance BMP pathway signalling</u>

5.1 <u>Introduction</u>

Ubiquitylation of the TGFβ/BMP pathway components plays a critical role in fine tuning TGFβ/BMP-mediated cellular responses (section 1.3.2). Receptor ubiquitylation through feedback mechanism attenuates signalling. Much is known about the E3 ubiquitin ligases that target TGFβ/BMP receptors for ubiquitylation. Recently several deubiquitylating enzymes that reverse type I TGFβ receptor ubiquitylation have been reported. However, no DUBs that target the type I BMP receptors have been discovered. USP15 was identified in a proteomic screen as an interactor of SMAD6, which is a negative regulator of the BMP pathway (Figure 5-2A). Hence, the aim of this chapter was to characterise the role of USP15 in the BMP pathway.

5.1.1 *Structure and function of USP15*

USP15 is a cysteine protease (Komander *et al.*, 2009, Baker *et al.*, 1999), which also harbours a zinc finger that is essential for the cleavage of polyubiquitin chains (Hetfeld *et al.*, 2005). It belongs to the USP family of DUBs and is highly related to USP4 and USP11, as defined by conserved sequences and structural similarities (Figure 5-1A) (Komander *et al.*, 2009). USP4, USP11 and USP15 harbour a DUSP (domain present in USPs) at the N-terminus and two UBLs (ubiquitin like domains), one preceding the USP catalytic domain and one within (Komander *et al.*, 2009). The crystal structures of the DUSP and UBL domains of USP15 (Figure 5-1B) have been resolved (de Jong *et al.*, 2006, Harper *et al.*, 2011, Elliott *et al.*, 2011).

The surface properties of the DUSP domain suggest a potential role in protein-protein interaction or substrate recognition (de Jong *et al.*, 2006). The UBL domains of multiple-domain proteins can function as protein-protein interaction motifs and recognise ubiquitylated substrates (Zhu *et al.*, 2007). The UBL domain within the catalytic domain (UBL2) of USP4 also serves an autoinhibitory role as a ubiquitin mimic (Luna-Vargas *et al.*, 2011). The UBL1 domain of USP15 is closely related to ubiquitin, however has longer loop regions and different surface characteristics, suggesting that it does not act as a ubiquitin mimic (Figure 5-1C) (Harper *et al.*, 2011). The DUSP and UBL domains of USP15 are arranged in tandem, which is conserved in USP4 but not in USP11. The tandem architecture of the DUSP and UBL domains is stabilised by a β-hairpin structure that forms a hydrogen-bonding network between the domains (Figure 5-1B, orange linker region) (Harper *et al.*, 2011).
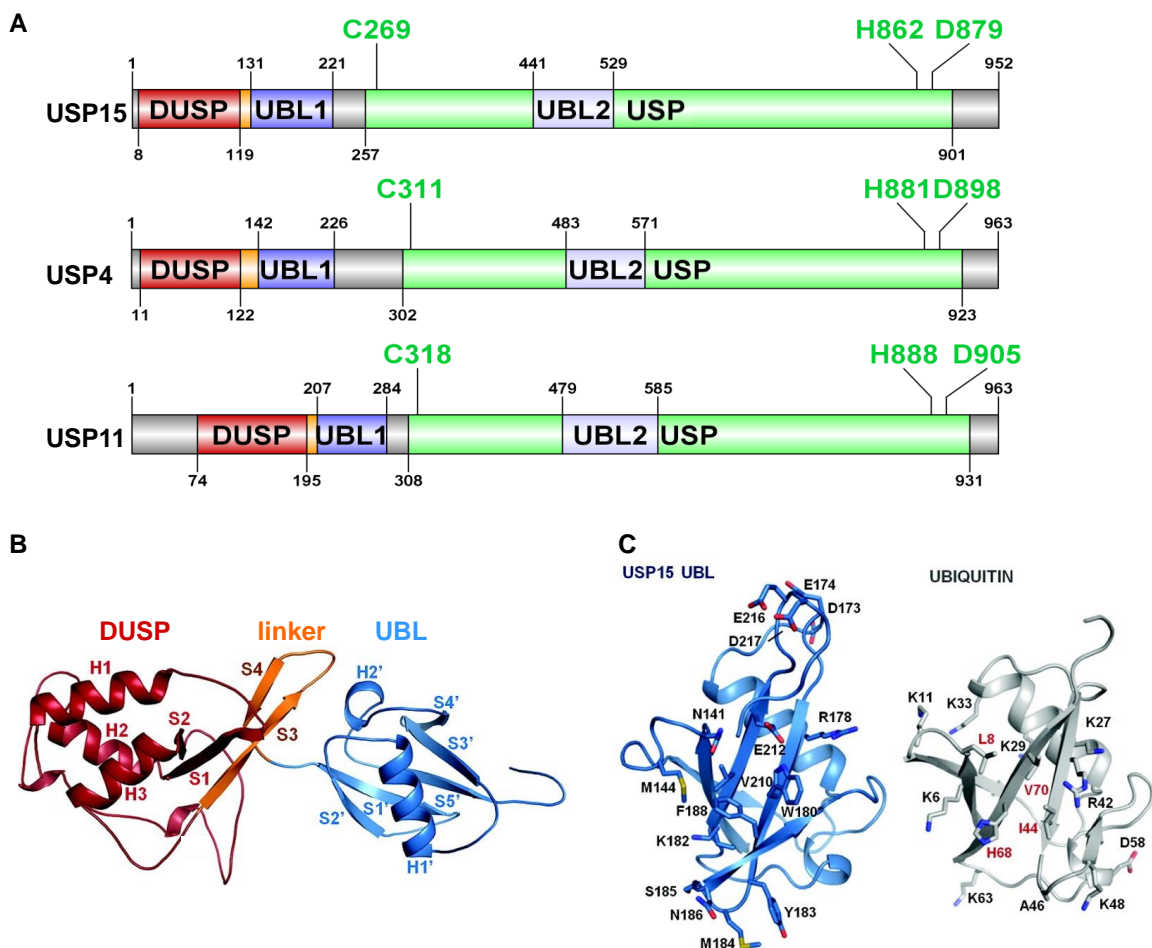
Figure 5-1 Structure of USP15 DUSP and UBL domains

A) Schematic representation of human USP15, USP4 and USP11 indicating the domain structures and catalytic residues. **B)** USP15 DUSP (red), linker (orange) and UBL (blue) domains in cartoon representation. The β-hairpin structure at the interface of the DUSP and UBL domains (orange linker region) creates an extensive hydrogen-bonding network and creates the DUSP and UBL interface, thereby determining the fixed tandem orientation. H=α-helix, S=β-strand. **C)** USP15 UBL domain and ubiquitin shown in the same orientation. Residues creating the hydrophobic surface patch in ubiquitin that most often engages in protein interactions are labelled in red. This Figure was adapted from Harper *et al.*, 2011.

5.1.2 Deubiquitylation targets of USP15

USP15 affects diverse signalling pathways and is linked to various pathologies, including cancers. USP15 is implicated in chemo-resistance to the anticancer agent Paclitaxel (Taxol), through the regulation of Caspase3 stability by inhibiting Paclitaxel-induced apoptosis (Xu *et al.*, 2009). Furthermore, it has been reported to act as a negative regulator of T cell activation by deubiquitylating the E3 ubiquitin ligase MDM2 (Zou *et al.*, 2014) and to antagonise the Parkin-mediated mitochondrial ubiquitylation and inhibit mitophagy (Cornelissen *et al.*, 2014). USP15 has been shown to deubiquitylate the skeletal muscle LIM protein 1 (SLIM1), which is implicated in the pathogenesis of myopathies (Isumi *et al.*, 2011). Additionally, USP15 has been reported to deubiquitylate the K48-, but not K63-, linked polyubiquitin chains on TRIM25, thereby preventing its proteasomal degradation while promoting the RIG1-mediated antiviral immune response (Pauli *et al.*, 2014). USP15 is involved in the transcriptional regulation by associating with SART3, which enhances USP15 binding to ubiquitylated histone H2B and facilitating its deubiquitylation (Long *et al.*, 2014). Moreover, USP15 has been shown to stabilise HPV16, ROC1, APC, REST and Keap1 through deubiquitylation (Vos *et al.*, 2009, Hetfeld *et al.*, 2005, Huang *et al.*, 2009, Faronato *et al.*, 2013, Villeneuve *et al.*, 2013). USP15 activity might be regulated in a feedback loop, as the DUSP-UBL domain of USP15 binds the coiled coil region of the E3 ligase BRAP and stabilises it, whereas BRAP then promotes the ubiquitylation of USP15 (Hayes *et al.*, 2012). USP15 has also been implicated in TGFβ signalling (*cf.* section 1.3.2), by deubiquitylating ALK5 and monoubiquitylated R-SMADs (Eichhorn *et al.*, 2012, Inui *et al.*, 2011). Its role in the BMP pathway through its association with SMAD6 had not been investigated.

5.2 <u>Results</u>

5.2.1 *USP15 interacts with SMAD6 and is ubiquitously expressed*

In order to identify novel regulators of the BMP signalling pathway, a proteomic screen on SMAD6-interacting proteins was performed. Flp-IN HEK293 cells stably expressing N-terminal tagged GFP-SMAD6 under the control of a tetracycline-inducible promoter were generated. GFP-immunoprecipitates (IPs) were resolved by SDS-PAGE and the interacting proteins excised, digested with trypsin and identified by mass spectrometry. USP15 was identified as an interactor of GFP-SMAD6 but not GFP control (Figure 5-2A). As expected SMURF2, WWP1, ITCH and USP11 were also identified in GFP-SMAD6 IPs (Zhang *et al.*, 2013c).

To test the specificity of the interaction between USP15 and SMAD6, FLAG-SMADs1, 3, 4, 6 and 7 were overexpressed in HEK293 cells. Only FLAG-SMAD6, but not other SMADs, was detected in the endogenous USP15 IPs (Figure 5-2B), indicating a selective interaction. Analysis of the expression pattern of USP15 in mouse tissues showed that USP15 is ubiquitously expressed (Figure 5-3).
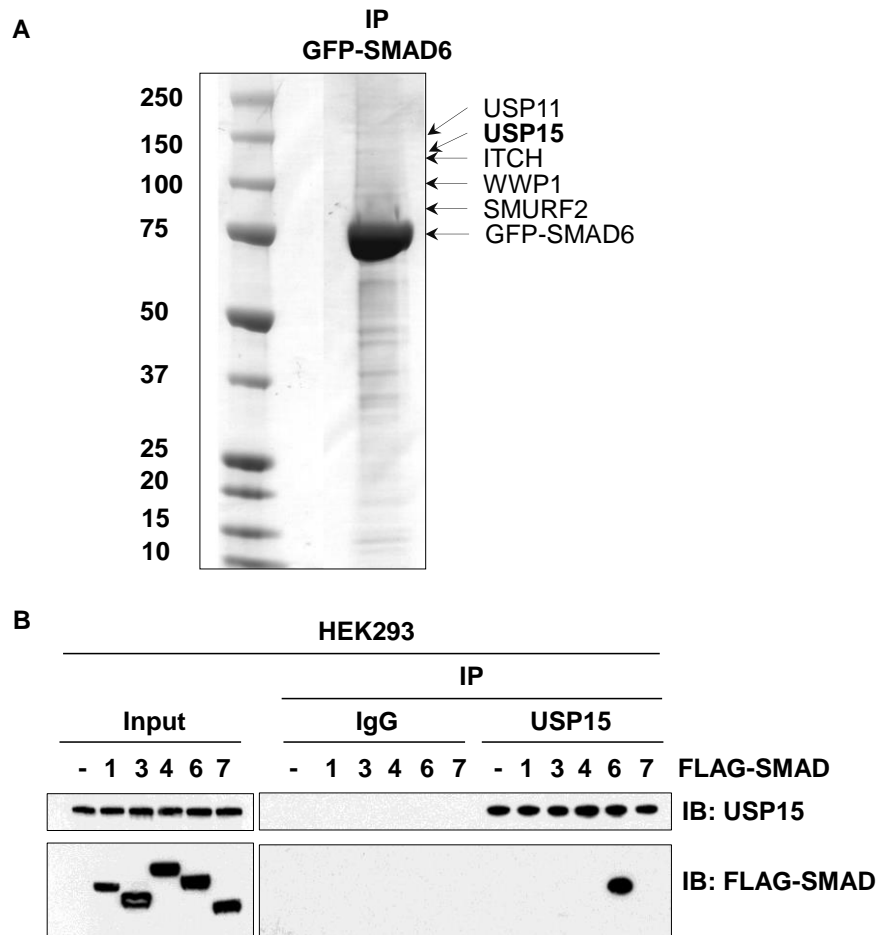
Figure 5-2 USP15 interacts with SMAD6

A) HEK293 cells stably expressing GFP-SMAD6 were lysed in the presence of DSP. GFP-immunoprecipitates (IPs) were separated by SDS-PAGE and interacting partners identified by mass spectrometry (performed by D. Bruce). **B)** HEK293 cells were transfected with constructs encoding N-terminal FLAG-tagged SMADs. USP15 or IgG-immunoprecipitates or lysate inputs were resolved by SDS-PAGE and immunoblotted with the indicated antibodies (performed by M. Al-Salihi).

wild type mouse tissues

brain, muscle, heart, adipose, lung, liver, pancreas, kidney, spleen, thymus, uterus, testis, epididymis

IB: USP15

IB: GAPDH
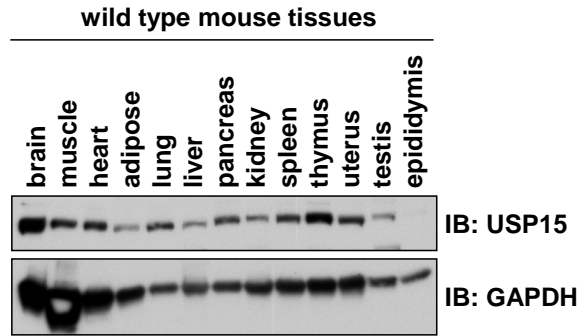
Figure 5-3 USP15 is ubiquitously expressed

Indicated mouse tissues were homogenised in lysis buffer and 20 µg of protein lysates were resolved by SDS-PAGE and immunoblotted with antibodies against USP15 and GAPDH.

5.2.2 USP15 modulates the intensity of SMAD1 phosphorylation upon BMP Signalling

SMAD6 is a negative regulator of BMP signalling. It is transcribed upon BMP stimulation and acts in a feedback loop by blocking access of R-SMADs to type I BMP receptors and directing E3 ubiquitin ligases to the receptor complexes, resulting in their ubiquitin-mediated degradation (Goto *et al.*, 2007, Murakami *et al.*, 2003). In order to investigate whether the binding of USP15 to SMAD6 implies a role for USP15 in BMP signalling, HEK293 cells were transiently transfected with three different siRNAs against USP15 (Figure 5-4A). siRNAs 1-3 resulted in a knockdown of USP15 protein levels, as compared to control siRNA (*iFoxO4*). Additionally the cells were treated with BMP_2 (6.25 ng/ml) for 1 hour[2], which resulted in the tail-phosphorylation of SMAD1 (SMAD1-TP) in control siRNA transfected cells. USP15 depletion caused a reduction in the levels of BMP-induced SMAD1-TP without affecting

---

[2] If not stated otherwise, cells were always serum starved overnight and treated for 1 hour with 6.25 ng/ml BMP_2.

the total levels of SMAD1 (Figure 5-4A). *iUSP15#3* was selected for further experiments.

To verify that USP15 depletion inhibits SMAD1 phosphorylation across cell lines, HeLa and U2OS cells were used in addition to the HEK293 cells (Figure 5-4B,C,D). siRNA-mediated reduction of USP15 in HeLa (Figure 5-4B,C) and U2OS (Figure 5-4D) cells strongly suppressed the BMP-induced phosphorylation of SMAD1 even in presence of excessive ligand (25 ng/ml BMP) (Figure 5-4B). A quantification of Western Blot bands representing SMAD1-TP and total SMAD1 from 5 independent experiments using control or *USP15* siRNA showed that *iUSP15#3* caused a statistically significant reduction in BMP-induced SMAD1-TP levels (Figure 5-4E). In contrast to the inhibition of BMP signalling by USP15 depletion, the overexpression of HA-USP15 in HEK293 cells slightly enhanced the levels of tail-phosphorylated SMAD1 in response to BMP (Figure 5-4F).
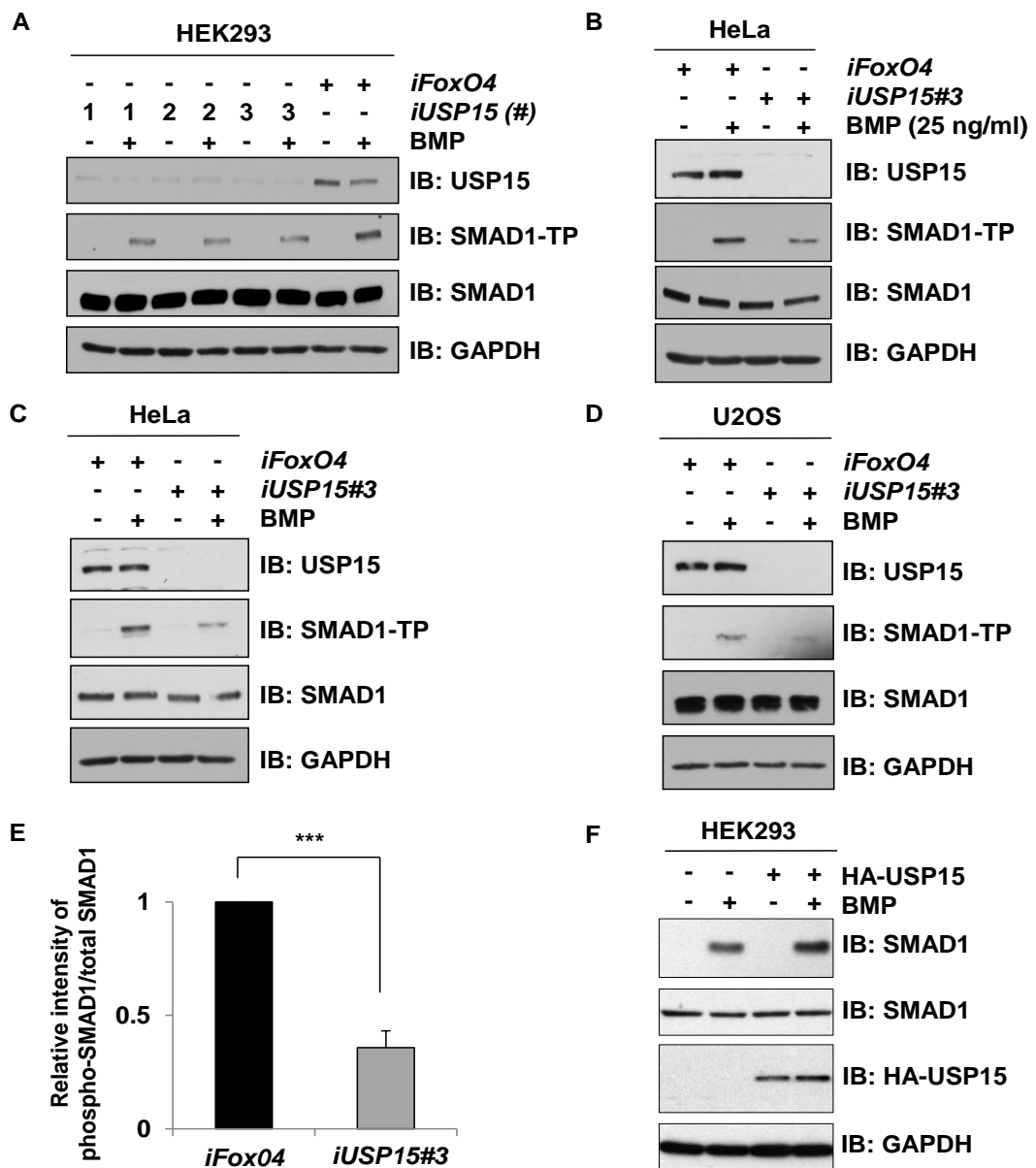
Figure 5-4 USP15 modulates the intensity of BMP-induced SMAD1 tail-phosphorylation

A) HEK293 cells were transiently transfected with siRNAs targeting USP15 and stimulated with 6.25 ng/ml BMP for 1 hour prior to lysis. Extracts were resolved by SDS-PAGE and immunoblotted with the indicated antibodies. **B)** As in A, except that HeLa cells were transiently transfected with *iUSP15#3* and stimulated with 25 ng/ml BMP for 1 hour prior to lysis. **C)** As in B, except that cells were stimulated with 6.25 ng/ml BMP for 1 hour. **D)** As in C, except that U2OS cells were employed. **E)** Western Blot bands representing phospho-SMAD1 and total SMAD1 from 5 independent experiments using *iUSP15#3* or *FoxO4* siRNA were quantified using Image J. Data are represented as mean and error bars indicate standard deviation (n=5). Student's t-test was performed and differences with p<0.001 were annotated as ***. **F)** HEK293 cells transiently expressing control HA-vector or HA-USP15 were stimulated with 6.25 ng/ml BMP for 1 hour prior to lysis. Extracts were resolved by SDS-PAGE and immunoblotted with the indicated antibodies.

5.2.3 Reduction of phospho-SMAD1 caused by a loss of USP15 can be rescued by Bortezomib and HA-USP15

To verify that the decrease in levels of tail-phosphorylated SMAD1 by USP15 depletion were not due to off target effects of siRNAs, rescue experiments were performed. The inhibition of BMP-induced SMAD1-TP levels by *iUSP15#3* were rescued by the overexpression of FLAG-USP15 in HEK293 cells (Figure 5-5A). Furthermore, the proteasomal inhibitor Bortezomib resulted in the stabilisation of BMP-induced SMAD1-TP levels caused by USP15 depletion (Figure 5-5B). In both cases, the total levels of SMAD1 protein remained unchanged (Figure 5-5).
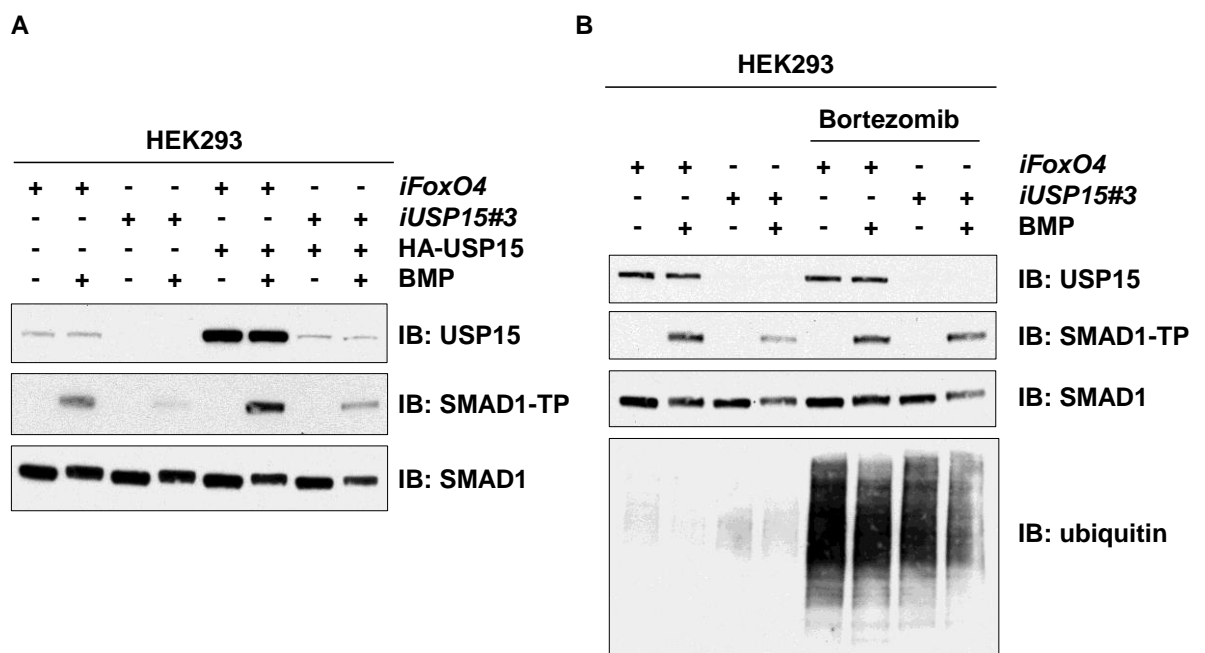
Figure 5-5 Reduction of phospho-SMAD1 caused by a loss of USP15 can be rescued by Bortezomib and HA-USP15

A) HEK293 cells were transiently transfected with *iFoxO4* or *iUSP15#3*. 24 hours post siRNA transfection, cells were transfected with HA-control or HA-USP15. Cells were stimulated with or without BMP for 1 hour prior to lysis. Extracts were resolved by SDS-PAGE and immunoblotted with the indicated antibodies (performed by M. Al-Salihi). **B)** HEK293 cells were transiently transfected with *iUSP15#3* or *iFoxO4.* Cells were treated with or without 10 µM Bortezomib for 3 hours and stimulated with 6.25 ng/ml BMP for 1 hour prior to lysis. Extracts were resolved by SDS-PAGE and immunoblotted with the indicated antibodies (performed by M. Al-Salihi).

5.2.4 USP15 depletion inhibits BMP-induced transcription

Next, it was investigated whether phospho-SMAD1 reduction caused by USP15 depletion (Figure 5-4) also resulted in inhibition of BMP-induced transcriptional activity (Figure 5-6). RNAi-mediated depletion of USP15 in HEK293 cells significantly reduced the expression of inhibitor of differentiation 1 (*ID-1*) mRNA, which is a transcriptional target of BMP (Figure 5-6A). In contrast, depletion of USP11, which is highly similar to USP15 (Figure 5-1A) and impacts TGFβ-induced transcription (Al-Salihi *et al.*, 2012a), did not cause any reduction in *ID-1* expression upon BMP induction (Figure 5-6B).
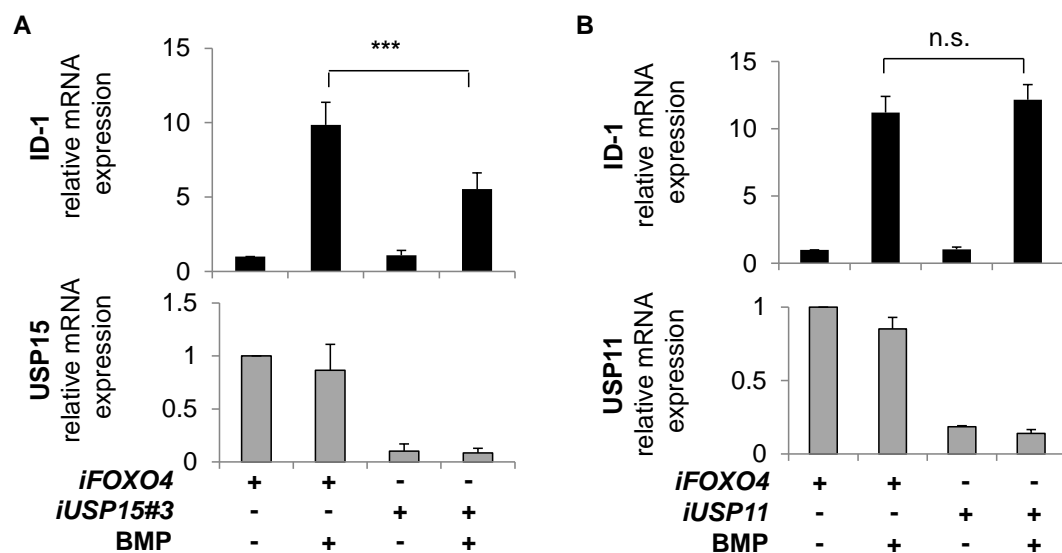
Figure 5-6 USP15 depletion inhibits BMP-induced transcription

A) HEK293 cells were transiently transfected with *iUSP15#3* and stimulated with 6.25 ng/ml BMP for 1 hour. Cells were then washed and lysed 2 hours later. The mRNA expression levels of *USP15* and the BMP-target gene *ID-1* were analysed by qRT-PCR. Data are represented as mean and error bars indicate standard deviation (n=6). Differences with p<0.001 were annotated as ***. **B)** As in A, except that HEK293 cells were transfected with siRNA against *USP11*. Differences with p>0.05 were annotated as ns (not significant).

5.2.5 USP15 and SMAD6 impact the BMP pathway in opposite ways

SMAD6 is a negative regulator of BMP signalling by directing E3 ubiquitin ligases to ALK3, thereby inducing ubiquitin-mediated degradation of the receptors. This results in reduced SMAD1 phosphorylation. Furthermore, SMAD6 can compete with SMAD1 for receptor binding, thus further inhibiting SMAD1 phosphorylation. Hence, the overexpression of HA-SMAD6 in HEK293 cells significantly reduced the BMP-induced tail-phosphorylation of SMAD1 (Figure 5-7A). The reduction in SMAD1 tail-phosphorylation could be partly rescued by the overexpression of USP15, indicating that in contrast to SMAD6, USP15 is a positive regulator of BMP signalling (Figure 5-7A).

In accordance with these findings, siRNA-mediated knockdown of *SMAD6* was also able to rescue the inhibition of BMP signalling caused by *USP15* depletion (Figure 5-7B). The depletion of *SMAD6* by siRNA resulted in enhanced BMP-mediated phosphorylation of SMAD1, whereas the depletion of *USP15* caused a decrease in SMAD1 phosphorylation in HEK293 cells. The knockdown of *SMAD6* and *USP15* together resulted in SMAD1 phosphorylation levels similar to control cells (*iFoxO4*) treated with BMP (Figure 5-7B). This indicates that SMAD6 and USP15 have opposing roles in regulating the BMP pathway. In the absence of SMAD6 antibodies, siRNA-mediated depletion of *SMAD6* was confirmed by qRT-PCR (Figure 5-7C).
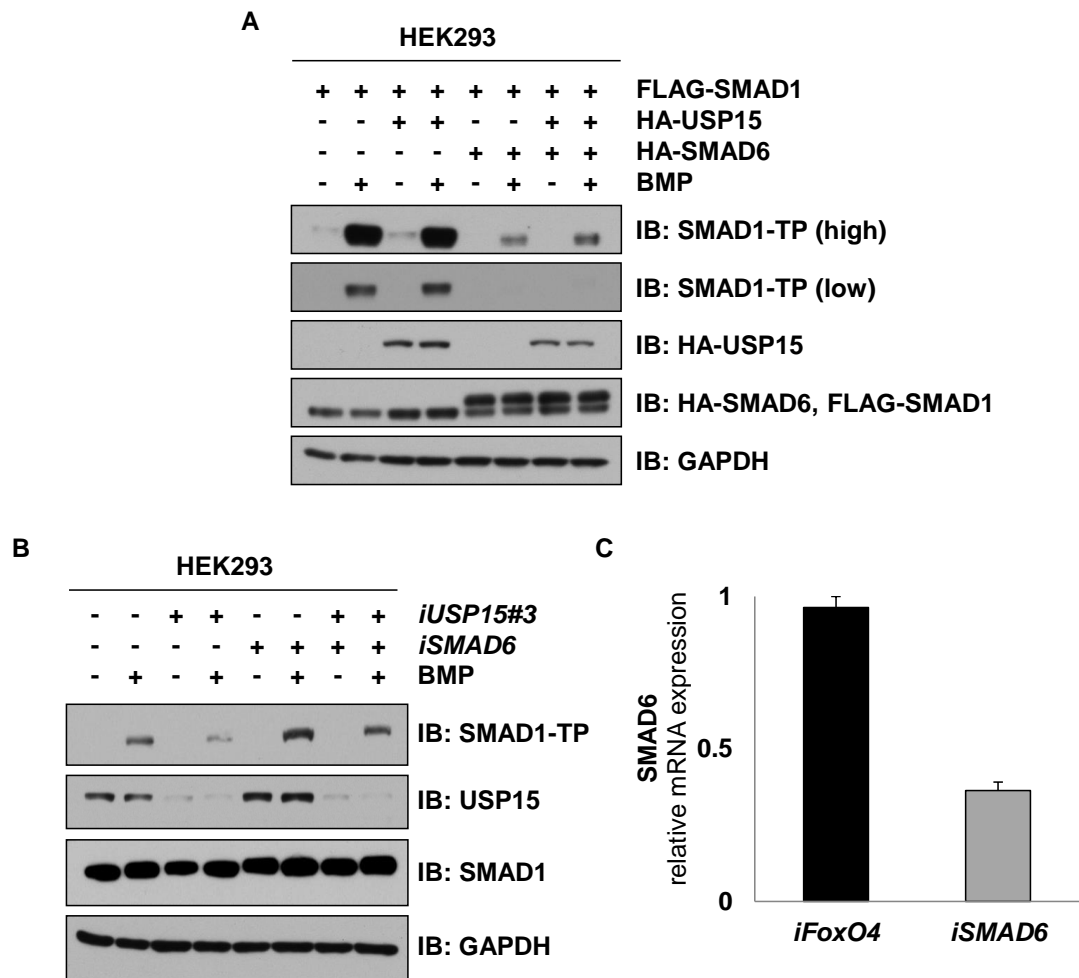
Figure 5-7 Opposing roles for USP15 and SMAD6 in the BMP pathway

A) HEK293 cells were co-transfected with constructs encoding N-terminal HA-tagged USP15, SMAD6 and N-terminal FLAG-tagged SMAD1. Cells were stimulated with 6.25 ng/ml BMP for 1 hour prior to lysis. Extracts were resolved by SDS-PAGE and immunoblotted with the indicated antibodies. **B)** HEK293 cells were transiently transfected with *iUSP15#3, iSMAD6* or *iFoxO4.* 48 hours post transfection cells were stimulated with 6.25 ng/ml BMP for 1 hour prior to lysis. Extracts were resolved by SDS-PAGE and immunoblotted with the indicated antibodies. **C)** The *SMAD6* knockdown from B was confirmed by qRT-PCR. HEK293 cells were transiently transfected with *iFoxO4* or *iSMAD6*. Cells were then washed and lysed 48 hours later. The expression of *SMAD6* transcript was assessed by qRT-PCR. The error bars indicate standard deviation.

5.2.6 USP15 interacts and co-localises with ALK3

Although USP15 was identified as an interactor of SMAD6 (Figure 5-2A) the results above indicate that it is unlikely to target SMAD6 for deubiquitylation (Figure 5-4, Figure 5-6), as stabilisation of SMAD6 would result in inhibition of BMP signalling. The observation that the total levels of SMAD1 are unaffected by either USP15 overexpression or depletion suggests that the target of USP15 in the BMP pathway lies upstream of SMAD1. Immediately upstream of SMAD1 are the type I BMP receptors (ALK2/3/6), which induce SMAD1 phosphorylation (Murakami *et al.*, 2003). ALK3 is targeted for ubiquitylation by E3 ligases, which are recruited to the receptors by SMAD6. Hence, it was hypothesised that SMAD6 could escort USP15 to ALK3 in a similar manner and that USP15 deubiquitylates ALK3, thereby opposing the effect of SMAD6 and its associated E3 ubiquitin ligases.

Firstly, the ability of USP15 to interact with ALKs, including ALK3, was tested in HEK293 cells. GFP-USP15 interacted with FLAG-ALK5/2/3/6, with the strongest interaction observed between USP15 and ALK2 (Figure 5-8A). Secondly, the ability of SMAD6 to influence the interaction between USP15 and ALK3 was investigated. The expression of HA-SMAD6 reduced the interaction between GFP-USP15 and FLAG-ALK3, indicating that SMAD6 might disrupt the USP15-ALK3 complex formation (Figure 5-8B). Additionally, the interaction between GFP-USP15 and HA-SMAD6 was completely abolished in the presence of FLAG-ALK3. This could suggest that the interactions of USP15 with SMAD6 or ALK3 are mutually exclusive (Figure 5-8B).

In order to verify this assumption, U2OS cells were transfected with GFP-USP15, HA-SMAD6 and FLAG-ALK3 and their localisations analysed by immunofluorescence microscopy (Figure 5-9). In the absence of SMAD6 or

ALK3 overexpression, USP15 was observed pan-cellularly (Figure 5-9A). ALK3 was present in the cytosol and at the membrane (Figure 5-9C,E,F,G), whereas SMAD6 expression was predominantly nuclear (Figure 5-9B,D,F,G). In the presence of ALK3, USP15 localised to the plasma membrane (Figure 5-9C,D,E,F,G). USP15 co-localised partially with SMAD6 in the nucleus (Figure 5-9B,D,E,F,G) and predominantly interacted with ALK3 at the membrane and the cytosol (Figure 5-9B,D,E,F,G). The nuclear presence of SMAD6 indicates that SMAD6 is unlikely to direct USP15 to ALK3 at the membrane. It might be possible that the expression of SMAD6 induces modulations on USP15 and/or ALK3 (or induces further proteins) that limit the interaction between ALK3 and USP15.
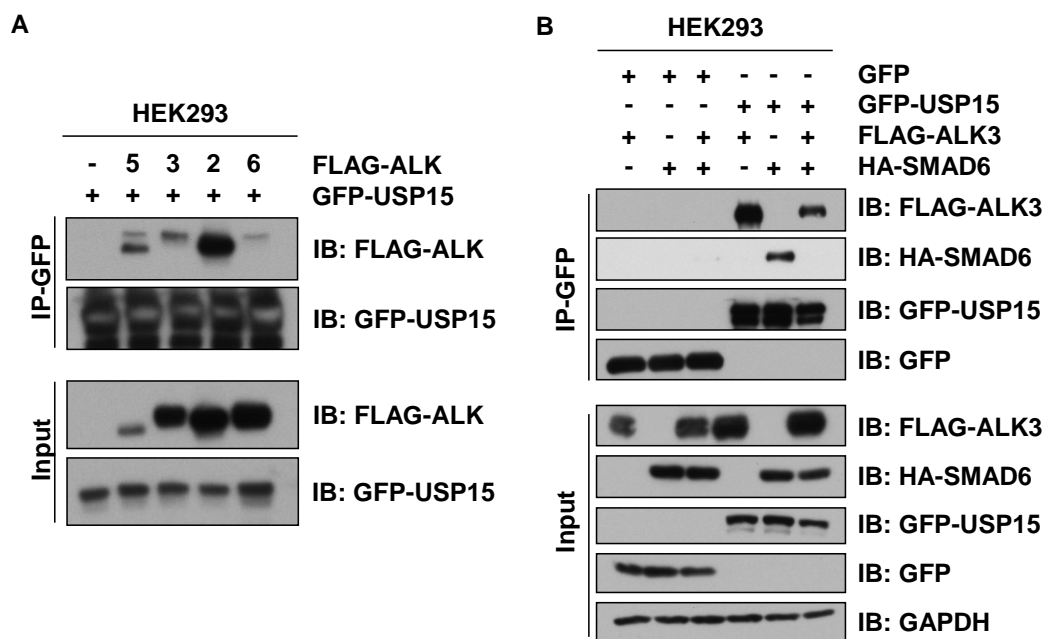
Figure 5-8 USP15 interacts with SMAD6 and ALK3

A) HEK293 cells were co-transfected with N-terminal FLAG-tagged ALK5, ALK3, ALK2, ALK6, control and GFP-USP15. GFP-IPs or extracts were resolved by SDS-PAGE and immunoblotted with the indicated antibodies. **B)** HEK293 cells expressing GFP control or GFP-USP15 were transfected with FLAG-ALK3, HA-SMAD6 or both as indicated. GFP-IPs or extracts were resolved by SDS-PAGE and subjected to immunoblotting with the indicated antibodies.
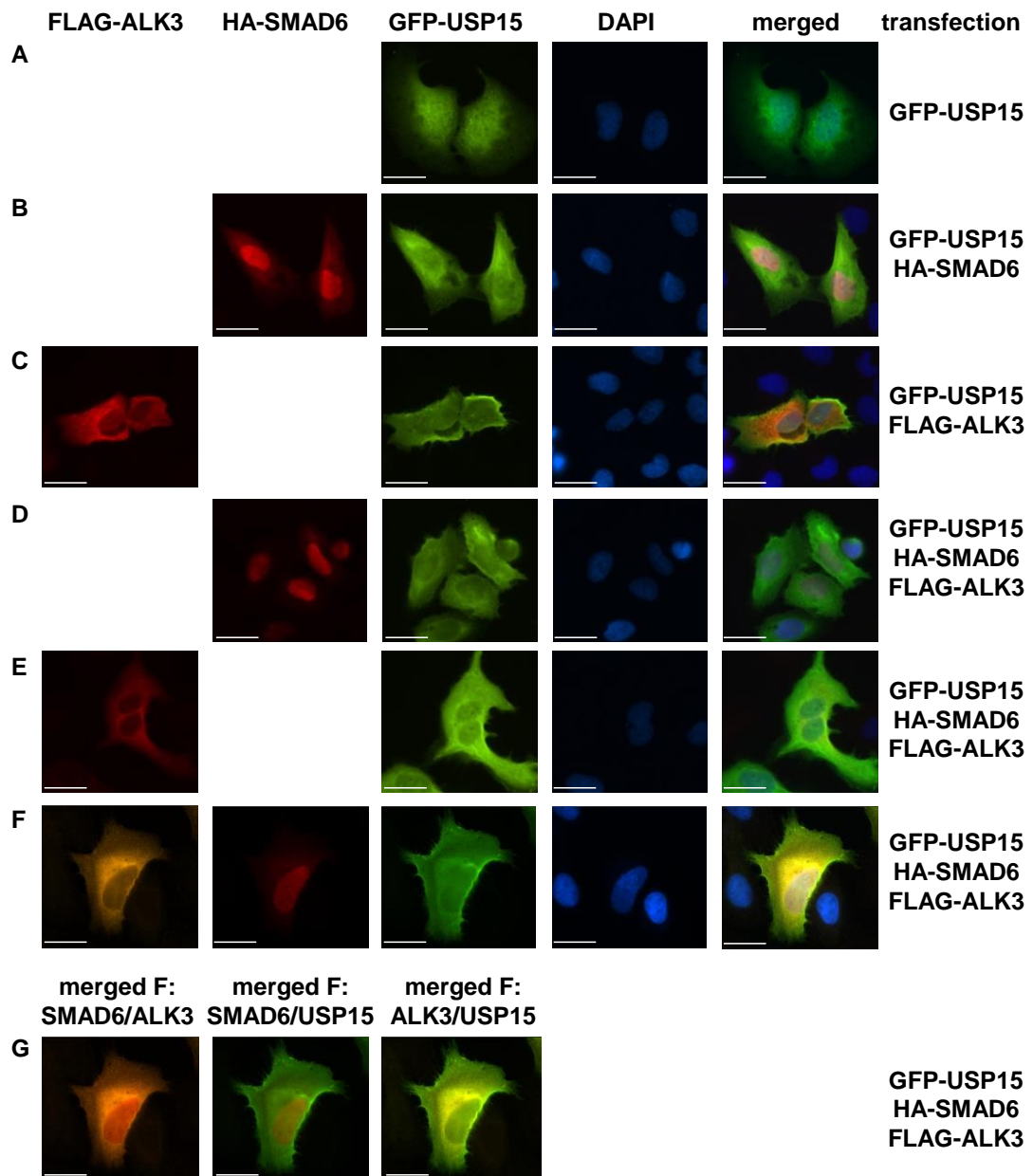
Figure 5-9 USP15 localises to membranes when co-transfected with ALK3

A-G) Fixed cell immunofluorescence was performed on U2OS cells transfected with FLAG-ALK3, HA-SMAD6 and GFP-USP15. Individual and merged pictures are shown. Pictures were taken using a 60x lens, scale bar represents 30 µm.

5.2.7 USP15 deubiquitylates ALK3

The interaction between USP15 and ALK3, their co-localisation and the positive effect of USP15 on BMP signalling suggest that USP15 could act as a DUB for ALK3. USP15 has been shown to cleave K6-, K11-, K27-, K29-, K33-, K48- and K63- but not M1-linked ubiquitin (McGouran *et al.*, 2014, Herhaus *et al.*, 2014). Recombinant GST-USP15 was able to cleave K48-linked polyubiquitin chains (Figure 5-10A). To test whether USP15 was able to deubiquitylate polyubiquitylated ALK3 *in vitro*, FLAG-ALK3 was immunoprecipitated from HEK293 cells treated with Bortezomib (to prevent polyubiquitylated ALK3 form degradation) and used as a substrate (alongside a FLAG control) for GST-USP15 in an *in vitro* DUB assay. USP15 was capable of deubiquitylating ALK3, resulting in the accumulation of monoubiquitin (Figure 5-10B).

To test the ability of USP15 to deubiquitylate ALK3 in cells, HEK293 cells were transfected with either a FLAG-control or FLAG-ALK3 in the presence or absence of HA-USP15 (Figure 5-11A). In the absence of HA-USP15, K48-linked polyubiquitin and total ubiquitin chains were observed in FLAG-ALK3 IPs, whereas no ubiquitylation was observed in FLAG control-IPs. Both K48-linked polyubiquitin and total ubiquitin chains on ALK3 IPs were significantly reduced in the presence of HA-USP15 (Figure 5-11A). Additionally, the level of overall polyubiquitylation in extracts was reduced upon overexpression of HA-USP15, which reflects the ability of USP15 to cleave multiple ubiquitin chain linkages (section 5.1.2, (McGouran *et al.*, 2013)). The observed polyubiquitylation of ALK3 does not depend on its kinase activity, as catalytically inactive ALK3 D380A mutant was also polyubiquitylated to a similar extent as the wild-type ALK3 (Figure 5-11B).

In order to establish whether the catalytic activity of USP15 was required for ALK3 deubiquitylation, FLAG-ALK3 was immunoprecipitated from HEK293 cells expressing control HA, wild type HA-USP15 or catalytically inactive HA-USP15 C269S mutant (Figure 5-12A). In the absence of HA-USP15, FLAG-ALK3 is efficiently polyubiquitylated, especially featuring K48-linked ubiquitin chains (Figure 5-12A). Treatment of cells with BMP did not alter the levels of FLAG-ALK3 polyubiquitylation (Figure 5-12A). Overexpression of wild-type HA-USP15 but not HA-USP15 C269S mutant resulted in the loss of polyubiquitylated ALK3, indicating that USP15 requires its catalytic activity in order to reduce ubiquitylation on ALK3 (Figure 5-12A).

Because the overall ubiquitylation was reduced in cell extracts upon wild type USP15 but not catalytically inactive USP15 overexpression (Figure 5-10D, Figure 5-12A), the role of endogenous USP15 in deubiquitylating ALK3 was established by performing a loss-of function experiment (Figure 5-12B). Depletion of endogenous USP15 led to an increase in total as well as K48-linked ubiquitin chains on FLAG-ALK3 IPs (Figure 5-12B). This increased polyubiquitylation was significantly inhibited when cells were transfected with siRNA-resistant mutant of HA-USP15 (rescue), suggesting that the observed effects were unlikely to be due to off-target effects of *USP15* siRNA (Figure 5-12B).
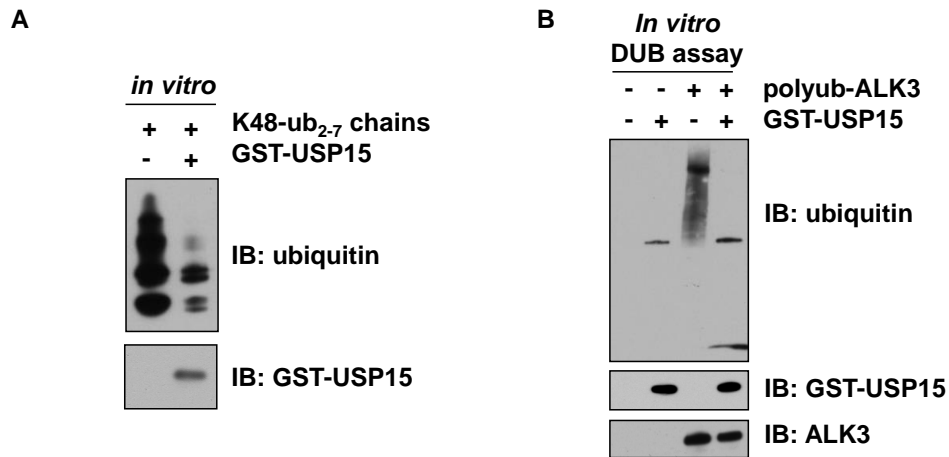
Figure 5-10 USP15 deubiquitylates ALK3 *in vitro*

A) Human recombinant GST-USP15 was incubated with K48-linked 2-7 polyubiquitin chains in a DUB assay buffer for 1 hour at 30 °C. The reaction was stopped by the addition of SDS sample buffer and the assay mix was resolved by SDS-PAGE and immunoblotted with the indicated antibodies. **B)** HEK293 cells transfected with FLAG control or FLAG-ALK3 vectors were treated with Bortezomib (10 µM) for 3 hours prior to lysis. FLAG-IPs from extracts were used as substrates for GST-USP15 in an *in vitro* deubiquitylation assay. The reactions were stopped by adding SDS sample buffer. The samples were resolved by SDS-PAGE and immunoblotted with the indicated antibodies.
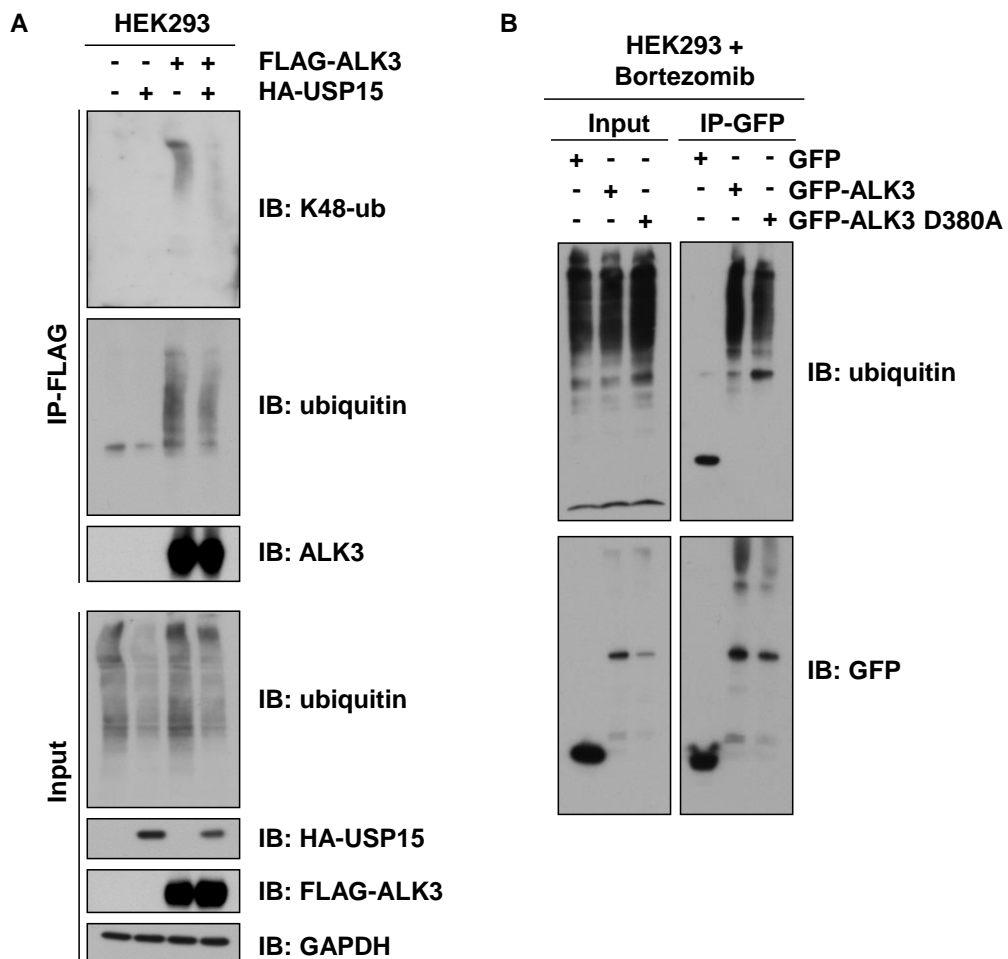
Figure 5-11 USP15 deubiquitylates ALK3 *in vivo*

A) HEK293 cells were transiently transfected with FLAG control or FLAG-ALK3 vectors with or without HA-USP15. Prior to lysis, cells were treated with 10 µM Bortezomib for 3 hours. FLAG-IPs and extract inputs were resolved by SDS-PAGE and immunoblotted with the indicated antibodies. **B)** HEK293 cells were transfected with GFP control, GFP-ALK3 or GFP-ALK3 D380A (kinase dead) vectors. Prior to lysis, cells were treated with 10 µM Bortezomib for 3 hours. GFP-IPs and extracts were resolved by SDS-PAGE and immunoblotted with the indicated antibodies.
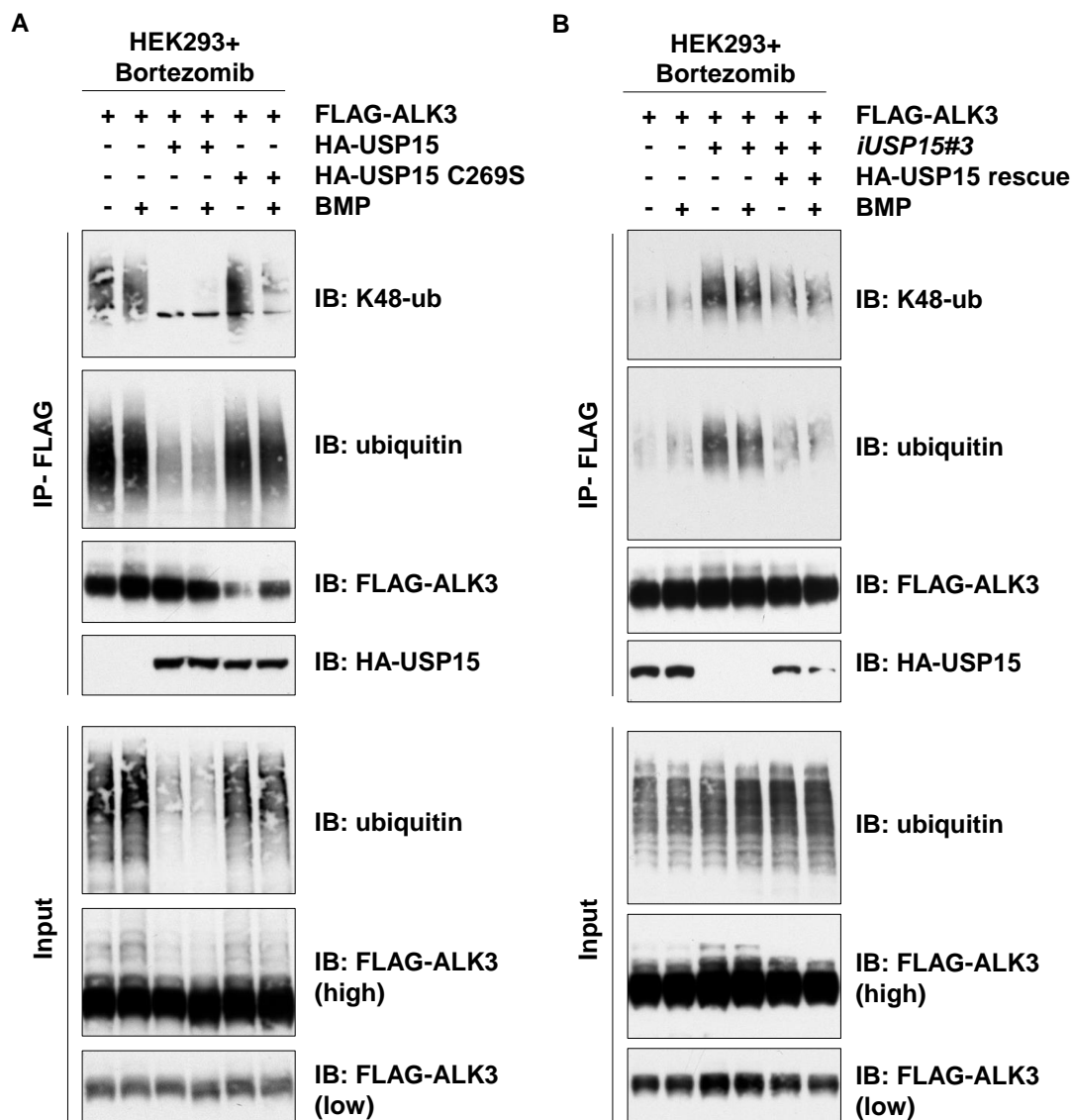
Figure 5-12 USP15 requires catalytic activity to reduce polyubiquitylation on ALK3

A) HEK293 cells transiently expressing FLAG-ALK3, HA-USP15, and USP15 C269S (DUB dead) were pretreated with 10 µM Bortezomib for 3 hours and then stimulated with 6.25 ng/ml BMP for 1 hour prior to lysis. FLAG-IPs and extract inputs were resolved by SDS-PAGE and immunoblotted with the indicated antibodies (performed by M. Al-Salihi). **B)** HEK293 cells transiently expressing *iUSP15#3*, FLAG-ALK3, and *iUSP15#3* resistant silent mutant of HA-USP15 (HA-USP15 rescue), were pretreated with 10 µM Bortezomib for 3 hours and then stimulated with 6.25 ng/ml BMP for 1 hour prior to lysis. FLAG-IPs and extract inputs were resolved by SDS-PAGE and immunoblotted with the indicated antibodies (performed by M. Al-Salihi).

5.2.8 Polyubiquitylated ALK3 undergoes proteasomal degradation

The degradation of polyubiquitylated ALK3 could be mediated via the proteasome or the lysosome (Bonifacino and Weissman, 1998), or possibly both (Zhao *et al.*, 2012). Hence, the turnover of untagged human ALK3 was monitored in the presence of the proteasomal inhibitor Bortezomib and lysosomal fusion inhibitor Bafilomycin A1 in HEK293 cells (Yoshimori *et al.*, 1991). As expected, Bortezomib resulted in the accumulation of polyubiquitin chains in extracts, whereas Bafilomycin A1 caused increased levels of the autophagic marker LC3-II (Allen *et al.*, 2013) (Figure 5-13A). Enhanced levels of ALK3 were detected in cells treated with Bortezomib, but not with control or Bafilomycin A1 treated cells. The treatment of cells with Cycloheximide for 24 hours prevented *de novo* ALK3 synthesis and also resulted in the accumulation of ALK3 only in the presence of Bortezomib (Figure 5-13A). Similar results were obtained when *Xenopus* ALK3-HA was overexpressed in HEK293 cells (Figure 5-13B). The pre-treatment of cells with Bortezomib, but not Bafilomycin A1, resulted in enhanced levels of ALK3 in extracts treated with Cycloheximide and increased ALK3 polyubiquitylation in HA-ALK3 IPs (Figure 5-13B). Human FLAG-ALK3, like untagged and *Xenopus* HA-ALK3, was degraded via the proteasome, as indicated by increased polyubiquitylation of FLAG-ALK3 IPs in the presence of Bortezomib but not Bafilomycin A1 (Figure 5-13C). Together, these results suggest that ALK3 polyubiquitylation leads to its proteasomal degradation.
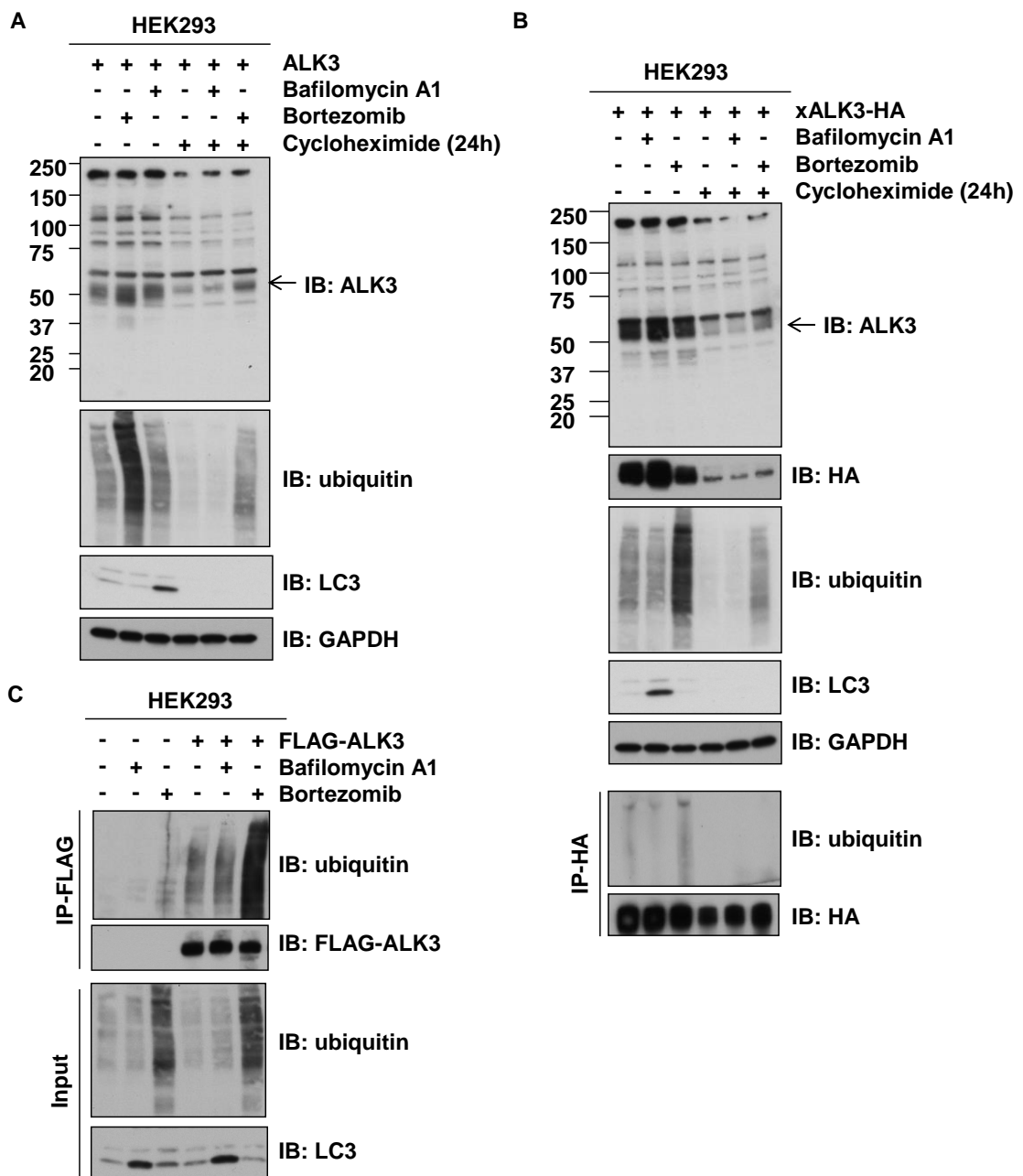
Figure 5-13 Polyubiquitylated ALK3 undergoes proteasomal degradation

A) HEK293 cells transfected with untagged ALK3 were treated with or without 20 µM Cycloheximide for 21 and then with DMSO control, 100 nM Bafilomycin A1 or 10 µM Bortezomib for 3 hours prior to lysis. Extracts were resolved by SDS-PAGE and immunoblotted with the indicated antibodies. **B)** HEK293 cells transfected with *Xenopus* ALK3 (xALK3-HA) were treated with or without 20 µM Cycloheximide for 21 hours and then with DMSO control, 100 nM Bafilomycin A1 or 10 µM Bortezomib for 3 hours prior to lysis. Extracts or HA-IPs were resolved by SDS-PAGE and immunoblotted with the indicated antibodies. **C)** HEK293 cells transfected with or without human FLAG-ALK3 were treated with DMSO control, 100 nM Bafilomycin A1 or 10 µM Bortezomib for 3 hours prior to lysis. Extracts or FLAG-IPs were resolved by SDS-PAGE and immunoblotted with the indicated antibodies.

5.2.9 *USP15 impacts BMP-induced osteoblastic differentiation*

Mesenchymal cells differentiate into chondrocytes, myocytes, adipocytes and osteoblasts (Moses and Serra, 1996). The differentiation into osteoblasts is driven by the commitment of the undifferentiated mesenchymal cells into osteoblast progenitors, which then mature into osteoblasts that exhibit phenotypes of bone-forming cells. These phenotypes include production of extracellular matrix proteins (i.e. type I collagen, osteocalcin), responsiveness to calcitropic hormones and high levels of alkaline phosphatase (AP) activity (Katagiri *et al.*, 1994). BMP_2 has been shown to induce alkaline phosphatase activity, inhibit myotube formation of myoblastic C2C12 cells and convert their differentiation pathway into the osteoblast lineage (Katagiri *et al.*, 1994).

To investigate whether USP15 has a physiological function in BMP signalling, the impact of its depletion on differentiation of the mouse myoblast progenitor C2C12 cells into osteoblasts by BMP was tested. RNAi-mediated depletion of *USP15* in C2C12 cells resulted in reduced BMP-induced SMAD1 phosphorylation levels (Figure 5-14A), and a significantly reduced BMP-induced alkaline phosphatase activity at both 48 hours and 96 hours post BMP-stimulation (Figure 5-14B). USP15 is conserved in mice (Angelats *et al.*, 2003) and the knockdown of USP15 was confirmed by immunoblotting (Figure 5-14B).
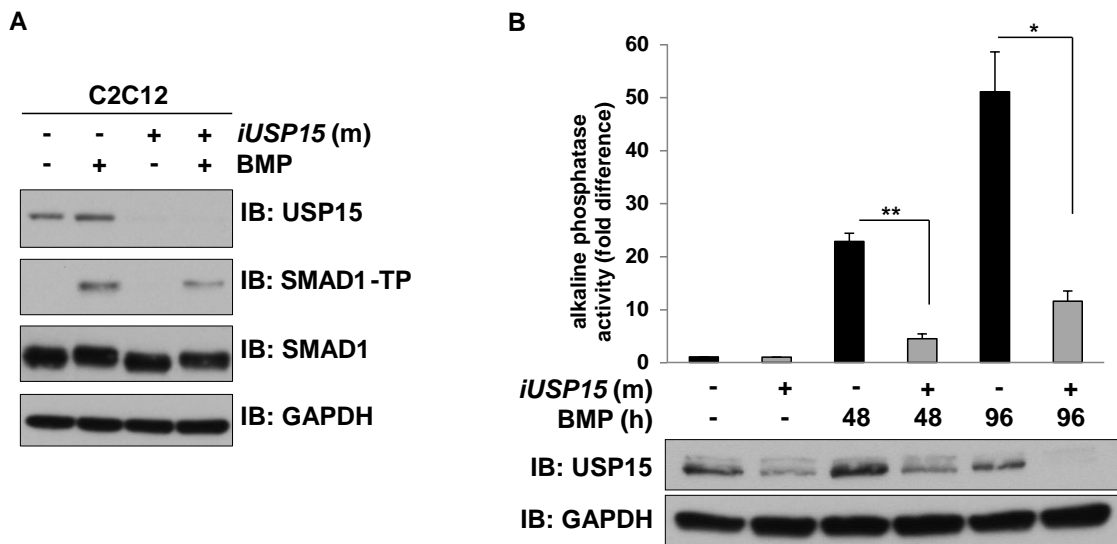
Figure 5-14 USP15 impacts mouse osteoblastic differentiation

A) The mouse myoblast cell line C2C12 was transfected with siRNAs targeting mouse (m) *FoxO4* or *USP15*. Cells were treated with or without BMP for 1 hour prior to lysis. Extracts were resolved by SDS-PAGE and immunoblotted with the indicated antibodies. **B)** C2C12 cells transfected with mouse (m) *iFoxO4* or *iUSP15* were grown for up to 96 hours in the presence of 100 ng/ml BMP_2. Cells were lysed and the alkaline phosphatase activity measured using a fluorescence plate reader. Data are represented as mean and error bars indicate standard deviation (n=3). Differences with $p<0.05$ were annotated as *. Representative extracts were resolved by SDS-PAGE and immunoblotted with the indicated antibodies.

5.2.10 USP15 modulates BMP signalling in Xenopus embryogenesis

Xenopus laevis is an established experimental model system to study vertebrate embryogenesis. During gastrulation (stages 5.25-10) the ventral centre expresses BMP and BMP related cytokines, whereas in the dorsal side (Spemann organiser) BMP antagonists are produced, resulting in a gradient of BMP signalling along the dorsal-ventral axis (Eivers *et al.*, 2008, De Robertis and Kuroda, 2004). BMP-mediated phosphorylation of SMAD1 in *Xenopus* embryos is detected after stage 9 (based on staging by Niewkoop and Faber, 1975) of development and is sustained thereafter (Figure 5-15A) (Sapkota *et al.*, 2007). *USP15* depletion in *Xenopus* embryos by morpholinos (xUSP15-*MO*)

decreased SMAD1 tail-phosphorylation (Figure 5-15A). To investigate whether USP15 influences BMP-mediated *Xenopus* development, the effect of USP15 depletion was measured by the mRNA expression of *xVENT1*, a marker of BMP signalling in *Xenopus* embryos (Figure 5-15B). Antisense morpholino oligonucleotides targeting *Xenopus USP15* (xUSP15-*MO*) or control (control-*MO*) were injected into one-cell-stage embryos and animal caps were cut at stage 8.5. The animal caps were collected at stage 10 and mRNA isolated for subsequent qRT-PCR analysis. Depletion of *USP15* resulted in a reduction of the BMP-induced *xVENT1* mRNA levels, indicating that USP15 controls BMP signalling during *Xenopus* embryogenesis (Figure 5-15B).
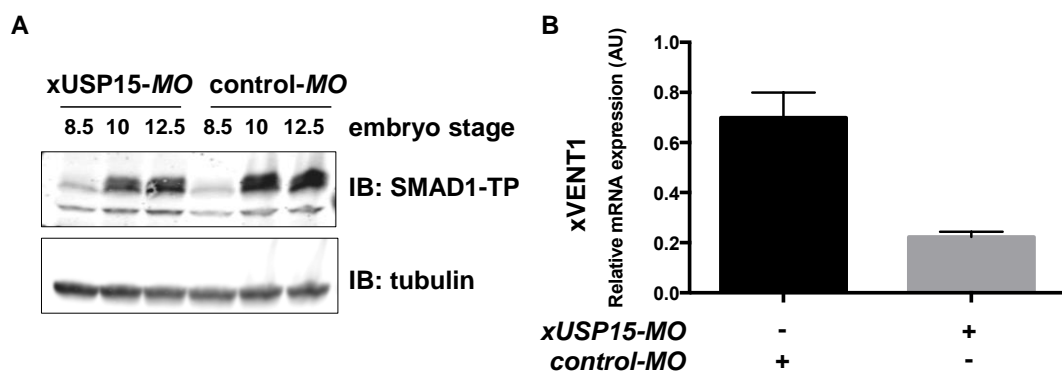
Figure 5-15 USP15 modulates BMP signalling in *Xenopus* embryogenesis

A) *Xenopus* embryos were injected with 80 ng of either xUSP15- (xUSP15-*MO*) or control- (control-*MO*) morpholinos at the 1-cell stage and then collected at the indicated stages. Lysates were resolved by SDS-PAGE and immunoblotted with the indicated antibodies (performed by K. Dingwell). **B)** qRT-PCR analysis of *xVENT1* mRNA expression. Embryos were injected with 80 ng of either USP15-*MO* or control-*MO* at the 1-cell stage and animal caps were cut at stage 8.5. The animal caps were collected at the equivalent embryo stage of 10 and processed for qRT-PCR. Data are represented as mean and error bars indicate standard deviation (n=3) (performed by K. Dingwell).

5.3 <u>Discussion</u>

Several DUBs targeting the TGFβ type I receptors have been reported (Zhang *et al.*, 2012b, Eichhorn *et al.*, 2012, Al-Salihi *et al.*, 2012a), however the DUBs acting on BMP type I receptors remained undefined. This study describes the discovery of USP15 as a DUB for ALK3. In the course of a proteomic approach to identify novel regulators of the BMP pathway, USP15 was identified as an interactor of SMAD6. Here, it is shown that USP15 binds to and deubiquitylates ALK3, thereby enhancing BMP signalling. Consequently, USP15 impacts BMP-induced SMAD1 phosphorylation, mouse osteoblastic differentiation and *Xenopus* embryogenesis.

5.3.1 *USP15 impacts BMP signalling in multiple species*

Depletion of USP15 from human, mouse and *Xenopus* cells confirms that USP15 plays a critical role in BMP signalling. In multiple human cell lines (HEK293, HeLa and U2OS), mouse C2C12 cells and *Xenopus* embryos, RNAi-mediated depletion of *USP15* resulted in the inhibition of BMP-induced tail-phosphorylation of SMAD1. Although USP15 had been reported to bind to and deubiquitylate monoubiquitylated R-SMADs (Inui *et al.*, 2011), perturbation of USP15 expression did not alter the total SMAD1 levels in all of the above species. Furthermore, no interaction was detected between endogenous USP15 and overexpressed R-SMADs, suggesting other targets for USP15 in the BMP pathway. The significance of USP15-mediated BMP signalling regulation was confirmed in a genome wide loss-of-function screen in zebrafish, where USP15 was identified as a critical player in dorsal-ventral patterning (Tse *et al.*, 2013). In accordance with this finding, USP15 also affects the expression of the ventral marker *xVENT1* in *Xenopus laevis* embryos. Vent1 is a homeobox

transcriptional repressor expressed during gastrulation in the ventral region of the animal cap and acts downstream of BMP_4 in the ventral signalling pathway. It antagonises the dorsal signalling centre and results in ventral mesoderm formation (Onichtchouk *et al.*, 1998, Gawantka *et al.*, 1995).

5.3.2 USP15 targets ALK3 for deubiquitylation and degradation via the proteasome

USP15 interacts with and deubiquitylates the type I BMP receptor ALK3. Ubiquitylated proteins can be degraded through the proteasomal, the lysosomal or the autophagic pathway (Komander and Rape, 2012). The ubiquitylation of the receptor kinase EGFR causes endocytosis-mediated degradation via the lysosome (Ganley *et al.*, 2011). Additionally, the type I TGFβ receptor has been reported to associate with the transmembrane prostate androgen-induced protein (TMEPAI), which is localised to the lysosome and late endosome. TMEPAI also binds NEDD4 and together they promote the degradation of TβR-I through lysosomes (Bai *et al.*, 2014). Lysosomal degradation can be blocked experimentally with Bafilomycin A1, which inhibits lysosomal acidification via the vacuolar-type H^+-ATPase (Yoshimori *et al.*, 1991). Polyubiquitylation of ALK3 results in its degradation, which is not inhibited by Bafilomycin A1. This indicates that the lysosomal-autophagic pathway does not mediate ALK3 turnover. In contrast, by blocking the proteasome with Bortezomib, ALK3 is stabilised. This is consistent with the presence of K48-linked polyubiquitin chains on ALK3, which promote proteasomal degradation (Pickart, 1997). By cleaving K48-linked ubiquitin chains on ALK3, USP15 rescues the type I BMP receptor from ubiquitin-mediated proteasomal degradation. It is possible that other ubiquitin-chain types are present on ALK3 in addition to K48-chains and

as USP15 can cleave several different chain linkages (McGouran *et al.*, 2013), it would be predicted that USP15 can remove other ubiquitin-chain linkages on ALK3 in addition to K48-linked ubiquitin chains. It would be interesting to determine which residues of ALK3 are polyubiquitylated, if other chain linkages are present on ALK3 and if so, which cellular function these chain types confer on ALK3.

BMP stimulation or ALK3 kinase activity did not affect the polyubiquitylation of ALK3. The accumulation of SMAD6 and its associated E3 ubiquitin ligases on ALK3 is possibly a late event during BMP signalling, as it serves as a feedback function. Hence, it would be interesting to investigate whether endogenous ALK3 polyubiquitylation increases at later stages of BMP treatment.

5.3.3 The role of SMAD6 in USP15 mediated deubiquitylation of ALK3

It is well established that I-SMADs direct E3 ubiquitin ligases to type I and II TGFβ and BMP receptors to catalyse their polyubiquitylation and subsequent degradation (Ebisawa *et al.*, 2001, Kavsak *et al.*, 2000, Murakami *et al.*, 2003, Fukasawa *et al.*, 2010, Komuro *et al.*, 2004, Kuratomi *et al.*, 2005, Seo *et al.*, 2004, Lin *et al.*, 2000). However, interaction and co-localisation data suggest that SMAD6 does not direct USP15 to ALK3. SMAD6 is predominantly found in the nucleus, whereas ALK3 and USP15 are cytosolic and present at the membrane. SMAD6 overexpression slightly inhibits the association of USP15 with ALK3, and ALK3 overexpression totally disrupts binding of USP15 to SMAD6. This suggests that USP15-SMAD6 and USP15-ALK3 interactions are mutually exclusive. Nevertheless, USP15 counters the inhibitory effect of SMAD6 on BMP signalling. Hence, in addition to deubiquitylating the receptors,

USP15 may restrict SMAD6-E3 ligase complexes from reaching the receptors. The role of USP15 in the BMP signalling pathway is most likely to strike a balance between BMP receptor degradation and stabilisation. Thus, it would also be interesting to study the effect of USP15 on the interaction between ALK3 and SMAD6. SMAD6 can inhibit ALK3 and ALK6, but not ALK2, receptor function through physical interaction, possibly because ALK3 and ALK6 are structurally related (Goto *et al.*, 2007). USP15 interacts equally strong with ALK3, ALK5 and ALK6 but the strongest binding of USP15 with type I receptors was observed between USP15 and ALK2. ALK3 is widely expressed (as is USP15), however ALK6 expression is restricted to certain cell types and tissues. Furthermore, ALK3 and ALK6 mostly signal through BMP_2, whereas ALK2 mostly signals through BMP_6 and BMP_9 (Ebisawa *et al.*, 1999, Brown *et al.*, 2005, Scharpfenecker *et al.*, 2007). Thus, it would be interesting to test whether USP15 also protects ALK2 from proteasomal degradation and if BMP_6 or BMP_9-induced target gene transcription is influenced by USP15 perturbation.

In conclusion, the differential binding affinities, subcellular and tissue specific distributions of ALKs, SMAD6 and USP15 possibly add an additional layer to the feedback induced regulation of BMP signalling by SMAD6 and USP15.

5.3.4 Substrate specificity of USP4, USP11 and USP15

The closely related DUBs USP4, USP11 and USP15 have been reported to modulate TGFβ signalling by deubiquitylating ALK5 through distinct modes of action (Al-Salihi *et al.*, 2012a, Eichhorn *et al.*, 2012, Zhang *et al.*, 2012b) (*cf.* section 1.3.2.2). USP15 interacts with ALKs that signal through BMP, as well as

with TGFβ receptor ALK5, which has been described previously (Eichhorn *et al.*, 2012).

USP4, USP11 and USP15 are closely related DUBs (Elliott *et al.*, 2011) and thus are likely to have similar cellular targets, however the role in BMP signalling is unique to USP15. Depletion of USP15 caused a reduction in BMP-induced transcription, but depletion of USP11 or USP4 (Zhang *et al.*, 2012b) did not affect BMP-mediated gene expression. Pathway specificity is possibly conferred by their relative binding affinities to type I TGFβ/BMP receptors and/or I-SMADs, among other regulatory factors.

The DUSP-UBL domains in USP4, 11 and 15 could be key features to determine substrate specificity as they adopt different configurations that could regulate substrate binding (Elliott *et al.*, 2011). The electrostatic characteristics of the DUSP-UBL region of USP4/11/15 are very similar, however the linker region is distinct in these three DUBs. The linker region connects the DUSP and UBL domains and determines their arrangement (Figure 5-1). In USP4 the UBL domain is independent of the DUSP domain and the linker region stabilises dimerisation of USP4, which locks the two DUSP domains into one unit. USP11 is only present as a monomer due to a shortened linker region and the DUSP and UBL domains can move independently from each other. In USP15, the DUSP and UBL domains form a single unit in a fixed orientation, which is defined by the linker region (Figure 5-1B). These differences in the DUSP-UBL domain arrangements of USP4, 11 and 15 can modify surface properties and are the likely features to provide selective binding properties (Elliott *et al.*, 2011). It would be interesting to map the USP15-ALK3 or USP15-SMAD6 interaction domains and test if the binding of USP15 to ALK3 or SMAD6 is mediated by the USP15 DUSP and UBL domains. If so, it would be interesting

to investigate whether swapping the DUSP-UBL domains from USP4, 11 and 15 alters their substrate specificity towards different ALKs and I-SMADs.

The activity and substrate specificity of USP4, 11 and 15 might further be influenced by PTMs within the DUBs or their targets. Phosphorylation of USP4 by AKT induces membrane localisation, binding to ALK5 and even influences stability and catalytic activity of USP4 (Zhang *et al.*, 2012b). The AKT phosphorylation site in USP4 (S445) is not conserved in USP11 or USP15 and whether USP11 and USP15 are further regulated by PTMs has not been investigated so far. Phosphorylation on S445 of USP4 is also required for homomeric and heteromeric complex formation with USP11, USP15 and USP19 (Zhang *et al.*, 2012b). This suggests that these DUBs could act as a complex and potentially individually compensate for the loss of the other. In addition to PTMs, differential expression patterns of USP4, 11 and 15 in cells and tissues could also contribute to the context-dependent regulation of TGFβ/BMP signalling. The generation of single, double and triple USP4, USP11 and USP15 knockout (or catalytically inactive knockin) mice might give molecular insights into their pathway-selectivity and redundancy. It has already been suggested that USP15 knockout T cells exhibit normal TGFβ signalling (Zou *et al.*, 2014), indicating possible redundancy in the TGFβ pathway.

5.3.5 USP15 as a potential drug target

USP15 is implicated in the regulation of various cellular signalling pathways (section 5.1.2) and altered in different cancers. Amplification of USP15 was observed in glioblastoma, breast and ovarian cancers (Eichhorn *et al.*, 2012), whereas in pancreatic cancers lower USP15 copy numbers were detected and USP15 deletion events were probably enriched by selective

pressures (Srihari and Ragan, 2013). USP15 has already been suggested as a potential drug target for the treatment of glioblastoma, a pathology associated with TGFβ signalling (Eichhorn *et al.*, 2012). Apart from its critical role in TGFβ signalling, the catalytic activity of USP15 is also essential for BMP signalling. Loss of USP15 inhibits BMP signalling in human and mouse cells, as well as during *Xenopus* embryogenesis. Mutations leading to overactive BMP signalling are associated with diseases such as Duchenne muscular dystrophy, heterotopic ossification and bone metastasis (Shi *et al.*, 2013). Duchenne muscular dystrophy is a pathology that results in muscle degeneration due to constitutive muscle fiber damage, chronic inflammation and fibrosis (Mann *et al.*, 2011). Heterotopic ossification is characterised by the formation of cartilage and bone at aberrant locations outside the skeleton and is caused by inflammation associated with traumatic injury. Furthermore, endothelial-mesenchymal transition and mesoderm cell differentiation into chondrocytes and osteocytes contribute to heterotopic ossification (Ramirez *et al.*, 2014). Bone metastasis is the most common secondary tumour site in prostate cancer progression (Ye *et al.*, 2007). Prostate cancer metastasis to bone is associated with increased osteoblast activity, which is characterised by high levels of alkaline phosphatase (AP). In normal bone tissue or bone metastasis originating from other organs, only few osteoblasts are present. Therefore, AP activity, a marker of osteoblast differentiation, was found to be significantly increased in prostate cancer patients that exhibited bone metastases compared to patients without metastasis. Patients with increased AP also showed significantly lower survival rates than patients with low AP concentrations (Jung *et al.*, 2004). Moreover, it has been suggested that increased AP activity is linked to bone resorption in women with severe osteoporosis (Hulth *et al.*, 1979). Depletion of

USP15 inhibited BMP-induced alkaline phosphatase activity and decreased BMP-mediated downstream signalling. Therefore, the inhibition of USP15 could be employed as a therapeutic strategy to inhibit BMP signalling in pathologies caused by elevated BMP pathway activity.

However, USP15 inhibition could have adverse effects on muscle regeneration after damage (Ono *et al.*, 2011, Clever *et al.*, 2010). Thus, the administration of USP15 inhibitors has to be cautioned and would only be beneficial in certain context-dependent physiological settings, which might differ in patients. Moreover, USP15 has multiple other targets (*cf.* section 5.1.2) and USP15 inhibitors could be non-selective and affect many cellular processes beyond those controlled by the BMP pathway. Therefore, it would be essential to map the USP15-ALK3 interaction, in order to design small molecule inhibitors that could act BMP signalling specific.

6 O-GlcNAc modification in the TGFβ/BMP pathway

6.1 Introduction

O-GlcNAcylation is a post-translational modification on Serine/Threonine residues of target proteins that is catalysed by O-GlcNAc transferase (OGT) (section 1.1.3). A proteomic approach identified OGT as an interactor of GFP-SMAD2. To date, SMADs have not been associated with O-GlcNAc modifications. Interestingly, a closer inspection of their conserved tail-phosphorylation "SXS" motif revealed that the first Serine potentially conforms to a putative O-GlcNAcylation motif (Figure 6-1). Extensive crosstalk between O-GlcNAcylation and phosphorylation has been reported in various signalling pathways (Hart *et al.*, 2011). The occupancy of O-GlcNAc on one of the TGFβ/BMP-mediated phosphorylation sites on R-SMADs could potentially cause delayed or alternative downstream signalling. Therefore, the aim of this chapter was to establish whether SMADs bind to O-GlcNAcylated proteins or are modified by OGT through O-GlcNAcylation and if so, whether this influenced TGFβ/BMP signalling.
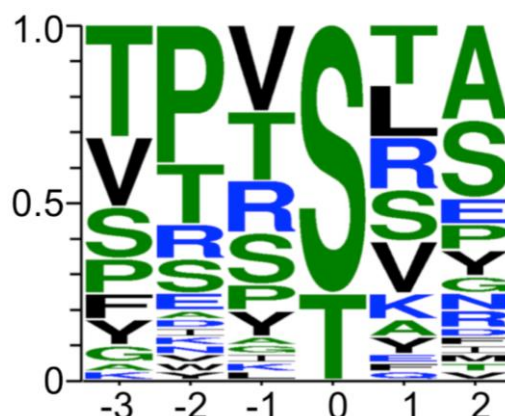
Figure 6-1 Putative optimal motif for O-GlcNAc modification by OGT

Schematic representation of the amino acid sequence that is preferentially targeted by OGT to catalyse O-GlcNAc modification on position 0 of substrates. Unpublished information provided by S. Pathak and D. van Aalten.

6.1.1 The effect of high glucose on TGFβ signalling

The limiting factor in the synthesis of O-GlcNAc is the availability of glucose, which is processed through the metabolically controlled hexosamine biosynthetic pathway (HBP) (Figure 1-3). High glucose concentrations have been reported to cause an increase in $TGF\beta_1$ ligand expression, through the HBP pathway (Kolm-Litty *et al.*, 1998). In the HBP pathway, GFAT (glutamine:fructose-6-phosphate amidotransferase) catalyses the conversion of glucose into glucosamine (Figure 1-3), which enhances $TGF\beta_1$ protein production, promotes conversion of latent $TGF\beta_1$ to the active form and subsequently increases the production of extracellular matrix proteins (Weigert *et al.*, 2004, Cheng *et al.*, 2013, Ye *et al.*, 2013, Kolm-Litty *et al.*, 1998). The increase in $TGF\beta_1$ protein levels in high glucose conditions also coincides with increases in expression of TβR-II, SMAD2/3 and activation of TGFβ signalling as well as the AKT/mTOR pathway (Aguilar *et al.*, 2014, Hong *et al.*, 2001, Singh *et al.*, 2008, Wu and Derynck, 2009). High concentrations of glucose result in increased cell size and protein synthesis, which are dependent on TGFβ receptor activity (Wu and Derynck, 2009).

6.1.2 O-GlcNAcylation and the TGFβ/BMP pathways

Increased glucose availability correlates with increased O-GlcNAc modification (Aguilar *et al.*, 2014). Although O-GlcNAc modification of the TGFβ/BMP pathway components would be predicted to impact signalling in response to glucose, not much is known about this. TGFβ promotes site-specific O-GlcNAcylation of oncofetal fibronectin, which is an ECM component expressed by cancer cells and embryonic tissues (Freire-de-Lima *et al.*, 2011). BMP_{15}, an oocyte-secreted factor critical for the regulation of ovarian

physiology, is O-GlcNAcylated on T10, however the physiological significance of O-GlcNAcylation on BMP_{15} is still unknown (Saito *et al.*, 2008).

In this chapter, it was investigated whether SMADs interact with OGT and are modified by O-GlcNAcylation or bind to O-GlcNAcylated proteins.

6.2 <u>Results</u>

6.2.1 R-SMADs interact with endogenous OGT and co-precipitate O-GlcNAc modification

In order to test whether OGT interacts with R-SMADs at the endogenous level, SMAD1, SMAD2 and SMAD3 IPs from HeLa extracts were subjected to immunoblotting with anti-OGT antibody. OGT was detected in SMAD1, SMAD2 and SMAD3 IPs. As expected, stimulation of cells with BMP and TGFβ caused enhanced phosphorylation of SMAD1 and SMAD2/3 respectively, however this did not affect the interaction between OGT and SMAD1, SMAD2 or SMAD3 (Figure 6-2, Figure 6-3, Figure 6-4). Treatment of HeLa cells with small molecule inhibitors of OGT (4Ac-5S-glcNAc, iT) resulted in a decrease in O-GlcNAc modification from cell extracts. In order to completely remove O-GlcNAc from IPs treated with iT, the IPs were additionally incubated with bacterially expressed O-GlcNAcase (cpOGA, iT*). The O-GlcNAcase (OGA) inhibitor (GlcNAcstatin G, iA) resulted in significant accumulation of O-GlcNAc modified proteins in cell extracts (Pathak *et al.*, 2012). Neither inhibitor altered the interaction between R-SMADs and OGT (Figure 6-2, Figure 6-3, Figure 6-4).

To investigate whether R-SMADs were O-GlcNAcylated or pulled-down O-GlcNAc modified proteins from cell extracts, endogenous R-SMAD IPs were subjected to immunoblotting with an antibody that recognises O-GlcNAc modification. O-GlcNAcylation was detected in IPs from endogenous SMAD1 (Figure 6-2), SMAD2 (Figure 6-3), as well as SMAD3 (Figure 6-4) independent of BMP or TGFβ stimulation. Treatment of HeLa cells with the small molecule inhibitor of OGT resulted in complete loss of O-GlcNAc modification from all R-SMAD IPs (Figure 6-2, Figure 6-3, Figure 6-4). No O-GlcNAc was detected in anti-IgG IPs employed as control (Figure 6-2, Figure 6-3, Figure 6-4).
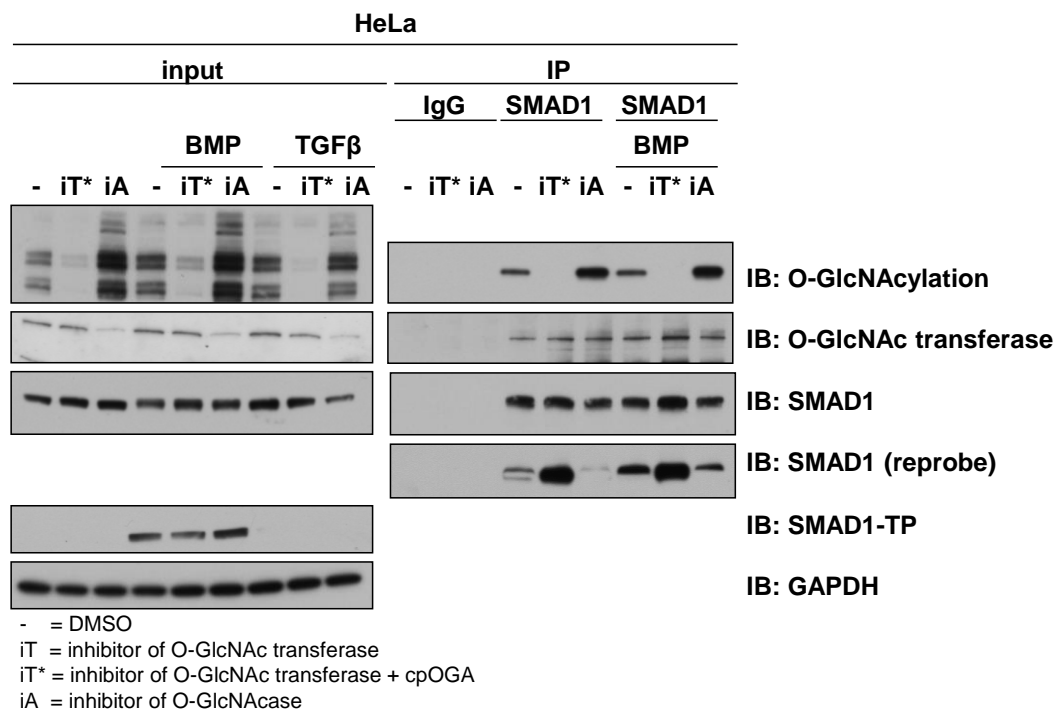
Figure 6-2 O-GlcNAc modification around 50 kDa is detected in SMAD1 IPs

An endogenous IP with anti-SMAD1 antibody or pre-immune sheep IgG was performed in HeLa cell extracts, stimulated with or without 25 ng/ml BMP$_2$ for 1 hour in the presence or absence of O-GlcNAc transferase inhibitor (4Ac-5S-glcNAc, iT, 10 µM) or O-GlcNAcase inhibitor (GlcNAcstatin G, iA, 2 µM) which were added 16 hours prior to ligand stimulation. Indicated cell extracts and IPs were additionally treated with cpOGA (iT*) to remove residual O-GlcNAcylation. Cell extracts (input), endogenous IgG or anti-SMAD1 IPs were resolved by SDS-PAGE and immunoblotted with the indicated antibodies. Reprobe= the membrane was stripped of the first primary antibody (O-GlcNAcylation) and the same membrane was probed with a second primary antibody (SMAD1).
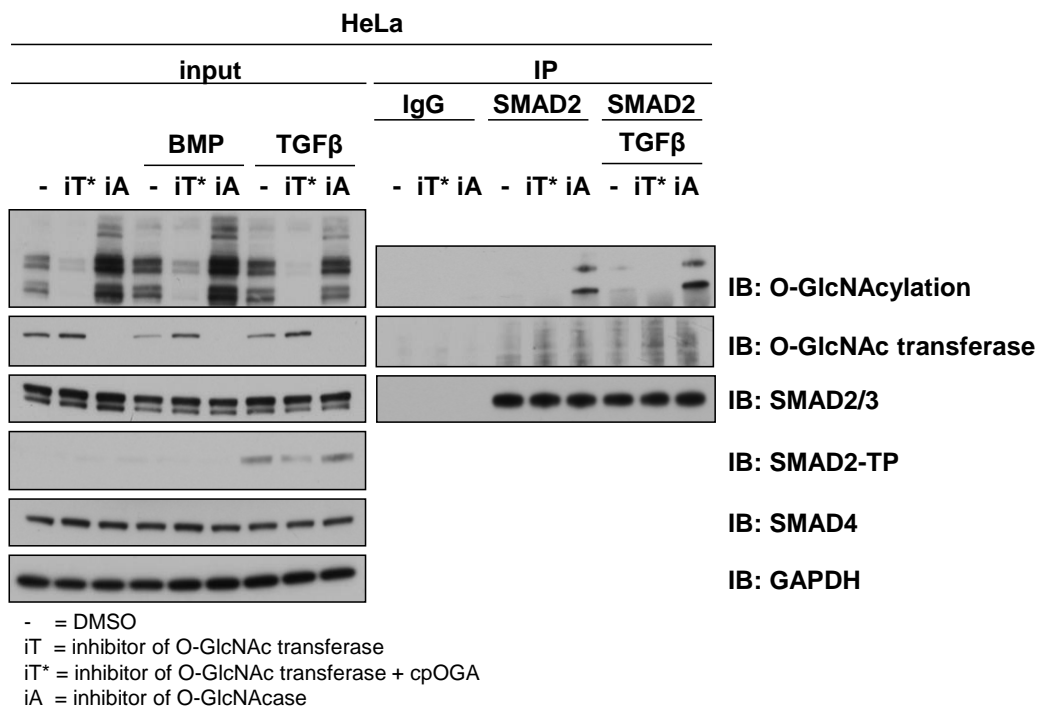
Figure 6-3 O-GlcNAc modifications around 50 kDa and 55 kDa are detected in SMAD2 IPs

An endogenous IP with anti-SMAD2 antibody or pre-immune sheep IgG was performed in HeLa cell extracts, stimulated with or without 50 pM TGFβ for 1 hour in the presence or absence of O-GlcNAc transferase inhibitor (4Ac-5S-glcNAc, iT, 10 µM) or O-GlcNAcase inhibitor (GlcNAcstatin G, iA, 2 µM) which were added 16 hours prior to ligand stimulation. Indicated cell extracts and IPs were additionally treated with cpOGA (iT*) to remove residual O-GlcNAcylation. Cell extracts (input), endogenous IgG or anti-SMAD2 IPs were resolved by SDS-PAGE and immunoblotted with the indicated antibodies.

HeLa

| input | IP |

| | IgG | SMAD3 | SMAD3 |
| | | | TGFβ |

| | TGFβ | | |
| - iT iT* iA | - iT iT* iA | - iT* iA | - iT* iA | - iT* iA |

IB: O-GlcNAcylation
IB: O-GlcNAc transferase
IB: SMAD2-TP
IB: SMAD2/3
IB: SMAD2/3 (long)
IB: GAPDH

- = DMSO
iT = inhibitor of O-GlcNAc transferase
iT* = inhibitor of O-GlcNAc transferase + cpOGA
iA = inhibitor of O-GlcNAcase

Figure 6-4 O-GlcNAc modifications around 50 kDa and 55 kDa are detected in SMAD3 IPs

An endogenous IP with anti-SMAD3 antibody or pre-immune sheep IgG was performed in HeLa cell extracts, stimulated with or without 50 pM TGFβ for 1 hour in the presence or absence of O-GlcNAc transferase inhibitor (4Ac-5S-glcNAc, iT, 10 µM) or O-GlcNAcase inhibitor (GlcNAcstatin G, iA, 2 µM) which were added 16 hours prior to ligand stimulation. Indicated cell extracts and IPs were additionally treated with cpOGA (iT*) to remove residual O-GlcNAcylation. Cell extracts (input), endogenous IgG or anti-SMAD3 IPs were resolved by SDS-PAGE and immunoblotted with the indicated antibodies.

6.2.2 R-SMADs bind to unidentified O-GlcNAcylated proteins

A single band of O-GlcNAc modification was observed in SMAD1 IPs proximal to the 50 kDa marker, where SMAD1 itself migrates (Figure 6-2). A reprobe immunoblot with SMAD1 antibody on the same membrane (reprobe, Figure 6-2), indicated a superimposition of SMAD1 and the O-GlcNAc signal, suggesting that SMAD1 itself might be O-GlcNAcylated or binds to an O-GlcNAcylated protein of ~50 kDa. Two distinct O-GlcNAcylation bands at ~50 kDa and ~55 kDa were observed in SMAD2 and SMAD3 IPs (Figure 6-3, Figure

6-4). Because SMAD2 (~55 kDa) and SMAD3 (~50 kDa) exhibit similar patterns of O-GlcNAc modifications at their respective molecular weights, it could be that SMADs2/3 are O-GlcNAc modified and each protein also pulls down the other (Nakao *et al.*, 1997), or that SMADs2/3 pull down other O-GlcNAc modified proteins. To investigate these possibilities, the R-SMAD IPs were run and analysed on the same gel (Figure 6-5A). The O-GlcNAc double band observed in SMAD3 IPs exhibited a similar electrophoretic migration pattern as the bands observed in SMAD2 IPs, however the levels of O-GlcNAc present in SMAD2 IPs were significantly lower (Figure 6-5A). Furthermore, the relative locations of O-GlcNAc modification in SMAD1 and SMAD3 IPs were similar, although SMAD3 (aa 425) is slightly smaller than SMAD1 (aa 465) (Figure 6-5A). This indicates that the observed O-GlcNAc modification is potentially an R-SMAD-interacting protein rather than O-GlcNAc modified R-SMADs themselves (Figure 6-5A). To evaluate this further, O-GlcNAc modification and SMAD3 levels on SMAD3 IPs were compared using LI-COR analysis (Figure 6-5B). The LI-COR image revealed that the O-GlcNAcylation signal was detected at a higher molecular weight than SMAD3 itself. Therefore, it is more likely that SMAD3 is not O-GlcNAcylated, but binds to O-GlcNAc modified proteins.

O-GlcNAc is a nutrient sensitive PTM and the amount of O-GlcNAc present in cells is dependent on the glucose concentration (section 1.1.3). In order to test whether the amount of glucose regulates the levels of O-GlcNAc present in SMAD1 and SMAD3 IPs, HeLa cells were grown in glucose free media for 16 hours (Figure 6-6). Glucose depletion reduced the amount of O-GlcNAc present in inputs, depleted the O-GlcNAc signal in SMAD1 IPs (Figure 6-6A) and reduced the O-GlcNAc doublet observed in SMAD3 IPs (Figure 6-6B).
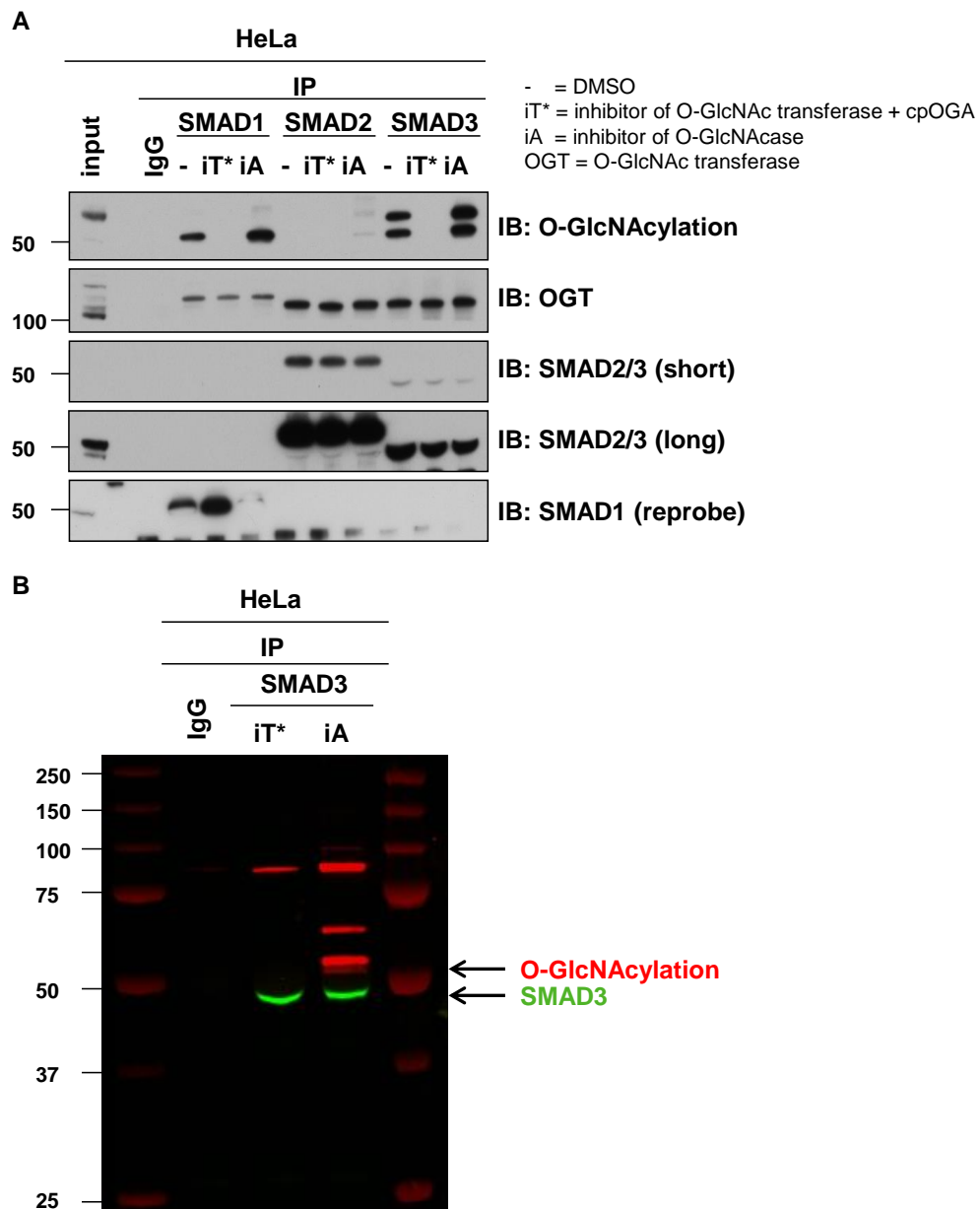
Figure 6-5 SMAD3 is unlikely to be O-GlcNAcylated

A) Endogenous IPs with anti-SMAD1, 2 and 3 antibody or pre-immune sheep IgG were performed in HeLa cell extracts. Cells were treated for 16 hours with or without O-GlcNAcase inhibitor (GlcNAcstatin G, iA, 2 µM) or O-GlcNAc transferase inhibitor (4Ac-5S-glcNAc, iT, 10 µM) and cpOGA (iT*). Cell extracts (input), endogenous IgG or anti-SMAD IPs were resolved by SDS-PAGE and immunoblotted with the indicated antibodies. **B)** An endogenous IP with anti-SMAD3 antibody or pre-immune sheep IgG was performed in HeLa cell extracts. Cells were treated for 16 hours with or without O-GlcNAcase inhibitor (GlcNAcstatin G, iA, 2 µM) or O-GlcNAc transferase inhibitor (4Ac-5S-glcNAc, iT, 10 µM) and cpOGA (iT*). IPs were resolved by SDS-PAGE and immunoblotted with the indicated antibodies. The Western Blot was analysed using LI-COR.
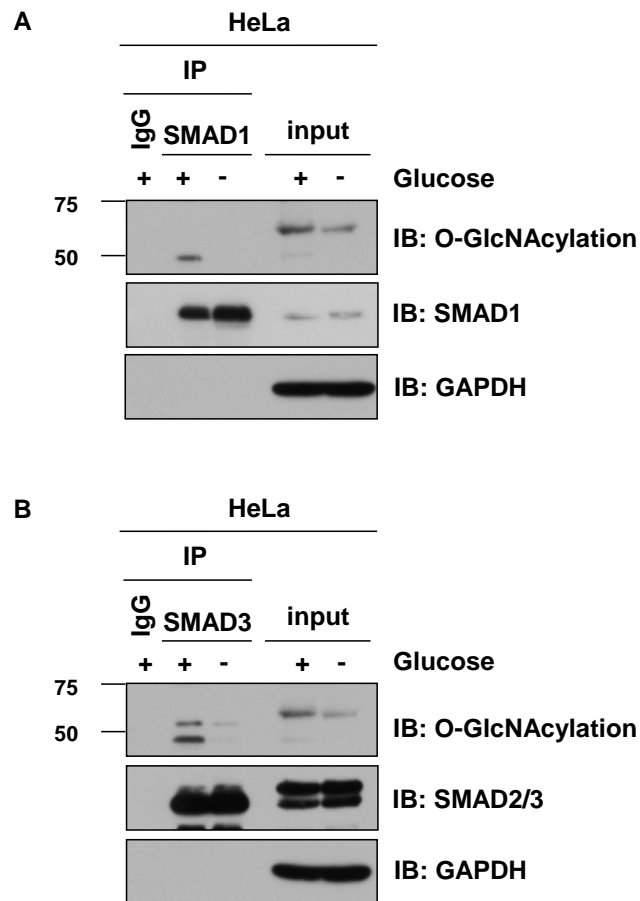
Figure 6-6 Low glucose conditions weaken the O-GlcNAc signal in SMAD1 and SMAD3 IPs

A) HeLa cells were grown in the presence or absence of glucose for 16 hours and IgG or anti-SMAD1 was immunoprecipitated from extracts. Cell extracts (input), endogenous IgG or anti-SMAD1 IPs were resolved by SDS-PAGE and immunoblotted with the indicated antibodies. **B)** As in A, except that SMAD3 was immunoprecipitated.

6.2.3 SMAD4, but not R-SMADs or I-SMADs, is O-GlcNAcylated in vitro

To test whether R-SMADs are O-GlcNAcylated themselves, an *in vitro* O-GlcNAcylation assay was performed with human recombinant GST-SMADs1-7 (except SMAD5). GST-TAB1 was employed as a positive control (Pathak *et al.*, 2012) (Figure 6-7). The SMAD2Δ3 mutant (that resembles SMAD3), was also included, as the levels of O-GlcNAc modification observed in SMAD2 IPs were less than that observed in SMAD3 IPs (Figure 6-5A). As expected, TAB1 was only O-GlcNAcylated in the presence of OGT. None of the R-SMADs or I-

SMADs were O-GlcNAcylated *in vitro*, however OGT O-GlcNAcylated SMAD4 (Figure 6-7). This confirms that SMAD1, SMAD2 and SMAD3 are unlikely to be O-GlcNAcylated.
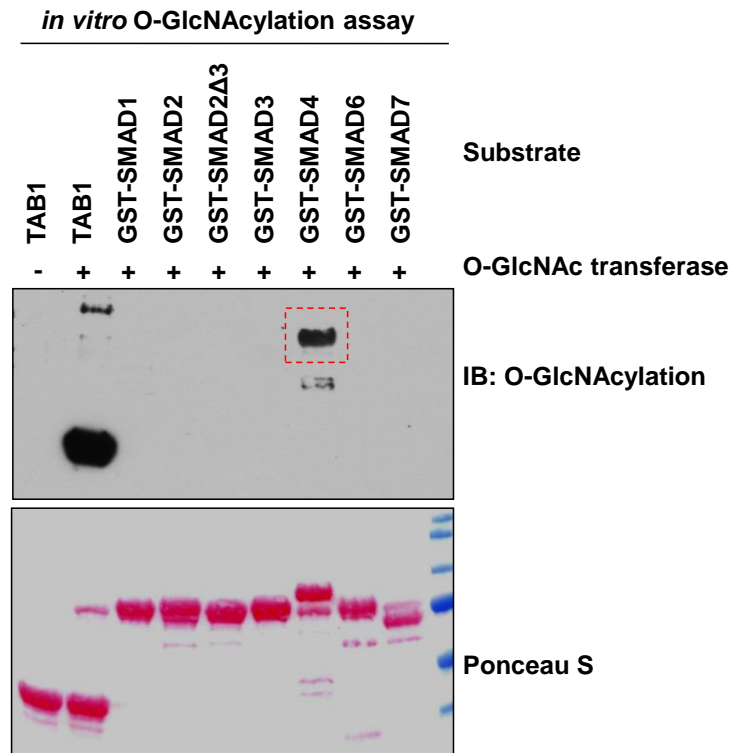
Figure 6-7 SMAD4 is O-GlcNAcylated *in vitro*

An *in vitro* O-GlcNAcylation assay was performed with human recombinant SMADs and TAB1 used as substrates. The substrate proteins were incubated with O-GlcNAc transferase and UDP-GlcNAc in an assay buffer containing 50 mM Tris-HCl, pH 7.5, 1 mM DTT and 12.5 mM $MgCl_2$ for 90 min at 37 °C. Proteins were resolved by SDS-PAGE and transferred to nitrocellulose membranes, which were stained with Ponceau S or immunoblotted with the indicated antibody.

6.2.4 SMAD4 O-GlcNAcylation

In order to test if SMAD4 is O-GlcNAcylated *in vivo*, endogenous SMAD4 IPs from HeLa and HEK293 cells grown in the presence or absence of glucose or OGT/OGA inhibitors were subjected to immunoblotting with O-GlcNAc antibody (Figure 6-8). O-GlcNAcylation was observed in SMAD4 IPs at or near

the predicted molecular weight of SMAD4 from cell extracts that were treated with O-GlcNAcase inhibitors (Figure 6-8).

An online O-GlcNAc modification prediction tool (Gupta and Brunak, 2002), predicted that SMAD4 could be O-GlcNAcylated at S221 and S483 (Figure 6-9A). An *in vitro* O-GlcNAcylation assay was set up in order to test whether GST-SMAD4 was O-GlcNAcylated at S221 and S483 (Figure 6-9B). SMAD4 wild type, SMAD4 S221A, SMAD4 S483A and the S221/483A double mutant were O-GlcNAcylated to the same extent, indicating that SMAD4 is O-GlcNAcylated at a different residue(s). In order to identify this residue(s), SMAD4 was *in vitro* O-GlcNAcylated and processed for mass spectrometry analysis (Figure 6-9C), which has so far not been successful in identifying the O-GlcNAc site within SMAD4.
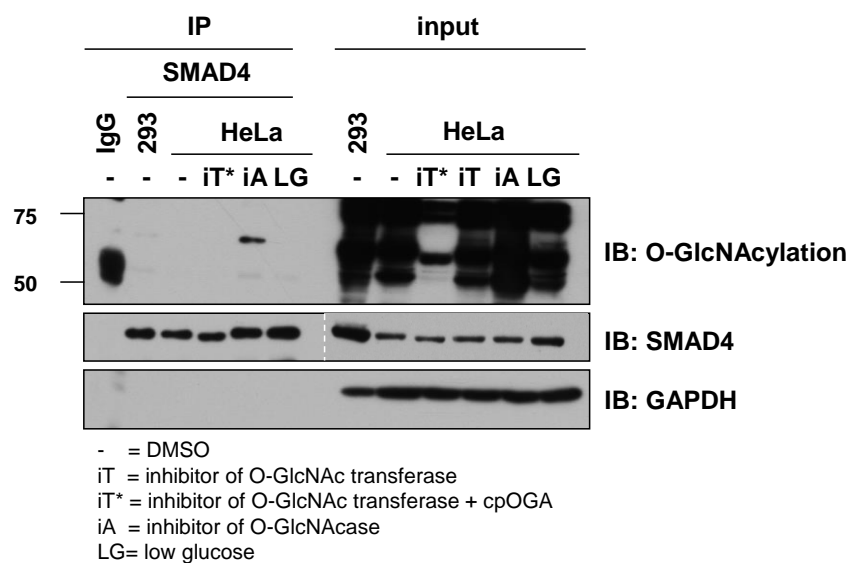
Figure 6-8 SMAD4 is O-GlcNAcylated *in vivo*

An endogenous IP with anti-SMAD4 antibody or pre-immune sheep IgG was performed in HeLa and HEK293 cell extracts, in the presence or absence of glucose, O-GlcNAc transferase inhibitor (4Ac-5S-glcNAc, iT, 10 µM) or O-GlcNAcase inhibitor (GlcNAcstatin G, iA, 2 µM) for 16 hours. Indicated cell extracts and IPs were additionally treated with cpOGA (iT*). Cell extracts (input), endogenous IgG or anti-SMAD4 IPs were resolved by SDS-PAGE and immunoblotted with the indicated antibodies.
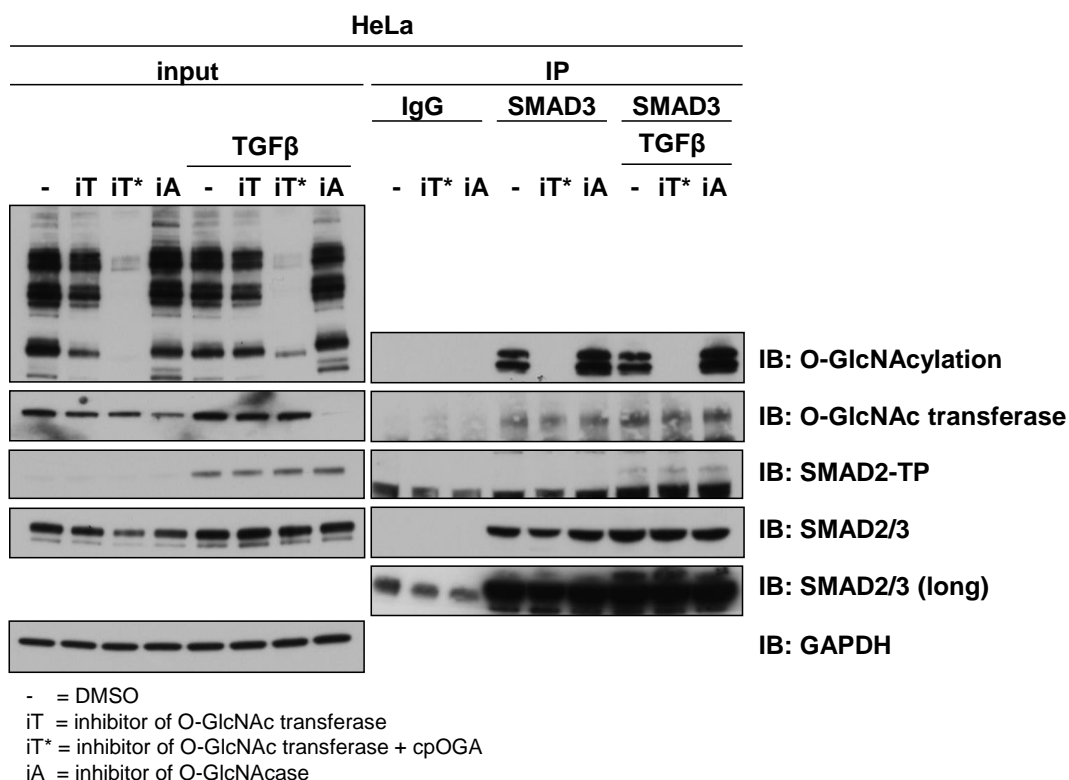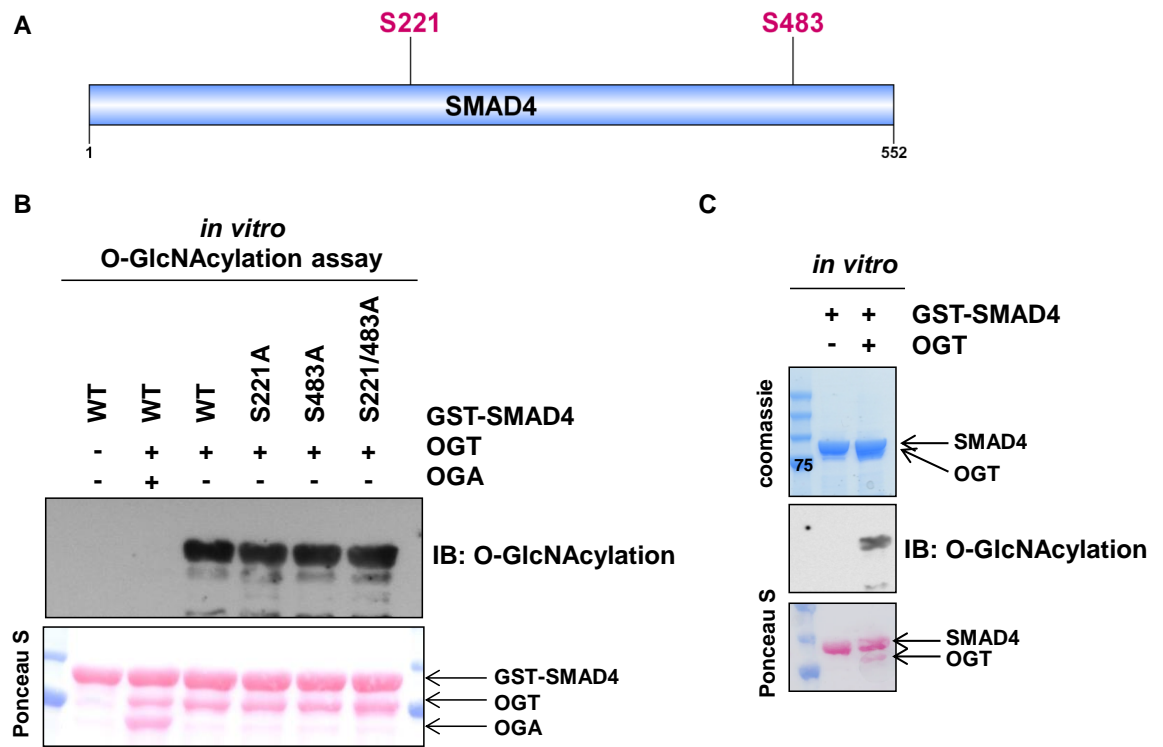
Figure 6-9 Identification of SMAD4 O-GlcNAcylation sites

A) Schematic representation of human SMAD4 indicating S221 and S483 as possible O-GlcNAcylation sites, as predicted using O-GlcNAcScan (Gupta and Brunak, 2002). **B)** An *in vitro* O-GlcNAcylation assay was performed with human recombinant SMAD4 and SMAD4 mutants employed as substrates. The substrate proteins and UDP-GlcNAc were incubated with or without O-GlcNAc transferase or O-GlcNAcase in the assay buffer (50 mM Tris–HCl, pH 7.5, 1 mM DTT, 12.5 mM MgCl$_2$) for 90 min at 37 °C. Proteins were resolved by SDS-PAGE and transferred to nitrocellulose membranes, which were stained with Ponceau S or immunoblotted with the indicated antibody. **C)** Same as in B, except that O-GlcNAcylated SMAD4 was excised and processed for mass spectrometry analysis.

6.2.5 O-GlcNAcylation does not impact TGFβ-induced R-SMAD tail-phosphorylation

As mentioned above (section 6.2.2), it is unlikely that R-SMADs are O-GlcNAcylated. In order to assess whether O-GlcNAcylation has a direct impact on the TGFβ/BMP-mediated activation of SMADs, a TGFβ or BMP stimulation time course in the presence or absence of OGT and OGA inhibitors was performed in different cell lines (Figure 6-10, Figure 6-11). The presence of the OGT inhibitor decreased the total O-GlcNAc modifications on proteins in cell extracts, whereas the addition of the OGA inhibitor resulted in enhanced O-GlcNAc levels (Figure 6-10, Figure 6-11). The levels of SMADs2/3 tail-phosphorylation following a TGFβ-stimulation time course was not affected by changes in the cellular O-GlcNAcylation levels caused by OGT or OGA inhibitors in HeLa (Figure 6-10A) or RPE-1 (Figure 6-10B) cells. Similarly, the tail-phosphorylation of SMAD1 was not influenced by the cellular O-GlcNAc levels during a BMP-stimulation time course in HeLa (Figure 6-11A) or HEK293 (Figure 6-11B) cells.
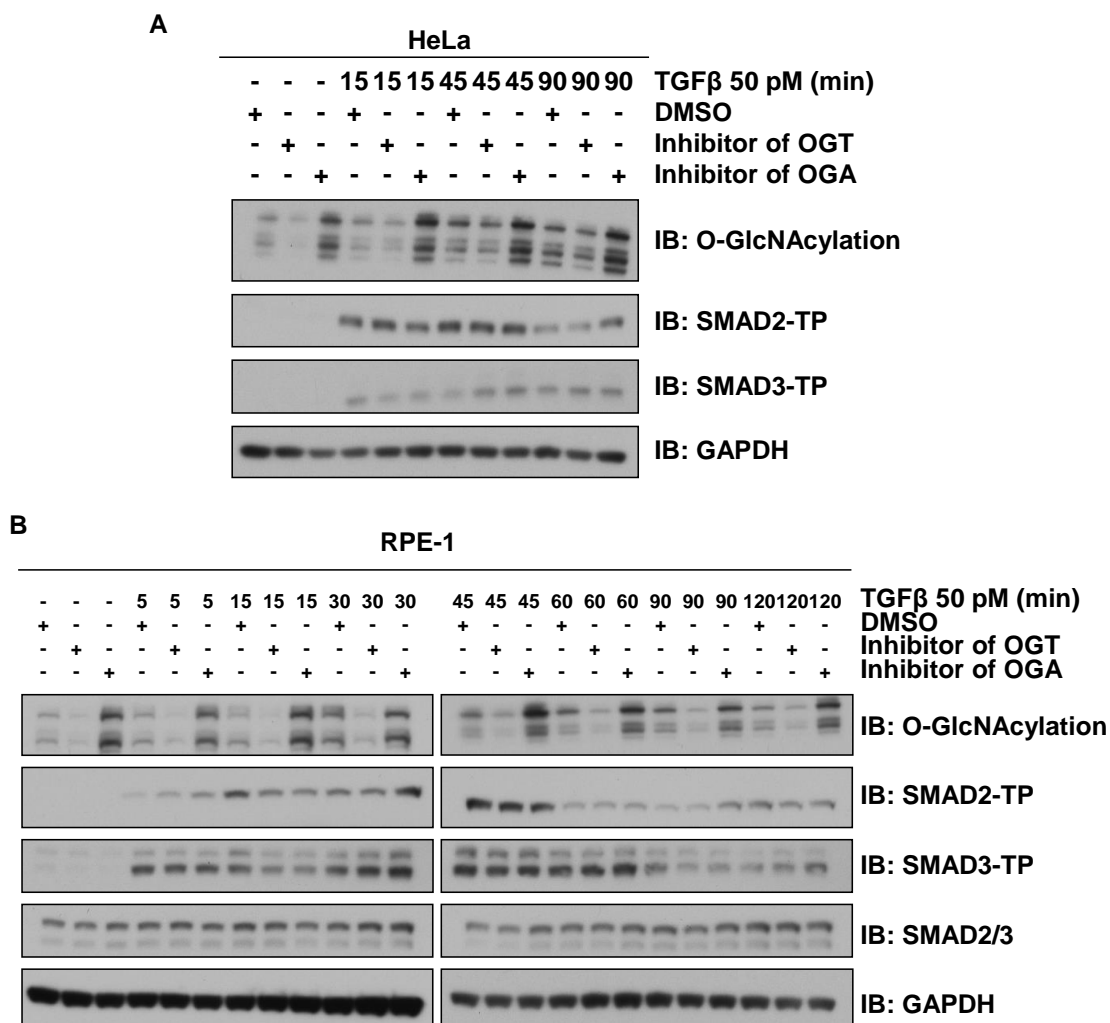
Figure 6-10 O-GlcNAcylation does not appear to interfere with TGFβ-mediated SMAD2/3 tail-phosphorylation

A) HeLa cells were treated with O-GlcNAc transferase inhibitor (4Ac-5S-glcNAc, iT, 10 µM), O-GlcNAcase inhibitor (GlcNAcstatin G, iA, 2 µM) or DMSO for 16 hours prior to a TGFβ (50 pM) stimulation time course. Extracts were resolved by SDS-PAGE and immunoblotted with the indicated antibodies. **B)** As in A, except that retinal epithelial RPE-1 cells were used.
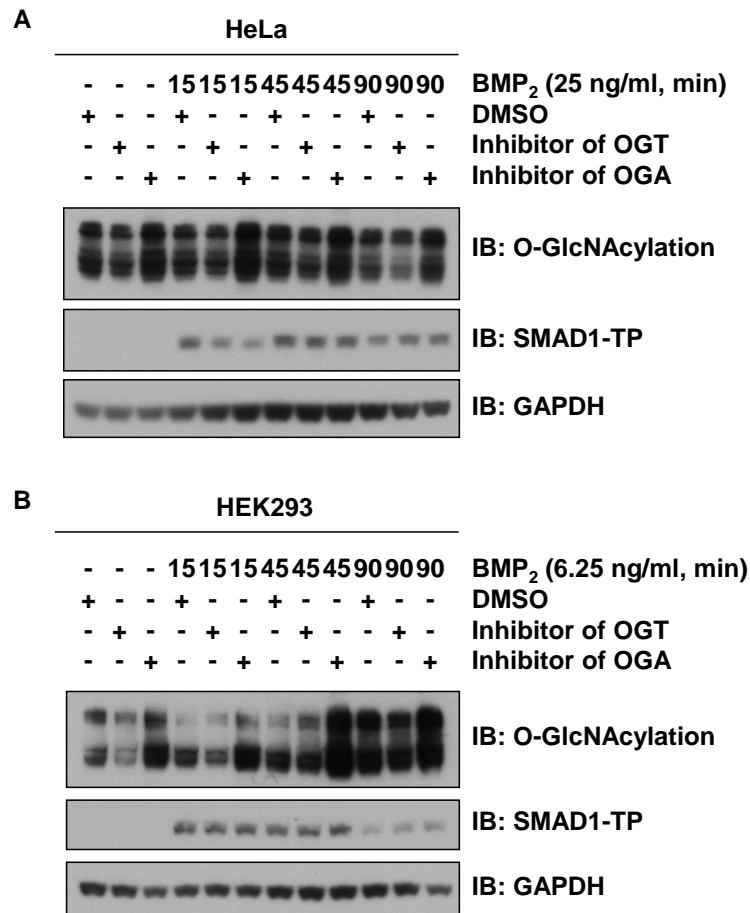
Figure 6-11 O-GlcNAcylation does not appear to interfere with BMP-mediated SMAD1 tail-phosphorylation

A) HeLa cells were treated with O-GlcNAc transferase inhibitor (4Ac-5S-glcNAc, iT, 10 μM), O-GlcNAcase inhibitor (GlcNAcstatin G, iA, 2 μM) or DMSO for 16 hours prior to a BMP$_2$ (25 ng/ml) stimulation time course. Extracts were resolved by SDS-PAGE and immunoblotted with the indicated antibodies. **B)** As in A, except that HEK293 cells were treated with 6.25 ng/ml BMP$_2$.

6.3   Discussion

The regulation of TGFβ/BMP signalling by O-GlcNAcylation has not been investigated previously. The observations that R-SMADs interact with OGT and pull down potential O-GlcNAc modified protein(s), in addition to SMAD4 possibly being O-GlcNAcylated imply that O-GlcNAc modification could regulate TGFβ/BMP signalling. Further investigation is needed to decipher the precise molecular mechanisms of this potential regulation.

6.3.1 The possible impact of SMAD1 and SMAD3 binding to O-GlcNAcylated proteins

Extensive crosstalk occurs between O-GlcNAcylation and phosphorylation in different signalling pathways (Hart *et al.*, 2011). Analogous, reciprocal occupancy of O-GlcNAc and phosphates could occur on residues of SMADs, which could potentially influence the TGFβ/BMP signalling cascade. O-GlcNAc cycling does not appear to influence the ability of TGFβ/BMP receptors to tail-phosphorylate R-SMADs, which excludes competition of these two PTMs at the C-terminal "SXS" motif on SMADs. Indeed, SMADs 1, 2, 3, 6, and 7 are unlikely to be O-GlcNAcylated themselves, although OGT interacts with R-SMADs and O-GlcNAcylation was detected in R-SMAD IPs around the 50 kDa marker, where these proteins migrate. SMAD1, 2 and 3 probably bind to the same O-GlcNAc modified protein, as its electrophoretic mobility pattern is identical in both SMAD1 and SMAD3 IPs. The second band in SMAD3 IPs could be an additional O-GlcNAc modified protein. An immunoprecipitation of SMADs1/2/3/4 under denaturing conditions might give further clues as to whether SMADs bind to O-GlcNAcylated proteins. The O-GlcNAc signal in SMAD1/3 IPs weakens in the presence of OGT inhibitors and under low

glucose conditions, indicating that this protein is genuinely affected by O-GlcNAc cycling in cells. The binding of SMADs to OGT could potentially alter the catalytic activity or specificity of OGT or act as a scaffold to facilitate O-GlcNAcylation of the SMAD-binding proteins. The O-GlcNAc signal in SMAD IPs is enriched, as the same O-GlcNAc signal is not visible in whole cell extracts at the same molecular weight. It would be interesting to find out which O-GlcNAc modified protein(s) is bound to endogenous SMAD1/2/3. Detection of O-GlcNAcylation by mass spectrometry is challenging, as the sugar modification is labile and could be lost during this process. Hence, the identification of the O-GlcNAc modified R-SMAD-bound protein(s) will be difficult, but could be attempted through a double enrichment pull down using a mutant version of cpOGA coupled to beads that traps O-GlcNAc and then by further selecting with a second IP of SMAD1 or SMAD3. Furthermore, it would be interesting to investigate whether the O-GlcNAc modification of the R-SMAD binding protein(s) is essential for their interaction.

Upon TGFβ/BMP stimulation SMAD3 interacts with SMAD2/SMAD4 and SMAD1 with SMAD4 (Souchelnytskyi *et al.*, 1997), however the interaction of the O-GlcNAcylated proteins with SMAD1 or SMAD3 was independent of TGFβ/BMP stimulation. Moreover, the O-GlcNAc modified binding protein exhibited significantly reduced affinity towards SMAD2, which is highly similar to SMAD3 but in contrast to SMAD1/3 has less affinity towards DNA (Dennler *et al.*, 1999).

It has been reported that 21 proteins change their O-GlcNAcylation status upon TGFβ treatment. Most of the identified hits were proteins of unknown function and regulators of cell survival, apoptosis, trafficking, and RNA processing (Iwahana *et al.*, 2006). SMAD proteins or known interacting partners

have not been shown to be post-translationally modified by O-GlcNAc in this study. TGFβ/BMP signalling could be altered through the binding of SMADs to proteins that are regulated by O-GlcNAcylation. O-GlcNAcylated proteins could potentially regulate SMAD nuclear translocation, binding to interacting proteins and/or affect SMAD-mediated transcription. O-GlcNAcylation has been reported to regulate several signalling pathways at the transcriptional level and O-GlcNAcylation of R-SMAD-binding transcription co-factors could link TGFβ/BMP signalling to nutrient sensing and glucose metabolism (Özcan *et al.*, 2010). Furthermore, it has been suggested that differences in BMP-SMAD signalling, lipid metabolism and glucose utilisation determine the differentiation and lipid accumulation between intramuscular and subcutaneous preadipocytes (Wang *et al.,* 2013b). The SMAD-interacting O-GlcNAcylated protein possibly regulates SMAD function at the basal level, as their interaction was not influenced by ligands.

6.3.2 *The possible impact of O-GlcNAcylation on SMAD4*

In contrast to SMAD1 and SMAD3, SMAD4 is O-GlcNAcylated *in vitro* and potentially *in vivo. In vivo* SMAD4 O-GlcNAcylation is only visible in the presence of OGA inhibitors, indicating high O-GlcNAc cycling and constant removal of O-GlcNAc from SMAD4. This could infer an inhibitory function of O-GlcNAcylation on SMAD4. The O-GlcNAcScan software is unreliable and did not predict the actual SMAD4 O-GlcNAcylation sites. Therefore, it will be critical to identify the *bona fide* O-GlcNAc sites on SMAD4, which might be possible by performing a SMAD4 *in vitro* O-GlcNAcylation assay and identifying the residues on SMAD4 by mass spectrometry (Ma and Hart, 2014). To confirm the O-GlcNAcylation of SMAD4 *in vivo*, an antibody directed against the O-

GlcNAcylation site(s) in SMAD4 should be raised. This antibody would clarify under which conditions SMAD4 is O-GlcNAcylated or if SMAD4 potentially also binds to an O-GlcNAcylated protein which has a similar electrophoretic mobility. If the O-GlcNAcylation sites on SMAD4 can be determined, then wild type SMAD4 or SMAD4 harbouring mutations of these specific sites could be stably integrated into cells lacking endogenous SMAD4. These cells could then be used to determine the impact and significance of SMAD4 O-GlcNAcylation, by monitoring the transcription of SMAD4-dependent target genes, the ability of SMAD4 to shuttle between the nucleus and cytoplasm and its affinity towards R-SMADs or other SMAD4 binding proteins. SMAD4 could be regulated by O-GlcNAcylation in an alagous manner to other transcription factors such as CREB, YY1, STAT, p53, ERα, c-Myc and C/EBPβ (Özcan *et al.*, 2010). SMAD4-mediated gene transcription could be monitored under high and low glucose conditions in the presence or absence of TGFβ/BMP ligands or kinase inhibitors, using luciferase reporter constructs or qRT-PCR. This would give a better insight into the magnitude of TGFβ/BMP pathway regulation goverened by O-GlcNAc modification.

References

ADAMS, C. O., HOUSLEY, W. J., BHOWMICK, S., CONE, R. E., RAJAN, T. V., FOROUHAR, F. & CLARK, R. B. 2010. Cbl-b(-/-) T cells demonstrate in vivo resistance to regulatory T cells but a context-dependent resistance to TGF-beta. *Journal of immunology,* 185**,** 2051-8.

ADAMS, J. 2003. The proteasome: structure, function, and role in the cell. *Cancer Treatment Reviews,* 29, Supplement 1**,** 3-9.

ADAMS, J., PALOMBELLA, V. J., SAUSVILLE, E. A., JOHNSON, J., DESTREE, A., LAZARUS, D. D., MAAS, J., PIEN, C. S., PRAKASH, S. & ELLIOTT, P. J. 1999. Proteasome Inhibitors: A Novel Class of Potent and Effective Antitumor Agents. *Cancer Research,* 59**,** 2615-2622.

AFRAKHTE, M., MOREN, A., JOSSAN, S., ITOH, S., SAMPATH, K., WESTERMARK, B., HELDIN, C. H., HELDIN, N. E. & TEN DIJKE, P. 1998. Induction of inhibitory Smad6 and Smad7 mRNA by TGF-beta family members. *Biochemical and Biophysical Research Communications,* 249**,** 505-11.

AGRICOLA, E., RANDALL, R. A., GAARENSTROOM, T., DUPONT, S. & HILL, C. S. 2011. Recruitment of TIF1γ to chromatin via its PHD finger-bromodomain activates its ubiquitin ligase and transcriptional repressor activities. *Molecular cell,* 43**,** 85-96.

AGUILAR, H., FRICOVSKY, E., IHM, S., SCHIMKE, M., MAYA-RAMOS, L., AROONSAKOOL, N., CEBALLOS, G., DILLMANN, W., VILLARREAL, F. & RAMIREZ-SANCHEZ, I. 2014. Role for high-glucose-induced protein O-GlcNAcylation in stimulating cardiac fibroblast collagen synthesis. *American journal of physiology. Cell physiology,* 306**,** C794-804.

AKHURST, R. J. & DERYNCK, R. 2001. TGF-beta signaling in cancer--a double-edged sword. *Trends in cell biology,* 11**,** S44-51.

AKHURST, R. J. & HATA, A. 2012. Targeting the TGF-beta signalling pathway in disease. *Nature Reviews Drug Discovery,* 11**,** 790-811.

AL-SALIHI, M. A., HERHAUS, L., MACARTNEY, T. & SAPKOTA, G. P. 2012a. USP11 augments TGFbeta signalling by deubiquitylating ALK5. *Open biology,* 2**,** 120063.

AL-SALIHI, M. A., HERHAUS, L. & SAPKOTA, G. P. 2012b. Regulation of the transforming growth factor beta pathway by reversible ubiquitylation. *Open Biology,* 2**,** 120082-120082.

ALARCÓN, C., ZAROMYTIDOU, A.-I., XI, Q., GAO, S., YU, J., FUJISAWA, S., BARLAS, A., MILLER, A. N., MANOVA-TODOROVA, K., MACIAS, M. J., SAPKOTA, G., PAN, D. & MASSAGUÉ, J. 2009. Nuclear CDKs drive Smad transcriptional activation and turnover in BMP and TGF-beta pathways. *Cell,* 139**,** 757-769.

ALLEN, G. F., TOTH, R., JAMES, J. & GANLEY, I. G. 2013. Loss of iron triggers PINK1/Parkin-independent mitophagy. *EMBO reports,* 14**,** 1127-35.

AMERIK, A. Y. & HOCHSTRASSER, M. 2004. Mechanism and function of deubiquitinating enzymes. *Biochimica et biophysica acta,* 1695**,** 189-207.

ANGELATS, C., WANG, X.-W., JERMIIN, L. S., COPELAND, N. G., JENKINS, N. A. & BAKER, R. T. 2003. Isolation and characterization of the mouse ubiquitin-specific protease Usp15. *Mammalian Genome,* 14**,** 31-46.

ANNES, J. P., MUNGER, J. S. & RIFKIN, D. B. 2003. Making sense of latent TGFbeta activation. *Journal of cell science,* 116**,** 217-24.

ARAGON, E., GOERNER, N., ZAROMYTIDOU, A. I., XI, Q., ESCOBEDO, A., MASSAGUE, J. & MACIAS, M. J. 2011. A Smad action turnover switch

operated by WW domain readers of a phosphoserine code. *Genes & development,* 25**,** 1275-88.

ARASE, M., HORIGUCHI, K., EHATA, S., MORIKAWA, M., TSUTSUMI, S., ABURATANI, H., MIYAZONO, K. & KOINUMA, D. 2014. Transforming growth factor-beta-induced lncRNA-Smad7 inhibits apoptosis of mouse breast cancer JygMC(A) cells. *Cancer science,* doi: 10.1111/cas.

BAI, X., JING, L., LI, Y., LUO, S., WANG, S., ZHOU, J., LIU, Z. & DIAO, A. 2014. TMEPAI inhibits TGF-beta signaling by promoting lysosome degradation of TGF-beta receptor and contributes to lung cancer development. *Cellular signalling,* 26**,** 2030-2039.

BAI, Y., YANG, C., HU, K., ELLY, C. & LIU, Y.-C. 2004. Itch E3 ligase-mediated regulation of TGF-beta signaling by modulating smad2 phosphorylation. *Mol Cell,* 15**,** 825-831.

BAKER, R. T., WANG, X.-W., WOOLLATT, E., WHITE, J. A. & SUTHERLAND, G. R. 1999. Identification, Functional Characterization, and Chromosomal Localization of USP15, a Novel Human Ubiquitin-Specific Protease Related to the UNP Oncoprotein, and a Systematic Nomenclature for Human Ubiquitin-Specific Proteases. *Genomics,* 59**,** 264-274.

BAKIN, A. V., RINEHART, C., TOMLINSON, A. K. & ARTEAGA, C. L. 2002. p38 mitogen-activated protein kinase is required for TGFβ-mediated fibroblastic transdifferentiation and cell migration. *Journal of Cell Science,* 115**,** 3193-3206.

BAKIN, A. V., TOMLINSON, A. K., BHOWMICK, N. A., MOSES, H. L. & ARTEAGA, C. L. 2000. Phosphatidylinositol 3-kinase function is required for transforming growth factor beta-mediated epithelial to mesenchymal transition and cell migration. *The Journal of biological chemistry,* 275**,** 36803-10.

BALAKIREV, M. Y., TCHERNIUK, S. O., JAQUINOD, M. & CHROBOCZEK, J. 2003. Otubains: a new family of cysteine proteases in the ubiquitin pathway. *EMBO reports,* 4**,** 517-22.

BATTISTUTTA, R. 2009. Protein kinase CK2 in health and disease: Structural bases of protein kinase CK2 inhibition. *Cellular and molecular life sciences : CMLS,* 66**,** 1868-89.

BATTISTUTTA, R. & LOLLI, G. 2011. Structural and functional determinants of protein kinase CK2alpha: facts and open questions. *Molecular and Cellular Biochemistry,* 356**,** 67-73.

BAUGHN, L. B., DI LIBERTO, M., NIESVIZKY, R., CHO, H. J., JAYABALAN, D., LANE, J., LIU, F. & CHEN-KIANG, S. 2009. CDK2 Phosphorylation of Smad2 Disrupts TGF-β Transcriptional Regulation in Resistant Primary Bone Marrow Myeloma Cells. *The Journal of Immunology,* 182**,** 1810-1817.

BELVILLE, C., JOSSO, N. & PICARD, J. Y. 1999. Persistence of Mullerian derivatives in males. *American journal of medical genetics,* 89**,** 218-23.

BERNDSEN, C. E. & WOLBERGER, C. 2014. New insights into ubiquitin E3 ligase mechanism. *Nature structural & molecular biology,* 21**,** 301-7.

BETTELLI, E., CARRIER, Y., GAO, W., KORN, T., STROM, T. B., OUKKA, M., WEINER, H. L. & KUCHROO, V. K. 2006. Reciprocal developmental pathways for the generation of pathogenic effector TH17 and regulatory T cells. *Nature,* 441**,** 235-238.

BIZET, A. A., LIU, K., TRAN-KHANH, N., SAKSENA, A., VORSTENBOSCH, J., FINNSON, K. W., BUSCHMANN, M. D. & PHILIP, A. 2011. The TGF-beta co-receptor, CD109, promotes internalization and degradation of TGF-beta receptors. *Biochimica et biophysica acta,* 1813**,** 742-53.

BIZET, A. A., TRAN-KHANH, N., SAKSENA, A., LIU, K., BUSCHMANN, M. D. & PHILIP, A. 2012. CD109-mediated degradation of TGF-beta receptors and

inhibition of TGF-beta responses involve regulation of SMAD7 and Smurf2 localization and function. *Journal of Cellular Biochemistry,* 113**,** 238-46.

BLAHNA, M. T. & HATA, A. 2012. Smad-mediated regulation of microRNA biosynthesis. *FEBS letters,* 586**,** 1906-12.

BLAYDES, J. P. & HUPP, T. R. 1998. DNA damage triggers DRB-resistant phosphorylation of human p53 at the CK2 site. *Oncogene,* 17**,** 1045-52.

BLITZ, I. L., ANDELFINGER, G. & HORB, M. E. 2006. Germ layers to organs: using Xenopus to study "later" development. *Seminars in cell & developmental biology,* 17**,** 133-45.

BLOBE, G. C., SCHIEMANN, W. P. & LODISH, H. F. 2000. Role of transforming growth factor beta in human disease. *The New England journal of medicine,* 342**,** 1350-8.

BLOCK, K., APPIKONDA, S., LIN, H. R., BLOOM, J., PAGANO, M. & YEW, P. R. 2005. The acidic tail domain of human Cdc34 is required for p27Kip1 ubiquitination and complementation of a cdc34 temperature sensitive yeast strain. *Cell cycle,* 4**,** 1421-7.

BOGDAHN, U., HAU, P., STOCKHAMMER, G., VENKATARAMANA, N. K., MAHAPATRA, A. K., SURI, A., BALASUBRAMANIAM, A., NAIR, S., OLIUSHINE, V., PARFENOV, V., POVERENNOVA, I., ZAAROOR, M., JACHIMCZAK, P., LUDWIG, S., SCHMAUS, S., HEINRICHS, H. & SCHLINGENSIEPEN, K. H. 2011. Targeted therapy for high-grade glioma with the TGF-beta2 inhibitor trabedersen: results of a randomized and controlled phase IIb study. *Neuro-oncology,* 13**,** 132-42.

BOND, M. R. & HANOVER, J. A. 2013. O-GlcNAc Cycling: A Link Between Metabolism and Chronic Disease. *Annual Review of Nutrition,* 33**,** 205-229.

BONIFACINO, J. S. & WEISSMAN, A. M. 1998. Ubiquitin and the control of protein fate in the secretory and endocytic pathways. *Annual review of cell and developmental biology,* 14**,** 19-57.

BONNI, S., WANG, H.-R., CAUSING, C. G., KAVSAK, P., STROSCHEIN, S. L., LUO, K. & WRANA, J. L. 2001. TGF-[beta] induces assembly of a Smad2-Smurf2 ubiquitin ligase complex that targets SnoN for degradation. *Nature cell biology,* 3**,** 587-595.

BOWEN, T., JENKINS, R. H. & FRASER, D. J. 2013. MicroRNAs, transforming growth factor beta-1, and tissue fibrosis. *The Journal of Pathology,* 229**,** 274-285.

BRADFORD, M. M. 1976. A rapid and sensitive method for the quantitation of microgram quantities of protein utilizing the principle of protein-dye binding. *Analytical biochemistry,* 72**,** 248-54.

BREMM, A. & KOMANDER, D. 2011. Emerging roles for Lys11-linked polyubiquitin in cellular regulation. *Trends in Biochemical Sciences,* 36**,** 355-363.

BROWN, M. A., ZHAO, Q., BAKER, K. A., NAIK, C., CHEN, C., PUKAC, L., SINGH, M., TSAREVA, T., PARICE, Y., MAHONEY, A., ROSCHKE, V., SANYAL, I. & CHOE, S. 2005. Crystal structure of BMP-9 and functional interactions with pro-region and receptors. *The Journal of biological chemistry,* 280**,** 25111-8.

BRUCE, D. L. & SAPKOTA, G. P. 2012. Phosphatases in SMAD regulation. *FEBS Letters,* 586**,** 1897-1905.

BUIJS, J. T., HENRIQUEZ, N. V., VAN OVERVELD, P. G., VAN DER HORST, G., QUE, I., SCHWANINGER, R., RENTSCH, C., TEN DIJKE, P., CLETON-JANSEN, A. M., DRIOUCH, K., LIDEREAU, R., BACHELIER, R., VUKICEVIC, S., CLEZARDIN, P., PAPAPOULOS, S. E., CECCHINI, M. G., LOWIK, C. W. & VAN DER PLUIJM, G. 2007. Bone morphogenetic protein 7

in the development and treatment of bone metastases from breast cancer. *Cancer Research,* 67**,** 8742-51.

BUTZ, H., RÁCZ, K., HUNYADY, L. & PATÓCS, A. 2012. Crosstalk between TGF-β signaling and the microRNA machinery. *Trends in Pharmacological Sciences,* 33**,** 382-393.

CALONGE, M. J. & MASSAGUE, J. 1999. Smad4/DPC4 silencing and hyperactive Ras jointly disrupt transforming growth factor-beta antiproliferative responses in colon cancer cells. *The Journal of biological chemistry,* 274**,** 33637-43.

CAMPBELL, D. & MORRICE, N. 2002. Identification of protein phosphorylation sites by a combination of mass spectrometry and solid phase Edman sequencing. *Journal of Biomolecular Techniques,* 13**,** 119-130.

CHAI, J., WU, J. W., YAN, N., MASSAGUE, J., PAVLETICH, N. P. & SHI, Y. 2003. Features of a Smad3 MH1-DNA complex. Roles of water and zinc in DNA binding. *The Journal of biological chemistry,* 278**,** 20327-31.

CHEN, G., DENG, C. & LI, Y. P. 2012. TGF-beta and BMP signaling in osteoblast differentiation and bone formation. *International journal of biological sciences,* 8**,** 272-88.

CHEN, H. B., SHEN, J., IP, Y. T. & XU, L. 2006. Identification of phosphatases for Smad in the BMP/DPP pathway. *Genes & Development,* 20**,** 648-53.

CHENG, P. L., LU, H., SHELLY, M., GAO, H. & POO, M. M. 2011. Phosphorylation of E3 ligase Smurf1 switches its substrate preference in support of axon development. *Neuron,* 69**,** 231-43.

CHENG, T. Y., WU, M. S., HUA, K. T., KUO, M. L. & LIN, M. T. 2014. Cyr61/CTGF/Nov family proteins in gastric carcinogenesis. *World journal of gastroenterology : WJG,* 20**,** 1694-700.

CHENG, X., GAO, W., DANG, Y., LIU, X., LI, Y., PENG, X. & YE, X. 2013. Both ERK/MAPK and TGF-Beta/Smad signaling pathways play a role in the kidney fibrosis of diabetic mice accelerated by blood glucose fluctuation. *Journal of diabetes research,* 2013**,** 463740.

CHOI, M. E., DING, Y. & KIM, S. I. 2012. TGF-beta signaling via TAK1 pathway: role in kidney fibrosis. *Seminars in nephrology,* 32**,** 244-52.

CLAGUE, M. J., COULSON, J. M. & URBE, S. 2012a. Cellular functions of the DUBs. *Journal of cell science,* 125**,** 277-86.

CLAGUE, MICHAEL J., LIU, H. & URBÉ, S. 2012b. Governance of Endocytic Trafficking and Signaling by Reversible Ubiquitylation. *Developmental Cell,* 23**,** 457-467.

CLEVER, J. L., SAKAI, Y., WANG, R. A. & SCHNEIDER, D. B. 2010. Inefficient skeletal muscle repair in inhibitor of differentiation knockout mice suggests a crucial role for BMP signaling during adult muscle regeneration. *American journal of physiology. Cell physiology,* 298**,** C1087-99.

COCCETTI, P., TRIPODI, F., TEDESCHI, G., NONNIS, S., MARIN, O., FANTINATO, S., CIRULLI, C., VANONI, M. & ALBERGHINA, L. 2008. The CK2 phosphorylation of catalytic domain of Cdc34 modulates its activity at the G1 to S transition in Saccharomyces cerevisiae. *Cell cycle,* 7**,** 1391-401.

COHEN, P. 2002. The origins of protein phosphorylation. *Nature cell biology,* 4**,** E127-30.

COHEN, P. & ALESSI, D. R. 2013. Kinase drug discovery-what's next in the field? *ACS chemical biology,* 8**,** 96-104.

COHEN, P. T. W. 2009. Phosphatase families dephosphorylating serine and threonine residues in proteins. *In:* DENNIS, E. A. & BRADSHAW, R. A. (eds.) *Handbook of Cell Signaling.* Oxford: Academic Press.

CONERY, A. R., CAO, Y., THOMPSON, E. A., TOWNSEND, C. M., JR., KO, T. C. & LUO, K. 2004. Akt interacts directly with Smad3 to regulate the sensitivity to TGF-beta induced apoptosis. *Nature cell biology,* 6**,** 366-72.

CONSTAM, D. B. & ROBERTSON, E. J. 1999. Regulation of bone morphogenetic protein activity by pro domains and proprotein convertases. *The Journal of Cell Biology,* 144**,** 139-49.

CORDEIRO, M. F. 2003. Technology evaluation: lerdelimumab, Cambridge Antibody Technology. *Current opinion in molecular therapeutics,* 5**,** 199-203.

CORNELISSEN, T., HADDAD, D., WAUTERS, F., VAN HUMBEECK, C., MANDEMAKERS, W., KOENTJORO, B., SUE, C., GEVAERT, K., DE STROOPER, B., VERSTREKEN, P. & VANDENBERGHE, W. 2014. The deubiquitinase USP15 antagonizes Parkin-mediated mitochondrial ubiquitination and mitophagy. *Human Molecular Genetics,* doi: 10.1093/hmg/ddu244.

COZZA, G., BORTOLATO, A. & MORO, S. 2010. How druggable is protein kinase CK2? *Medicinal research reviews,* 30**,** 419-62.

COZZA, G., GIRARDI, C., RANCHIO, A., LOLLI, G., SARNO, S., ORZESZKO, A., KAZIMIERCZUK, Z., BATTISTUTTA, R., RUZZENE, M. & PINNA, L. 2014. Cell-permeable dual inhibitors of protein kinases CK2 and PIM-1: structural features and pharmacological potential. *Cellular and Molecular Life Sciences***,** 1-13.

COZZA, G., MAZZORANA, M., PAPINUTTO, E., BAIN, J., ELLIOTT, M., DI MAIRA, G., GIANONCELLI, A., PAGANO, M. A., SARNO, S., RUZZENE, M., BATTISTUTTA, R., MEGGIO, F., MORO, S., ZAGOTTO, G. & PINNA, L. A. 2009. Quinalizarin as a potent, selective and cell-permeable inhibitor of protein kinase CK2. *The Biochemical journal,* 421**,** 387-95.

COZZA, G., SARNO, S., RUZZENE, M., GIRARDI, C., ORZESZKO, A., KAZIMIERCZUK, Z., ZAGOTTO, G., BONAIUTO, E., DI PAOLO, M. L. & PINNA, L. A. 2013. Exploiting the repertoire of CK2 inhibitors to target DYRK and PIM kinases. *Biochimica et Biophysica Acta (BBA) - Proteins and Proteomics,* 1834**,** 1402-1409.

CUTTS, A. J., SOOND, S. M., POWELL, S. & CHANTRY, A. 2011. Early phase TGFβ receptor signalling dynamics stabilised by the deubiquitinase UCH37 promotes cell migratory responses. *The International Journal of Biochemistry & Cell Biology,* 43**,** 604-612.

DAI, F., SHEN, T., LI, Z., LIN, X. & FENG, X. H. 2011. PPM1A dephosphorylates RanBP3 to enable efficient nuclear export of Smad2 and Smad3. *EMBO reports,* 12**,** 1175-81.

DALY, A. C., RANDALL, R. A. & HILL, C. S. 2008. Transforming Growth Factor β-Induced Smad1/5 Phosphorylation in Epithelial Cells Is Mediated by Novel Receptor Complexes and Is Essential for Anchorage-Independent Growth. *Molecular and Cellular Biology,* 28**,** 6889-6902.

DAVIS, B. N., HILYARD, A. C., LAGNA, G. & HATA, A. 2008. SMAD proteins control DROSHA-mediated microRNA maturation. *Nature,* 454**,** 56-61.

DAVIS, B. N., HILYARD, A. C., NGUYEN, P. H., LAGNA, G. & HATA, A. 2010. Smad proteins bind a conserved RNA sequence to promote microRNA maturation by Drosha. *Molecular cell,* 39**,** 373-84.

DE BOECK, M. & TEN DIJKE, P. 2012. Key role for ubiquitin protein modification in TGFbeta signal transduction. *Upsala journal of medical sciences,* 117**,** 153-65.

DE JONG, R. N., AB, E., DIERCKS, T., TRUFFAULT, V., DANIELS, M., KAPTEIN, R. & FOLKERS, G. E. 2006. Solution structure of the human ubiquitin-specific protease 15 DUSP domain. *The Journal of biological chemistry,* 281**,** 5026-31.

DE ROBERTIS, E. M. & KURODA, H. 2004. Dorsal-ventral patterning and neural induction in Xenopus embryos. *Annual review of cell and developmental biology,* 20**,** 285-308.

DECKERS, M., VAN DINTHER, M., BUIJS, J., QUE, I., LOWIK, C., VAN DER PLUIJM, G. & TEN DIJKE, P. 2006. The tumor suppressor Smad4 is required for transforming growth factor beta-induced epithelial to mesenchymal transition and bone metastasis of breast cancer cells. *Cancer research,* 66**,** 2202-9.

DENG, L., WANG, C., SPENCER, E., YANG, L., BRAUN, A., YOU, J., SLAUGHTER, C., PICKART, C. & CHEN, Z. J. 2000. Activation of the IκB Kinase Complex by TRAF6 Requires a Dimeric Ubiquitin-Conjugating Enzyme Complex and a Unique Polyubiquitin Chain. *Cell,* 103**,** 351-361.

DENNLER, S., HUET, S. & GAUTHIER, J. M. 1999. A short amino-acid sequence in MH1 domain is responsible for functional differences between Smad2 and Smad3. *Oncogene,* 18**,** 1643-8.

DERYNCK, R. & AKHURST, R. J. 2007. Differentiation plasticity regulated by TGF-[beta] family proteins in development and disease. *Nat Cell Biol,* 9**,** 1000-1004.

DESHAIES, R. J. & JOAZEIRO, C. A. 2009. RING domain E3 ubiquitin ligases. *Annual review of biochemistry,* 78**,** 399-434.

DI MAIRA, G., SALVI, M., ARRIGONI, G., MARIN, O., SARNO, S., BRUSTOLON, F., PINNA, L. A. & RUZZENE, M. 2005. Protein kinase CK2 phosphorylates and upregulates Akt//PKB. *Cell Death Differ,* 12**,** 668-677.

DIETZ, H. C., CUTTING, G. R., PYERITZ, R. E., MASLEN, C. L., SAKAI, L. Y., CORSON, G. M., PUFFENBERGER, E. G., HAMOSH, A., NANTHAKUMAR, E. J., CURRISTIN, S. M. & ET AL. 1991. Marfan syndrome caused by a recurrent de novo missense mutation in the fibrillin gene. *Nature,* 352**,** 337-9.

DIETZ, H. C., LOEYS, B., CARTA, L. & RAMIREZ, F. 2005. Recent progress towards a molecular understanding of Marfan syndrome. *American journal of medical genetics. Part C, Seminars in medical genetics,* 139C**,** 4-9.

DRABSCH, Y. & TEN DIJKE, P. 2011. TGF-beta signaling in breast cancer cell invasion and bone metastasis. *Journal of mammary gland biology and neoplasia,* 16**,** 97-108.

DRABSCH, Y. & TEN DIJKE, P. 2012. TGF-beta signalling and its role in cancer progression and metastasis. *Cancer metastasis reviews,* 31**,** 553-68.

DUAN, X., LIANG, Y. Y., FENG, X. H. & LIN, X. 2006. Protein serine/threonine phosphatase PPM1A dephosphorylates Smad1 in the bone morphogenetic protein signaling pathway. *The Journal of biological chemistry,* 281**,** 36526-32.

DUBOIS, C. M., LAPRISE, M. H., BLANCHETTE, F., GENTRY, L. E. & LEDUC, R. 1995. Processing of transforming growth factor beta 1 precursor by human furin convertase. *The Journal of biological chemistry,* 270**,** 10618-24.

DUNCAN, L. M., PIPER, S., DODD, R. B., SAVILLE, M. K., SANDERSON, C. M., LUZIO, J. P. & LEHNER, P. J. 2006. Lysine-63-linked ubiquitination is required for endolysosomal degradation of class I molecules. *The EMBO Journal,* 25**,** 1635-1645.

DUPONT, S., INUI, M. & NEWFELD, S. J. 2012. Regulation of TGF-beta signal transduction by mono- and deubiquitylation of Smads. *FEBS letters,* 586**,** 1913-20.

DUPONT, S., MAMIDI, A., CORDENONSI, M., MONTAGNER, M., ZACCHIGNA, L., ADORNO, M., MARTELLO, G., STINCHFIELD, M. J., SOLIGO, S., MORSUT, L., INUI, M., MORO, S., MODENA, N., ARGENTON, F., NEWFELD, S. J. & PICCOLO, S. 2009. FAM/USP9x, a Deubiquitinating

Enzyme Essential for TGFβ Signaling, Controls Smad4 Monoubiquitination. *Cell,* 136**,** 123-135.

DUPONT, S., ZACCHIGNA, L., CORDENONSI, M., SOLIGO, S., ADORNO, M., RUGGE, M. & PICCOLO, S. 2005. Germ-Layer Specification and Control of Cell Growth by Ectodermin, a Smad4 Ubiquitin Ligase. *Cell,* 121**,** 87-99.

EBISAWA, T., FUKUCHI, M., MURAKAMI, G., CHIBA, T., TANAKA, K., IMAMURA, T. & MIYAZONO, K. 2001. Smurf1 interacts with transforming growth factor-beta type I receptor through Smad7 and induces receptor degradation. *J Biol Chem,* 276**,** 12477-12480.

EBISAWA, T., TADA, K., KITAJIMA, I., TOJO, K., SAMPATH, T. K., KAWABATA, M., MIYAZONO, K. & IMAMURA, T. 1999. Characterization of bone morphogenetic protein-6 signaling pathways in osteoblast differentiation. *Journal of Cell Science,* 112 (Pt 20)**,** 3519-27.

EDELMANN, M. J., IPHÖFER, A., AKUTSU, M., ALTUN, M., DI GLERIA, K., KRAMER, H. B., FIEBIGER, E., DHE-PAGANON, S. & KESSLER, B. M. 2009. Structural basis and specificity of human otubain 1-mediated deubiquitination. *Biochemical Journal,* 418**,** 379.

EDELMANN, M. J., KRAMER, H. B., ALTUN, M. & KESSLER, B. M. 2010. Post-translational modification of the deubiquitinating enzyme otubain 1 modulates active RhoA levels and susceptibility to Yersinia invasion. *FEBS Journal,* 277**,** 2515-2530.

EDLUND, S., BU, S., SCHUSTER, N., ASPENSTROM, P., HEUCHEL, R., HELDIN, N. E., TEN DIJKE, P., HELDIN, C. H. & LANDSTROM, M. 2003. Transforming growth factor-beta1 (TGF-beta)-induced apoptosis of prostate cancer cells involves Smad7-dependent activation of p38 by TGF-beta-activated kinase 1 and mitogen-activated protein kinase kinase 3. *Molecular biology of the cell,* 14**,** 529-44.

EICHHORN, P. J., RODON, L., GONZALEZ-JUNCA, A., DIRAC, A., GILI, M., MARTINEZ-SAEZ, E., AURA, C., BARBA, I., PEG, V., PRAT, A., CUARTAS, I., JIMENEZ, J., GARCIA-DORADO, D., SAHUQUILLO, J., BERNARDS, R., BASELGA, J. & SEOANE, J. 2012. USP15 stabilizes TGF-beta receptor I and promotes oncogenesis through the activation of TGF-beta signaling in glioblastoma. *Nature medicine,* 18**,** 429-35.

EIVERS, E., FUENTEALBA, L. C. & DE ROBERTIS, E. M. 2008. Integrating positional information at the level of Smad1/5/8. *Current opinion in genetics & development,* 18**,** 304-10.

ELLIOTT, P. R., LIU, H., PASTOK, M. W., GROSSMANN, G. J., RIGDEN, D. J., CLAGUE, M. J., URBÉ, S. & BARSUKOV, I. L. 2011. Structural variability of the ubiquitin specific protease DUSP-UBL double domains. *FEBS Letters,* 585**,** 3385-3390.

EMMERICH, C. H., ORDUREAU, A., STRICKSON, S., ARTHUR, J. S., PEDRIOLI, P. G., KOMANDER, D. & COHEN, P. 2013. Activation of the canonical IKK complex by K63/M1-linked hybrid ubiquitin chains. *Proceedings of the National Academy of Sciences of the United States of America,* 110**,** 15247-52.

EMRE, N. C. T. & BERGER, S. L. 2004. Histone H2B Ubiquitylation and Deubiquitylation in Genomic Regulation. *Cold Spring Harbor Symposia on Quantitative Biology,* 69**,** 289-300.

FAFEUR, V., O'HARA, B. & BÖHLEN, P. 1993. A glycosylation-deficient endothelial cell mutant with modified responses to transforming growth factor-beta and other growth inhibitory cytokines: evidence for multiple growth inhibitory signal transduction pathways. *Molecular biology of the cell,* 4**,** 135-144.

FAN, Y. H., YU, Y., MAO, R. F., TAN, X. J., XU, G. F., ZHANG, H., LU, X. B., FU, S. B. & YANG, J. 2011. USP4 targets TAK1 to downregulate TNF[alpha]-induced NF-[kappa]B activation. *Cell Death and Differentiation,* 18**,** 1547-1560.

FANG, Z., GRUTTER, C. & RAUH, D. 2013. Strategies for the selective regulation of kinases with allosteric modulators: exploiting exclusive structural features. *ACS chemical biology,* 8**,** 58-70.

FARONATO, M., PATEL, V., DARLING, S., DEARDEN, L., CLAGUE, M. J., URBE, S. & COULSON, J. M. 2013. The deubiquitylase USP15 stabilizes newly synthesized REST and rescues its expression at mitotic exit. *Cell cycle,* 12**,** 1964-77.

FERNANDES-ALNEMRI, T., LITWACK, G. & ALNEMRI, E. S. 1994. CPP32, a novel human apoptotic protein with homology to Caenorhabditis elegans cell death protein Ced-3 and mammalian interleukin-1 beta-converting enzyme. *Journal of Biological Chemistry,* 269**,** 30761-4.

FERNANDEZ, I. E. & EICKELBERG, O. 2012. The impact of TGF-beta on lung fibrosis: from targeting to biomarkers. *Proceedings of the American Thoracic Society,* 9**,** 111-6.

FERRER, C. M., LYNCH, T. P., SODI, V. L., FALCONE, J. N., SCHWAB, L. P., PEACOCK, D. L., VOCADLO, D. J., SEAGROVES, T. N. & REGINATO, M. J. 2014. O-GlcNAcylation Regulates Cancer Metabolism and Survival Stress Signaling via Regulation of the HIF-1 Pathway. *Molecular cell,* 54**,** 820-31.

FINNSON, K. W., ARANY, P. R. & PHILIP, A. 2013. Transforming Growth Factor Beta Signaling in Cutaneous Wound Healing: Lessons Learned from Animal Studies. *Advances in wound care,* 2**,** 225-237.

FLAVELL, R. A., SANJABI, S., WRZESINSKI, S. H. & LICONA-LIMON, P. 2010. The polarization of immune cells in the tumour environment by TGFbeta. *Nature reviews. Immunology,* 10**,** 554-67.

FONG, Y. C., LI, T. M., WU, C. M., HSU, S. F., KAO, S. T., CHEN, R. J., LIN, C. C., LIU, S. C., WU, C. L. & TANG, C. H. 2008. BMP-2 increases migration of human chondrosarcoma cells via PI3K/Akt pathway. *Journal of cellular physiology,* 217**,** 846-55.

FRAILE, J. M., QUESADA, V., RODRIGUEZ, D., FREIJE, J. M. & LOPEZ-OTIN, C. 2011. Deubiquitinases in cancer: new functions and therapeutic options. *Oncogene,* 31**,** 2373-88.

FRAPPIER, L. & VERRIJZER, C. P. 2011. Gene expression control by protein deubiquitinases. *Current opinion in genetics & development,* 21**,** 207-13.

FREIRE-DE-LIMA, L., GELFENBEYN, K., DING, Y., MANDEL, U., CLAUSEN, H., HANDA, K. & HAKOMORI, S. I. 2011. Involvement of O-glycosylation defining oncofetal fibronectin in epithelial-mesenchymal transition process. *Proceedings of the National Academy of Sciences of the United States of America,* 108**,** 17690-5.

FRIAS-STAHELI, N., GIANNAKOPOULOS, N. V., KIKKERT, M., TAYLOR, S. L., BRIDGEN, A., PARAGAS, J., RICHT, J. A., ROWLAND, R. R., SCHMALJOHN, C. S., LENSCHOW, D. J., SNIJDER, E. J., GARCÍA-SASTRE, A. & VIRGIN, H. W. 2007. Ovarian Tumor Domain-Containing Viral Proteases Evade Ubiquitin- and ISG15-Dependent Innate Immune Responses. *Cell host & microbe,* 2**,** 404-416.

FUKASAWA, H., YAMAMOTO, T., FUJIGAKI, Y., MISAKI, T., OHASHI, N., TAKAYAMA, T., SUZUKI, S., MUGIYA, S., ODA, T., UCHIDA, C., KITAGAWA, K., HATTORI, T., HAYASHI, H., OZONO, S., KITAGAWA, M. & HISHIDA, A. 2010. Reduction of transforming growth factor-β type II

receptor is caused by the enhanced ubiquitin-dependent degradation in human renal cell carcinoma. *International Journal of Cancer,* 127**,** 1517-1525.

FUKUCHI, M., IMAMURA, T., CHIBA, T., EBISAWA, T., KAWABATA, M., TANAKA, K. & MIYAZONO, K. 2001. Ligand-dependent degradation of Smad3 by a ubiquitin ligase complex of ROC1 and associated proteins. *Mol Biol Cell,* 12**,** 1431-1443.

GAARENSTROOM, T. & HILL, C. S. 2014. TGF-β signaling to chromatin: How Smads regulate transcription during self-renewal and differentiation. *Seminars in cell & developmental biology,* 32C**,** 107-118.

GALLIHER-BECKLEY, A. J. & SCHIEMANN, W. P. 2008. Grb2 binding to Tyr284 in TbetaR-II is essential for mammary tumor growth and metastasis stimulated by TGF-beta. *Carcinogenesis,* 29**,** 244-51.

GANLEY, I. G., WONG, P. M., GAMMOH, N. & JIANG, X. J. 2011. Distinct Autophagosomal-Lysosomal Fusion Mechanism Revealed by Thapsigargin-Induced Autophagy Arrest. *Molecular cell,* 42**,** 731-743.

GAO, S., ALARCÓN, C., SAPKOTA, G., RAHMAN, S., CHEN, P.-Y., GOERNER, N., MACIAS, M. J., ERDJUMENT-BROMAGE, H., TEMPST, P. & MASSAGUÉ, J. 2009. Ubiquitin ligase Nedd4L targets activated Smad2/3 to limit TGF-β signaling. *Molecular Cell,* 36**,** 457-468.

GAWANTKA, V., DELIUS, H., HIRSCHFELD, K., BLUMENSTOCK, C. & NIEHRS, C. 1995. Antagonizing the Spemann organizer: role of the homeobox gene Xvent-1. *The EMBO Journal,* 14**,** 6268-79.

GEOFFROY, M. C. & HAY, R. T. 2009. An additional role for SUMO in ubiquitin-mediated proteolysis. *Nature reviews. Molecular cell biology,* 10**,** 564-8.

GEYER, C. R. 2010. Strategies to re-express epigenetically silenced p15(INK4b) and p21(WAF1) genes in acute myeloid leukemia. *Epigenetics : official journal of the DNA Methylation Society,* 5**,** 696-703.

GHAVIDEL, A. & SCHULTZ, M. C. 2001. TATA binding protein-associated CK2 transduces DNA damage signals to the RNA polymerase III transcriptional machinery. *Cell,* 106**,** 575-84.

GHOSH, A. K., QUAGGIN, S. E. & VAUGHAN, D. E. 2013. Molecular basis of organ fibrosis: potential therapeutic approaches. *Experimental biology and medicine,* 238**,** 461-81.

GOETSCHY, J. F., LETOURNEUR, O., CERLETTI, N. & HORISBERGER, M. A. 1996. The unglycosylated extracellular domain of type-II receptor for transforming growth factor-beta. A novel assay for characterizing ligand affinity and specificity. *European journal of biochemistry / FEBS,* 241**,** 355-62.

GOGGINS, M., SHEKHER, M., TURNACIOGLU, K., YEO, C. J., HRUBAN, R. H. & KERN, S. E. 1998. Genetic alterations of the transforming growth factor beta receptor genes in pancreatic and biliary adenocarcinomas. *Cancer research,* 58**,** 5329-32.

GONCHAROV, T., NIESSEN, K., DE ALMAGRO, M. C., IZRAEL-TOMASEVIC, A., FEDOROVA, A. V., VARFOLOMEEV, E., ARNOTT, D., DESHAYES, K., KIRKPATRICK, D. S. & VUCIC, D. 2013. OTUB1 modulates c-IAP1 stability to regulate signalling pathways. *EMBO J,* 32**,** 1103-1114.

GOTO, K., KAMIYA, Y., IMAMURA, T., MIYAZONO, K. & MIYAZAWA, K. 2007. Selective inhibitory effects of Smad6 on bone morphogenetic protein type I receptors. *The Journal of biological chemistry,* 282**,** 20603-11.

GOTO, K., TONG, K. I., IKURA, J. & OKADA, H. 2011. HLA-B-associated transcript 3 (Bat3/Scythe) negatively regulates Smad phosphorylation in BMP signaling. *Cell death & disease,* 2**,** e236.

GOUDIE, D. R., D'ALESSANDRO, M., MERRIMAN, B., LEE, H., SZEVERENYI, I., AVERY, S., O'CONNOR, B. D., NELSON, S. F., COATS, S. E., STEWART, A., CHRISTIE, L., PICHERT, G., FRIEDEL, J., HAYES, I., BURROWS, N., WHITTAKER, S., GERDES, A. M., BROESBY-OLSEN, S., FERGUSON-SMITH, M. A., VERMA, C., LUNNY, D. P., REVERSADE, B. & LANE, E. B. 2011. Multiple self-healing squamous epithelioma is caused by a disease-specific spectrum of mutations in TGFBR1. *Nature genetics,* 43**,** 365-9.

GOUMANS, M. J., VAN ZONNEVELD, A. J. & TEN DIJKE, P. 2008. Transforming growth factor beta-induced endothelial-to-mesenchymal transition: a switch to cardiac fibrosis? *Trends in cardiovascular medicine,* 18**,** 293-8.

GOVANI, F. S. & SHOVLIN, C. L. 2009. Hereditary haemorrhagic telangiectasia: a clinical and scientific review. *European journal of human genetics : EJHG,* 17**,** 860-71.

GRIPP, K. W., WOTTON, D., EDWARDS, M. C., ROESSLER, E., ADES, L., MEINECKE, P., RICHIERI-COSTA, A., ZACKAI, E. H., MASSAGUE, J., MUENKE, M. & ELLEDGE, S. J. 2000. Mutations in TGIF cause holoprosencephaly and link NODAL signalling to human neural axis determination. *Nature genetics,* 25**,** 205-208.

GRONROOS, E., HELLMAN, U., HELDIN, C.-H. & ERICSSON, J. 2002. Control of Smad7 Stability by Competition between Acetylation and Ubiquitination. *Molecular cell,* 10**,** 483-493.

GRONROOS, E., KINGSTON, I. J., RAMACHANDRAN, A., RANDALL, R. A., VIZAN, P. & HILL, C. S. 2012. Transforming growth factor beta inhibits bone morphogenetic protein-induced transcription through novel phosphorylated Smad1/5-Smad3 complexes. *Molecular and Cellular Biology,* 32**,** 2904-16.

GROSICKI, S., BARCHNICKA, A., JURCZYSZYN, A. & GROSICKA, A. 2014. Bortezomib for the treatment of multiple myeloma. *Expert Review of Hematology,* 7**,** 173-185.

GUO, X., RAMIREZ, A., WADDELL, D. S., LI, Z., LIU, X. & WANG, X. F. 2008. Axin and GSK3- control Smad3 protein stability and modulate TGF- signaling. *Genes & Development,* 22**,** 106-20.

GUPTA, R. & BRUNAK, S. 2002. Prediction of glycosylation across the human proteome and the correlation to protein function. *Pacific Symposium on Biocomputing. Pacific Symposium on Biocomputing***,** 310-22.

GURDON, J. B., ELSDALE, T. R. & FISCHBERG, M. 1958. Sexually mature individuals of Xenopus laevis from the transplantation of single somatic nuclei. *Nature,* 182**,** 64-5.

HAHN, S. A., SCHUTTE, M., HOQUE, A. T., MOSKALUK, C. A., DA COSTA, L. T., ROZENBLUM, E., WEINSTEIN, C. L., FISCHER, A., YEO, C. J., HRUBAN, R. H. & KERN, S. E. 1996. DPC4, a candidate tumor suppressor gene at human chromosome 18q21.1. *Science,* 271**,** 350-3.

HANAHAN, D. & WEINBERG, ROBERT A. 2011. Hallmarks of Cancer: The Next Generation. *Cell,* 144**,** 646-674.

HANNA, J., HATHAWAY, N. A., TONE, Y., CROSAS, B., ELSASSER, S., KIRKPATRICK, D. S., LEGGETT, D. S., GYGI, S. P., KING, R. W. & FINLEY, D. 2006. Deubiquitinating enzyme Ubp6 functions noncatalytically to delay proteasomal degradation. *Cell,* 127**,** 99-111.

HANOVER, J. A., KRAUSE, M. W. & LOVE, D. C. 2012. Bittersweet memories: linking metabolism to epigenetics through O-GlcNAcylation. *Nature Reviews Molecular Cell Biology,* 13**,** 312-321.

HARDING, J. L., HORSWELL, S., HELIOT, C., ARMISEN, J., ZIMMERMAN, L. B., LUSCOMBE, N. M., MISKA, E. A. & HILL, C. S. 2014. Small RNA profiling

of Xenopus embryos reveals novel miRNAs and a new class of small RNAs derived from intronic transposable elements. *Genome research,* 24**,** 96-106.

HARPER, S., BESONG, T. M., EMSLEY, J., SCOTT, D. J. & DREVENY, I. 2011. Structure of the USP15 N-terminal domains: a beta-hairpin mediates close association between the DUSP and UBL domains. *Biochemistry,* 50**,** 7995-8004.

HART, G. W., SLAWSON, C., RAMIREZ-CORREA, G. & LAGERLOF, O. 2011. Cross Talk Between O-GlcNAcylation and Phosphorylation: Roles in Signaling, Transcription, and Chronic Disease. *Annual Review of Biochemistry,* 80**,** 825-858.

HARWOOD, K. R. & HANOVER, J. A. 2014. Nutrient-driven O-GlcNAc cycling – think globally but act locally. *Journal of Cell Science,* 127**,** 1857-1867.

HAWINKELS, L. J. & TEN DIJKE, P. 2011. Exploring anti-TGF-beta therapies in cancer and fibrosis. *Growth factors,* 29**,** 140-52.

HAY, R. T. 2007. SUMO-specific proteases: a twist in the tail. *Trends in Cell Biology,* 17**,** 370-6.

HAY, R. T. 2013. Decoding the SUMO signal. *Biochemical Society transactions,* 41**,** 463-73.

HAYES, S. D., LIU, H., MACDONALD, E., SANDERSON, C. M., COULSON, J. M., CLAGUE, M. J. & URBE, S. 2012. Direct and indirect control of mitogen-activated protein kinase pathway-associated components, BRAP/IMP E3 ubiquitin ligase and CRAF/RAF1 kinase, by the deubiquitylating enzyme USP15. *The Journal of biological chemistry,* 287**,** 43007-18.

HE, W., DORN, D. C., ERDJUMENT-BROMAGE, H., TEMPST, P., MOORE, M. A. S. & MASSAGUÉ, J. 2006. Hematopoiesis Controlled by Distinct TIF1γ and Smad4 Branches of the TGFβ Pathway. *Cell,* 125**,** 929-941.

HEIKKINEN, P. T., NUMMELA, M., LEIVONEN, S. K., WESTERMARCK, J., HILL, C. S., KAHARI, V. M. & JAAKKOLA, P. M. 2010. Hypoxia-activated Smad3-specific dephosphorylation by PP2A. *The Journal of biological chemistry,* 285**,** 3740-9.

HELDIN, C. H., LANDSTROM, M. & MOUSTAKAS, A. 2009. Mechanism of TGF-beta signaling to growth arrest, apoptosis, and epithelial-mesenchymal transition. *Current opinion in cell biology,* 21**,** 166-76.

HELDIN, C. H., MIYAZONO, K. & TEN DIJKE, P. 1997. TGF-beta signalling from cell membrane to nucleus through SMAD proteins. *Nature,* 390**,** 465-71.

HELDIN, C. H., VANLANDEWIJCK, M. & MOUSTAKAS, A. 2012. Regulation of EMT by TGFbeta in cancer. *FEBS letters,* 586**,** 1959-70.

HELLWINKEL, O. J., ASONG, L. E., ROGMANN, J. P., SULTMANN, H., WAGNER, C., SCHLOMM, T. & EICHELBERG, C. 2011. Transcription alterations of members of the ubiquitin-proteasome network in prostate carcinoma. *Prostate cancer and prostatic diseases,* 14**,** 38-45.

HERHAUS, L., AL-SALIHI, M., DINGWELL, K. S., CUMMINS, T. D., WASMUS, L., VOGT, J., EWAN, R., BRUCE, D., MACARTNEY, T., WEIDLICH, S., SMITH, J. C. & SAPKOTA, G. P. 2014. USP15 targets ALK3/BMPR1A for deubiquitylation to enhance bone morphogenetic protein signalling. *Open Biology,* 4**,** 140065.

HERHAUS, L., AL-SALIHI, M., MACARTNEY, T., WEIDLICH, S. & SAPKOTA, G. P. 2013. OTUB1 enhances TGFβ signalling by inhibiting the ubiquitylation and degradation of active SMAD2/3. *Nature Communications,* 4**,** 2519.

HERHAUS, L. & SAPKOTA, G. P. 2014. The emerging roles of deubiquitylating enzymes (DUBs) in the TGFβ and BMP pathways. *Cellular signalling,* 26**,** 2186-2192.

HERSHKO, A., CIECHANOVER, A. & ROSE, I. A. 1979. Resolution of the ATP-dependent proteolytic system from reticulocytes: a component that interacts with ATP. *Proceedings of the National Academy of Sciences of the United States of America,* 76**,** 3107-10.

HERSHKO, A., HELLER, H., ELIAS, S. & CIECHANOVER, A. 1983. Components of ubiquitin-protein ligase system. Resolution, affinity purification, and role in protein breakdown. *The Journal of biological chemistry,* 258**,** 8206-14.

HETFELD, B. K., HELFRICH, A., KAPELARI, B., SCHEEL, H., HOFMANN, K., GUTERMAN, A., GLICKMAN, M., SCHADE, R., KLOETZEL, P. M. & DUBIEL, W. 2005. The zinc finger of the CSN-associated deubiquitinating enzyme USP15 is essential to rescue the E3 ligase Rbx1. *Current biology : CB,* 15**,** 1217-21.

HILL, C. S. 2009. Nucleocytoplasmic shuttling of Smad proteins. *Cell research,* 19**,** 36-46.

HINCK, A. P. 2012. Structural studies of the TGF-betas and their receptors - insights into evolution of the TGF-beta superfamily. *FEBS Letters,* 586**,** 1860-70.

HO, J., COCOLAKIS, E., DUMAS, V. M., POSNER, B. I., LAPORTE, S. A. & LEBRUN, J. J. 2005. The G protein-coupled receptor kinase-2 is a TGFbeta-inducible antagonist of TGFbeta signal transduction. *The EMBO Journal,* 24**,** 3247-58.

HOCHSTRASSER, M. 2009. Origin and function of ubiquitin-like proteins. *Nature,* 458**,** 422-9.

HOFMANN, R. M. & PICKART, C. M. 1999. Noncanonical MMS2-Encoded Ubiquitin-Conjugating Enzyme Functions in Assembly of Novel Polyubiquitin Chains for DNA Repair. *Cell,* 96**,** 645-653.

HOLTZHAUSEN, A., GOLZIO, C., HOW, T., LEE, Y.-H., SCHIEMANN, W. P., KATSANIS, N. & BLOBE, G. C. 2014. Novel bone morphogenetic protein signaling through Smad2 and Smad3 to regulate cancer progression and development. *The FASEB Journal,* 28**,** 1248-1267.

HONG, S. W., ISONO, M., CHEN, S., IGLESIAS-DE LA CRUZ, M. C., HAN, D. C. & ZIYADEH, F. N. 2001. Increased glomerular and tubular expression of transforming growth factor-beta1, its type II receptor, and activation of the Smad signaling pathway in the db/db mouse. *The American journal of pathology,* 158**,** 1653-63.

HOSPENTHAL, M. K., FREUND, S. M. V. & KOMANDER, D. 2013. Assembly, analysis and architecture of atypical ubiquitin chains. *Nat Struct Mol Biol,* 20**,** 555-565.

HOUGH, C., RADU, M. & DORÉ, J. J. E. 2012. TGF-Beta Induced Erk Phosphorylation of Smad Linker Region Regulates Smad Signaling. *PLoS ONE,* 7**,** e42513.

HOWE, J. R., SAYED, M. G., AHMED, A. F., RINGOLD, J., LARSEN-HAIDLE, J., MERG, A., MITROS, F. A., VACCARO, C. A., PETERSEN, G. M., GIARDIELLO, F. M., TINLEY, S. T., AALTONEN, L. A. & LYNCH, H. T. 2004. The prevalence of MADH4 and BMPR1A mutations in juvenile polyposis and absence of BMPR2, BMPR1B, and ACVR1 mutations. *Journal of medical genetics,* 41**,** 484-91.

HUANG, O. W., MA, X., YIN, J., FLINDERS, J., MAURER, T., KAYAGAKI, N., PHUNG, Q., BOSANAC, I., ARNOTT, D., DIXIT, V. M., HYMOWITZ, S. G., STAROVASNIK, M. A. & COCHRAN, A. G. 2012. Phosphorylation-dependent activity of the deubiquitinase DUBA. *Nature Structural and Molecular Biology,* 19**,** 171-175.

HUANG, S. S. & HUANG, J. S. 2005. TGF-β control of cell proliferation. *Journal of Cellular Biochemistry,* 96**,** 447-462.

HUANG, X., LANGELOTZ, C., HETFELD-PECHOC, B. K., SCHWENK, W. & DUBIEL, W. 2009. The COP9 signalosome mediates beta-catenin degradation by deneddylation and blocks adenomatous polyposis coli destruction via USP15. *Journal of molecular biology,* 391**,** 691-702.

HULTH, A. G., NILSSON, B. E., WESTLIN, N. E. & WIKLUND, P. E. 1979. Alkaline Phosphatase in Women with Osteoporosis. *Acta Medica Scandinavica,* 206**,** 201-203.

HURTADO-GUERRERO, R., DORFMUELLER, H. C. & VAN AALTEN, D. M. F. 2008. Molecular mechanisms of O-GlcNAcylation. *Current Opinion in Structural Biology,* 18**,** 551-557.

HUSE, M., CHEN, Y. G., MASSAGUE, J. & KURIYAN, J. 1999. Crystal structure of the cytoplasmic domain of the type I TGF beta receptor in complex with FKBP12. *Cell,* 96**,** 425-36.

HUSE, M., MUIR, T. W., XU, L., CHEN, Y. G., KURIYAN, J. & MASSAGUE, J. 2001. The TGF beta receptor activation process: an inhibitor- to substrate-binding switch. *Molecular cell,* 8**,** 671-82.

HUSNJAK, K. & DIKIC, I. 2012. Ubiquitin-binding proteins: decoders of ubiquitin-mediated cellular functions. *Annual Review of Biochemistry,* 81**,** 291-322.

HWANG, I. W., MAKISHIMA, Y., KATO, T., PARK, S., TERZIC, A. & PARK, E. Y. 2014. Human acetyl-CoA carboxylase 2 expressed in silkworm Bombyx mori exhibits posttranslational biotinylation and phosphorylation. *Applied microbiology and biotechnology,* Epub ahead of print.

IBARROLA, N., KRATCHMAROVA, I., NAKAJIMA, D., SCHIEMANN, W., MOUSTAKAS, A., PANDEY, A. & MANN, M. 2004. Cloning of a novel signaling molecule, AMSH-2, that potentiates transforming growth factor beta signaling. *BMC Cell Biology,* 5**,** 2.

IGARASHI, A., OKOCHI, H., BRADHAM, D. M. & GROTENDORST, G. R. 1993. Regulation of connective tissue growth factor gene expression in human skin fibroblasts and during wound repair. *Molecular biology of the cell,* 4**,** 637-45.

IMAMURA, T., OSHIMA, Y. & HIKITA, A. 2013. Regulation of TGF-β family signalling by ubiquitination and deubiquitination. *Journal of Biochemistry,* 154**,** 481-489.

INAMITSU, M., ITOH, S., HELLMAN, U., TEN DIJKE, P. & KATO, M. 2006. Methylation of Smad6 by protein arginine N-methyltransferase 1. *FEBS Letters,* 580**,** 6603-11.

INMAN, G. J. 2011. Switching TGFbeta from a tumor suppressor to a tumor promoter. *Current opinion in genetics & development,* 21**,** 93-9.

INOUE, Y. & IMAMURA, T. 2008. Regulation of TGF-beta family signaling by E3 ubiquitin ligases. *Cancer science,* 99**,** 2107-12.

INUI, M., MANFRIN, A., MAMIDI, A., MARTELLO, G., MORSUT, L., SOLIGO, S., ENZO, E., MORO, S., POLO, S., DUPONT, S., CORDENONSI, M. & PICCOLO, S. 2011. USP15 is a deubiquitylating enzyme for receptor-activated SMADs. *Nature cell biology,* 13**,** 1368-75.

ISUMI, Y., HIRATA, T., SAITOH, H., MIYAKAWA, T., MURAKAMI, K., KUDOH, G., DOI, H., ISHIBASHI, K. & NAKAJIMA, H. 2011. Transgenic overexpression of USP15 in the heart induces cardiac remodeling in mice. *Biochemical and Biophysical Research Communications,* 405**,** 216-21.

ITO, I., HANYU, A., WAYAMA, M., GOTO, N., KATSUNO, Y., KAWASAKI, S., NAKAJIMA, Y., KAJIRO, M., KOMATSU, Y., FUJIMURA, A., HIROTA, R., MURAYAMA, A., KIMURA, K., IMAMURA, T. & YANAGISAWA, J. 2010.

Estrogen inhibits transforming growth factor beta signaling by promoting Smad2/3 degradation. *The Journal of biological chemistry,* 285**,** 14747-55.

ITOH, F., ASAO, H., SUGAMURA, K., HELDIN, C. H., TEN DIJKE, P. & ITOH, S. 2001. Promoting bone morphogenetic protein signaling through negative regulation of inhibitory Smads. *The EMBO Journal,* 20**,** 4132-4142.

ITOH, F., WATABE, T. & MIYAZONO, K. 2014. Roles of TGF-β family signals in the fate determination of pluripotent stem cells. *Seminars in cell & developmental biology,* 32C**,** 98-106.

ITOH, S. & TEN DIJKE, P. 2007. Negative regulation of TGF-beta receptor/Smad signal transduction. *Current opinion in cell biology,* 19**,** 176-84.

IWAHANA, H., YAKYMOVYCH, I., DUBROVSKA, A., HELLMAN, U. & SOUCHELNYTSKYI, S. 2006. Glycoproteome profiling of transforming growth factor-beta (TGFbeta) signaling: nonglycosylated cell death-inducing DFF-like effector A inhibits TGFbeta1-dependent apoptosis. *Proteomics,* 6**,** 6168-80.

JIANG, F., LIU, G. S., DUSTING, G. J. & CHAN, E. C. 2014. NADPH oxidase-dependent redox signaling in TGF-beta-mediated fibrotic responses. *Redox biology,* 2**,** 267-72.

JO, M., LESTER, R. D., MONTEL, V., EASTMAN, B., TAKIMOTO, S. & GONIAS, S. L. 2009. Reversibility of epithelial-mesenchymal transition (EMT) induced in breast cancer cells by activation of urokinase receptor-dependent cell signaling. *The Journal of biological chemistry,* 284**,** 22825-33.

JOHNSON, D. W., BERG, J. N., BALDWIN, M. A., GALLIONE, C. J., MARONDEL, I., YOON, S. J., STENZEL, T. T., SPEER, M., PERICAK-VANCE, M. A., DIAMOND, A., GUTTMACHER, A. E., JACKSON, C. E., ATTISANO, L., KUCHERLAPATI, R., PORTEOUS, M. E. & MARCHUK, D. A. 1996. Mutations in the activin receptor-like kinase 1 gene in hereditary haemorrhagic telangiectasia type 2. *Nature genetics,* 13**,** 189-95.

JOSSO, N., BELVILLE, C., DI CLEMENTE, N. & PICARD, J. Y. 2005. AMH and AMH receptor defects in persistent Mullerian duct syndrome. *Human reproduction update,* 11**,** 351-6.

JUANG, Y. C., LANDRY, M. C., SANCHES, M., VITTAL, V., LEUNG, C. C., CECCARELLI, D. F., MATEO, A. R., PRUNEDA, J. N., MAO, D. Y., SZILARD, R. K., ORLICKY, S., MUNRO, M., BRZOVIC, P. S., KLEVIT, R. E., SICHERI, F. & DUROCHER, D. 2012. OTUB1 Co-opts Lys48-Linked Ubiquitin Recognition to Suppress E2 Enzyme Function. *Molecular cell,* 45**,** 384-97.

JUNG, K., LEIN, M., STEPHAN, C., VON HÖSSLIN, K., SEMJONOW, A., SINHA, P., LOENING, S. A. & SCHNORR, D. 2004. Comparison of 10 serum bone turnover markers in prostate carcinoma patients with bone metastatic spread: Diagnostic and prognostic implications. *International Journal of Cancer,* 111**,** 783-791.

JUNG, S. M., LEE, J.-H., PARK, J., OH, Y. S., LEE, S. K., PARK, J. S., LEE, Y. S., KIM, J. H., LEE, J. Y., BAE, Y.-S., KOO, S.-H., KIM, S.-J. & PARK, S. H. 2013. Smad6 inhibits non-canonical TGF-β1 signalling by recruiting the deubiquitinase A20 to TRAF6. *Nature Communications,* 4.

JURIS, S. J., SHAH, K., SHOKAT, K., DIXON, J. E. & VACRATSIS, P. O. 2006. Identification of otubain 1 as a novel substrate for the Yersinia protein kinase using chemical genetics and mass spectrometry. *FEBS Letters,* 580**,** 179-183.

KAMADURAI, H. B., QIU, Y., DENG, A., HARRISON, J. S., MACDONALD, C., ACTIS, M., RODRIGUES, P., MILLER, D. J., SOUPHRON, J., LEWIS, S. M., KURINOV, I., FUJII, N., HAMMEL, M., PIPER, R., KUHLMAN, B. &

SCHULMAN, B. A. 2013. Mechanism of ubiquitin ligation and lysine prioritization by a HECT E3. *eLife,* 2**,** e00828.

KAMADURAI, H. B., SOUPHRON, J., SCOTT, D. C., DUDA, D. M., MILLER, D. J., STRINGER, D., PIPER, R. C. & SCHULMAN, B. A. 2009. Insights into ubiquitin transfer cascades from a structure of a UbcH5B approximately ubiquitin-HECT(NEDD4L) complex. *Molecular cell,* 36**,** 1095-102.

KANG, J. S., SAUNIER, E. F., AKHURST, R. J. & DERYNCK, R. 2008. The type I TGF-[beta] receptor is covalently modified and regulated by sumoylation. *Nature cell biology,* 10**,** 654-664.

KATAGIRI, T., IMADA, M., YANAI, T., SUDA, T., TAKAHASHI, N. & KAMIJO, R. 2002. Identification of a BMP-responsive element in Id1, the gene for inhibition of myogenesis. *Genes to cells : devoted to molecular & cellular mechanisms,* 7**,** 949-60.

KATAGIRI, T., YAMAGUCHI, A., KOMAKI, M., ABE, E., TAKAHASHI, N., IKEDA, T., ROSEN, V., WOZNEY, J. M., FUJISAWA-SEHARA, A. & SUDA, T. 1994. Bone morphogenetic protein-2 converts the differentiation pathway of C2C12 myoblasts into the osteoblast lineage. *The Journal of Cell Biology,* 127**,** 1755-1766.

KATO, M., DANG, V., WANG, M., PARK, J. T., DESHPANDE, S., KADAM, S., MARDIROS, A., ZHAN, Y., OETTGEN, P., PUTTA, S., YUAN, H., LANTING, L. & NATARAJAN, R. 2013. TGF-{beta} Induces Acetylation of Chromatin and of Ets-1 to Alleviate Repression of miR-192 in Diabetic Nephropathy. *Sci. Signal.,* 6**,** ra43-.

KATZ, E. J., ISASA, M. & CROSAS, B. 2010. A new map to understand deubiquitination. *Biochemical Society transactions,* 38**,** 21-8.

KAVSAK, P., RASMUSSEN, R. K., CAUSING, C. G., BONNI, S., ZHU, H., THOMSEN, G. H. & WRANA, J. L. 2000. Smad7 binds to Smurf2 to form an E3 ubiquitin ligase that targets the TGF beta receptor for degradation. *Mol Cell,* 6**,** 1365-1375.

KESSLER, B. M. & EDELMANN, M. J. 2011. PTMs in conversation: activity and function of deubiquitinating enzymes regulated via post-translational modifications. *Cell biochemistry and biophysics,* 60**,** 21-38.

KIELTY, C. M., BALDOCK, C., LEE, D., ROCK, M. J., ASHWORTH, J. L. & SHUTTLEWORTH, C. A. 2002. Fibrillin: from microfibril assembly to biomechanical function. *Philosophical transactions of the Royal Society of London. Series B, Biological sciences,* 357**,** 207-17.

KIM, H. J., KIM, J. G., MOON, M. Y., PARK, S. H. & PARK, J. B. 2014. IkappaB kinase gamma/nuclear factor-kappaB-essential modulator (IKKgamma/NEMO) facilitates RhoA GTPase activation, which, in turn, activates Rho-associated KINASE (ROCK) to phosphorylate IKKbeta in response to transforming growth factor (TGF)-beta1. *The Journal of biological chemistry,* 289**,** 1429-40.

KIM, W., BENNETT, ERIC J., HUTTLIN, EDWARD L., GUO, A., LI, J., POSSEMATO, A., SOWA, MATHEW E., RAD, R., RUSH, J., COMB, MICHAEL J., HARPER, J. W. & GYGI, STEVEN P. 2011. Systematic and Quantitative Assessment of the Ubiquitin-Modified Proteome. *Molecular cell,* 44**,** 325-340.

KIM, Y. W., PARK, J., LEE, H. J., LEE, S. Y. & KIM, S. J. 2012. TGF-beta sensitivity is determined by N-linked glycosylation of the type II TGF-beta receptor. *The Biochemical journal,* 445**,** 403-11.

KNOCKAERT, M., SAPKOTA, G., ALARCON, C., MASSAGUE, J. & BRIVANLOU, A. H. 2006. Unique players in the BMP pathway: small C-terminal domain phosphatases dephosphorylate Smad1 to attenuate BMP

signaling. *Proceedings of the National Academy of Sciences of the United States of America,* 103**,** 11940-5.

KODACH, L. L., BLEUMING, S. A., PEPPELENBOSCH, M. P., HOMMES, D. W., VAN DEN BRINK, G. R. & HARDWICK, J. C. 2007. The effect of statins in colorectal cancer is mediated through the bone morphogenetic protein pathway. *Gastroenterology,* 133**,** 1272-81.

KOINUMA, D., SHINOZAKI, M., KOMURO, A., GOTO, K., SAITOH, M., HANYU, A., EBINA, M., NUKIWA, T., MIYAZAWA, K., IMAMURA, T. & MIYAZONO, K. 2003. Arkadia amplifies TGF-beta superfamily signalling through degradation of Smad7. *The EMBO Journal,* 22**,** 6458-70.

KOKABU, S., NOJIMA, J., KANOMATA, K., OHTE, S., YODA, T., FUKUDA, T. & KATAGIRI, T. 2010. Protein phosphatase magnesium-dependent 1A-mediated inhibition of BMP signaling is independent of Smad dephosphorylation. *Journal of bone and mineral research : the official journal of the American Society for Bone and Mineral Research,* 25**,** 653-60.

KOLM-LITTY, V., SAUER, U., NERLICH, A., LEHMANN, R. & SCHLEICHER, E. D. 1998. High glucose-induced transforming growth factor beta1 production is mediated by the hexosamine pathway in porcine glomerular mesangial cells. *The Journal of clinical investigation,* 101**,** 160-9.

KOMANDER, D., CLAGUE, M. J. & URBE, S. 2009. Breaking the chains: structure and function of the deubiquitinases. *Nature reviews. Molecular cell biology,* 10**,** 550-63.

KOMANDER, D., LORD, C. J., SCHEEL, H., SWIFT, S., HOFMANN, K., ASHWORTH, A. & BARFORD, D. 2008. The Structure of the CYLD USP Domain Explains Its Specificity for Lys63-Linked Polyubiquitin and Reveals a B Box Module. *Molecular cell,* 29**,** 451-464.

KOMANDER, D. & RAPE, M. 2012. The ubiquitin code. *Annual review of biochemistry,* 81**,** 203-29.

KOMURO, A., IMAMURA, T., SAITOH, M., YOSHIDA, Y., YAMORI, T., MIYAZONO, K. & MIYAZAWA, K. 2004. Negative regulation of transforming growth factor-beta (TGF-beta) signaling by WW domain-containing protein 1 (WWP1). *Oncogene,* 23**,** 6914-23.

KONG, W., YANG, H., HE, L., ZHAO, J. J., COPPOLA, D., DALTON, W. S. & CHENG, J. Q. 2008. MicroRNA-155 is regulated by the transforming growth factor beta/Smad pathway and contributes to epithelial cell plasticity by targeting RhoA. *Molecular and Cellular Biology,* 28**,** 6773-84.

KORN, I., GUTKIND, S., SRINIVASAN, N., BLUNDELL, T. L., ALLENDE, C. C. & ALLENDE, J. E. 1999. Interactions of protein kinase CK2 subunits. *Molecular and Cellular Biochemistry,* 191**,** 75-83.

KRAUSE, C., KLOEN, P. & TEN DIJKE, P. 2011. Elevated transforming growth factor beta and mitogen-activated protein kinase pathways mediate fibrotic traits of Dupuytren's disease fibroblasts. *Fibrogenesis & tissue repair,* 4**,** 14.

KREPPEL, L. K., BLOMBERG, M. A. & HART, G. W. 1997. Dynamic Glycosylation of Nuclear and Cytosolic Proteins: cloning and characterization of a unique O-GlcNAc transferase with multiple tetratricopeptide repeats. *Journal of Biological Chemistry,* 272**,** 9308-9315.

KULATHU, Y. & KOMANDER, D. 2012. Atypical ubiquitylation — the unexplored world of polyubiquitin beyond Lys48 and Lys63 linkages. *Nature Reviews Molecular Cell Biology,* 13**,** 508-523.

KUME, S., HANEDA, M., KANASAKI, K., SUGIMOTO, T., ARAKI, S.-I., ISSHIKI, K., ISONO, M., UZU, T., GUARENTE, L., KASHIWAGI, A. & KOYA, D. 2007. SIRT1 Inhibits Transforming Growth Factor β-Induced Apoptosis in

Glomerular Mesangial Cells via Smad7 Deacetylation. *Journal of Biological Chemistry,* 282**,** 151-158.

KURATOMI, G., KOMURO, A., GOTO, K., SHINOZAKI, M., MIYAZAWA, K., MIYAZONO, K. & IMAMURA, T. 2005. NEDD4-2 (neural precursor cell expressed, developmentally down-regulated 4-2) negatively regulates TGF-beta (transforming growth factor-beta) signalling by inducing ubiquitin-mediated degradation of Smad2 and TGF-beta type I receptor. *The Biochemical journal,* 386**,** 461-70.

KWEI, K. A., SHAIN, A. H., BAIR, R., MONTGOMERY, K., KARIKARI, C. A., VAN DE RIJN, M., HIDALGO, M., MAITRA, A., BASHYAM, M. D. & POLLACK, J. R. 2011. SMURF1 amplification promotes invasiveness in pancreatic cancer. *PLoS ONE,* 6**,** e23924.

LAGNA, G., HATA, A., HEMMATI-BRIVANLOU, A. & MASSAGUE, J. 1996. Partnership between DPC4 and SMAD proteins in TGF-beta signalling pathways. *Nature,* 383**,** 832-6.

LALLEMAND, F., SEO, S. R., FERRAND, N., PESSAH, M., L'HOSTE, S., RAWADI, G., ROMAN-ROMAN, S., CAMONIS, J. & ATFI, A. 2005. AIP4 restricts transforming growth factor-beta signaling through a ubiquitination-independent mechanism. *The Journal of biological chemistry,* 280**,** 27645-53.

LAMOUILLE, S., CONNOLLY, E., SMYTH, J. W., AKHURST, R. J. & DERYNCK, R. 2012. TGF-beta-induced activation of mTOR complex 2 drives epithelial-mesenchymal transition and cell invasion. *Journal of Cell Science,* 125**,** 1259-73.

LAMOUILLE, S. & DERYNCK, R. 2007. Cell size and invasion in TGF-beta-induced epithelial to mesenchymal transition is regulated by activation of the mTOR pathway. *The Journal of cell biology,* 178**,** 437-51.

LAN, T. H., HUANG, X. Q. & TAN, H. M. 2013. Vascular fibrosis in atherosclerosis. *Cardiovascular pathology : the official journal of the Society for Cardiovascular Pathology,* 22**,** 401-7.

LATCHFORD, A. R., NEALE, K., PHILLIPS, R. K. & CLARK, S. K. 2012. Juvenile polyposis syndrome: a study of genotype, phenotype, and long-term outcome. *Diseases of the colon and rectum,* 55**,** 1038-43.

LAWLER, S., FENG, X. H., CHEN, R. H., MARUOKA, E. M., TURCK, C. W., GRISWOLD-PRENNER, I. & DERYNCK, R. 1997. The type II transforming growth factor-beta receptor autophosphorylates not only on serine and threonine but also on tyrosine residues. *The Journal of biological chemistry,* 272**,** 14850-9.

LAZARUS, M. B., NAM, Y., JIANG, J., SLIZ, P. & WALKER, S. 2011. Structure of human O-GlcNAc transferase and its complex with a peptide substrate. *Nature,* 469**,** 564-7.

LEASK, A. & ABRAHAM, D. J. 2004. TGF-beta signaling and the fibrotic response. *FASEB journal : official publication of the Federation of American Societies for Experimental Biology,* 18**,** 816-27.

LEE, H. S. 2012. Paracrine role for TGF-beta-induced CTGF and VEGF in mesangial matrix expansion in progressive glomerular disease. *Histology and histopathology,* 27**,** 1131-41.

LEE, M. J., LEE, B. H., HANNA, J., KING, R. W. & FINLEY, D. 2011. Trimming of ubiquitin chains by proteasome-associated deubiquitinating enzymes. *Molecular & cellular proteomics : MCP,* 10**,** R110 003871.

LEE, M. K., PARDOUX, C., HALL, M. C., LEE, P. S., WARBURTON, D., QING, J., SMITH, S. M. & DERYNCK, R. 2007. TGF-beta activates Erk MAP kinase signalling through direct phosphorylation of ShcA. *The EMBO journal,* 26**,** 3957-67.

LEE, P. S. W., CHANG, C., LIU, D. & DERYNCK, R. 2003. Sumoylation of Smad4, the Common Smad Mediator of Transforming Growth Factor-β Family Signaling. *Journal of Biological Chemistry,* 278**,** 27853-27863.

LEE, R. C., FEINBAUM, R. L. & AMBROS, V. 1993. The C. elegans heterochronic gene lin-4 encodes small RNAs with antisense complementarity to lin-14. *Cell,* 75**,** 843-54.

LEHMANN, K., SEEMANN, P., SILAN, F., GOECKE, T. O., IRGANG, S., KJAER, K. W., KJAERGAARD, S., MAHONEY, M. J., MORLOT, S., REISSNER, C., KERR, B., WILKIE, A. O. & MUNDLOS, S. 2007. A new subtype of brachydactyly type B caused by point mutations in the bone morphogenetic protein antagonist NOGGIN. *American journal of human genetics,* 81**,** 388-96.

LEVY, L. & HILL, C. S. 2005. Smad4 dependency defines two classes of transforming growth factor-beta (TGF-beta) target genes and distinguishes TGF-beta-induced epithelial-mesenchymal transition from its antiproliferative and migratory responses. *Molecular and Cellular Biology,* 25**,** 8108-25.

LEVY, L., HOWELL, M., DAS, D., HARKIN, S., EPISKOPOU, V. & HILL, C. S. 2007. Arkadia Activates Smad3/Smad4-Dependent Transcription by Triggering Signal-Induced SnoN Degradation. *Molecular and cellular biology,* 27**,** 6068-6083.

LI, L., XIN, H., XU, X., HUANG, M., ZHANG, X., CHEN, Y., ZHANG, S., FU, X.-Y. & CHANG, Z. 2004. CHIP mediates degradation of Smad proteins and potentially regulates Smad-induced transcription. *Mol Cell Biol,* 24**,** 856-864.

LI, S., ZHENG, H., MAO, A. P., ZHONG, B., LI, Y., LIU, Y., GAO, Y., RAN, Y., TIEN, P. & SHU, H. B. 2010. Regulation of virus-triggered signaling by OTUB1- and OTUB2-mediated deubiquitination of TRAF3 and TRAF6. *The Journal of biological chemistry,* 285**,** 4291-7.

LI, Y., SUN, X. X., ELFERICH, J., SHINDE, U., DAVID, L. L. & DAI, M. S. 2014. Monoubiquitination is critical for ovarian tumor domain-containing ubiquitin aldehyde binding protein 1 (Otub1) to suppress UbcH5 enzyme and stabilize p53 protein. *The Journal of biological chemistry,* 289**,** 5097-108.

LIANG, M., LIANG, Y.-Y., WRIGHTON, K., UNGERMANNOVA, D., WANG, X.-P., BRUNICARDI, F. C., LIU, X., FENG, X.-H. & LIN, X. 2004. Ubiquitination and Proteolysis of Cancer-Derived Smad4 Mutants by SCFSkp2. *Molecular and Cellular Biology,* 24**,** 7524-7537.

LIM, J. H., JONO, H., KOMATSU, K., WOO, C.-H., LEE, J., MIYATA, M., MATSUNO, T., XU, X., HUANG, Y., ZHANG, W., PARK, S. H., KIM, Y.-I., CHOI, Y.-D., SHEN, H., HEO, K.-S., XU, H., BOURNE, P., KOGA, T., XU, H., YAN, C., WANG, B., CHEN, L.-F., FENG, X.-H. & LI, J.-D. 2012. CYLD negatively regulates transforming growth factor-β-signalling via deubiquitinating Akt. *Nature Communications,* 3**,** 771.

LIN, K. W., YAKYMOVYCH, I., JIA, M., YAKYMOVYCH, M. & SOUCHELNYTSKYI, S. 2010. Phosphorylation of eEF1A1 at Ser300 by TbetaR-I results in inhibition of mRNA translation. *Current biology : CB,* 20**,** 1615-25.

LIN, S. J., LERCH, T. F., COOK, R. W., JARDETZKY, T. S. & WOODRUFF, T. K. 2006a. The structural basis of TGF-β, bone morphogenetic protein, and activin ligand binding. *Reproduction,* 132**,** 179-190.

LIN, X., DUAN, X., LIANG, Y. Y., SU, Y., WRIGHTON, K. H., LONG, J., HU, M., DAVIS, C. M., WANG, J., BRUNICARDI, F. C., SHI, Y., CHEN, Y. G., MENG, A. & FENG, X. H. 2006b. PPM1A functions as a Smad phosphatase to terminate TGFbeta signaling. *Cell,* 125**,** 915-28.

LIN, X., LIANG, M. & FENG, X. H. 2000. Smurf2 is a ubiquitin E3 ligase mediating proteasome-dependent degradation of Smad2 in transforming growth factor-beta signaling. *The Journal of biological chemistry,* 275**,** 36818-22.

LIN, X., LIANG, M., LIANG, Y.-Y., BRUNICARDI, F. C., MELCHIOR, F. & FENG, X.-H. 2003. Activation of Transforming Growth Factor-β Signaling by SUMO-1 Modification of Tumor Suppressor Smad4/DPC4. *Journal of Biological Chemistry,* 278**,** 18714-18719.

LITCHFIELD, D. W. 2003. Protein kinase CK2: structure, regulation and role in cellular decisions of life and death. *The Biochemical journal,* 369**,** 1-15.

LIU, D., BLACK, B. L. & DERYNCK, R. 2001. TGF-β inhibits muscle differentiation through functional repression of myogenic transcription factors by Smad3. *Genes & Development,* 15**,** 2950-2966.

LIU, W., RUI, H., WANG, J., LIN, S., HE, Y., CHEN, M., LI, Q., YE, Z., ZHANG, S., CHAN, S. C., CHEN, Y. G., HAN, J. & LIN, S. C. 2006. Axin is a scaffold protein in TGF-beta signaling that promotes degradation of Smad7 by Arkadia. *The EMBO Journal,* 25**,** 1646-58.

LIU, X., JIANG, W.-N., WANG, J.-G. & CHEN, H. 2014a. Colon cancer bears overexpression of OTUB1. *Pathology - Research and Practice,* doi: 10.1016/j.prp.2014.05.008.

LIU, X., LI, H., ZHONG, B., BLONSKA, M., GORJESTANI, S., YAN, M., TIAN, Q., ZHANG, D.-E., LIN, X. & DONG, C. 2013. USP18 inhibits NF-κB and NFAT activation during Th17 differentiation by deubiquitinating the TAK1−TAB1 complex. *The Journal of Experimental Medicine,* 210**,** 1575-1590.

LIU, X., LI, L., WANG, Y., YAN, H., MA, X., WANG, P. G. & ZHANG, L. 2014b. A peptide panel investigation reveals the acceptor specificity of O-GlcNAc transferase. *FASEB journal,* Epub ahead of print.

LOEYS, B. L., CHEN, J., NEPTUNE, E. R., JUDGE, D. P., PODOWSKI, M., HOLM, T., MEYERS, J., LEITCH, C. C., KATSANIS, N., SHARIFI, N., XU, F. L., MYERS, L. A., SPEVAK, P. J., CAMERON, D. E., DE BACKER, J., HELLEMANS, J., CHEN, Y., DAVIS, E. C., WEBB, C. L., KRESS, W., COUCKE, P., RIFKIN, D. B., DE PAEPE, A. M. & DIETZ, H. C. 2005. A syndrome of altered cardiovascular, craniofacial, neurocognitive and skeletal development caused by mutations in TGFBR1 or TGFBR2. *Nature genetics,* 37**,** 275-81.

LOIZOU, J. I., EL-KHAMISY, S. F., ZLATANOU, A., MOORE, D. J., CHAN, D. W., QIN, J., SARNO, S., MEGGIO, F., PINNA, L. A. & CALDECOTT, K. W. 2004. The protein kinase CK2 facilitates repair of chromosomal DNA single-strand breaks. *Cell,* 117**,** 17-28.

LONG, L., THELEN, J. P., FURGASON, M., HAJ-YAHYA, M., BRIK, A., CHENG, D., PENG, J. & YAO, T. 2014. The U4/U6 recycling factor SART3 has histone chaperone activity and associates with USP15 to regulate H2B deubiquitination. *The Journal of biological chemistry,* 289**,** 8916-30.

LONG, X. & MIANO, J. M. 2011. Transforming Growth Factor-β1 (TGF-β1) Utilizes Distinct Pathways for the Transcriptional Activation of MicroRNA 143/145 in Human Coronary Artery Smooth Muscle Cells. *Journal of Biological Chemistry,* 286**,** 30119-30129.

LÖNN, P., MORÉN, A., RAJA, E., DAHL, M. & MOUSTAKAS, A. 2009. Regulating the stability of TGFβ receptors and Smads. *Cell research,* 19**,** 21-35.

LOVE, D. C. & HANOVER, J. A. 2005. The hexosamine signaling pathway: deciphering the "O-GlcNAc code". *Science's STKE: signal transduction knowledge environment.,* 2005**,** re13.

LUBAS, W. A., FRANK, D. W., KRAUSE, M. & HANOVER, J. A. 1997. O-Linked GlcNAc Transferase Is a Conserved Nucleocytoplasmic Protein Containing Tetratricopeptide Repeats. *Journal of Biological Chemistry,* 272**,** 9316-9324.

LUISE, C., CAPRA, M., DONZELLI, M., MAZZAROL, G., JODICE, M. G., NUCIFORO, P., VIALE, G., DI FIORE, P. P. & CONFALONIERI, S. 2011. An Atlas of Altered Expression of Deubiquitinating Enzymes in Human Cancer. *PLoS ONE,* 6**,** e15891.

LUNA-VARGAS, M. P., FAESEN, A. C., VAN DIJK, W. J., RAPE, M., FISH, A. & SIXMA, T. K. 2011. Ubiquitin-specific protease 4 is inhibited by its ubiquitin-like domain. *EMBO reports,* 12**,** 365-72.

LUND, L. R., RICCIO, A., ANDREASEN, P. A., NIELSEN, L. S., KRISTENSEN, P., LAIHO, M., SAKSELA, O., BLASI, F. & DANO, K. 1987. Transforming growth factor-beta is a strong and fast acting positive regulator of the level of type-1 plasminogen activator inhibitor mRNA in WI-38 human lung fibroblasts. *The EMBO journal,* 6**,** 1281-6.

LUO, K., STROSCHEIN, S. L., WANG, W., CHEN, D., MARTENS, E., ZHOU, S. & ZHOU, Q. 1999. The Ski oncoprotein interacts with the Smad proteins to repress TGFbeta signaling. *Genes & development,* 13**,** 2196-206.

MA, J. & HART, G. W. 2014. O-GlcNAc profiling: from proteins to proteomes. *Clinical proteomics,* 11**,** 8.

MA, Z. & VOSSELLER, K. 2013. O-GlcNAc in cancer biology. *Amino Acids,* 45**,** 719-733.

MANCINI, M. L. & SONIS, S. T. 2014. Mechanisms of cellular fibrosis associated with cancer regimen-related toxicities. *Frontiers in pharmacology,* 5**,** 51.

MANN, C. J., PERDIGUERO, E., KHARRAZ, Y., AGUILAR, S., PESSINA, P., SERRANO, A. L. & MUNOZ-CANOVES, P. 2011. Aberrant repair and fibrosis development in skeletal muscle. *Skeletal muscle,* 1**,** 21.

MANNING, G., WHYTE, D. B., MARTINEZ, R., HUNTER, T. & SUDARSANAM, S. 2002. The Protein Kinase Complement of the Human Genome. *Science,* 298**,** 1912-1934.

MARKIV, A., RAMBARUTH, N. D. S. & DWEK, M. V. 2012. Beyond the genome and proteome: targeting protein modifications in cancer. *Current Opinion in Pharmacology,* 12**,** 408-413.

MASSAGUE, J. 2008. TGFbeta in cancer. *Cell,* 134**,** 215-230.

MASSAGUE, J. 2012. TGFβ signalling in context. *Nature Reviews Molecular Cell Biology,* 13**,** 616-630.

MASSAGUÉ, J. & GOMIS, R. R. 2006. The logic of TGFβ signaling. *FEBS Letters,* 580**,** 2811-2820.

MASSAGUÉ, J. & XI, Q. 2012. TGF-β control of stem cell differentiation genes. *FEBS Letters,* 586**,** 1953-1958.

MATSUURA, I., DENISSOVA, N. G., WANG, G., HE, D., LONG, J. & LIU, F. 2004. Cyclin-dependent kinases regulate the antiproliferative function of Smads. *Nature,* 430**,** 226-31.

MATYAS, G., ARNOLD, E., CARREL, T., BAUMGARTNER, D., BOILEAU, C., BERGER, W. & STEINMANN, B. 2006. Identification and in silico analyses of novel TGFBR1 and TGFBR2 mutations in Marfan syndrome-related disorders. *Human mutation,* 27**,** 760-9.

MCDOWELL, N. & GURDON, J. B. 1999. Activin as a morphogen in Xenopus mesoderm induction. *Seminars in cell & developmental biology,* 10**,** 311-7.

MCDOWELL, N., GURDON, J. B. & GRAINGER, D. J. 2001. Formation of a functional morphogen gradient by a passive process in tissue from the early

Xenopus embryo. *The International journal of developmental biology,* 45**,** 199-207.

MCGOURAN, J. F., GAERTNER, S. R., ALTUN, M., KRAMER, H. B. & KESSLER, B. M. 2013. Deubiquitinating enzyme specificity for ubiquitin chain topology profiled by di-ubiquitin activity probes. *Chemistry & biology,* 20**,** 1447-55.

MEDICI, D., POTENTA, S. & KALLURI, R. 2011. Transforming growth factor-beta2 promotes Snail-mediated endothelial-mesenchymal transition through convergence of Smad-dependent and Smad-independent signalling. *The Biochemical journal,* 437**,** 515-20.

MEGGIO, F. & PINNA, L. A. 2003. One-thousand-and-one substrates of protein kinase CK2? *The FASEB Journal,* 17**,** 349-368.

MESSICK, T. E., RUSSELL, N. S., IWATA, A. J., SARACHAN, K. L., SHIEKHATTAR, R., SHANKS, J. R., REYES-TURCU, F. E., WILKINSON, K. D. & MARMORSTEIN, R. 2008. Structural basis for ubiquitin recognition by the Otu1 ovarian tumor domain protein. *The Journal of biological chemistry,* 283**,** 11038-49.

METZGER, M. B., HRISTOVA, V. A. & WEISSMAN, A. M. 2012. HECT and RING finger families of E3 ubiquitin ligases at a glance. *Journal of Cell Science,* 125**,** 531-7.

METZGER, M. B., PRUNEDA, J. N., KLEVIT, R. E. & WEISSMAN, A. M. 2014. RING-type E3 ligases: master manipulators of E2 ubiquitin-conjugating enzymes and ubiquitination. *Biochimica et biophysica acta,* 1843**,** 47-60.

MEULMEESTER, E. & TEN DIJKE, P. 2011. The dynamic roles of TGF-beta in cancer. *The Journal of Pathology,* 223**,** 205-18.

MEVISSEN, TYCHO E. T., HOSPENTHAL, MANUELA K., GEURINK, PAUL P., ELLIOTT, PAUL R., AKUTSU, M., ARNAUDO, N., EKKEBUS, R., KULATHU, Y., WAUER, T., EL OUALID, F., FREUND, STEFAN M. V., OVAA, H. & KOMANDER, D. 2013. OTU Deubiquitinases Reveal Mechanisms of Linkage Specificity and Enable Ubiquitin Chain Restriction Analysis. *Cell,* 154**,** 169-184.

MEYER, A. E., GATZA, C. E., HOW, T., STARR, M., NIXON, A. B. & BLOBE, G. C. 2014. The role of TGF-beta receptor III localization in polarity and breast cancer progression. *Molecular biology of the cell,* pii: mbc.E14-03-0825.

MILES, W. O., JAFFRAY, E., CAMPBELL, S. G., TAKEDA, S., BAYSTON, L. J., BASU, S. P., LI, M., RAFTERY, L. A., ASHE, M. P., HAY, R. T. & ASHE, H. L. 2008. Medea SUMOylation restricts the signaling range of the Dpp morphogen in the Drosophila embryo. *Genes & Development,* 22**,** 2578-90.

MIYATA, Y. & NISHIDA, E. 2004. CK2 Controls Multiple Protein Kinases by Phosphorylating a Kinase-Targeting Molecular Chaperone, Cdc37. *Molecular and Cellular Biology,* 24**,** 4065-4074.

MONTENARH, M. 2010. Cellular regulators of protein kinase CK2. *Cell and Tissue Research,* 342**,** 139-46.

MORÉN, A., IMAMURA, T., MIYAZONO, K., HELDIN, C.-H. & MOUSTAKAS, A. 2005. Degradation of the tumor suppressor Smad4 by WW and HECT domain ubiquitin ligases. *J Biol Chem,* 280**,** 22115-22123.

MORENO-BUENO, G., PEINADO, H., MOLINA, P., OLMEDA, D., CUBILLO, E., SANTOS, V., PALACIOS, J., PORTILLO, F. & CANO, A. 2009. The morphological and molecular features of the epithelial-to-mesenchymal transition. *Nature Protocols,* 4**,** 1591-1613.

MORRISON, C. D., PARVANI, J. G. & SCHIEMANN, W. P. 2013. The relevance of the TGF-beta Paradox to EMT-MET programs. *Cancer Letters,* 341**,** 30-40.

MORSUT, L., YAN, K. P., ENZO, E., ARAGONA, M., SOLIGO, S. M., WENDLING, O., MARK, M., KHETCHOUMIAN, K., BRESSAN, G., CHAMBON, P., DUPONT, S., LOSSON, R. & PICCOLO, S. 2010. Negative control of Smad activity by ectodermin/Tif1gamma patterns the mammalian embryo. *Development,* 137**,** 2571-8.

MOSES, H. L. & SERRA, R. 1996. Regulation of differentiation by TGF-beta. *Current opinion in genetics & development,* 6**,** 581-6.

MOUSTAKAS, A. & HELDIN, C. H. 2005. Non-Smad TGF-beta signals. *Journal of cell science,* 118**,** 3573-84.

MOUSTAKAS, A. & HELDIN, C. H. 2009. The regulation of TGFβ signal transduction. *Development,* 136**,** 3699-3714.

MU, Y., SUNDAR, R., THAKUR, N., EKMAN, M., GUDEY, S. K., YAKYMOVYCH, M., HERMANSSON, A., DIMITRIOU, H., BENGOECHEA-ALONSO, M. T., ERICSSON, J., HELDIN, C. H. & LANDSTROM, M. 2011. TRAF6 ubiquitinates TGFbeta type I receptor to promote its cleavage and nuclear translocation in cancer. *Nature communications,* 2**,** 330.

MUELLER, T., BREUER, P., SCHMITT, I., WALTER, J., EVERT, B. O. & WULLNER, U. 2009. CK2-dependent phosphorylation determines cellular localization and stability of ataxin-3. *Human Molecular Genetics,* 18**,** 3334-43.

MUKAI, A., YAMAMOTO-HINO, M., KOMADA, M., OKANO, H. & GOTO, S. 2012. Balanced ubiquitination determines cellular responsiveness to extracellular stimuli. *Cellular and Molecular Life Sciences,* 69**,** 4007-4016.

MURAKAMI, G., WATABE, T., TAKAOKA, K., MIYAZONO, K. & IMAMURA, T. 2003. Cooperative inhibition of bone morphogenetic protein signaling by Smurf1 and inhibitory Smads. *Molecular biology of the cell,* 14**,** 2809-17.

NAGANO, Y., MAVRAKIS, K. J., LEE, K. L., FUJII, T., KOINUMA, D., SASE, H., YUKI, K., ISOGAYA, K., SAITOH, M., IMAMURA, T., EPISKOPOU, V., MIYAZONO, K. & MIYAZAWA, K. 2007. Arkadia induces degradation of SnoN and c-Ski to enhance transforming growth factor-beta signaling. *J Biol Chem,* 282**,** 20492-20501.

NAGARAJ, N. S. & DATTA, P. K. 2010. Targeting the transforming growth factor-beta signaling pathway in human cancer. *Expert opinion on investigational drugs,* 19**,** 77-91.

NAKADA, S., TAI, I., PANIER, S., AL-HAKIM, A., IEMURA, S., JUANG, Y. C., O'DONNELL, L., KUMAKUBO, A., MUNRO, M., SICHERI, F., GINGRAS, A. C., NATSUME, T., SUDA, T. & DUROCHER, D. 2010. Non-canonical inhibition of DNA damage-dependent ubiquitination by OTUB1. *Nature,* 466**,** 941-6.

NAKANO, A., KOINUMA, D., MIYAZAWA, K., UCHIDA, T., SAITOH, M., KAWABATA, M., HANAI, J.-I., AKIYAMA, H., ABE, M., MIYAZONO, K., MATSUMOTO, T. & IMAMURA, T. 2009. Pin1 Down-regulates Transforming Growth Factor-β (TGF-β) Signaling by Inducing Degradation of Smad Proteins. *Journal of Biological Chemistry,* 284**,** 6109-6115.

NAKAO, A., IMAMURA, T., SOUCHELNYTSKYI, S., KAWABATA, M., ISHISAKI, A., OEDA, E., TAMAKI, K., HANAI, J., HELDIN, C. H., MIYAZONO, K. & TEN DIJKE, P. 1997. TGF-beta receptor-mediated signalling through Smad2, Smad3 and Smad4. *The EMBO Journal,* 16**,** 5353-62.

NAKASONE, M. A., LIVNAT-LEVANON, N., GLICKMAN, MICHAEL H., COHEN, ROBERT E. & FUSHMAN, D. 2013. Mixed-Linkage Ubiquitin Chains Send Mixed Messages. *Structure,* 21**,** 727-740.

NATHAN, J. A., TAE KIM, H., TING, L., GYGI, S. P. & GOLDBERG, A. L. 2013. Why do cellular proteins linked to K63-polyubiquitin chains not associate with proteasomes? *The EMBO Journal,* 32**,** 552-565.

NEMUNAITIS, J., DILLMAN, R. O., SCHWARZENBERGER, P. O., SENZER, N., CUNNINGHAM, C., CUTLER, J., TONG, A., KUMAR, P., PAPPEN, B., HAMILTON, C., DEVOL, E., MAPLES, P. B., LIU, L., CHAMBERLIN, T., SHAWLER, D. L. & FAKHRAI, H. 2006. Phase II study of belagenpumatucel-L, a transforming growth factor beta-2 antisense gene-modified allogeneic tumor cell vaccine in non-small-cell lung cancer. *Journal of clinical oncology : official journal of the American Society of Clinical Oncology,* 24**,** 4721-30.

NEMUNAITIS, J., NEMUNAITIS, M., SENZER, N., SNITZ, P., BEDELL, C., KUMAR, P., PAPPEN, B., MAPLES, P. B., SHAWLER, D. & FAKHRAI, H. 2009. Phase II trial of Belagenpumatucel-L, a TGF-beta2 antisense gene modified allogeneic tumor vaccine in advanced non small cell lung cancer (NSCLC) patients. *Cancer gene therapy,* 16**,** 620-4.

NEPTUNE, E. R., FRISCHMEYER, P. A., ARKING, D. E., MYERS, L., BUNTON, T. E., GAYRAUD, B., RAMIREZ, F., SAKAI, L. Y. & DIETZ, H. C. 2003. Dysregulation of TGF-beta activation contributes to pathogenesis in Marfan syndrome. *Nature genetics,* 33**,** 407-11.

NICHOLSON, D. W., ALI, A., THORNBERRY, N. A., VAILLANCOURT, J. P., DING, C. K., GALLANT, M., GAREAU, Y., GRIFFIN, P. R., LABELLE, M., LAZEBNIK, Y. A., MUNDAY, N. A., RAJU, S. M., SMULSON, M. E., YAMIN, T.-T., YU, V. L. & MILLER, D. K. 1995. Identification and inhibition of the ICE/CED-3 protease necessary for mammalian apoptosis. *Nature,* 376**,** 37-43.

NIEFIND, K., GUERRA, B., ERMAKOWA, I. & ISSINGER, O. G. 2001. Crystal structure of human protein kinase CK2: insights into basic properties of the CK2 holoenzyme. *The EMBO Journal,* 20**,** 5320-31.

NIEFIND, K. & ISSINGER, O.-G. 2010. Conformational plasticity of the catalytic subunit of protein kinase CK2 and its consequences for regulation and drug design. *Biochimica et Biophysica Acta (BBA) - Proteins and Proteomics,* 1804**,** 484-492.

NIEWKOOP, P. D. & FABER, J. 1975. *Normal Table of Xenopus laevis (Daudin),* Amsterdam, North-Holland.

NIH. 2014. *Clinical trials* [Online]. U.S. National Institutes of Health. Available: https://clinicaltrials.gov/ 2014].

NIJMAN, S. M., LUNA-VARGAS, M. P., VELDS, A., BRUMMELKAMP, T. R., DIRAC, A. M., SIXMA, T. K. & BERNARDS, R. 2005. A genomic and functional inventory of deubiquitinating enzymes. *Cell,* 123**,** 773-86.

OGUNJIMI, A. A., BRIANT, D. J., PECE-BARBARA, N., LE ROY, C., DI GUGLIELMO, G. M., KAVSAK, P., RASMUSSEN, R. K., SEET, B. T., SICHERI, F. & WRANA, J. L. 2005. Regulation of Smurf2 ubiquitin ligase activity by anchoring the E2 to the HECT domain. *Molecular cell,* 19**,** 297-308.

OLSEN, B. B., WANG, S. Y., SVENSTRUP, T. H., CHEN, B. P. & GUERRA, B. 2012. Protein kinase CK2 localizes to sites of DNA double-strand break regulating the cellular response to DNA damage. *BMC molecular biology,* 13**,** 7.

ONICHTCHOUK, D., CHEN, Y. G., DOSCH, R., GAWANTKA, V., DELIUS, H., MASSAGUE, J. & NIEHRS, C. 1999. Silencing of TGF-beta signalling by the pseudoreceptor BAMBI. *Nature,* 401**,** 480-5.

ONICHTCHOUK, D., GLINKA, A. & NIEHRS, C. 1998. Requirement for Xvent-1 and Xvent-2 gene function in dorsoventral patterning of Xenopus mesoderm. *Development,* 125**,** 1447-56.

ONO, Y., CALHABEU, F., MORGAN, J. E., KATAGIRI, T., AMTHOR, H. & ZAMMIT, P. S. 2011. BMP signalling permits population expansion by preventing premature myogenic differentiation in muscle satellite cells. *Cell death and differentiation,* 18**,** 222-34.

OSADA, S., OHMORI, S. Y. & TAIRA, M. 2003. XMAN1, an inner nuclear membrane protein, antagonizes BMP signaling by interacting with Smad1 in Xenopus embryos. *Development,* 130**,** 1783-94.

ÖZCAN, S., ANDRALI, S. S. & CANTRELL, J. E. L. 2010. Modulation of transcription factor function by O-GlcNAc modification. *Biochimica et Biophysica Acta (BBA) - Gene Regulatory Mechanisms,* 1799**,** 353-364.

OZDAMAR, B., BOSE, R., BARRIOS-RODILES, M., WANG, H. R., ZHANG, Y. & WRANA, J. L. 2005. Regulation of the polarity protein Par6 by TGFbeta receptors controls epithelial cell plasticity. *Science,* 307**,** 1603-9.

PAGANO, M. A., BAIN, J., KAZIMIERCZUK, Z., SARNO, S., RUZZENE, M., DI MAIRA, G., ELLIOTT, M., ORZESZKO, A., COZZA, G., MEGGIO, F. & PINNA, L. A. 2008. The selectivity of inhibitors of protein kinase CK2: an update. *Biochemical Journal,* 415**,** 353-365.

PAKYARI, M., FARROKHI, A., MAHARLOOEI, M. K. & GHAHARY, A. 2013. Critical Role of Transforming Growth Factor Beta in Different Phases of Wound Healing. *Advances in wound care,* 2**,** 215-224.

PAN, D., ESTEVEZ-SALMERON, L. D., STROSCHEIN, S. L., ZHU, X., HE, J., ZHOU, S. & LUO, K. 2005. The integral inner nuclear membrane protein MAN1 physically interacts with the R-Smad proteins to repress signaling by the transforming growth factor-{beta} superfamily of cytokines. *The Journal of biological chemistry,* 280**,** 15992-6001.

PANNU, J., NAKERAKANTI, S., SMITH, E., TEN DIJKE, P. & TROJANOWSKA, M. 2007. Transforming growth factor-beta receptor type I-dependent fibrogenic gene program is mediated via activation of Smad1 and ERK1/2 pathways. *The Journal of biological chemistry,* 282**,** 10405-13.

PAPALEO, E., RANZANI, V., TRIPODI, F., VITRIOLO, A., CIRULLI, C., FANTUCCI, P., ALBERGHINA, L., VANONI, M., DE GIOIA, L. & COCCETTI, P. 2011. An acidic loop and cognate phosphorylation sites define a molecular switch that modulates ubiquitin charging activity in Cdc34-like enzymes. *PLoS computational biology,* 7**,** e1002056.

PARDALI, E. & TEN DIJKE, P. 2012. TGFbeta signaling and cardiovascular diseases. *International journal of biological sciences,* 8**,** 195-213.

PARK, H.-S., HOHN, M. J., UMEHARA, T., GUO, L.-T., OSBORNE, E. M., BENNER, J., NOREN, C. J., RINEHART, J. & SÖLL, D. 2011. Expanding the Genetic Code of Escherichia coli with Phosphoserine. *Science,* 333**,** 1151-1154.

PARK, M. H., WOLFF, E. C. & FOLK, J. E. 1993. Hypusine: its post-translational formation in eukaryotic initiation factor 5A and its potential role in cellular regulation. *BioFactors,* 4**,** 95-104.

PATHAK, S., BORODKIN, V. S., ALBARBARAWI, O., CAMPBELL, D. G., IBRAHIM, A. & VAN AALTEN, D. M. 2012. O-GlcNAcylation of TAB1 modulates TAK1-mediated cytokine release. *The EMBO Journal,* 31**,** 1394-404.

PATTISON, M. J., MACKENZIE, K. F. & ARTHUR, J. S. C. 2012. Inhibition of JAKs in Macrophages Increases Lipopolysaccharide-Induced Cytokine Production by Blocking IL-10–Mediated Feedback. *The Journal of Immunology,* 189**,** 2784-2792.

PAULI, E. K., CHAN, Y. K., DAVIS, M. E., GABLESKE, S., WANG, M. K., FEISTER, K. F. & GACK, M. U. 2014. The ubiquitin-specific protease USP15

promotes RIG-I-mediated antiviral signaling by deubiquitylating TRIM25. *Science signaling,* 7**,** ra3.

PENG, Y., XU, R. & ZHENG, X. 2014. HSCARG Negatively Regulates the Cellular Antiviral RIG-I Like Receptor Signaling Pathway by Inhibiting TRAF3 Ubiquitination via Recruiting OTUB1. *PLoS Pathog,* 10**,** e1004041.

PERSSON, U., IZUMI, H., SOUCHELNYTSKYI, S., ITOH, S., GRIMSBY, S., ENGSTROM, U., HELDIN, C. H., FUNA, K. & TEN DIJKE, P. 1998. The L45 loop in type I receptors for TGF-beta family members is a critical determinant in specifying Smad isoform activation. *FEBS Letters,* 434**,** 83-7.

PFAFFL, M. W. 2001. A new mathematical model for relative quantification in real-time RT-PCR. *Nucleic acids research,* 29**,** e45.

PICKART, C. M. 1997. Targeting of substrates to the 26S proteasome. *The FASEB Journal,* 11**,** 1055-66.

PICKART, C. M. 2001. Mechanisms underlying ubiquitination. *Annual review of biochemistry,* 70**,** 503-33.

PICKART, C. M. & EDDINS, M. J. 2004. Ubiquitin: structures, functions, mechanisms. *Biochimica et Biophysica Acta (BBA) - Molecular Cell Research,* 1695**,** 55-72.

PINNA, L. A. 2002. Protein kinase CK2: a challenge to canons. *Journal of Cell Science,* 115**,** 3873-3878.

PINNA, L. A. 2003. The Raison D'Être of Constitutively Active Protein Kinases: The Lesson of CK2. *Accounts of Chemical Research,* 36**,** 378-384.

PLECHANOVOVA, A., JAFFRAY, E. G., TATHAM, M. H., NAISMITH, J. H. & HAY, R. T. 2012. Structure of a RING E3 ligase and ubiquitin-loaded E2 primed for catalysis. *Nature,* 489**,** 115-20.

POZUELO RUBIO, M., GERAGHTY, K. M., WONG, B. H. C., WOOD, N. T., CAMPBELL, D. G., MORRICE, N. & MACKINTOSH, C. 2004. 14-3-3-affinity purification of over 200 human phosphoproteins reveals new links to regulation of cellular metabolism, proliferation and trafficking. *Biochem. J.,* 379**,** 395-408.

RAFTERY, L. A., TWOMBLY, V., WHARTON, K. & GELBART, W. M. 1995. Genetic screens to identify elements of the decapentaplegic signaling pathway in Drosophila. *Genetics,* 139**,** 241-54.

RAMIREZ, D. M., RAMIREZ, M. R., REGINATO, A. M. & MEDICI, D. 2014. Molecular and cellular mechanisms of heterotopic ossification. *Histology and histopathology,* Epub ahead of print.

REMY, I., MONTMARQUETTE, A. & MICHNICK, S. W. 2004. PKB/Akt modulates TGF-beta signalling through a direct interaction with Smad3. *Nature cell biology,* 6**,** 358-65.

REYES-TURCU, F. E., VENTII, K. H. & WILKINSON, K. D. 2009. Regulation and cellular roles of ubiquitin-specific deubiquitinating enzymes. *Annual review of biochemistry,* 78**,** 363-97.

ROSS, S., CHEUNG, E., PETRAKIS, T. G., HOWELL, M., KRAUS, W. L. & HILL, C. S. 2006. Smads orchestrate specific histone modifications and chromatin remodeling to activate transcription. *EMBO Journal,* 25**,** 4490-4502.

ROSS, S. & HILL, C. S. 2008. How the Smads regulate transcription. *The International Journal of Biochemistry & Cell Biology,* 40**,** 383-408.

ROTIN, D. & KUMAR, S. 2009. Physiological functions of the HECT family of ubiquitin ligases. *Nature Reviews Molecular Cell Biology,* 10**,** 398-409.

RUAN, H.-B., SINGH, J. P., LI, M.-D., WU, J. & YANG, X. 2013. Cracking the O-GlcNAc code in metabolism. *Trends in Endocrinology & Metabolism,* 24**,** 301-309.

RUMPF, S. & JENTSCH, S. 2006. Functional Division of Substrate Processing Cofactors of the Ubiquitin-Selective Cdc48 Chaperone. *Molecular cell,* 21**,** 261-269.

RUZZENE, M. & PINNA, L. A. 2010. Addiction to protein kinase CK2: A common denominator of diverse cancer cells? *Biochimica et Biophysica Acta (BBA) - Proteins and Proteomics,* 1804**,** 499-504.

SAITO, S., YANO, K., SHARMA, S., MCMAHON, H. E. & SHIMASAKI, S. 2008. Characterization of the post-translational modification of recombinant human BMP-15 mature protein. *Protein science : a publication of the Protein Society,* 17**,** 362-70.

SAMARAKOON, R. & HIGGINS, P. J. 2008. Integration of non-SMAD and SMAD signaling in TGF-beta1-induced plasminogen activator inhibitor type-1 gene expression in vascular smooth muscle cells. *Thrombosis and haemostasis,* 100**,** 976-83.

SAMARAKOON, R., OVERSTREET, J. M. & HIGGINS, P. J. 2013. TGF-beta signaling in tissue fibrosis: redox controls, target genes and therapeutic opportunities. *Cellular signalling,* 25**,** 264-8.

SAMARAKOON, R., OVERSTREET, J. M., HIGGINS, S. P. & HIGGINS, P. J. 2012. TGF-beta1 --> SMAD/p53/USF2 --> PAI-1 transcriptional axis in ureteral obstruction-induced renal fibrosis. *Cell and tissue research,* 347**,** 117-28.

SANCHEZ, N. S. & BARNETT, J. V. 2012. TGFbeta and BMP-2 regulate epicardial cell invasion via TGFbetaR3 activation of the Par6/Smurf1/RhoA pathway. *Cellular signalling,* 24**,** 539-48.

SAPKOTA, G., ALARCÓN, C., SPAGNOLI, F. M., BRIVANLOU, A. H. & MASSAGUÉ, J. 2007. Balancing BMP signaling through integrated inputs into the Smad1 linker. *Molecular cell,* 25**,** 441-454.

SAPKOTA, G., KNOCKAERT, M., ALARCON, C., MONTALVO, E., BRIVANLOU, A. H. & MASSAGUE, J. 2006. Dephosphorylation of the linker regions of Smad1 and Smad2/3 by small C-terminal domain phosphatases has distinct outcomes for bone morphogenetic protein and transforming growth factor-beta pathways. *The Journal of biological chemistry,* 281**,** 40412-9.

SAPKOTA, G. P. 2013. The TGFβ-induced phosphorylation and activation of p38 mitogen-activated protein kinase is mediated by MAP3K4 and MAP3K10 but not TAK1. *Open Biology,* 3.

SARKARI, F., SHENG, Y. & FRAPPIER, L. 2010. USP7/HAUSP Promotes the Sequence-Specific DNA Binding Activity of p53. *PLoS ONE,* 5**,** e13040.

SATO, Y., YAMAGATA, A., GOTO-ITO, S., KUBOTA, K., MIYAMOTO, R., NAKADA, S. & FUKAI, S. 2012. Molecular basis of Lys-63-linked polyubiquitination inhibition by the interaction between human deubiquitinating enzyme OTUB1 and ubiquitin-conjugating enzyme UBC13. *The Journal of biological chemistry,* 287**,** 25860-8.

SATO, Y., YOSHIKAWA, A., YAMAGATA, A., MIMURA, H., YAMASHITA, M., OOKATA, K., NUREKI, O., IWAI, K., KOMADA, M. & FUKAI, S. 2008. Structural basis for specific cleavage of Lys63-linked polyubiquitin chains. *Nature,* 455**,** 358-362.

SATOW, R., KURISAKI, A., CHAN, T. C., HAMAZAKI, T. S. & ASASHIMA, M. 2006. Dullard promotes degradation and dephosphorylation of BMP receptors and is required for neural induction. *Developmental cell,* 11**,** 763-74.

SAVAGE, C., DAS, P., FINELLI, A. L., TOWNSEND, S. R., SUN, C. Y., BAIRD, S. E. & PADGETT, R. W. 1996. Caenorhabditis elegans genes sma-2, sma-3, and sma-4 define a conserved family of transforming growth factor beta pathway

components. *Proceedings of the National Academy of Sciences of the United States of America,* 93**,** 790-4.

SAYED, M. G., AHMED, A. F., RINGOLD, J. R., ANDERSON, M. E., BAIR, J. L., MITROS, F. A., LYNCH, H. T., TINLEY, S. T., PETERSEN, G. M., GIARDIELLO, F. M., VOGELSTEIN, B. & HOWE, J. R. 2002. Germline SMAD4 or BMPR1A mutations and phenotype of juvenile polyposis. *Annals of surgical oncology,* 9**,** 901-6.

SCHARPFENECKER, M., VAN DINTHER, M., LIU, Z., VAN BEZOOIJEN, R. L., ZHAO, Q., PUKAC, L., LOWIK, C. W. & TEN DIJKE, P. 2007. BMP-9 signals via ALK1 and inhibits bFGF-induced endothelial cell proliferation and VEGF-stimulated angiogenesis. *Journal of Cell Science,* 120**,** 964-72.

SCHECHTER, I. & BERGER, A. 1967. On the size of the active site in proteases. I. Papain. *Biochemical and Biophysical Research Communications,* 27**,** 157-162.

SCHEFFNER, M. & KUMAR, S. 2014. Mammalian HECT ubiquitin-protein ligases: biological and pathophysiological aspects. *Biochimica et biophysica acta,* 1843**,** 61-74.

SCHLESINGER, D. H. & GOLDSTEIN, G. 1975. Molecular conservation of 74 amino acid sequence of ubiquitin between cattle and man. *Nature,* 255**,** 423-4.

SCHLINGENSIEPEN, K. H., JASCHINSKI, F., LANG, S. A., MOSER, C., GEISSLER, E. K., SCHLITT, H. J., KIELMANOWICZ, M. & SCHNEIDER, A. 2011. Transforming growth factor-beta 2 gene silencing with trabedersen (AP 12009) in pancreatic cancer. *Cancer science,* 102**,** 1193-200.

SCHULMAN, B. A. 2011. Twists and turns in ubiquitin-like protein conjugation cascades. *Protein science : a publication of the Protein Society,* 20**,** 1941-54.

SCHUSTER, N. & KRIEGLSTEIN, K. 2002. Mechanisms of TGF-β-mediated apoptosis. *Cell and Tissue Research,* 307**,** 1-14.

SCUDIERO, D. A., SHOEMAKER, R. H., PAULL, K. D., MONKS, A., TIERNEY, S., NOFZIGER, T. H., CURRENS, M. J., SENIFF, D. & BOYD, M. R. 1988. Evaluation of a Soluble Tetrazolium/Formazan Assay for Cell Growth and Drug Sensitivity in Culture Using Human and Other Tumor Cell Lines. *Cancer Research,* 48**,** 4827-4833.

SEKELSKY, J. J., NEWFELD, S. J., RAFTERY, L. A., CHARTOFF, E. H. & GELBART, W. M. 1995. Genetic characterization and cloning of mothers against dpp, a gene required for decapentaplegic function in Drosophila melanogaster. *Genetics,* 139**,** 1347-58.

SEMPLICI, F., MEGGIO, F., PINNA, L. A. & OLIVIERO, S. 2002. CK2-dependent phosphorylation of the E2 ubiquitin conjugating enzyme UBC3B induces its interaction with beta-TrCP and enhances beta-catenin degradation. *Oncogene,* 21**,** 3978-87.

SEO, S. R., LALLEMAND, F., FERRAND, N., PESSAH, M., L'HOSTE, S., CAMONIS, J. & ATFI, A. 2004. The novel E3 ubiquitin ligase Tiul1 associates with TGIF to target Smad2 for degradation. *The EMBO Journal,* 23**,** 3780-92.

SEOANE, J., LE, H.-V., SHEN, L., ANDERSON, S. A. & MASSAGUÉ, J. 2004. Integration of Smad and Forkhead Pathways in the Control of Neuroepithelial and Glioblastoma Cell Proliferation. *Cell,* 117**,** 211-223.

SFLOMOS, G., KOSTARAS, E., PANOPOULOU, E., PAPPAS, N., KYRKOU, A., POLITOU, A. S., FOTSIS, T. & MURPHY, C. 2011. ERBIN is a new SARA-interacting protein: competition between SARA and SMAD2 and SMAD3 for binding to ERBIN. *Journal of cell science,* 124**,** 3209-22.

SHA, X., BRUNNER, A. M., PURCHIO, A. F. & GENTRY, L. E. 1989. Transforming growth factor beta 1: importance of glycosylation and acidic proteases for processing and secretion. *Molecular endocrinology,* 3**,** 1090-8.

SHEN, R., CHEN, M., WANG, Y.-J., KANEKI, H., XING, L., O'KEEFE, R. J. & CHEN, D. 2006. Smad6 Interacts with Runx2 and Mediates Smad Ubiquitin Regulatory Factor 1-induced Runx2 Degradation. *Journal of Biological Chemistry,* 281**,** 3569-3576.

SHI, S., DE GORTER, D. J., HOOGAARS, W. M., T HOEN, P. A. & TEN DIJKE, P. 2013. Overactive bone morphogenetic protein signaling in heterotopic ossification and Duchenne muscular dystrophy. *Cellular and molecular life sciences : CMLS,* 70**,** 407-23.

SHI, W., SUN, C., HE, B., XIONG, W., SHI, X., YAO, D. & CAO, X. 2004. GADD34-PP1c recruited by Smad7 dephosphorylates TGFbeta type I receptor. *The Journal of cell biology,* 164**,** 291-300.

SHI, Y. & MASSAGUE, J. 2003. Mechanisms of TGF-beta signaling from cell membrane to the nucleus. *Cell,* 113**,** 685-700.

SHI, Y. & MASSAGUÉ, J. 2003. Mechanisms of TGF-β Signaling from Cell Membrane to the Nucleus. *Cell,* 113**,** 685-700.

SHI, Y., WANG, Y.-F., JAYARAMAN, L., YANG, H., MASSAGUÉ, J. & PAVLETICH, N. P. 1998. Crystal Structure of a Smad MH1 Domain Bound to DNA: Insights on DNA Binding in TGF-β Signaling. *Cell,* 94**,** 585-594.

SIEGEL, P. M. & MASSAGUE, J. 2003. Cytostatic and apoptotic actions of TGF-beta in homeostasis and cancer. *Nature reviews. Cancer,* 3**,** 807-21.

SIMEONI, I. & GURDON, J. B. 2007. Interpretation of BMP signaling in early Xenopus development. *Developmental biology,* 308**,** 82-92.

SIMONSSON, M., KANDURI, M., GRÖNROOS, E., HELDIN, C. H. & ERICSSON, J. 2006. The DNA binding activities of Smad2 and Smad3 are regulated by coactivator-mediated acetylation. *Journal of Biological Chemistry,* 281**,** 39870-39880.

SINGH, J. P., ZHANG, K., WU, J. & YANG, X. 2014. O-GlcNAc signaling in cancer metabolism and epigenetics. *Cancer Letters,* doi: 10.1016/j.canlet.2014.04.014.

SINGH, V. P., BAKER, K. M. & KUMAR, R. 2008. Activation of the intracellular renin-angiotensin system in cardiac fibroblasts by high glucose: role in extracellular matrix production. *American journal of heart and Circulatory Physiology,* 294**,** H1675-H1684.

SINGHAL, S., TAYLOR, M. C. & BAKER, R. T. 2008. Deubiquitylating enzymes and disease. *BMC biochemistry,* 9 Suppl 1**,** S3.

SLACK, J. M. W. 1984. Regional biosynthetic markers in the early amphibian embryo. *Journal of Embryology and Experimental Morphology,* 80**,** 289-319.

SMITH, J. C. 1993. *Purifying and assaying mesoderm-inducing factors from vertebrate embryos,* Oxford, Oxford University Press.

SOARES, L., SEROOGY, C., SKRENTA, H., ANANDASABAPATHY, N., LOVELACE, P., CHUNG, C. D., ENGLEMAN, E. & FATHMAN, C. G. 2004. Two isoforms of otubain 1 regulate T cell anergy via GRAIL. *Nature immunology,* 5**,** 45-54.

SOOND, S. M. & CHANTRY, A. 2011. Selective targeting of activating and inhibitory Smads by distinct WWP2 ubiquitin ligase isoforms differentially modulates TGFbeta signalling and EMT. *Oncogene,* 30**,** 2451-62.

SORRENTINO, A., THAKUR, N., GRIMSBY, S., MARCUSSON, A., VON BULOW, V., SCHUSTER, N., ZHANG, S., HELDIN, C. H. & LANDSTROM, M. 2008. The type I TGF-beta receptor engages TRAF6 to activate TAK1 in a receptor kinase-independent manner. *Nature cell biology,* 10**,** 1199-207.

SOUCHELNYTSKYI, S., TAMAKI, K., ENGSTROM, U., WERNSTEDT, C., TEN DIJKE, P. & HELDIN, C. H. 1997. Phosphorylation of Ser465 and Ser467 in the C terminus of Smad2 mediates interaction with Smad4 and is required for

transforming growth factor-beta signaling. *The Journal of biological chemistry,* 272**,** 28107-15.

SPRATT, D. E., WALDEN, H. & SHAW, G. S. 2014. RBR E3 ubiquitin ligases: new structures, new insights, new questions. *The Biochemical journal,* 458**,** 421-37.

SRIHARI, S. & RAGAN, M. A. 2013. Systematic tracking of dysregulated modules identifies novel genes in cancer. *Bioinformatics,* 29**,** 1553-61.

STANISIC, V., MALOVANNAYA, A., QIN, J., LONARD, D. M. & O'MALLEY, B. W. 2009. OTU Domain-containing ubiquitin aldehyde-binding protein 1 (OTUB1) deubiquitinates estrogen receptor (ER) alpha and affects ERalpha transcriptional activity. *The Journal of biological chemistry,* 284**,** 16135-45.

STEGEMAN, S., JOLLY, L. A., PREMARATHNE, S., GECZ, J., RICHARDS, L. J., MACKAY-SIM, A. & WOOD, S. A. 2013. Loss of *Usp9x* Disrupts Cortical Architecture, Hippocampal Development and TGFβ-Mediated Axonogenesis. *PLoS ONE,* 8**,** e68287.

STINCHFIELD, M. J., TAKAESU, N. T., QUIJANO, J. C., CASTILLO, A. M., TIUSANEN, N., SHIMMI, O., ENZO, E., DUPONT, S., PICCOLO, S. & NEWFELD, S. J. 2012. Fat facets deubiquitylation of Medea/Smad4 modulates interpretation of a Dpp morphogen gradient. *Development,* 139**,** 2721-9.

STROSCHEIN, S. L., BONNI, S., WRANA, J. L. & LUO, K. 2001. Smad3 recruits the anaphase-promoting complex for ubiquitination and degradation of SnoN. *Genes Dev,* 15**,** 2822-2836.

SUGIMORI, K., MATSUI, K., MOTOMURA, H., TOKORO, T., WANG, J., HIGA, S., KIMURA, T. & KITAJIMA, I. 2005. BMP-2 prevents apoptosis of the N1511 chondrocytic cell line through PI3K/Akt-mediated NF-kappaB activation. *Journal of bone and mineral metabolism,* 23**,** 411-9.

SUN, P. D. & DAVIES, D. R. 1995. The cystine-knot growth-factor superfamily. *Annual review of biophysics and biomolecular structure,* 24**,** 269-91.

SUN, S.-C. 2008. Deubiquitylation and regulation of the immune response. *Nature Reviews Immunology,* 8**,** 501-511.

SUN, X.-X., CHALLAGUNDLA, K. B. & DAI, M.-S. 2011. Positive regulation of p53 stability and activity by the deubiquitinating enzyme Otubain 1. *The EMBO journal,* 31**,** 576-592.

TAN, M., LUO, H., LEE, S., JIN, F., YANG, JEONG S., MONTELLIER, E., BUCHOU, T., CHENG, Z., ROUSSEAUX, S., RAJAGOPAL, N., LU, Z., YE, Z., ZHU, Q., WYSOCKA, J., YE, Y., KHOCHBIN, S., REN, B. & ZHAO, Y. 2011. Identification of 67 Histone Marks and Histone Lysine Crotonylation as a New Type of Histone Modification. *Cell,* 146**,** 1016-1028.

TANG, L.-Y., YAMASHITA, M., COUSSENS, N. P., TANG, Y., WANG, X., LI, C., DENG, C.-X., CHENG, S. Y. & ZHANG, Y. E. 2011. Ablation of Smurf2 reveals an inhibition in TGF-β signalling through multiple mono-ubiquitination of Smad3. *EMBO J,* 30**,** 4777-4789.

TANG, L.-Y. & ZHANG, Y. E. 2011. Non-degradative ubiquitination in Smad-dependent TGF-beta signaling. *Cell & bioscience,* 1**,** 43.

TEN DIJKE, P., EGOROVA, A. D., GOUMANS, M. J., POELMANN, R. E. & HIERCK, B. P. 2012. TGF-beta signaling in endothelial-to-mesenchymal transition: the role of shear stress and primary cilia. *Science signaling,* 5**,** pt2.

TEN DIJKE, P., FU, J., SCHAAP, P. & ROELEN, B. A. 2003. Signal transduction of bone morphogenetic proteins in osteoblast differentiation. *The Journal of bone and joint surgery. American volume,* 85-A Suppl 3**,** 34-8.

TEN DIJKE, P., GOUMANS, M. J., ITOH, F. & ITOH, S. 2002. Regulation of cell proliferation by Smad proteins. *Journal of cellular physiology,* 191**,** 1-16.

TEN DIJKE, P., GOUMANS, M. J. & PARDALI, E. 2008. Endoglin in angiogenesis and vascular diseases. *Angiogenesis,* 11**,** 79-89.

TEN DIJKE, P. & HILL, C. S. 2004. New insights into TGF-beta-Smad signalling. *Trends in Biochemical Sciences,* 29**,** 265-73.

THROWER, J. S., HOFFMAN, L., RECHSTEINER, M. & PICKART, C. M. 2000. Recognition of the polyubiquitin proteolytic signal. *The EMBO journal,* 19**,** 94-102.

TIAN, M., BAI, C., LIN, Q., LIN, H., LIU, M., DING, F. & WANG, H. R. 2011. Binding of RhoA by the C2 domain of E3 ligase Smurf1 is essential for Smurf1-regulated RhoA ubiquitination and cell protrusive activity. *FEBS Letters,* 585**,** 2199-204.

TODOROVIC, V. & RIFKIN, D. B. 2012. LTBPs, more than just an escort service. *Journal of cellular biochemistry,* 113**,** 410-8.

TOKUNAGA, F., SAKATA, S.-I., SAEKI, Y., SATOMI, Y., KIRISAKO, T., KAMEI, K., NAKAGAWA, T., KATO, M., MURATA, S., YAMAOKA, S., YAMAMOTO, M., AKIRA, S., TAKAO, T., TANAKA, K. & IWAI, K. 2009. Involvement of linear polyubiquitylation of NEMO in NF-kappaB activation. *Nature Cell Biolology,* 11**,** 123-132.

TORRES, C. R. & HART, G. W. 1984. Topography and polypeptide distribution of terminal N-acetylglucosamine residues on the surfaces of intact lymphocytes. Evidence for O-linked GlcNAc. *Journal of Biological Chemistry,* 259**,** 3308-3317.

TOWNSEND, T. A., ROBINSON, J. Y., DEIG, C. R., HILL, C. R., MISFELDT, A., BLOBE, G. C. & BARNETT, J. V. 2011. BMP-2 and TGFbeta2 shared pathways regulate endocardial cell transformation. *Cells, tissues, organs,* 194**,** 1-12.

TSE, W., EISENHABER, B., HO, S., NG, Q., EISENHABER, F. & JIANG, Y.-J. 2009. Genome-wide loss-of-function analysis of deubiquitylating enzymes for zebrafish development. *BMC Genomics,* 10**,** 637.

TSE, W. K. F., JIANG, Y.-J. & WONG, C. K. C. 2013. Zebrafish transforming growth factor-β-stimulated clone 22 domain 3 (TSC22D3) plays critical roles in Bmp-dependent dorsoventral patterning via two deubiquitylating enzymes Usp15 and Otud4. *Biochimica et Biophysica Acta (BBA) - General Subjects,* 1830**,** 4584-4593.

TSUKAZAKI, T., CHIANG, T. A., DAVISON, A. F., ATTISANO, L. & WRANA, J. L. 1998. SARA, a FYVE domain protein that recruits Smad2 to the TGFbeta receptor. *Cell,* 95**,** 779-91.

VALDIMARSDOTTIR, G., GOUMANS, M. J., ITOH, F., ITOH, S., HELDIN, C. H. & TEN DIJKE, P. 2006. Smad7 and protein phosphatase 1alpha are critical determinants in the duration of TGF-beta/ALK1 signaling in endothelial cells. *BMC cell biology,* 7**,** 16.

VAN DE WATER, L., VARNEY, S. & TOMASEK, J. J. 2013. Mechanoregulation of the Myofibroblast in Wound Contraction, Scarring, and Fibrosis: Opportunities for New Therapeutic Intervention. *Advances in wound care,* 2**,** 122-141.

VARKI, A., CUMMINGS, R. D., ESKO, J. D., FREEZE, H. H., STANLEY, P., BERTOZZI, C. R., HART, G. W. & ETZLER, M. E. 2009. Essentials of Glycobiology. *Essentials of Glycobiology.* 2nd ed. Cold Spring Harbor (NY).

VARSHAVSKY, A. 2006. The early history of the ubiquitin field. *Protein science : a publication of the Protein Society,* 15**,** 647-54.

VILLENEUVE, N. F., TIAN, W., WU, T., SUN, Z., LAU, A., CHAPMAN, E., FANG, D. & ZHANG, D. D. 2013. USP15 negatively regulates Nrf2 through deubiquitination of Keap1. *Molecular cell,* 51**,** 68-79.

VO, B., T., MORTON, D., KOMARAGIRI, S., MILLENA, A. C., LEATH, C. & KHAN, S., A. 2013. TGF-β Effects on Prostate Cancer Cell Migration and Invasion Are Mediated by PGE2 through Activation of PI3K/AKT/mTOR Pathway. *Endocrinology,* 154**,** 1768-1779.

VOCADLO, D. J. 2012. O-GlcNAc processing enzymes: catalytic mechanisms, substrate specificity, and enzyme regulation. *Current opinion in chemical biology,* 16**,** 488-97.

VOGT, J., DINGWELL, K. S., HERHAUS, L., GOURLAY, R., MACARTNEY, T., CAMPBELL, D., SMITH, J. C. & SAPKOTA, G. P. 2014. Protein associated with SMAD1 (PAWS1/FAM83G) is a substrate for type I bone morphogenetic protein receptors and modulates bone morphogenetic protein signalling. *Open Biology,* 4.

VOGT, J., TRAYNOR, R. & SAPKOTA, G. P. 2011. The specificities of small molecule inhibitors of the TGFss and BMP pathways. *Cell Signal.,* 23**,** 1831-1842.

VOORNEVELD, P. W., KODACH, L. L., JACOBS, R. J., LIV, N., ZONNEVYLLE, A. C., HOOGENBOOM, J. P., BIEMOND, I., VERSPAGET, H. W., HOMMES, D. W., DE ROOIJ, K., VAN NOESEL, C. J., MORREAU, H., VAN WEZEL, T., OFFERHAUS, G. J., VAN DEN BRINK, G. R., PEPPELENBOSCH, M. P., TEN DIJKE, P. & HARDWICK, J. C. 2014. Loss of SMAD4 Alters BMP Signaling to Promote Colorectal Cancer Cell Metastasis via Activation of Rho and ROCK. *Gastroenterology,* 147**,** 196-208 e13.

VOS, R. M., ALTREUTER, J., WHITE, E. A. & HOWLEY, P. M. 2009. The ubiquitin-specific peptidase USP15 regulates human papillomavirus type 16 E6 protein stability. *Journal of virology,* 83**,** 8885-92.

VOSSELLER, K., TRINIDAD, J. C., CHALKLEY, R. J., SPECHT, C. G., THALHAMMER, A., LYNN, A. J., SNEDECOR, J. O., GUAN, S., MEDZIHRADSZKY, K. F., MALTBY, D. A., SCHOEPFER, R. & BURLINGAME, A. L. 2006. O-linked N-acetylglucosamine proteomics of postsynaptic density preparations using lectin weak affinity chromatography and mass spectrometry. *Molecular & cellular proteomics : MCP,* 5**,** 923-34.

WAGNER, S. A., BELI, P., WEINERT, B. T., NIELSEN, M. L., COX, J., MANN, M. & CHOUDHARY, C. 2011. A Proteome-wide, Quantitative Survey of In Vivo Ubiquitylation Sites Reveals Widespread Regulatory Roles. *Molecular & Cellular Proteomics,* 10.

WAKEFIELD, L. M. & HILL, C. S. 2013. Beyond TGFbeta: roles of other TGFbeta superfamily members in cancer. *Nature Reviews Cancer,* 13**,** 328-341.

WAN, M., HUANG, J., JHALA, N. C., TYTLER, E. M., YANG, L., VICKERS, S. M., TANG, Y., LU, C., WANG, N. & CAO, X. 2005. SCF(beta-TrCP1) controls Smad4 protein stability in pancreatic cancer cells. *The American journal of pathology,* 166**,** 1379-92.

WAN, M., TANG, Y., TYTLER, E. M., LU, C., JIN, B., VICKERS, S. M., YANG, L., SHI, X. & CAO, X. 2004. Smad4 Protein Stability Is Regulated by Ubiquitin Ligase SCFβ-TrCP1. *Journal of Biological Chemistry,* 279**,** 14484-14487.

WAN, Y., LIU, X. & KIRSCHNER, M. W. 2001. The anaphase-promoting complex mediates TGF-beta signaling by targeting SnoN for destruction. *Mol Cell,* 8**,** 1027-1039.

WANG, G., LI, C., WANG, Y. & CHEN, G. 2013a. Cooperative assembly of Co-Smad4 MH1 with R-Smad1/3 MH1 on DNA: a molecular dynamics simulation study. *PLoS ONE,* 8**,** e53841.

WANG, H. R., ZHANG, Y., OZDAMAR, B., OGUNJIMI, A. A., ALEXANDROVA, E., THOMSEN, G. H. & WRANA, J. L. 2003. Regulation of cell polarity and protrusion formation by targeting RhoA for degradation. *Science,* 302**,** 1775-9.

WANG, S., ZHOU, G., SHU, G., WANG, L., ZHU, X., GAO, P., XI, Q., ZHANG, Y., YUAN, L. & JIANG, Q. 2013b. Glucose utilization, lipid metabolism and BMP-Smad signaling pathway of porcine intramuscular preadipocytes compared with subcutaneous preadipocytes. *Cellular physiology and biochemistry,* 31**,** 981-96.

WANG, T., YIN, L., COOPER, E. M., LAI, M. Y., DICKEY, S., PICKART, C. M., FUSHMAN, D., WILKINSON, K. D., COHEN, R. E. & WOLBERGER, C. 2009. Evidence for bidentate substrate binding as the basis for the K48 linkage specificity of otubain 1. *Journal of molecular biology,* 386**,** 1011-23.

WEIGERT, C., BRODBECK, K., SAWADOGO, M., HARING, H. U. & SCHLEICHER, E. D. 2004. Upstream stimulatory factor (USF) proteins induce human TGF-beta1 gene activation via the glucose-response element-1013/-1002 in mesangial cells: up-regulation of USF activity by the hexosamine biosynthetic pathway. *The Journal of biological chemistry,* 279**,** 15908-15.

WEINERT, BRIAN T., SCHÖLZ, C., WAGNER, SEBASTIAN A., IESMANTAVICIUS, V., SU, D., DANIEL, JEREMY A. & CHOUDHARY, C. 2013. Lysine Succinylation Is a Frequently Occurring Modification in Prokaryotes and Eukaryotes and Extensively Overlaps with Acetylation. *Cell Reports,* 4**,** 842-851.

WEISKIRCHEN, R. & MEURER, S. K. 2013. BMP-7 counteracting TGF-beta1 activities in organ fibrosis. *Frontiers in bioscience,* 18**,** 1407-34.

WENZEL, D. M., LISSOUNOV, A., BRZOVIC, P. S. & KLEVIT, R. E. 2011. UBCH7 reactivity profile reveals parkin and HHARI to be RING/HECT hybrids. *Nature,* 474**,** 105-108.

WHELAN, S. A., DIAS, W. B., THIRUNEELAKANTAPILLAI, L., LANE, M. D. & HART, G. W. 2010. Regulation of insulin receptor substrate 1 (IRS-1)/AKT kinase-mediated insulin signaling by O-Linked beta-N-acetylglucosamine in 3T3-L1 adipocytes. *The Journal of biological chemistry,* 285**,** 5204-11.

WICKLIFFE, K. E., WILLIAMSON, A., MEYER, H.-J., KELLY, A. & RAPE, M. 2011. K11-linked ubiquitin chains as novel regulators of cell division. *Trends in Cell Biology,* 21**,** 656-663.

WICKS, S. J., HAROS, K., MAILLARD, M., SONG, L., COHEN, R. E., DIJKE, P. T. & CHANTRY, A. 2005. The deubiquitinating enzyme UCH37 interacts with Smads and regulates TGF-[beta] signalling. *Oncogene,* 24**,** 8080-8084.

WIENER, R., DIBELLO, A. T., LOMBARDI, P. M., GUZZO, C. M., ZHANG, X., MATUNIS, M. J. & WOLBERGER, C. 2013. E2 ubiquitin-conjugating enzymes regulate the deubiquitinating activity of OTUB1. *Nature Structural and Molecular Biology,* 20**,** 1033-1039.

WIENER, R., ZHANG, X., WANG, T. & WOLBERGER, C. 2012. The mechanism of OTUB1-mediated inhibition of ubiquitination. *Nature,* 483**,** 612-622.

WIESER, R., WRANA, J. L. & MASSAGUE, J. 1995. GS domain mutations that constitutively activate T beta R-I, the downstream signaling component in the TGF-beta receptor complex. *The EMBO Journal,* 14**,** 2199-208.

WIESNER, S., OGUNJIMI, A. A., WANG, H. R., ROTIN, D., SICHERI, F., WRANA, J. L. & FORMAN-KAY, J. D. 2007. Autoinhibition of the HECT-type ubiquitin ligase Smurf2 through its C2 domain. *Cell,* 130**,** 651-62.

WIGGIN, G. R., SOLOAGA, A., FOSTER, J. M., MURRAY-TAIT, V., COHEN, P. & ARTHUR, J. S. C. 2002. MSK1 and MSK2 Are Required for the Mitogen- and Stress-Induced Phosphorylation of CREB and ATF1 in Fibroblasts. *Molecular and Cellular Biology,* 22**,** 2871-2881.

WILLIS, S. A., ZIMMERMAN, C. M., LI, L. I. & MATHEWS, L. S. 1996. Formation and activation by phosphorylation of activin receptor complexes. *Molecular endocrinology,* 10**,** 367-79.

WOHLFERT, E. A., GORELIK, L., MITTLER, R., FLAVELL, R. A. & CLARK, R. B. 2006. Cutting edge: deficiency in the E3 ubiquitin ligase Cbl-b results in a multifunctional defect in T cell TGF-beta sensitivity in vitro and in vivo. *Journal of immunology,* 176**,** 1316-20.

WRANA, J. L., ATTISANO, L., WIESER, R., VENTURA, F. & MASSAGUE, J. 1994. Mechanism of activation of the TGF-beta receptor. *Nature,* 370**,** 341-7.

WRIGHTON, K. H., LIN, X. & FENG, X.-H. 2009. Phospho-control of TGF-β superfamily signaling. *Cell research,* 19**,** 8-20.

WRIGHTON, K. H., WILLIS, D., LONG, J., LIU, F., LIN, X. & FENG, X. H. 2006. Small C-terminal domain phosphatases dephosphorylate the regulatory linker regions of Smad2 and Smad3 to enhance transforming growth factor-beta signaling. *The Journal of biological chemistry,* 281**,** 38365-75.

WU, L. & DERYNCK, R. 2009. Essential role of TGF-beta signaling in glucose-induced cell hypertrophy. *Developmental Cell,* 17**,** 35-48.

XI, Q., WANG, Z., ZAROMYTIDOU, A.-I., ZHANG, X. H. F., CHOW-TSANG, L.-F., LIU, J. X., KIM, H. J., BARLAS, A., MANOVA-TODOROVA, K., KAARTINEN, V., STUDER, L., MARK, W., PATEL, D. J. & MASSAGUÉ, J. 2011. A Poised Chromatin Platform for TGF-β Access to Master Regulators. *Cell,* 147**,** 1511-1524.

XIA, Q., LIAO, L., CHENG, D., DUONG, D. M., GEARING, M., LAH, J. J., LEVEY, A. I. & PENG, J. 2008. Proteomic identification of novel proteins associated with Lewy bodies. *Frontiers in bioscience : a journal and virtual library,* 13**,** 3850-6.

XIN, H., XU, X., LI, L., NING, H., RONG, Y., SHANG, Y., WANG, Y., FU, X.-Y. & CHANG, Z. 2005. CHIP controls the sensitivity of transforming growth factor-beta signaling by modulating the basal level of Smad3 through ubiquitin-mediated degradation. *J Biol Chem,* 280**,** 20842-20850.

XU, J., WANG, A. H., OSES-PRIETO, J., MAKHIJANI, K., KATSUNO, Y., PEI, M., YAN, L., ZHENG, Y. G., BURLINGAME, A., BRÜCKNER, K. & DERYNCK, R. 2013. Arginine Methylation Initiates BMP-Induced Smad Signaling. *Molecular cell,* 51**,** 5-19.

XU, M., TAKANASHI, M., OIKAWA, K., TANAKA, M., NISHI, H., ISAKA, K., KUDO, M. & KURODA, M. 2009. USP15 plays an essential role for caspase-3 activation during Paclitaxel-induced apoptosis. *Biochemical and Biophysical Research Communications,* 388**,** 366-71.

XU, P., LIU, J. & DERYNCK, R. 2012. Post-translational regulation of TGF-β receptor and Smad signaling. *FEBS Letters,* 586**,** 1871-1884.

XU, Y. & PASCHE, B. 2007. TGF-beta signaling alterations and susceptibility to colorectal cancer. *Human molecular genetics,* 16 Spec No 1**,** R14-20.

YAMASHITA, M., FATYOL, K., JIN, C., WANG, X., LIU, Z. & ZHANG, Y. E. 2008. TRAF6 mediates Smad-independent activation of JNK and p38 by TGF-beta. *Molecular cell,* 31**,** 918-24.

YAN, X., LIU, Z. & CHEN, Y. 2009. Regulation of TGF- signaling by Smad7. *Acta Biochimica et Biophysica Sinica,* 41**,** 263-272.

YAN, X., ZHANG, J., PAN, L., WANG, P., XUE, H., ZHANG, L., GAO, X., ZHAO, X., NING, Y. & CHEN, Y. G. 2011. TSC-22 promotes transforming growth factor beta-mediated cardiac myofibroblast differentiation by antagonizing Smad7 activity. *Molecular and Cellular Biology,* 31**,** 3700-9.

YANAGITA, M. 2012. Inhibitors/antagonists of TGF-beta system in kidney fibrosis. *Nephrology, dialysis, transplantation,* 27**,** 3686-91.

YANG, L., WANG, N., TANG, Y., CAO, X. & WAN, M. 2006. Acute myelogenous leukemia-derived SMAD4 mutations target the protein to ubiquitin-proteasome degradation. *Human mutation,* 27**,** 897-905.

YANG, X., TENG, Y., HOU, N., FAN, X., CHENG, X., LI, J., WANG, L., WANG, Y. & WU, X. 2011. Delayed Re-epithelialization in Ppm1a Gene-deficient Mice Is Mediated by Enhanced Activation of Smad2. *The Journal of biological chemistry,* 286**,** 42267-73.

YANG, Y. R., SONG, M., LEE, H., JEON, Y., CHOI, E. J., JANG, H. J., MOON, H. Y., BYUN, H. Y., KIM, E. K., KIM, D. H., LEE, M. N., KOH, A., GHIM, J., CHOI, J. H., LEE-KWON, W., KIM, K. T., RYU, S. H. & SUH, P. G. 2012. O-GlcNAcase is essential for embryonic development and maintenance of genomic stability. *Aging cell,* 11**,** 439-48.

YE, L., LEWIS-RUSSELL, J. M., KYANASTON, H. G. & JIANG, W. G. 2007. Bone morphogenetic proteins and their receptor signaling in prostate cancer. *Histology and histopathology,* 22**,** 1129-47.

YE, X., CHENG, X., LIU, L., ZHAO, D. & DANG, Y. 2013. Blood glucose fluctuation affects skin collagen metabolism in the diabetic mouse by inhibiting the mitogen-activated protein kinase and Smad pathways. *Clinical and experimental dermatology,* 38**,** 530-7.

YE, Y. & RAPE, M. 2009. Building ubiquitin chains: E2 enzymes at work. *Nature reviews. Molecular cell biology,* 10**,** 755-64.

YI, J. Y., SHIN, I. & ARTEAGA, C. L. 2005. Type I transforming growth factor beta receptor binds to and activates phosphatidylinositol 3-kinase. *The Journal of biological chemistry,* 280**,** 10870-6.

YOSHIMORI, T., YAMAMOTO, A., MORIYAMA, Y., FUTAI, M. & TASHIRO, Y. 1991. Bafilomycin A1, a specific inhibitor of vacuolar-type H(+)-ATPase, inhibits acidification and protein degradation in lysosomes of cultured cells. *Journal of Biological Chemistry,* 266**,** 17707-17712.

YU, J., PAN, L., QIN, X., CHEN, H., XU, Y., CHEN, Y. & TANG, H. 2010. MTMR4 attenuates transforming growth factor beta (TGFbeta) signaling by dephosphorylating R-Smads in endosomes. *The Journal of biological chemistry,* 285**,** 8454-62.

YUAN, H., REDDY, M. A., SUN, G., LANTING, L., WANG, M., KATO, M. & NATARAJAN, R. 2013. Involvement of p300/CBP and epigenetic histone acetylation in TGF-β1-mediated gene transcription in mesangial cells. *American Journal of Physiology - Renal Physiology,* 304**,** F601-F613.

YUAN, J. H., YANG, F., WANG, F., MA, J. Z., GUO, Y. J., TAO, Q. F., LIU, F., PAN, W., WANG, T. T., ZHOU, C. C., WANG, S. B., WANG, Y. Z., YANG, Y., YANG, N., ZHOU, W. P., YANG, G. S. & SUN, S. H. 2014. A long noncoding RNA activated by TGF-beta promotes the invasion-metastasis cascade in hepatocellular carcinoma. *Cancer cell,* 25**,** 666-81.

YUZAWA, H., KOINUMA, D., MAEDA, S., YAMAMOTO, K., MIYAZAWA, K. & IMAMURA, T. 2009. Arkadia represses the expression of myoblast differentiation markers through degradation of Ski and the Ski-bound Smad complex in C2C12 myoblasts. *Bone,* 44**,** 53-60.

ZACHARA, N. E. 2012. The roles of O-linked β-N-acetylglucosamine in cardiovascular physiology and disease. *American journal of Heart and Circulatory Physiology,* 302**,** H1905-H1918.

ZAVADIL, J., BITZER, M., LIANG, D., YANG, Y. C., MASSIMI, A., KNEITZ, S., PIEK, E. & BOTTINGER, E. P. 2001. Genetic programs of epithelial cell

plasticity directed by transforming growth factor-beta. *Proceedings of the National Academy of Sciences of the United States of America,* 98**,** 6686-91.

ZAWEL, L., DAI, J. L., BUCKHAULTS, P., ZHOU, S., KINZLER, K. W., VOGELSTEIN, B. & KERN, S. E. 1998. Human Smad3 and Smad4 are sequence-specific transcription activators. *Molecular cell,* 1**,** 611-7.

ZHANG, B., HALDER, S. K., KASHIKAR, N. D., CHO, Y. J., DATTA, A., GORDEN, D. L. & DATTA, P. K. 2010. Antimetastatic role of Smad4 signaling in colorectal cancer. *Gastroenterology,* 138**,** 969-80 e1-3.

ZHANG, J., ZHANG, X., XIE, F., ZHANG, Z., DAM, H., ZHANG, L. & ZHOU, F. 2014a. The regulation of TGF-β/SMAD signaling by protein deubiquitination. *Protein & Cell***,** 1-15.

ZHANG, L., HUANG, H., ZHOU, F., SCHIMMEL, J., PARDO, C. G., ZHANG, T., BARAKAT, T. S., SHEPPARD, K. A., MICKANIN, C., PORTER, J. A., VERTEGAAL, A. C., VAN DAM, H., GRIBNAU, J., LU, C. X. & TEN DIJKE, P. 2012a. RNF12 controls embryonic stem cell fate and morphogenesis in zebrafish embryos by targeting Smad7 for degradation. *Molecular cell,* 46**,** 650-61.

ZHANG, L., ZHOU, F., DRABSCH, Y., GAO, R., SNAAR-JAGALSKA, B. E., MICKANIN, C., HUANG, H., SHEPPARD, K.-A., PORTER, J. A., LU, C. X. & TEN DIJKE, P. 2012b. USP4 is regulated by AKT phosphorylation and directly deubiquitylates TGF-beta type I receptor. *Nature Cell Biolology,* 14**,** 717-726.

ZHANG, L., ZHOU, F., GARCIA DE VINUESA, A., DE KRUIJF, E. M., MESKER, W. E., HUI, L., DRABSCH, Y., LI, Y., BAUER, A., ROUSSEAU, A., SHEPPARD, K. A., MICKANIN, C., KUPPEN, P. J., LU, C. X. & TEN DIJKE, P. 2013a. TRAF4 promotes TGF-beta receptor signaling and drives breast cancer metastasis. *Molecular cell,* 51**,** 559-72.

ZHANG, L., ZHOU, F. & TEN DIJKE, P. 2013b. Signaling interplay between transforming growth factor-beta receptor and PI3K/AKT pathways in cancer. *Trends in Biochemical Sciences,* 38**,** 612-20.

ZHANG, Q., YU, N. & LEE, C. 2014b. Mysteries of TGF-beta Paradox in Benign and Malignant Cells. *Frontiers in oncology,* 4**,** 94.

ZHANG, X., ZHANG, J., BAUER, A., ZHANG, L., SELINGER, D. W., LU, C. X. & TEN DIJKE, P. 2013c. Fine-tuning BMP7 signalling in adipogenesis by UBE2O/E2-230K-mediated monoubiquitination of SMAD6. *The EMBO Journal,* 32**,** 996-1007.

ZHANG, Y., CHANG, C., GEHLING, D. J., HEMMATI-BRIVANLOU, A. & DERYNCK, R. 2001. Regulation of Smad degradation and activity by Smurf2, an E3 ubiquitin ligase. *Proceedings of the National Academy of Sciences of the United States of America,* 98**,** 974-9.

ZHANG, Y., FENG, X., WE, R. & DERYNCK, R. 1996. Receptor-associated Mad homologues synergize as effectors of the TGF-beta response. *Nature,* 383**,** 168-72.

ZHANG, Y., HU, R., WU, H., JIANG, W., SUN, Y., WANG, Y., SONG, Y., JIN, T., ZHANG, H., MAO, X., ZHAO, Z. & ZHANG, Z. 2012c. OTUB1 Overexpression in Mesangial Cells Is a Novel Regulator in the Pathogenesis of Glomerulonephritis through the Decrease of DCN Level. *PloS one,* 7**,** e29654.

ZHANG, Y. E. 2009. Non-Smad pathways in TGF-beta signaling. *Cell research,* 19**,** 128-39.

ZHAO, B., WANG, Q., DU, J., LUO, S., XIA, J. & CHEN, Y.-G. 2012. PICK1 promotes caveolin-dependent degradation of TGF-[beta] type I receptor. *Cell research,* 22**,** 1467-1478.

ZHAO, Y., THORNTON, A. M., KINNEY, M. C., MA, C. A., SPINNER, J. J., FUSS, I. J., SHEVACH, E. M. & JAIN, A. 2011. The Deubiquitinase CYLD Targets Smad7 Protein to Regulate Transforming Growth Factor β (TGF-β) Signaling and the Development of Regulatory T Cells. *Journal of Biological Chemistry,* 286**,** 40520-40530.

ZHOU, X., GAO, C., HUANG, W., YANG, M., CHEN, G., JIANG, L., GOU, F., FENG, H., AI, N. & XU, Y. 2014. High Glucose Induces Sumoylation of Smad4 via SUMO2/3 in Mesangial Cells. *BioMed research international,* 2014**,** 782625.

ZHU, H., KAVSAK, P., ABDOLLAH, S., WRANA, J. L. & THOMSEN, G. H. 1999. A SMAD ubiquitin ligase targets the BMP pathway and affects embryonic pattern formation. *Nature,* 400**,** 687-693.

ZHU, X., MENARD, R. & SULEA, T. 2007. High incidence of ubiquitin-like domains in human ubiquitin-specific proteases. *Proteins,* 69**,** 1-7.

ZI, Z., CHAPNICK, D. A. & LIU, X. 2012. Dynamics of TGF-β/Smad signaling. *FEBS Letters,* 586**,** 1921-8.

ZOU, Q., JIN, J., HU, H., LI, H. S., ROMANO, S., XIAO, Y., NAKAYA, M., ZHOU, X., CHENG, X., YANG, P., LOZANO, G., ZHU, C., WATOWICH, S. S., ULLRICH, S. E. & SUN, S.-C. 2014. USP15 stabilizes MDM2 to mediate cancer-cell survival and inhibit antitumor T cell responses. *Nature Immunology,* 15**,** 562-570.

ZUO, W., HUANG, F., CHIANG, Y. J., LI, M., DU, J., DING, Y., ZHANG, T., LEE, H. W., JEONG, L. S., CHEN, Y., DENG, H., FENG, X. H., LUO, S., GAO, C. & CHEN, Y. G. 2013. c-Cbl-mediated neddylation antagonizes ubiquitination and degradation of the TGF-beta type II receptor. *Molecular cell,* 49**,** 499-510.